Electrophysiological biomarkers for the study of new therapeutic strategies for motoneuron disease

Renzo Mancuso

ACADEMIC DISSERTATION

To obtain the degree of PhD in Neuroscience

by the Universitat Autònoma de Barcelona

2014

Supervisor: Dr. Xavier Navarro Acebes

Index

Introduction

Motoneuron disease

Motoneuron diseases (MND) are progressive neurodegenerative disorders with different etiologies and clinical spectra, but a common final event: loss of lower and/or upper motoneurons (MNs). Amyotrophic lateral sclerosis (ALS) and spinal muscular atrophy (SMA) are the most frequent forms of MND and therefore the most studied. ALS was first described by Charcot in 1869 and is the most common form of MND (incidence of 1–5 per 100.000) affecting adults. Despite that most ALS cases are sporadic (sALS), 5-10% are familiar (fALS), related with several genetic mutations (summarized in Table 1) (Shaw, 2005). No matter if they are sporadic or familiar, patients develop progressive weakness and muscle atrophy, with spasticity and contractures. Progressive weakness may start distally or proximally in the upper or lower limbs and reaches all muscles, including those related with breathing, speaking and swallowing. Patients die, mostly due to respiratory failure, 2-5 years after diagnosis (Wijesekera and Leigh, 2009; Worms, 2001). No satisfactory treatment is presently available for ALS. Patient care focuses on symptomatic treatment and physical therapy. Assisted ventilation and nutrition can transiently overcome the loss of upper airway and respiratory muscular control (Wijesekera and Leigh, 2009). A large number of therapeutic trials have been attempted, but it was not until the early 1990s that the first drug approved by the FDA for the treatment of patients with ALS reached the market: riluzole, an antiglutamatergic agent that blocks the presynaptic release of glutamate. However, the efficacy of riluzole is questionable, with minimal therapeutic benefits of about 3-4 months of survival increase (Ludolph and Jesse, 2009).

Table 1. Currently known genetic causes of fALS. Table includes data on mutations identified to date, and the percentage known for which the mutation accounts for fALS or sALS.

Protein/gene	Chromosome	Mutations	FALS cases (%)	SALS cases (%)	Reference
SOD1/*SOD1*	21q22.11	166	20	1-3	(Rosen, 1993)
Alsin/*ALS2*	2q33.2	19	-	-	(Yang et al., 2001)
Senataxin/*SEXT*	9q34.13	7	-	-	(Chen et al., 2004)
TDP-43/*TARDBP*	1p36.22	39	4	0.2-0-4	(Kabashi et al., 2008; Sreedharan et al., 2008)
FUS/*FUS*	16p11.2	27	4	0.2-0-4	(Kwiatkowski et al., 2009)

Optineurin/*OPTN*	10p13	3	-	-	(Maruyama et al., 2010)
VCP/*VCP*	14q11.1	4	-	-	(Johnson et al., 2010)
Angiongenin/*ANG*	20q13.33	18	-	-	(Greenway et al., 2006)
VAPB/*VAPB*	Xp11.21	2	<1	-	(Nishimura et al., 2004)
Ubiquilin-2/*UBQLN2*	9p21.2	5	-	-	(Deng et al., 2011)
C9orf72/*C9ORF72*	17p13.3	GGGGCC repeat expansion	20-40	10	(DeJesus-Hernandez et al., 2011; Renton et al., 2011)
Profilin 1/*PFN1*		4	-	.	(Wu et al., 2012)

"–" denotes that this information is unclear. Source: http://alsod.iop.kcl.ac.uk.

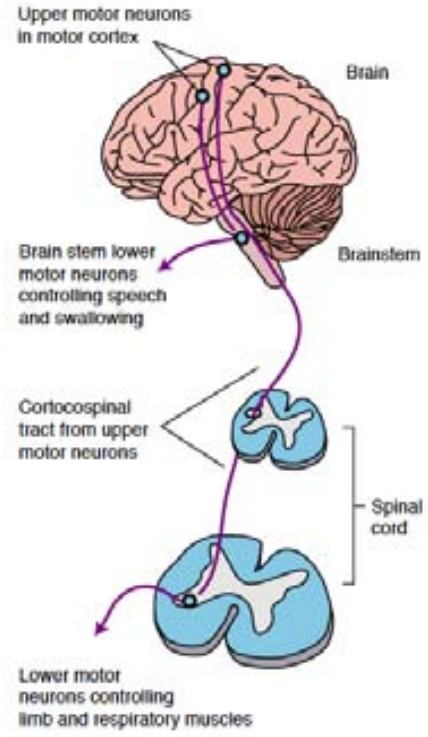

Figure 1. Outline of the human motor system. Upper motor neuron cell bodies are situated in the motor cortex and project axons via the corticospinal tracts to the spinal cord. There they synapse in the anterior horn with lower motor neurons, which project axons via peripheral nerves that then contact muscle fibers at the neuromuscular junction. Lower motor neurons originating in the brain stem that control speech and swallowing (bulbar motor neurons), and lower motor neurons that originate in the spinal cord that control limb and respiratory muscles, may both be affected.

Extracted from Goodall et al., 2006

Diagnostic criteria and methods

ALS is characterized by the loss of MNs of primary motor cortex, brainstem and spinal cord. This special combination of upper and lower MNs provokes physical signs of upper or lower MN involvement (Leigh and Ray-Chaudhuri, 1994): loss of upper MNs affects central motor drive

(reduced firing rates and recruitment of lower MNs), leading to slowing of contraction speed, slow repetitive movements, weakness, and decreased muscle activation, as well as hyperreflexia and spasticity. Loss of lower MNs and, consequently, loss of motor units results in muscle atrophy, fasciculations, hyporeflexia, and a comparable loss of both voluntary and electrically stimulated (tetanic) muscle force (Hardiman et al., 2011; Wijesekera and Leigh, 2009). Not all motor units are equally vulnerable to the disease process. Electromyographical analysis performed in ALS patients revealed that the larger and physiological stronger motor units are clearly more affected by the disease (Dengler et al., 1990). Moreover, histopathological studies also described a preferential degeneration of large MNs in ALS (Sobue et al., 1983).

One of the major problems of ALS is the delay in diagnosis, mainly because the initial symptoms mimic other spinal cord diseases, neuropathies and several neurological syndromes (Kraemer et al., 2010). With the advent of possible new therapies for ALS, there is an increasing need for early diagnosis, because is intuitively probable that early therapy will produce better results. Many efforts have been conducted to develop reliable biomarkers to early diagnose ALS mainly focused on either biochemical or live-imaging fields. However, physiological markers are still the most important approach in terms of ALS diagnosis and monitoring.

Electrophysiological tests for lower motoneuron involvement

Nerve conduction studies are crucial for the diagnosis of ALS since they permit to define and exclude other peripheral nerve, neuromuscular junction or muscle disorders that may mimic the ALS phenotype (Brooks et al., 2003). In ALS, the major electrophysiological feature is the reduction of the compound muscle action potentials (CMAP) (Brooks et al., 2003). On the contrary, the distal motor latency and the motor nerve conduction velocity remain almost normal, below 70% of upper or lower limits of normal (Cornblath et al., 1992; de Carvalho and Swash, 2000; Mills and Nithi, 1998). Motor studies are also important for excluding multifocal motor neuropathy by the detection of partial conduction blocks. A marked reduction of proximal amplitude or negative-peak area as compared with the distal ones (over 50%), in short segments (excluding entrapment sites) implies partial conduction block (de Carvalho et al., 2001).

F-wave tests are also useful in assessing proximal conduction and some abnormalities have been described in ALS patients (de Carvalho et al., 2008), including increased F-wave latency with normal frequency and increased amplitude, and slowed F-wave velocity with decreased F-wave

latency. Upper MN abnormalities may be associated with an increased F-wave rate (de Carvalho and Swash, 2000).

Sensory nerve conduction studies can be abnormal in the case of entrapment syndromes and peripheral nerve diseases (Brooks et al., 2003). There are also recent evidences pointing to a sub-clinical involvement of the sensory system in 10-20% of ALS patients, suggesting an additional polyneuropathy (Isaacs et al., 2007; Pugdahl et al., 2007).

Electromyography

Needle electromyography (EMG) provides evidences of lower MN dysfunction, which are required for ALS diagnosis (Krarup, 2011). Abnormal EMG should be found in muscles innervated by MNs from at least two of the following four CNS regions: brainstem (bulbar/cranial MN), cervical, thoracic or lumbosacral spinal MNs. For the brainstem region it is enough to find EMG changes in one muscle (e.g. tongue, facial muscles, jaw muscles, etc). For thoracic spinal cord region it is sufficient to demonstrate EMG alterations in either paraspinal muscles at or below T6 level or abdominal muscles. Finally, for cervical and lumbosacral spinal cord regions, at least two muscles innervated by different roots and peripheral nerves must show EMG abnormalities (Brooks et al., 2003; Mitsumoto et al., 2007). EMG alterations could be manifested as: 1) large motor unit potentials of increased duration with an increased proportion of polyphasic potentials, often of increased amplitude; 2) reduced interference pattern with firing rates higher tan 10 Hz (unless there is a significant upper MN component, in which case the firing rate may be lower than 10 Hz); 3) unstable motor unit potentials.

Fasciculation potentials are another important feature in ALS, although they can also be seen in normal muscles (benign fasciculations) and are not present in all muscles of ALS patients. In benign fasciculations the morphology of fasciculation potentials is normal, whereas pathological fasciculations have a complex morphology (de Carvalho et al., 2008; Janko et al., 1989). It has been suggested that abnormal fasciculation potentials can be considered as equivalent in importance to fibrillation potentials or positive sharp waves (de Carvalho et al., 2008).

Motor unit number estimation

Motor unit number estimation (MUNE) is an electrophysiological technique that provides

quantitative information about the number of axons innervating a muscle. MUNE can be performed using a number of different approaches (incremental method, multiple point stimulation, spike-triggered averaging, F-wave, and statistical method), with each presenting advantages and limitations. Despite the lack of a single method for MUNE performing, it is crucial for the evaluation of progressive motor axonal loss in ALS (Bromberg and Brownell, 2008; Mitsumoto et al., 2007).

Transcranial magnetic stimulation and central motor conduction studies

Transcranial magnetic stimulation allows non-invasive evaluation of corticospinal motor pathways and thus the detection of upper MN lesion even when patients do not show upper MN clinical signs (Mitsumoto et al., 2007). Using this technique, motor amplitude, stimulation threshold, central motor conduction time and silent periods can be easily evaluated (Eisen and Shtybel, 1990). Electrophysiological features reflecting upper MN involvement include (Brooks et al., 2003): 1) up to 30% increase in central motor conduction time determined by cortical magnetic stimulation. Marked increase in central motor conduction time was reported in fALS patients with D90A SOD1 mutation (Cappellari et al., 2008; Osei-Lah et al., 2004; Vucic and Kiernan, 2007); 2) low firing rates of motor unit potentials on maximal effort.

Neuroimaging studies

The most important use of neuroimaging for ALS diagnosis is to exclude treatable structural lesions that mimic ALS by producing varying degrees of upper and lower MNs signs, especially in those with clinically probable or possible ALS. Clinically definite ALS with bulbar or pseudobulbar onset is the only condition where imaging studies are not required, since structural lesions are unlikely to reproduce this kind of signs (Brooks et al., 2003). Magnetic resonance image (MRI) can be also used to reveal lesions in the corticospinal tract in ALS. The most characteristic feature in ALS is the hyperintensity of the corticospinal tract on T2-weighted, proton density weighted and FLAIR-weighted MRI, and is best visualized in the brain and brainstem and to a lesser extent in the spinal cord (Abe et al., 1997; Goodin et al., 1988; Thorpe et al., 1996; Waragai, 1997).

Muscle biopsy and neuropathalogical studies

Biopsy of skeletal muscle or other tissues is not required for diagnosis, unless to rule out a mimic syndrome (e.g. inclusion body myositis). In addition, muscle biopsy may be used to demonstrate lower MN dysfunction in a body region where clinical or electrophysiological findings do not evidence involvement (Brooks et al., 2003).

Frontotemporal lobal degeneration - ALS

Frontotemporal lobal degeneration (FTLD or FTD) is caused by a progressive neuronal atrophy and loss in the frontotemporal cortex, and is characterized by personality and behavioral changes, as well as gradual impairment of language skills. It is the second most common dementia after Alzheimer's disease (Van Langenhove et al., 2012).

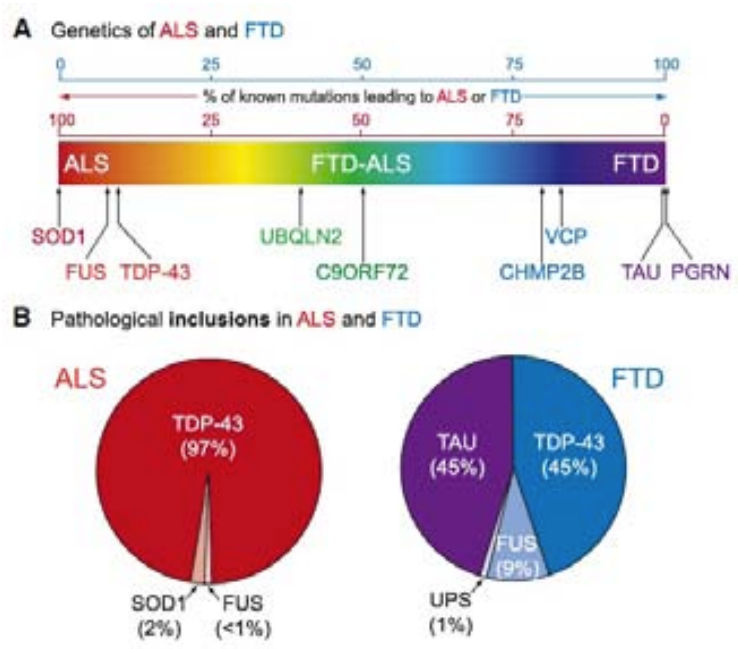

Figure 2. Clinical, genetic, and pathological overlap of ALS and FTLD (**A**) ALS and FTLD represent a continuum of a broad neurodegenerative disorder with each presenting as extremes of a spectrum of overlapping clinical symptoms (ALS in red and FTLD in purple). Major known genetic causes for ALS and FTLD are plotted according to the ratio of known mutations that give rise to ALS or FTLD. (**B**) Pathological protein inclusions in ALS and FTLD, according to the major protein misaccumulated. Inclusions of TDP-43 and FUS/TLS in ALS and FTLD reflect the pathological overlap of ALS and FTLD.

Extracted from Ling et al., 2013

Traditionally, ALS and FTLD were considered as two distinct identities. However, novel evidences suggest that both pathologies form one clinical continuum, where pure forms are linked by overlap syndromes. The first link established between FTLD and ALS was the identification of TDP-43 positive ubiquitinated cytoplasmic inclusions in almost all cases of ALS and more than a half of FTLD patients (Neumann et al., 2006; Van Langenhove et al., 2012). Although neuropsychological testing shows normal cognition in the majority of ALS patients, up to 50% of

them present some degree of cognitive impairment, while 15-18% meet the criteria for FTLD (Ringholz et al., 2005). On the contrary, few patients with FLTD develop ALS (Lomen-Hoerth et al., 2002). In fact, FTLD-only, ALS-only and coincident FTD-ALS were reported to occur inside a same family. Despite genetic alterations underlying these cases are unknown, some studies have identified a common locus on chromosome 9 (Vance et al., 2006). The recent finding of an hexanucleotid expansion in C9ORF72 constitutes a strong link between ALS and FTLD (DeJesus-Hernandez et al., 2011; Ling et al., 2013; Mori et al., 2013a; Renton et al., 2011).

Animal models

The development of transgenic animal models carrying genetic mutations described in fALS cases has facilitated the study of MNDs. These models show similar pathological events to the ones observed in patients. There are different mouse models for ALS, including those with spontaneous mutations, such as the MN degenerative (*mnd*) mouse, the wasted mouse, the wobbler mouse, and the progressive motoneuronopathy (*pmn*) mouse; and genetically engineered mice, such as the transgenic mouse that overexpresses mutant human SOD1 (mSOD1). During the last 20 years, the study of ALS-liked genetic mutations has led to the development of several transgenic animal models.

mSOD1 models

Missense *sod1* gene mutations on the chromosome 9 were the first identified genetic cause of ALS (Rosen, 1993). Research into the aberrant function of mSOD1 has formed the basis of much of our understanding of ALS pathogenesis through the generation and study of transgenic rodent models overexpressing the human mSOD1 protein. However, after 20 years of research, the exact mechanisms underlying mSOD1 pathology remain unknown. It was originally hypothesized that mSOD1 may cause ALS as a result of a loss of dismutase activity. However, further studies in *sod1* KO mice revealed that SOD1 deficiency was not the cause of motor dysfunction (Reaume et al., 1996). In contrast, the degeneration of MN in transgenic mice expressing mSOD1 is likely to result from a toxic gain-of-function (Gurney et al., 1994). Few years after the discovery of SOD1 mutations as a cause of familial ALS (Rosen, 1993), the transgenic mouse model $SOD1^{G93A}$ was developed, expressing the human mutation of a glycine to alanine conversion at the 93rd codon of SOD1 gene in high copy number (Ripps et al., 1995). These mice develop a rapidly progressive

MND, which leads to hindlimb paralysis and death in around 4-5 months of age. This phenotype recapitulates several clinical and histopathological features of both familial and sporadic forms of the human disease (Ripps et al., 1995). Since the development of this model, over twenty other mSOD1 models have been created carrying other mutations such as G37R or G85R, leading to heterogeneous phenotypes in terms of disease onset and progression. In fact, mSOD1 rodent models of ALS have variable ages of clinical disease onset, rates of progression and survival mostly depending upon the specific mutation on the gene (G93A, G85R, G37R, etc), the number of mSOD1 transgene copies or its expression level, the gender of the animals or their genetic background (Alexander et al., 2004; Heiman-Patterson et al., 2005; 2011). Although the high variety of existing mSOD1 mouse models, SOD1^{G93A} mice are still the most widely used on basic research and preclinical studies.

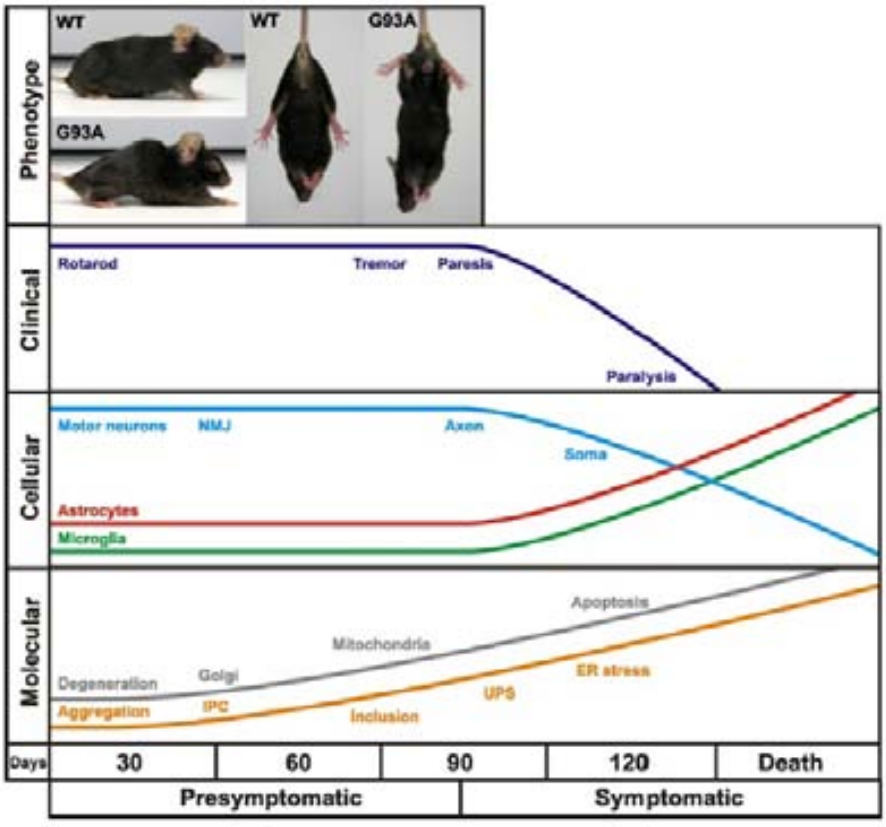

Figure 3. Time course of clinical and neuropathological events in high copy number transgenic SOD1^{G93A} mice.

Extracted from Turner et al., 2008

More recently, models of neuronal-specific (Jaarsma et al., 2008; Lino et al., 2002) or non-neuronal-specific (Clement et al., 2003; Yamanaka et al., 2008) mSOD1 expression have also been developed, leading to important findings about the role of non-neuronal cells on ALS physiopathology. In order to assess the possibility that the disease phenotype may be triggered by the overexpression of the SOD1 *per se*, some lines of transgenic mice overexpressing the human wild type SOD1 (wtSOD1) protein have been created and used as control in several studies (Gurney et al., 1994; Jaarsma et al., 2000; Saxena et al., 2009). It was originally described that wtSOD1 did not play a role in ALS, as mice overexpressing this protein show mild axonopathy with signs of abnormal mitochondrial morphology but without overt motor dysfunction (Jaarsma et al., 2000). However, more recently it has emerged that wtSOD1 could play a role in ALS pathogenesis, since overexpression of human wtSOD1 at similar levels to that seen in mSOD1 mouse models, causes progressive MN degeneration (Graffmo et al., 2013). In their work, Graffmo et al. reported that wtSOD1 overexpression resulted in an ataxic staggering gait with abnormal hindlimb reflexes and a reduced lifespan, with median survival of 367 days. These clinical signs were accompanied by gliosis and misfolded wtSOD1 in transgenic mice spinal cord from 100 days of age, and a 41% reduction of thoracic MN. These novel findings, together to those reporting a potential role of conformationally altered wtSOD1 in sporadic ALS patients (Bosco et al., 2010b) lead to the need of further investigation on the contribution of SOD1 in ALS pathology.

TDP-43 models

TDP-43 is a 43kDa nuclear protein originally discovered because of its effects on human immunodeficiency virus transcription (Ou et al., 1995). It is encoded by the *tardbp* gene on chromosome 1 and is composed by a nuclear localization signal, two RNA-binding motifs and a glycine-enriched region, which contains a "prion-like" domain and mediates protein and hnRNP interactions. In fact, it is in this glycine-enriched domain where most of ALS-associated mutations have been described (Kabashi et al., 2008; Sreedharan et al., 2008).

Although not all TDP-43 functions are known, it plays crucial roles in alterative splicing and gene expression (Buratti and Baralle, 2008), embryogenesis (Sephton et al., 2010) and neuronal development. Nevertheless, the effect of TDP mutations on such functions is not understood. Several *in vitro* and *in vivo* studies have identified a large range of aberrant cellular dysfunctions caused by mTDP-43, including abnormal neuronal function and synaptic defects (Godena et al.,

2011; Lin et al., 2011), mitochondrial alterations (Braun et al., 2011) proteasome dysfunction (Estes et al., 2011) and altered neuroinflammatory response (Swarup et al., 2011). Although it remains unclear how TDP-43 mutations cause ALS, both loss and gain of function have been proposed (Tsao et al., 2012). Several groups have attempted to generate TDP-43-ALS mouse models but results have shown varied phenotypes, with no TDP-43-ALS model completely replicating an ALS phenotype. Similar to mSOD1 murine models, development of disease phenotype in TDP-43-ALS transgenic rodents is highly dependent upon the level of transgene expression and, ultimately, the promoter used. However, in marked contrast to mSOD1 transgenic mice, these models develop mostly axonal alterations with relatively mild MN degeneration. Overexpression of human wild type TDP-43 has been shown to cause significant neurodegeneration (McGoldrick et al., 2013; Tsao et al., 2012).

FUS models

FUS was originally identified because its oncogenic properties following a chromosomal translocation resulting in the fusion of truncated FUS protein with the transcription factor CHOP (Crozat et al., 1993; Rabbitts et al., 1993). The FUS gene is located at 16p11.2 and comprises 15 exons encoding a multifunctional 526 amino-acid protein (Prasad et al., 1994) with a complex domain structure. The N-terminus contains a Gln-Gly-Ser-Tyr-rich domain and glycine rich domain, and is proposed to have 'prion-like' properties (Udan and Baloh, 2011). Adjacent to this domain is an RNA recognition motif (RRM) domain, which contains a nuclear export sequence, followed by two Arg-Gly-Gly domains, which flank a zinc-finger region. The C-terminus of the protein contains a non-classical nuclear localization signal, which is recognized by transportin (Dormann et al., 2010). FUS is ubiquitously expressed in all cells, despite some rodent data suggest that expression outside the CNS decreases with age, being absent in mouse skeletal muscle, liver and kidney from 80 days of age (Huang et al., 2010). FUS binds DNA and RNA and primarily shows nuclear localization (Bosco et al., 2010a; Gal et al., 2011) .

Mutations in FUS have been described as causative in similar proportion of fALS cases (FUS-ALS) as TDP-43 mutations, but it has been proposed that it may function downstream TDP-43 and in parallel to other RNA-binding proteins (Kabashi et al., 2011). Developing models of FUS-ALS models is important to clarify the mechanisms by which mutations in this protein cause ALS and how aberrant RNA metabolism may lead to neurodegeneration.

There are four published transgenic rodent lines overexpressing FUS: 1) transgenic mice which overexpressing HA-tagged human wild-type FUS under control of the mouse prion promoter (Mitchell et al., 2013); 2) somatic brain transgenic mice expressing V5-tagged human wild-type FUS, mutant R521C and FUS lacking its nuclear localization signal (Δ14) (Verbeeck et al., 2012); 3) transgenic rats which conditionally express human wild-type or mutant FUS under a TRE (Huang et al., 2011); and 4) transgenic rats which express mutant FUS under the CaMKIIα promoter with a TRE (Huang et al., 2012). Controversially, all four models display different phenotypic manifestations from pure motor involvement with muscle denervation, axonopathy and spinal MN degeneration, to pure cognitive deficits with memory impairment and hippocampal neurons death.

Controversies of preclinical studies

One of the most important problems regarding the development of new therapies for ALS is the failure to translate positive experimental results into successful human trials (Benatar, 2007; Rothstein, 2003). There are several possible explanations for the failure of successful translation from preclinical studies to effective human treatments. Firstly, mSOD1 rodent models represent a proportion of familial ALS rather than sporadic ALS cases. Given this, it can be argued that mSOD1 animals only model fALS or even only the fraction of cases caused by specific mutations that were introduced to the rodents. Since ALS pathophysiology is incompletely understood, it is possible that familial and sporadic ALS differ in some fundamental biological aspect that determines the effectiveness of a given treatment. Secondly, therapeutic approaches in animal models are usually applied prior to clinical onset of the disease. Despite this strategy might offer better results on preclinical studies and could be relevant for fALS cases, it cannot be replicated in human sALS. Thirdly, drug dosage and bioavailability are difficult to translate to humans based on rodent experimental data. And fourthly, drug effect discrepancies may be related to methodological shortcomings rather than drawbacks in the models themselves, increasing the importance of developing and applying techniques that lead to reliable, objective reliable preclinical results.

Pathophysiological mechanisms

The exact molecular pathway causing MN degeneration in ALS is unknown, but as with other neurodegenerative diseases, is likely to be a complex interplay between multiple pathogenic cellular

mechanisms that may not be mutually exclusive (Ferraiuolo et al., 2011; Pasinelli and Brown, 2006; Shaw, 2005).

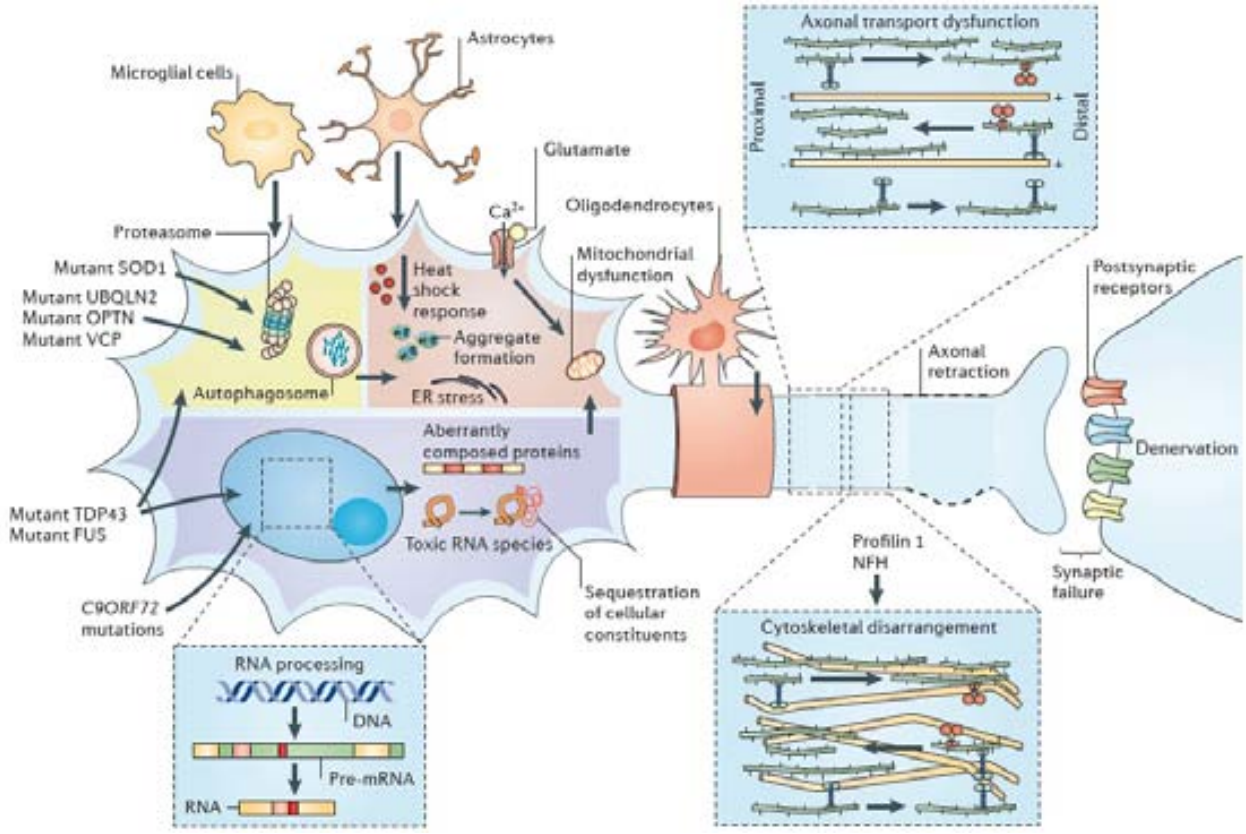

Figure 4. Overview of events in the pathogenesis of ALS.

Extracted from Robberecht et al., 2013

Oxidative stress

Oxidative stress results from the imbalance between the production of reactive oxygen species (ROS) and the biological system capacity to remove ROS or repair the ROS-induced damage. Although oxidative stress by itself may not be such harmful, accumulation of ROS may be an important factor that reduces the ability of the cell to cope with an underlying pathologic situation.

The discovery that defects in the gene encoding SOD1 (Rosen, 1993) were associated with cases of familial ALS has heightened interest in the possibility that oxidative stress may contribute to MN death. However, further experiments demonstrated that MN death was related to the accumulation of abnormal mSOD1 instead of a loss of dismutase activity, since SOD1 deletion in mice do not lead to MN degeneration (Reaume et al., 1996).

The analysis of CSF and serum from both familial and sporadic ALS patients showed increased concentrations of oxidative stress-induced damage (Lyras et al., 1996; Mitsumoto et al., 2008; Simpson et al., 2004; Smith et al., 1998). In this sense, evidences of oxidative damage to proteins (Shaw et al., 1995b), lipids (Simpson et al., 2004) and DNA (Bogdanov et al., 2000) have been reported in tissue of ALS patients.

Oxidative damage has been documented in both cellular and rodent models of ALS (Barber and Shaw, 2010; Parakh et al., 2013). One of the most important consequences of oxidative stress is the damage to RNA species. Chang et al. (2008) reported that mRNA oxidation primarily occurs in MNs and spinal cord oligodendrocytes in $SOD1^{G93A}$ mice at early pre-symptomatic disease stages, and that translation of oxidized mRNA species decreased. Some mRNA species seem to be more susceptible to oxidation, including those involved in the mitochondrial electron transport chain, protein biosynthesis, folding and degradation pathways, myelination, the cytoskeleton, and the tricarboxylic acid cycle and glycolysis pathways. Interestingly, aberrant oxidation of wtSOD1 present in sALS patients confers pathological properties similar to those observed in mSOD1, such as the inhibition of axonal transport (Bosco et al., 2010b).

Mitochondrial dysfunction

Mitochondria are the cellular organelle in charge of ATP production, calcium homeostasis maintenance and intrinsic apoptosis regulation. Numerous studies have highlighted the common role of mitochondria in the pathogenesis of neurodegenerative diseases (Lin and Beal, 2006). An important core of evidences implicates mitochondria as a key player in ALS physiopathology (Shi et al., 2010). Reduced mitochondrial DNA content associated to increased mutations of mitochondrial DNA, and respiratory chain complexes activity have been described in the spinal cord of ALS patients (Hirano et al., 1984; Wiedemann et al., 2002). In this sense, mitochondrial function impairments have been also reported in the skeletal muscle of ALS patients (Wiedemann et al., 1998). *In vitro* studies showed mitochondrial morphological and functional alterations in NSC-34 cells (a MN cell line) expressing mSOD1 (Menzies et al., 2002). Experiments performed in mSOD1 mice also revealed early mitochondrial morphological abnormalities prior to onset of symptoms (Kong and Xu, 1998).

Although the exact mechanism by which mSOD1 might disrupt mitochondrial function is not clear, several possible explanations have been postulated. mSOD1 could aggregate into the mitochondrial intermembrane space physically blocking the TOM/TIM protein import machines,

thus impeding mitochondrial protein import (Liu et al., 2004; Wong et al., 1995). MNs are large cells with important energy requirements. Despite several studies conducted, there is no consensus about the presence and contribution of mitochondrial respiratory chain alterations in mSOD1 models. Mitochondrial respiration, electron transfer chain, and ATP synthesis have been reported as defective in $SOD1^{G93A}$ mice at disease onset (Jung et al., 2002; Mattiazzi et al., 2002), and ATP is even depleted in pre-symptomatic $SOD1^{G93A}$ mice (Browne et al., 2006). On the contrary, Damiano et al. (2006) reported unchanged ATP synthesis in SOD^{G85R} mice.

Maintaining calcium homeostasis is a critical function of mitochondria. It has been reported that neural mitochondrial calcium buffering capacity is altered prior to symptoms onset in the brain and spinal cord of $SOD1^{G93A}$ mice (Damiano et al., 2006). Furthermore, mitochondrial calcium uptake deficits have been shown in hypoglossal (vulnerable) MNs of $SOD1^{G93A}$ mice (Fuchs et al., 2013). Calcium buffering impairments in MNs could increase their susceptibility to the altered calcium homeostasis associated with glutamate-mediated excitoxicity. Parone et al. (2013) explored the contribution of mitochondrial calcium buffering dysfunction by eliminating the expression of cyclophilin D, an important regulator of calcium-mediated opening of the mitochondrial permeability transition pore that determines mitochondrial calcium content. They determined that a chronic increase in mitochondrial calcium buffering capacity improved mitochondrial ATP synthesis, reduced mitochondrial swelling preserving their normal morphology.

Mitochondria are a central element controlling apoptosis since the opening of the permeability transition pore and release of cytochrome c from the mitochondrial intermembrane space is crucial for the activation of the caspase cascade. mSOD1 aggregates may interfere with mitochondrial anti-apoptotic elements, such as Bcl-2, thereby triggering abnormal activation of intrinsic apoptosis by the premature release of cytochrome c to the cytoplasm (Pasinelli et al., 2004). In this sense, Tan et al. (2013) reported that small peptides that specifically block the mSOD1-Bcl-2 complex formation rescue mitochondrial dysfunction. However, further experiments demonstrated that Bax deletion was able to rescue spinal MNs but failed to prevent neuromuscular denervation and mitochondrial vacuolization (Gould et al., 2006), suggesting that apoptosis contribution is limited to the last part of the MN degenerating process.

Recent findings from Wang et al. (2013) and Xu et al. (2010) showed that mTPD-43 also impairs mitochondrial morphology and function in transgenic mice.

Impaired axonal transport

Intracellular transport is an essential element for neuronal cells. Neurons are polarized cells and they require mechanisms to direct axonal vs. dendritic transport. Since neurons transmit signals along long distances, proteins and organelles have to travel more than in other cell types (axons of human MNs can reach 1 m long). Even within an axon, proteins must be delivered to specific compartments (e.g., sodium channels must go to the plasma membrane in the nodes of Ranvier, and synaptic proteins to the axon terminal) thus increasing the importance of axonal transport within MNs.

One of the main findings supporting axonal transport deficits as a hallmark of neurodegeneration is the axonal and cell body accumulation of organelles and other proteins observed in many human neurodegenerative diseases (De Vos et al., 2008). Regarding ALS, several works have demonstrated the accumulation of neurofilaments in MN cell bodies in human patients, suggesting that axonal transport is impaired in these cells (Hirano et al., 1984; Julien, 1997; Julien et al., 1998; Schmidt et al., 1987). Additionally, abnormalities of organelle axonal trafficking have been described in ALS patients (Breuer et al., 1987).

Axonal transport has been widely studied in animal models mimicking ALS. Similar to what was reported in patients, it has been demonstrated that transgenic mice overexpressing mSOD1 transgene develop neuronal cytoeskeletal pathology resembling human ALS (Tu et al., 1996). Further studies reported impaired anterograde axonal transport and neurofilament accumulation in $SOD1^{G93A}$ mice (Zhang et al., 1997). How mSOD1 perturbs axonal transport is not fully understood. It has been proposed that SOD1 mutations could indirectly alter axonal transport by increasing inflammatory and excitotoxic mediators, altering mitochondria or damaging transport cargos (De Vos et al., 2008). However, some evidences suggest a direct link between mSOD1 and axonal transport deficits since misfolded SOD1 specifically and abnormally binds to kinesin-associated protein 3 (KAP3) in the ventral grey matter of $SOD1^{G93A}$ spinal cord. KAP3 is a kinesin-2 subunit responsible for binding to divers cargos including choline acetyltransferase (ChAT). The consequent reduction of ChAT in the axon terminal may contribute to the synaptic deficit and, finally, to muscle denervation (Tateno et al., 2009). However, recent evidence from Marinkovic et al. (2012) suggests that axonal transport deficits may evolve independently from MN degeneration in $SOD1^{G93A}$ mice. In their work, Marinkovic et al., (2012) demonstrated that $SOD1^{G93A}$ axons can survive despite long-lasting transport deficits since these are present soon after birth, months before the first signs of muscle denervation (Fischer et al., 2004). Even more, they showed that MN

degeneration in SOD^{G85R} ALS mice occurs without axonal transport abnormalities. In light of these results, further experiments have to be performed to elucidate the role of axonal transport alterations in the specific MN degeneration in ALS.

Excitotoxicity

Glutamate is the main excitatory neurotransmitter in the CNS. It exerts its effect through the activation of several types of ionotropic and metabotropic receptors. Neuronal injury caused by excitatory mediators, known as excitotoxicity, results from the excessive activation of glutamate receptors, and may be due to failure in the neurotransmitter clearance from the synaptic cleft or increased postsynaptic sensitivity to glutamate. This enhanced activation induces massive calcium influxes that damage the cell through the activation of calcium-dependent protreases, lipases and nucleases. In fact, excitotoxicity is closely related to other important features of ALS, such as intracellular calcium disruption, with secondary activation of proteolitic and ROS-generating enzymes, and mitochondrial abnormalities and energy imbalance (Arundine and Tymianski, 2003). A large amount of evidences implicate excitotoxicity as a mechanism contributing to MN injury in ALS, although clear evidence that it is a primary disease mechanism is lacking. The most important evidences supporting the role of excitotoxicity in ALS physiopathology are the three-fold increased glutamate levels present in ALS patients CSF (Perry et al., 1990; Shaw et al., 1995a) and the benefits achieved by riluzole as an anti-excitotoxic drug (Ludolph and Jesse, 2009).

Excitotoxicity detrimental effects are mainly mediated through calcium-dependent pathways (Grosskreutz et al., 2010; Van Den Bosch et al., 2006). One possible explanation for the role of excitotoxic injury to MNs is that ALS-vulnerable spinal and brainstem MNs display low endogenous Ca^{2+} buffering capacity, that is 5-6 times lower than that found in ALS-resistant MNs (i.e. oculomotor MNs), making them more susceptible to excitotoxic insults (Alexianu et al., 1994).

Overactivation of α-Amino-3-hydroxy-5-methyl-4-isoxazolepropionic acid (AMPA) and N-methyl-D-aspartate (NMDA) receptors is considered one of the main causes of excitotoxiciy (Van Den Bosch et al., 2006). It has been demonstrated that MNs are especially vulnerable to AMPA-mediated excitotoxicity *in vitro* (Carriedo et al., 1996). AMPA receptor calcium permeability is largely determined by the GluR2 subunit. Most native AMPA receptors in the mammalian CNS contain the GluR2 subunit, which is post-transcriptionally edited at the Gln/Arg site 586 in the second transmembrane domain, making the receptor complex calcium-impermeable (Kwak et al., 2010; Williams et al., 1997). Williams et al., (1997) reported that GluR2 subunit is reduced in human spinal MNs, making them highly calcium permeable and more susceptible to excitotoxic

insults, while Kawahara et al., (2004) reported a defect in the editing of the GluR2 subunit mRNA in the spinal motoneurons of individuals affected by ALS. In contrast, mRNA analysis performed in $SOD1^{G93A}$ and $SOD1^{H46R}$ transgenic rats showed a complete edition of the GluR2 subunit (Kawahara et al., 2004; 2006).

Although the role of the NMDA receptor has received less attention, there is some evidence supporting its contribution to excitotoxicity in ALS. In fact, Texido et al., (2011) (Texidó et al., 2011) have reported that sera from ALS patients induces abnormal NMDA receptors activation. Moreover, Sunico et al. (2011) have recently showed an excitation/inhibition imbalance in MNs of $SOD1^{G93A}$ mice with an increased density of glutamatergic synapses, which could lead to an excitatory imbalance.

As above mentioned, excitotoxicity could also result from glutamate clearance alterations from the synaptic cleft. Excitatory amino-acid transporters (EAATs) are located at most synapses in the CNS and translocate glutamate from the synaptic space into astrocytes (Foran and Trotti, 2009). Glutamate transport deficits have been identified in the motor cortex and the spinal cord of ALS patients, especially focused in the astroglial specific EEAT2 (Bristol and Rothstein, 1996). Furthermore, loss of glial EEAT2 have been also reported in mSOD1 models of ALS (Howland et al., 2002; Trotti et al., 1999).

Finally, it has been reported that mSOD1 can directly alter calcium hemeostasis. Allen et al. (2011) recently demonstrated that misfolded A4V mSOD1 aggregates forming pores that integrate in the membrane permitting the influx of calcium into the cytoplasm. This finding suggests that mSOD1 can contribute to excitotoxic damage to MNs without contribution of other glutamatergic-related elements.

Protein aggregation

Protein aggregates or inclusions have long been recognized as a pathological hallmark of several neurodegenerative disorders, including ALS, in which protein aggregates are common in spinal MNs. Ubiquitin-positive inclusions are characteristic of ALS pathology. However, it remains unknown whether inclusion formation is responsible of cellular toxicity and ALS pathogenesis, if aggregates may be innocuous neurodegeneration-derived products, or if they may represent a protective mechanism of the cell to reduce intracellular concentrations of toxic proteins.

Most ALS cases present small eosinofil Bunina-bodies containing cystatin C and transferrin (Okamoto et al., 1993b; 2008). However, the significance of these inclusions remains unclear.

Neurofilament-rich hyaline aggregates are found in the citoplasm and proximal dendrites of spinal MNs in human patients (Schmidt et al., 1987) and animal models (Zhang et al., 1997) of ALS. Although for some time neurofilament accumulation was considered an evidence of MN dysfunction, nowadays it is not clear their real contribution to ALS physiopathology (Julien, 1997).

SOD1 inclusions are found in MNs of familial and sporadic ALS patients (Shibata et al., 1994). Aggregation of mSOD1 is also a pathophysiological hallmark in mSOD1 rodent models (Bruijn et al., 1998). Further studies revealed that conformational antibodies that react with structurally altered mSOD1 mainly labeled cell bodies and proximal axons of spinal MNs (Rakhit et al., 2007). Bosco et al. (2010b) recently demonstrated that conformational antibodies against mSOD1 also react with structurally altered wtSOD1 present in sALS patients. Extracellular aggregates of mSOD1 are also able to activate microglial cells *in vitro* (Roberts et al., 2012).

Non-mutated TDP-43 is found in aggregates both in neuronal and non-neuronal cells in all sALS patients and the vast majority of SOD1-negative familial ALS patients, but not in SOD1-related ALS (Mackenzie et al., 2007; Neumann et al., 2006). Under normal conditions, TDP-43 is predominantly localized in the nucleus, and loss of nuclear TDP-43 staining is seen in most cells containing TDP-43-positive cytoplasmic inclusions (Zhang et al., 2008). It has been hypothesized that cytoplasmic redistribution of TDP-43 is an early pathogenic event in ALS. In fact, mutations in TARDBP, the gene encoding TDP-43, were discovered in several familial ALS pedigrees, thereby consolidating the evidence for TDP-43 dysfunction in ALS and establishing this protein as a crucial player in both sporadic and familial disease (Sreedharan et al., 2008).

Similarly, cytoplasmic inclusions containing mutant FUS protein have been observed in some patients with FUS-related fALS (Groen et al., 2010; Hewitt et al., 2010).

Mutations in ubiquilin 2, which encodes a cytosolic ubiquitin-like protein, have recently been found to be associated with a dominantly inherited X-linked subtype of ALS (Deng et al., 2011). The exact function of ubiquilin 2 is unknown, but it has been implicated in protein degradation via both the Ubiquitin-Proteasome System (UPS) and autophagy (Lee and Brown, 2012).

An intronic hexanucleotide repeat expansion in C9ORF72 was recently identified as the most prevalent cause of ALS, FTD and ALS-FTD (DeJesus-Hernandez et al., 2011; Renton et al., 2011). Interestingly, TDP-43-negtive, ubiquilin 2-positive inclusions can distinguish expanded repeat from non-expanded repeat carriers (Brettschneider et al., 2012). In fact, these protein

accumulations contain polydipeptide repeat proteins generated by non-AGT-initiated translation from the C9ORF72 intronic repeat expansion (Ash et al., 2013; Mori et al., 2013a).

Endoplasmic reticulum stress

Physiologically, accumulation of misfolded protein elicits the ER stress response. ER-resident chaperons recognize the accumulation of misfolded proteins and activate the Unfolded-Protein Response (UPR), which can cause suppression of general translation and ER-associated protein degradation. Although these mechanisms are initially cytoprotective, prolonged UPR activation can trigger apoptotic signaling (Kaufman, 2002).

A deal of evidence implicates ER stress as an important feature of MN degeneration in ALS. UPR markers are up-regulated in sporadic ALS patients (Atkin et al., 2008) and mSOD1 rodent models (Atkin et al., 2006; Saxena et al., 2009). In fact, protein disulphide isomerase (PDI), an ER-resident chaperone is overexpressed in mSOD1 mice, where it co-localizes with SOD1 inclusions (Atkin et al., 2008). In mSOD1 mice, a longitudinally gene expression profile of vulnerable MNs (innervating fast fatigable muscles, e. g. *extensor digitorum longus*) vs. resistant MNs (innervating slow muscle fibers, e. g. *soleus*) revealed early up-regulation of several UPR markers prior to muscle denervation in vulnerable MNs. Similar changes eventually occurred in disease-resistant MNs but 25-30 days later (Saxena et al., 2009).

Addition of CSF from sporadic ALS patients on NSC-34 cells and primary rat spinal MNs cell cultures induces ER stress, including the up-regulation of UPR markers, such as GRP-78 and caspase-12 (Vijayalakshmi et al., 2011).

Under ER stress conditions, UPR is triggered by the activation of three sensor proteins, IRE1, ATF6, and PERK. Diminishing PERK activity in mSOD1^{G85R} mice dramatically accelerated disease onset as well as shortened disease duration and lifespan (Wang et al., 2010). Although UPR improves the ability of protein folding by inducing ER resident chaperones expression and protects the cell from ER stress, excessive ER stress leads to apoptosis by the activation of C/EBP homologous protein (CHOP). CHOP levels are increased in neurons, astroglia, microglia and oligodendrocytes of both sALS patients and mSOD1^{G93A} mice (Ito et al., 2009).

Neuroinflammation

Neuroinflammation is a common pathological event of neurodegenerative disorders (Khandelwal et al., 2011) and its modulation has been proposed as an important potential therapeutic target (Yong

and Rivest, 2009). Analysis of sporadic and familial ALS spinal cord tissue and CSF revealed increased microglial activation and T cells infiltration (Henkel et al., 2004; Sta et al., 2011), and higher concentration of some proinflammatory mediators, including monocyte chemoattractant protein 1 (MCP-1) and IL-8 (Kuhle et al., 2009). Consistent with these results gene array analysis of mSOD1 mice revealed an enhanced expression of inflammatory-related molecules especially at later stages of disease progression (Ferraiuolo et al., 2007; Lincecum et al., 2010). Additionally, Lincecum et al. (2010) reported a therapeutic improvement after the administration of an anti-CD40L in mSOD1 mice.

Microglial activation and proliferation is also evident in rodent models of ALS (Henkel et al., 2009). Gowing et al. (2008) reported an increased number of $CD45^{+}/CD11b^{+}$ microglial cells in $SOD1^{G93A}$ mice from 100 days of age. Additionally, they demonstrated an increased $CD45^{+}/CD11b^{+}/CD86^{+}$ ratio from 80 days of age, evidencing an increased proportion of activated microglial cells. Although it is still unknown whether microglial activation is a cause or a consequence of the MN degeneration, some works have been conducted manipulating microglial cells in mSOD1 mice. However, ablation of proliferating microglia in SOD^{G93A} mice did affect neither disease onset nor progression (Gowing et al., 2008).

Astrocytes also play a key role in the neuroinflammatory process by producing several inflammatory signals. Astrocytes from $SOD1^{G93A}$ secrete inflammatory mediators, such as prostaglandin E2, leukotriene B4, and nitric oxide both at basal (non-activated) and activated conditions (Hensley et al., 2006). Additionally, co-cultures of astrocytes from familial and sporadic ALS are toxic to MNs. This toxicity is in part mediated by the up-regulation of inflammatory gene expression (Haidet-Phillips et al., 2011).

The role of non-neuronal cells

It is now accepted that neighboring glial cells have a crucial role in the MN degeneration occurring in ALS. In 2003, Clement et al. (2003) generated a chimeric animal expressing mSOD1 in specific cell lines and demonstrated that normal MNs developed ALS signs when surrounded by mSOD1-expressing glia. Moreover, the proportion of non-neuronal cells that lacked the transgene positively correlated to the lifespan of the chimeric mice.

To determine the contribution of microglia, double transgenic mice were generated expressing the Cre–Lox recombination system to specifically suppress $mSOD1^{G37R}$ expression in MNs or microglia. mSOD1 deletion from MNs showed delayed disease onset but no modifications of disease progression once it had been initiated. On the contrary, mSOD1 suppression from

CD11b+ cells (microglia and macrophages) did not alter disease onset but significantly prolonged mice survival. These findings suggest that disease onset and propagation could be underlined by different mechanisms (Boillee et al., 2006a; 2006b). To deeply study the role of microglial cells in ALS disease progression, CD11b-Tkmut-30;SOD1^{G93A} double transgenic mice were generated to allow the selective elimination of proliferating microglial cells under the administration of ganciclovir. Surprisingly, a 50% reduction of reactive microglia in the lumbar spinal cord of these animals had no effect on MN degeneration (Gowing et al., 2008).

Although the generation of transgenic animals selectively expressing mSOD1 in astrocytes failed to induce MN degeneration (Gong et al., 2000), it is accepted that astrocytes play a crucial role in ALS. Astrocytes derived from postmortem tissue of familial and sporadic ALS patients are toxic to MNs. Interestingly, the toxic effect was restricted to MNs, since ALS-astrocytes are not toxic when co-cultured with GABAergic neurons. Surprisingly, blocking mSOD1 expression produced significant neuroprotective effects both on familial and sporadic ALS-derived astrocytes (Haidet-Phillips et al., 2011).

Rodent astrocytes expressing mSOD1 are toxic to spinal primary and embryonic mouse stem cell–derived motor neurons (Diaz-Amarilla et al., 2011; Nagai et al., 2007). Moreover, diminishing mutant expression in astrocytes does not affect onset, but delays microglial activation and sharply slows later disease progression (Yamanaka et al., 2008).

There is emerging evidence that oligodendrocytes provide crucial metabolic support to neurons (Nave, 2010) but their role in ALS has been not established. Kang et al. (2013) recently reported an extensive degeneration of gray matter oligodendrocytes in the spinal cord of mSOD1^{G93A} mice prior to disease onset. Moreover, they showed that selective removal of mSOD1 from oligodendroglia substantially delayed disease onset and prolonged survival.

Surprisingly, diminished mSOD1 synthesis exclusively within Schwann cells of SOD1^{G37R} significantly accelerates disease progression, accompanied by a reduction of insulin-like growth factor 1 (IGF-1) in nerves (Lobsiger et al., 2009).

Abnormal RNA processing

RNA processing abnormalities were first implicated in MND by the description of mutations in SMN1 as a cause of SMA (Lefebvre et al., 1995). The SMN protein participates in the assembly of small ribonucleoproteins, which have a role for pre-mRNA splicing (Burghes and Beattie, 2009).

Gene expression profiling revealed transcriptional repression in isolated MNs from $SOD1^{G93A}$ mice (Ferraiuolo et al., 2007; Kirby et al., 2005).

Later identification of TDP-43, a RNA-DNA binding protein, as a major component of the ubiquitinated inclusions in ALS (Neumann et al., 2006) focused the attention to RNA metabolism alteration as an important pathophysiological disease mechanism. TDP-43 is a predominantly nuclear protein implicated in several aspects of RNA processing, including transcriptional regulation, alterative splicing and microRNA processing. ALS-related TDP-43 positive cytoplasmic inclusions are present in both neuronal and glial cells, excluding those based on mSOD1 and FUS mutations (Mackenzie et al., 2007; 2010).

Recent studies using ultraviolet cross-linking and immunoprecipitation (CLIP) on brain and spinal cord of ALS mouse models and human patients have evaluated the RNA-binding targets of TDP-43 (Polymenidou et al., 2011; Tollervey et al., 2011; Xiao et al., 2011). Results revealed that TDP-43 binds to numerous RNA target molecules (approximately 30% of the mouse transcriptome). Binding commonly occurs to long UG-rich sequences in introns and less frequently to non-coding RNA molecules or to 3' untranslated regions of mRNA. This high proportion on intronic binding suggests a nuclear function for TDP-43. Blocking *tardbp43* expression with antisense oligonucleotides in adult mouse striatum altered the expression levels of 601 mRNA and changed the splicing pattern of 965 mRNA transcripts, including some relevant to neurodegeneration, such as FUS, progranulin and choline acetyltransferase (Polymenidou et al., 2011). A recent study shows that fibroblast cell lines derived from patients with TDP-43-related ALS loss nuclear expression of TDP-43, together with RNA splicing changes, including changes of transcripts of RNA-processing genes previously implicated in ALS (Highley et al., 2010). A note of caution relating to genetic studies is that although gene structures are often similar between species, intronic sequences show great variability. Given the key role of TDP-43 in binding to long intronic sequences, the intraspecies variability in introns may hinder accurate modeling of human TDP-43 proteinopathies in other species, including rodents (Xiao et al., 2011).

Further evidence of dysfunctional RNA metabolism in ALS emerges from the presence of mutations in angiogenin (ANG) (Greenway et al., 2006) and the DNA–RNA helicase senataxin (SETX) (Chen et al., 2004) in some cases. ANG, which expression is increased during hypoxia to promote angiogenesis, also acts as a transfer RNA-specific ribonuclease and regulates ribosomal RNA transcription (Kieran et al., 2008). A proposed mechanism by which ANG normally prevents cell death is inhibition of the translocation of apoptosis-inducing factor into the nucleus (Li et al.,

2012). Mutations in ANG are likely to have a deleterious effect through loss of function, as overexpression of ANG extends the lifespan of mSOD1 mice (Kieran et al., 2008). SETX autosomal dominant mutations are associated with juvenile-onset fALS (Chen et al., 2004). The SETX protein is predicted to be a component of large ribonucleoprotein complexes, with roles in maintaining DNA repair in response to oxidative stress, and RNA processing (Chen et al., 2004). The mechanisms by which mutant SETX causes ALS remain to be determined.

Additional evidence that dysregulated RNA processing may contribute to MN injury in ALS arises from the detection of biomarkers of RNA oxidation in human ALS and mSOD1 mice (Chang et al., 2008; Kieran et al., 2004) and the transcriptional repression within MNs that occurs in the presence of mSOD1 (Ferraiuolo et al., 2007; Kirby et al., 2005).

Most relevant current therapies

Drug-based therapy

The beneficial effect of riluzole in ALS is though to be due to its antiglutamatergic actions (non-competitive blocking of NMDA receptors) and by the blockage of voltage-dependent sodium channel (Doble, 1996). Although several trials targeting glutamate excitotoxicity (including gabapentin, toporimate, verapamil, lamotrignine or dextromethorphan) have been performed, the overall results have been disappointing (Choudry and Cudkowicz, 2005).

Several antioxidants, such as vitamin E, N-acetyl-L-cysteine (NAC) or catalase, produce benefits in mSOD1 mouse models but without successful translation in clinical trials (Orrell et al., 2005). Creatine, that promotes glutamate uptake into synaptic vesicles and stabilizes mitochondrial energy transfer complex through inhibiting the opening of the mitochondrial permeability pore, showed promising results when orally administered to mSOD1 mice (Klivenyi et al., 1999). However, three large clinical trials in human ALS failed to reproduce these benefits (Groeneveld et al., 2003; Rosenfeld et al., 2008; Shefner et al., 2004). Coenzyme Q10 is a co-factor of the electron-transport chain in the mitochondria. It prolongs survival in mSOD1 mice but it also failed to translate in successful human clinical trials (Kaufmann et al., 2009).

Increased interest is focused on the antibiotic minocycline since it has been one of the most effective agents in prolonging life in the rodent mSOD1 mouse models (Kriz et al., 2002). Although the exact mechanism underlying such effect is unclear, it is though that it inhibits microglial activation and modulates apoptosis (Yong et al., 2004). Unfortunately, recent phase III clinical trial

in human ALS patient revealed harmful effects after continuous minocycline administration (Gordon et al., 2007).

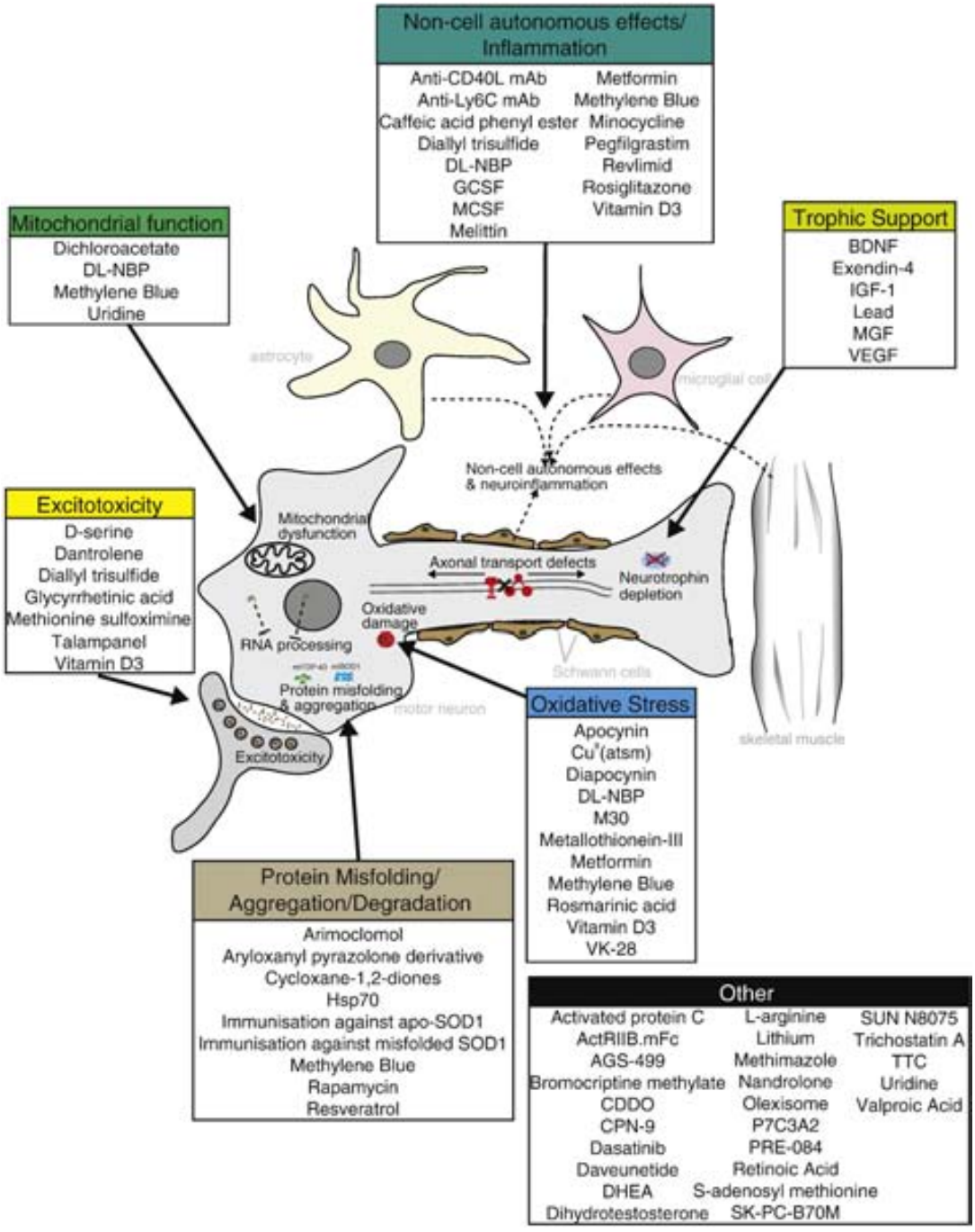

Figure 5. Summary of ALS therapeutic targets and agents tested on recent preclinical studies.

Extracted from McGoldrick et al., 2013

Glatiramer acetate (copaxone) was also proposed as a promising candidate since it produces almost 25% increased survival in mSOD1 mice (Angelov et al., 2003). However, a phase III clinical trial showed no impact on disease progression in human ALS patients (Meininger et al., 2009).

Arimoclomol is one compound of the novel "smart drugs" family that induces the expression of heat-shock proteins only under cellular stress conditions. Treatment with arimoclomol after symptoms onset slowed disease progression and increased survival in mSOD1 mice (Kieran et al., 2004). A phase III human trial is currently under recruiting phase (see www.alsa.org).

Growth factors

As the main hallmark of ALS disease progression is the loss of MNs, another therapeutic strategy has been the treatment with a variety of growth factors. Ciliary neurotrophic factor (CNTF), glial derived neurotrophic factor (GDNF) and insulin growth factor (IGF-1) showed promising effects on mSOD1 models, but clinical trials have been disappointing. IGF-1 was reported to produce some modest effects slowing disease progression and functional decline in American trials but these results were not confirmed in subsequent studies (Borasio et al., 1998; Lai et al., 1997). Neurotrophic factors lack of effect may be due to the low bioavailability and the poor delivery to MNs thus increasing the interest of the development of gene therapy approaches.

Gene therapy

Gene therapy is a promising therapeutic approach for ALS since it permits to specifically deliver treatments to damaged MNs overcoming the difficulty of crossing the blood-brain barrier. Several strategies have been developed, including the delivery of genes encoding for neurotrophic factors, anti-apoptotic proteins or blocking the expression or detrimental factors (e.g. by means of small interference RNAs). The main advantage of gene therapy is that viral vectors can be administered either directly to the CNS or systemically (intramuscular, intravenous, etc), but always affecting a determined cell target (Federici and Boulis, 2006). At present, gene therapy is restricted to preclinical studies in mSOD1 models. Retrograde adeno-associated virus (AAV) delivery systems for IGF-1 and GDNF have shown benefits in mSOD1 mice (Kaspar et al., 2003; Wang et al., 2002). Intramuscular injections of lentiviral-tagged VEGF or anti-apoptotic Bcl-2 also resulted successful in rodent models (Azzouz et al., 2000; 2004).

An alternative approach is to block the expression of genes that are causative of MNs degeneration, such as mutant *sod1*. Successful reports has been published using small interfering

RNAs (RNAi) targeted to mutant *sod1* (Ralph et al., 2005; Raoul et al., 2005). In fact, a phase I, randomized clinical trial has been recently performed intratecally delivering an antisense oligonucleotide against mutant *sod1* in SOD1 familial ALS patients (Miller et al., 2013).

Stem cell therapy

Several preclinical works have been carried out transplanting different types of cells in mouse models of ALS, including embryonic stem cells, neural stem cells, bone marrow cells, hematopoietic stem cells and mesenchymal stem cells (MSCs) (Giordano et al., 2007; Kim and de Vellis, 2009; Meamar et al., 2013). As in other contexts, there are potential complications after embryonic or neural stem cell transplantation since both have the ability for unlimited growth and could be associated with high risk of teratoma formation. In addition, the possibility to replace the lost MNs is low. Despite evidence of MN differentiation *in vivo*, it seems unlikely that single localized injections of stem cells will provide long-term benefit in ALS pathology. Furthermore, the new MNs would need to reestablish appropriate connections to both upper MNs and the correct target muscle to become functional. Even considering the successful integration of transplanted, MN axons growth at a rate of 1-3 mm/day requiring months for complete generations of new connections. This limitation is largely underappreciated and, among others, is the reason that MNs replacement cannot be currently considered as an effective therapeutic strategy for ALS (Lindvall and Kokaia, 2010; Meamar et al., 2013; Papadeas and Maragakis, 2009).

Induced pluripotencial stem (iPS) cells are capable of differentiating into any cell type, including MNs. Patient-specific iPS cells can be used for disease modeling, drug discovery, and perhaps autologous cell replacement therapies. iPS cells can also differentiate into MNs for drug screening or studying ALS cell mechanisms. Their ability to overcome immune rejection adds to their therapeutic potential.

MSCs are also being tested for ALS cell therapies. Following intravenous injection into $SOD1^{G93A}$ ALS mice, human MSCs showed neuroglia differentiation and migrated to the brain and spinal cord, surviving for long time (Zhao et al., 2007). In addition, hMSC-transplanted mice showed a significant delay in disease onset (14 days), increased lifespan (18 days), and delayed disease progression compared to untreated mice. Results from Phase I clinical trials have confirmed the safety of MSC transplantation into the spinal cords of ALS patients, suggesting that MSCs may have clinical utility (Mazzini et al., 2010).

Hematopoietic stem cells infusion into the spinal cord parenchyma of adult *mdf* mice, produced functional improvement, as well as an increase in the number of MNs in the anterior horn of the spinal cord when compared to sham mice (Pastor et al., 2012). However, no neural differentiation of the transplanted cells was observed. Further analysis of the experimental spinal cords showed that the grafted cells formed cellular nests surrounding the MNs and that they expressed GDNF, which has been hypothesized to be responsible for the neuroprotective effects of the transplant. A phase I clinical trial in which autologous bone marrow cells were infused into the thoracic spinal cord confirmed not only the safety of the procedure in ALS patients but also provided evidence strongly suggesting their neurotrophic activity (Blanquer et al., 2012).

Objectives

The general objective of the present thesis is to develop new therapeutic approaches for the SOD1^{G93A} mouse model of ALS. With this aim, we established the following specific objectives:

1. To characterize the SOD1^{G93A} mouse model of ALS in order to develop reliable, objective markers to assess disease onset and progression, and to evaluate new potential treatments.

2. To test the potential therapeutic effect of sigma-1 receptor modulation in SOD1^{G93A} ALS mice.

3. To test the potential therapeutic effect or resveratrol administration in SOD1^{G93A} ALS mice.

4. To assess the combinatory effect of sigma-1 receptor modulation and resveratrol in SOD1^{G93A} ALS mice.

Study design

The main goal of the present thesis was to assess by reliable biomarkers the potential effects on disease progression and MN protection of new therapeutic approaches in the SOD1^{G93A} mouse model of ALS. Here, we show a summary of the performed studies to facilitate understanding of the following chapters.

Chapter I: SOD1^{G93A} mouse model characterization

The fist chapter of this thesis focused on the characterization of the SOD1^{G93A} mouse model of ALS in order to develop reliable, objective tools for assessing disease onset and progression, and evaluating new potential treatments.

Electrophysiological characterization

We first made a detailed characterization of the SOD1^{G93A} mice by using electrophysiological tests, since they are the most important tool for monitoring disease progression in ALS patients. We found that alterations of lower MN function were evident from 8 weeks of age whereas concomitant upper MN abnormalities appeared at 12 weeks of age.

Evaluation of gait alterations

Then, we focused on the characterization of SOD1^{G93A} mice locomotion in order to evaluate whether alterations of both lower and upper MNs were translated into locomotor abnormalities. We performed a detailed locomotor assessment by means of a computerized system in which mouse gait was recorded, digitized and analyzed. Using this approach we found that first gait alterations were evident from 8 weeks of age, correlating with the first signs of lower MNs dysfunction.

Predictive value of electrophysiological tests

Following the electrophysiological and locomotor characterization, we focused on whether pre-symptomatic electrophysiological results were able of predict clinical disease onset and survival in SOD1^{G93A} ALS mice. We found that pre-symptomatic electrophysiological tests are accurate in differentiating transgenic vs. non-transgenic animals and can predict both clinical disease onset and survival.

Differences in disease progression depending on the genetic background of SOD1^{G93A} mice

Finally, we performed a proof of concept assessing whether electrophysiological and locomotion tests were able to discriminate differences on disease onset and progression in SOD1^{G93A} animals bread from distinct strains. The results revealed that although both strains have similar locomotor impairments in rotarod from 12 weeks of age, motor nerve conduction tests showed a quite different disease progression. Whereas muscle denervation began 2 weeks earlier in B6 than in B6SJL mice, disease progression was more pronounced in the latter strain leading to a reduced lifespan. Thereby, genetic background is an important factor determining disease onset and progression, and electrophysiological tests are a useful tool to discriminate even minor differences in the course of MND models.

Chapter II: Sigma-1 receptor agonist treatment

Once demonstrated that electrophysiological and locomotion tests were appropriate for assessing disease progression in SOD1^{G93A} ALS mice, we developed a first therapeutic approached based on the manipulation of the Sigma-1 receptor (Sigma-1R). Previous studies from our laboratory revealed that the sigma-1 receptor agonist PRE-084, produced neuroprotective effect of MNs both *in vitro* (after excitotoxic insult) and *in vivo* (after spinal root avulsion). PRE-084 administration in SOD1^{G93A} mice from 8 weeks of age significantly preserved lower MN function and extended animal survival. Further analyses led us to hypothesize that PRE-084 promoted neuroprotection by modulating the NMDA receptor function and reducing microglial reactivity.

Chapter III: Resveratrol treatment

Secondly, we evaluated a therapeutic approach based on the administration of a resveratrol (RSV) enriched-diet. Our results revealed that resveratrol promoted significant preservation of both upper and lower MN function accompanied by survival extension and reduced spinal MN degeneration. In this case, we hypothesized that resveratrol was acting through the activation of sirtuin 1 and AMPK leading ultimately to a normalization of autophagy and enhanced mitochondrial biogenesis.

Chapter IV: Combinatory PRE-084 + resveratrol treatment

The final step was to combine both Sigma-1R modulation and RSV administration in SOD1^{G93A} mice. Although we found a significant preservation of lower MN function, survival extension and reduction of spinal MN degeneration after the combinatorial treatment, these effects were not enhanced compared to single treatments. Although in the previous chapters we hypothesized that PRE-084 and RSV were acting through independent molecular pathways, the lack of synergistic effect of the combined administration pointed to possible overlapping. In this chapter we also raised the possibility of a limited therapeutic opportunity in SOD1^{G93A} mice as a potential explanation of the lack of effect of the combinatorial therapy.

Chapter I: SOD1^{G93A} mouse model characterization

1.1. Electrophysiological analysis of a murine model of motoneuron disease

Mancuso R, Santos-Nogueira E, Osta R, Navarro X. Electrophysiological analysis of a murine model of motoneuron disease. Clin Neurophysiol 2011, 122:1660-1670.

Clinical Neurophysiology 122 (2011) 1660–1670

Contents lists available at ScienceDirect

Clinical Neurophysiology

journal homepage: www.elsevier.com/locate/clinph

Electrophysiological analysis of a murine model of motoneuron disease

Renzo Mancuso [a], Eva Santos-Nogueira [a], Rosario Osta [b], Xavier Navarro [a,*]

[a] Group of Neuroplasticity and Regeneration, Institute of Neurosciences and Department of Cell Biology, Physiology and Immunology, Universitat Autònoma de Barcelona, and Centro de Investigación Biomédica en Red sobre Enfermedades Neurodegenerativas (CIBERNED), E-08193 Bellaterra, Spain
[b] Laboratory of Genetic Biochemistry (LAGENBIO-I3A), Veterinary Faculty, Aragon Institute of Health Sciences, Universidad de Zaragoza, Zaragoza, Spain

ARTICLE INFO

Article history:
Accepted 31 January 2011
Available online 25 February 2011

Keywords:
Electrophysiology
Motoneuron disease
Motor unit
Nerve conduction
Neurodegeneration

HIGHLIGHTS

- Electrophysiological tests for peripheral and central conduction are useful to evaluate the early detection and the temporal progression of motor dysfunction in the SOD1 transgenic mouse model.
- Motor evoked potentials revealed early abnormalities in central motor pathways.
- Motor nerve conduction tests revealed very early abnormalities in peripheral motor conduction.

ABSTRACT

Objective: Amyotrophic lateral sclerosis (ALS) is a fatal neurodegenerative disease characterized by loss of motoneurons of the primary motor cortex, the brainstem and the spinal cord, for which there are not effective treatments. Several transgenic mice that mimic motoneuron disease have been used to investigate potential treatments. The objective of this work is to characterize electrophysiologically the $SOD1^{G93A}$ transgenic mouse model of ALS, and to provide useful markers to improve early detection and monitoring of progression of the disease.
Methods: We performed nerve conduction tests, motor unit number estimation (MUNE), H reflex tests and motor evoked potentials (MEPs) in a cohort of transgenic and wild type mice from 4 to 16 weeks of age.
Results: The results revealed dysfunction of spinal motoneurons evidenced by deficits in motor nerve conduction tests starting at 8 weeks of age, earlier in proximal than in distal muscles of the hindlimb. MUNE demonstrated that spinal motoneurons loss muscle innervation and have a deficit in their sprouting capacity. Motor evoked potentials revealed that, coexisting with peripheral deficits, there was a dysfunction of central motor tracts that started also at 8 weeks, indicating progressive dysfunction of upper motoneurons.
Conclusions: These electrophysiological results provide important information about the $SOD1^{G93A}$ mouse model, as they demonstrate by the first time alterations of central motor pathways simultaneously to lower motoneuron dysfunction, well before functional abnormalities appear (by 12 weeks of age).
Significance: The finding of concomitant dysfunction of upper and lower motoneurons contributes to the validation of the $SOD1^{G93A}$ mouse as model of ALS, because this parallel involvement is a diagnostic condition for ALS. Electrophysiological tests can be used as early markers of the disease and to evaluate the potential benefits of new treatments on both upper and lower motoneurons.

1. Introduction

Motoneuron diseases are progressive neurodegenerative disorders characterized by the loss of upper and/or lower motoneurons (MN). Amyotrophic lateral sclerosis (ALS) is the most common form of MN disease and it differs from others because of the degeneration involves both upper and lower MN. Clinically, ALS is manifested as weakness, muscle atrophy and progressive paralysis and finishes with patient's death 2–5 years after diagnosis (Wijesekera and Leigh 2009; Worms 2001). No satisfactory treatment is presently available for ALS. Despite numerous therapeutic trials have been attempted, the only drug approved by the FDA for the treatment of ALS is riluzole, with limited therapeutic benefits of about 3–4 months survival increase (Ludolph and Jesse 2009). One of the problems of ALS is the delay in diagnosis, mainly because the initial symptoms mimic other spinal cord diseases, neuropathies and neurological syndromes (Kraemer et al., 2010). With the advent of possible new therapies for ALS, there is an increasing need for early diagnosis, because probably early therapies will produce better results.

* Corresponding author. Address: Unitat de Fisiologia Mèdica, Facultat de Medicina, Universitat Autònoma de Barcelona, E-08193 Bellaterra, Spain. Tel.: +34 935811966; fax: +34 935812986.
E-mail address: xavier.navarro@uab.cat (X. Navarro).

1388-2457/$36.00
doi:10.1016/j.clinph.2011.01.045

The development of transgenic animal models carrying genetic mutations described in familiar ALS cases has facilitated the study of ALS. The most widely used is a transgenic mouse with a glycine to alanine conversion at the 93rd codon of the SOD1 gene in high copy number ($SOD1^{G93A}$) (Ripps et al., 1995). These mice develop a rapidly progressive motoneuron degeneration, which leads to locomotor deficits starting at 12–13 weeks and ending up with hindlimb paralysis at 16 weeks and death around 17–19 weeks of age (Gurney et al., 1994; Miana-Mena et al., 2005, Turner and Talbot 2008). This phenotype recapitulates several clinical and histopathological features of both familial and sporadic forms of the human disease (Ripps et al., 1995). Although animal models carrying SOD1 mutations have been developed based on familial cases of ALS and their validity has been questioned, especially after the development of new models based on mutations in the TDP-43 protein (Wegorzewska et al., 2009), it has been recently found that alterations of SOD1 protein are also related to sporadic ALS cases (Bosco et al., 2010), thus, increasing the interest in the study of these transgenic animals.

Electrophysiological tests are fundamental for diagnosis and progression monitoring of patients suffering MN diseases (Mitsumoto et al., 2007; de Carvalho et al., 2008; Wijesekera and Leigh 2009; Krarup 2010). Several authors have used these techniques on the $SOD1^{G93A}$ model but, in most cases, only focusing on the analysis of lower MN function (Kennel et al., 1996; Azzouz et al., 1997; Shefner et al., 2006) and on several occasions using methods that do not allow a time follow-up of the same animal (Hegedus et al., 2007, 2008). The objective of this work is to provide a detailed electrophysiological characterization of the $SOD1^{G93A}$ transgenic mouse model of ALS. Lower and upper MN function was evaluated from early pre-symptomatic (4 weeks) to end stage of the disease (16 weeks) by means of nerve conduction and evoked potential tests. The advantages of electrophysiological tests compared to behavioral and histological methods are established for the early detection and evaluation of disease progression in this animal model. We have previously used the electrophysiology tests to assess peripheral nerve function in neuropathic diseases (Verdú et al., 1999; Bruna et al., 2010) and after nerve trauma (Navarro et al., 1994; Udina et al., 2003) in small laboratory animals, showing that these methods can reliably help in the early detection and quantitation of loss or recovery of motor and sensory functions (Navarro and Udina 2009).

2. Materials and methods

2.1. Transgenic mice

Transgenic mice with the G93A human SOD1 mutation (B6SJL-Tg[SOD1-G93A]1Gur) were obtained from The Jackson Laboratory (Bar Harbor, ME, USA), and provided from the colony maintained at the Animal Service of the Universidad de Zaragoza. Hemizygotes were maintained by breeding $SOD1^{G93A}$ males with female littermates. The offspring was identified by PCR amplification of DNA extracted from the tail tissue. All experimental procedures were approved by the Ethics Committee of the Universitat Autònoma de Barcelona. Rotarod and nerve conduction tests were performed comparing female SOD1 and wild type mice with 25 animals in each group, while motor unit number estimation (MUNE) was performed in subgroups of 10 mice.

2.2. Rotarod test

Rotarod test was performed to evaluate motor coordination, strength and balance of the animals (Miana-Mena et al., 2005), and to establish the onset of symptomatic disease. Mice were placed onto the rod rotating at a constant speed of 14 rpm (rotating cylinder 3.4 cm in diameter). The time for which each animal could remain on the rotating rod was measured. Each animal was given three trials and the longest latency without falling was recorded; 180 s was chosen as the arbitrary cut-off time. Rotarod was tested weekly from 4 to 16 weeks of age.

2.3. Nerve conduction tests

For motor nerve conduction tests, the sciatic nerve was stimulated percutaneously by means of single pulses of 0.02 ms duration (Grass S88) delivered through a pair of needle electrodes placed at the sciatic notch. The compound muscle action potential (CMAP, M wave) and the reflex H wave were recorded from the tibialis anterior (TA) and the plantar (interossei) muscles with microneedle electrodes (Navarro et al., 1994; Udina et al., 2003; Navarro and Udina 2009). The amplitude of the maximal M and H waves were measured, and the H/M amplitude ratio was calculated for assessment of spinal reflex function (Valero-Cabré and Navarro 2001). For evaluation of the motor central pathways, motor evoked potentials (MEP) were recorded from the TA and plantar muscles in response to transcranial electrical stimulation of the motor cortex by single rectangular pulses of 0.1 ms duration, delivered through needle electrodes inserted subcutaneously, the cathode over the skull overlaying the sensorimotor cortex and the anode at the nose (Garcia-Alias et al., 2003). For sensory nerve conduction tests, the recording electrodes were placed near the digital nerves of the fourth toe to record the compound sensory nerve action potential (CNAP) following stimulation of the sciatic nerve as above.

All potentials were amplified and displayed on a digital oscilloscope (Tektronix 450S) at settings appropriate to measure the amplitude from baseline to the maximal negative peak and the latency from stimulus to the onset of the first negative deflection, to the maximal negative peak and to the end of the wave. To ensure reproducibility, the recording needles were placed under microscope to secure the same placement on all animals guided by anatomical landmarks. During the tests, the mice body temperature was kept constant between 34–36 °C by means of a thermostated heating pad.

2.4. Motor unit number estimation

For motor unit number estimation (MUNE) a subset of 10 female SOD1 mice and their respective wild type littermates were used. The setting was the same as for the motor nerve conduction tests. The protocol used consisted in the incremental technique (Shefner et al., 2002; Lago et al., 2007). Starting from subthreshold intensity, the sciatic nerve was stimulated with single pulses of gradually increased intensity until the first response appeared, representing the first motor unit recruited. With the next stimuli, quantal increases in the response were recorded. Increments >50 μV were considered like the recruitment of an additional motor unit. The amplitude of a single motor unit was calculated as the mean of ~15 consistent increases. The estimated number of motor units results from the equation: MUNE = CMAP maximal amplitude/mean amplitude of single motor unit action potentials.

Inherent to this technique is a problem called "alternation", in which a difference in the amplitude of the CMAP could be due to a different combination of already recruited motor units rather than to the recruitment of a new motor unit. The influence of alternation on the MUNE causes the number of motor units to be overestimated (Arasaki et al., 1997). In order to minimize the effect of the "alternation" phenomenon only the increases >50 μV in the amplitude of the CMAP were considered as representing recruitment of a new motor unit. Moreover, MUNE of SOD1 animals is always referred to age matched control mice, evaluated in parallel,

so that an overestimation should not have an effect on the comparative results.

2.5. Histology

Subgroups of four mice were perfused with 4% paraformaldehyde in PBS at 4, 8, 12 or 16 weeks of age. The lumbar segment of the spinal cord was removed, post-fixed for 24 h, and cryopreserved in 30% sucrose. Transverse 40-μm thick sections were serially cut with a cryotome (Leica) at L2, L3 and L4 segmental levels. For each segment, each section of a series of 10 was collected sequentially on separate gelatin-coated slides. One slide was rehydrated for 1 min and stained for 2 h with an acidified solution of 3.1 mM cresyl violet. Then, the slides were washed in distilled water for 1 min, dehydrated and mounted with DPX (Fluka). MNs were identified by their localization in the ventral horn of the stained spinal cord sections and counted following strict size and morphological criteria: only MNs with diameters larger than 20 μm and with polygonal shape and prominent nucleoli were counted. The number of MNs present in both ventral horns was counted in four serial sections of each L2 and L4 segments (Penas et al., 2009).

2.6. Statistical analysis

All electrophysiological measurements were analyzed with repeated measurements ANOVA, applying Bonferroni post hoc test when necessary. Histological data was analyzed using Mann-Withney non-parametric test for each age group. Linear regression tests were used for correlation analysis between variables.

3. Results

3.1. Rotarod test

Rotarod test was performed to evaluate the locomotion capability of the animals and to determine the beginning of the symptomatic phase of the disease. The results showed differences between transgenic and wild type mice. The performance of the SOD1 mice started to decline between 12 and 13 weeks of age, and continued decreasing until the end stage of the disease, when the animals were paralyzed (Fig. 1). Control animals performance was maintained in 180s during all the follow-up.

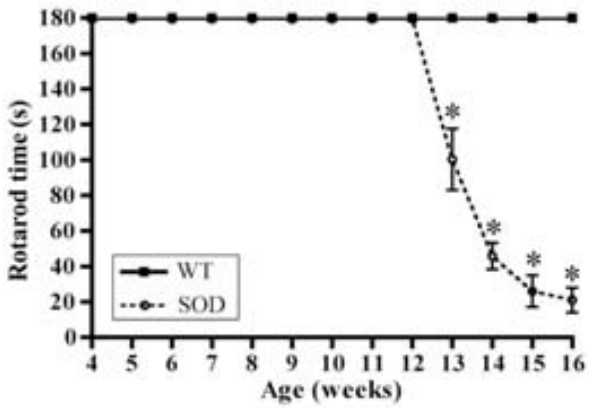

Fig. 1. Rotarod test was used to assess motor function, coordination and strength. The transgenic SOD1 mice performance declined from 12–13 weeks of age. Wild type mice maintained permanence in the rotarod during 180 s during all the follow up. Values are mean ± SEM; *$p < 0.05$ vs. wild type mice.

3.2. Motor nerve conduction

Motor nerve conduction test was performed to evaluate lower MNs function, by monitoring their capacity to transmit signals from the spinal cord to the hindlimb muscles. The results showed a progressive functional loss following a slightly different pattern depending on the muscle tested. The degree of neuromuscular functional innervation, assessed by the amplitude of the M wave, was significantly reduced at 12 weeks in the plantar muscle, evidenced by a 60–70% reduction in M wave amplitude, whereas in the TA muscle it started to decline earlier, at 8 weeks, when the M wave amplitude was 75% of control values (Table 1). Fibrillation potentials, indicative of muscle denervation, were detected at 8 weeks in the TA muscle, were moderately abundant at 12 weeks and increased at 16 weeks in both muscles tested. Fig. 2 shows representative recordings of CMAPs of plantar and TA muscles of wild type and SOD1 mice. The denervation of both muscles progressed with a different slope: the M wave showed a marked drop between 8 and 12 weeks in the plantar muscle, and a steadier decline in the TA muscle. At 16 weeks, the M wave amplitude for both muscles averaged about 25–30% of normal values (Table 1). Electrophysiological analysis also demonstrated slowing of motor nerve fibers conduction starting at 12 weeks in both plantar and TA muscles. The latency to the onset of the M wave, reflecting the conduction time of the largest motor fibers, showed slowing of 20–30% at 12 and 16 weeks in both muscles (Table 1). In contrast, the M wave duration was only significantly increased in the distal plantar muscle, suggesting also slowing in conduction of the small motor fibers (Table 1).

3.3. Sensory nerve conduction

Sensory nerve conduction tests were performed as a control, considering that ALS does not affect the sensory system. The electrophysiological recordings did not show any significant difference neither in the amplitude nor in the latency of the CNAP recorded from the digital nerves in the toes of SOD1 mice compared with wild type mice (Table 1). However, the latency showed a slight, not significant increase of about 10% in SOD1 animals at 12 and 16 weeks (Table 1).

3.4. Spinal motor reflexes

To evaluate the functional state of the spinal cord motor reflexes, the H/M ratio was calculated in the motor nerve conduction tests performed (Fig. 2). In the TA muscle at 12 weeks there was a slight increase of the H/M ratio with respect to control values that progressed to a large increase of almost 8-fold at 16 weeks (Table 1). In the plantar muscle, the H/M ratio of SOD1 mice was maintained similar to normal values until 16 weeks, when it showed an increase of 50% (Table 1).

3.5. Motor evoked potentials

The conduction of central motor pathways was tested to evaluate potential dysfunction of the descending corticospinal and brainstem-spinal tracts and, thus, of the upper MNs in the SOD1 transgenic mice. Fig. 3 shows representative recordings of MEPs. The results obtained from the TA muscle showed a marked decrease of the MEP amplitude of 40% as early as 8 weeks of age, well before the symptomatic phase started (Table 2). The mean MEP amplitude showed an important decline to about 15% of control values by 16 weeks of age. The MEP latency started to increase significantly at 12 weeks, as evidenced by an increment of 35% with respect to wild-type mice (Table 2). In contrast, the results obtained from plantar muscles showed a decline of both MEP latency and amplitude from 12 weeks of age.

Table 1
Electrophysiological results of peripheral nerve conduction comparing SOD1 and wild type (WT) mice at 4, 8, 12 and 16 weeks of age.

		4 weeks		8 weeks		12 weeks		16 weeks	
		WT (n = 14)	SOD (n = 14)	WT (n = 14)	SOD (n = 22)	WT (n = 21)	SOD (n = 22)	WT (n = 16)	SOD (n = 22)
Tibialis ant muscle	Latency (ms)	0.91 ± 0.02	0.92 ± 0.01	0.91 ± 0.02	0.95 ± 0.02	0.89 ± 0.02	1.06 ± 0.02*	0.86 ± 0.03	1.07 ± 0.03*
	Dur CMAP (ms)	1.35 ± 0.06	1.46 ± 0.03	1.42 ± 0.05	1.46 ± 0.02	1.50 ± 0.04	1.57 ± 0.03	1.41 ± 0.04	1.60 ± 0.08
	Amp CMAP (mV)	47.2 ± 2.54	53.0 ± 2.03	52.8 ± 2.47	38.9 ± 2.69*	52.6 ± 1.23	29.8 ± 2.79*	50.6 ± 2.90	13.2 ± 1.62*
	H/M ratio (%)	2.81 ± 0.27	2.39 ± 0.21	3.70 ± 0.90	2.98 ± 0.47	3.16 ± 0.38	4.91 ± 0.81	3.69 ± 0.62	11.3 ± 1.49*
Plantar muscle	Latency (ms)	1.73 ± 0.02	1.73 ± 0.02	1.85 ± 0.07	1.83 ± 0.04	1.70 ± 0.03	2.14 ± 0.06*	1.64 ± 0.07	2.09 ± 0.09*
	Dur CMAP (ms)	1.04 ± 0.06	1.11 ± 0.03	0.98 ± 0.03	1.0 ± 0.04	1.01 ± 0.03	1.49 ± 0.10*	0.96 ± 0.04	1.51 ± 0.19*
	Amp CMAP (mV)	6.58 ± 0.45	6.74 ± 0.42	6.48 ± 0.37	5.99 ± 0.49	6.86 ± 0.43	2.46 ± 0.28*	6.54 ± 0.65	1.93 ± 0.42*
	H/M ratio (%)	14.4 ± 3.32	12.0 ± 1.39	16.5 ± 2.95	17.5 ± 2.25	15.45 ± 2.03	12.0 ± 2.34	18.3 ± 3.18	27.2 ± 6.46*
Digital nerve	Latency (ms)	1.21 ± 0.02	1.19 ± 0.02	1.16 ± 0.04	1.13 ± 0.02	1.08 ± 0.02	1.18 ± 0.03	1.00 ± 0.03	1.07 ± 0.02
	Amp CNAP (μV)	54.2 ± 3.37	50.7 ± 4.3	50.4 ± 3.99	47.6 ± 2.65	47.0 ± 2.73	49.7 ± 2.29	47.9 ± 2.93	49.2 ± 2.66

CMAP, compound muscle action potential; CNAP, compound nerve action potential; Dur, duration; Amp, amplitude.
* $p < 0.05$ vs. wild type group.

To ascertain the involvement of central versus peripheral motor pathways, the MEP/M amplitude ratio and the MEP-M latency were calculated. For the TA muscle, there was a progressive decrease of the MEP/M ratio in SOD1 mice compared with wild type mice. The decline started at 8 weeks when the ratio was 22.5 ± 1.9%, about 80% of control values, and became significant at 12 and 16 weeks with ratios decreased to 15.4 ± 1.6% and 13.5 ± 2.4%, about 55% and 45% of control values, respectively (Table 2). The MEP-M difference latency showed a mild increase of central conduction time at 8 and 12 weeks, and marked at 16 weeks, being about 60% higher with respect to controls (Table 2). In the case of the plantar muscle, the MEP-M latency was significantly increased only at 16 weeks, when it was more than 100% higher than control values (Table 2).

3.6. Motor unit number estimation

The estimation of the number of functioning motor units (MUNE) was performed in a subset of animals as an indirect evidence of the survival of spinal MNs. The motor unit number started to decline significantly in SOD1 mice at 8 weeks in the TA muscle (176 ± 16 vs. 218 ± 13 motor units) and at 12 weeks in the plantar muscle (12 ± 2 vs. 31 ± 2 motor units). Disease progression resulted in a marked drop of the MUNE between 8 and 12 weeks that was more severe in the plantar than in the TA muscle, reaching 40% and 50% of control values, respectively. At 16 weeks, there were about 35% of functioning motor units compared with wild type mice in both muscles (Fig. 4).

The mean amplitude of single motor units in SOD1 mice showed a significant reduction compared with wild type mice, both in plantar and TA muscles (Fig. 4E and F). In the plantar muscle, the amplitude reduction started at 12 weeks (0.19 ± 0.02 vs. 0.24 ± 0.02 mV) and progressed until 16 weeks (0.15 ± 0.02 vs. 0.22 ± 0.02 mV), whereas in the TA muscle the decline became significant only at 16 weeks (0.17 ± 0.01 vs. 0.22 ± 0.01 mV).

The motor nerve conductions tests performed in this subgroup of animals revealed an evident decrease in the amplitude of the CMAP of plantar and TA muscles, which followed a similar trend that for the whole group of mice. Thus, the M wave amplitude started to decline at 8 weeks in the TA muscle (39.0 ± 4.4 vs. 51.1 ± 1.6 mV in wild type mice; 25% decrease), and at 12 weeks in the plantar muscle (2.26 ± 0.48 vs. 7.61 ± 0.48 mV; 30% decrease) (Fig. 5A and B). There was a significant linear regression between the MUNE and the M wave amplitude for both plantar and TA muscles (Fig. 5C and D).

3.7. Motoneuron loss

The extent of MN degeneration was determined by counting the number of stained MN soma in the ventral horns of lumbar spinal cord sections of wild type and SOD1 mice of 8, 12 and 16 weeks of age. The lumbar segments analyzed were L2 and L4, in which the TA and the plantar muscles motor nuclei are represented (McHanwell and Biscoe 1981). In all the sections, MN counts were made for the lateral (innervating hindlimb muscles) and the medial (innervating axial muscles) areas of the ventral horn lamina IX. Neurons smaller than 20 μm in diameter were excluded from counting, even if they could be atrophic MNs because they were unlikely to be functional.

The first pathological observation in SOD1 mice spinal cord was the appearance of MN degeneration evidenced by cytoplasm vacuolization and attenuation of the Nissl bodies staining (Fig. 6A). Fig. 6B shows representative microphotographs of L4 and L2 ventral horns from wild type and SOD1 mice at 12 weeks and 16 weeks of age. The number of lateral MNs started to decline at 12 weeks at both L2 and L4 segments, with a loss of approximately 25% compared to wild type mice. MN degeneration progressed at 16 weeks, when the surviving MNs were only 50% in both segments (Fig. 6C). The number of medial MNs did not show differences at 8 and 12 weeks compared with wild type animals, but it was reduced at 16 weeks to about 70% of controls for the two spinal segments (Fig. 6C).

4. Discussion

The results of the electrophysiological tests performed provide important information about the SOD1^{G93A} transgenic mouse animal model, as they demonstrate for the first time that dysfunction of central motor pathways is coexisting with peripheral motor deficits, and both are detected well before the loss of spinal motoneuron cell bodies or the first functional evidences appear (by 12 weeks of age). The results of this study show dysfunction of the lower MNs that progress from proximal to distal muscles, evidenced by a deficit in motor nerve conduction from 8 weeks of age. Moreover, the MUNE demonstrated that lower MNs lose muscle innervation and had a deficit in their sprouting capacity. The study of the MEPs showed that, in parallel to peripheral deficits, there is a dysfunction in central motor conduction in SOD1 mice starting also at 8 weeks. The finding of a concomitant dysfunction of upper and lower MN contributes to the validation of the SOD1^{G93A} mouse as a useful model of ALS, because this double contribution is an essential condition for ALS diagnosis in patients. Electrophysiological tests can be used as early markers of the disease and to evaluate new treatments and their potential beneficial effects both for upper and lower MN manifestations.

4.1. Lower motoneuron contribution to motor dysfunction

Motor nerve conduction and electromyography tests are widely used to analyze lower MN function in ALS patients, and may reveal

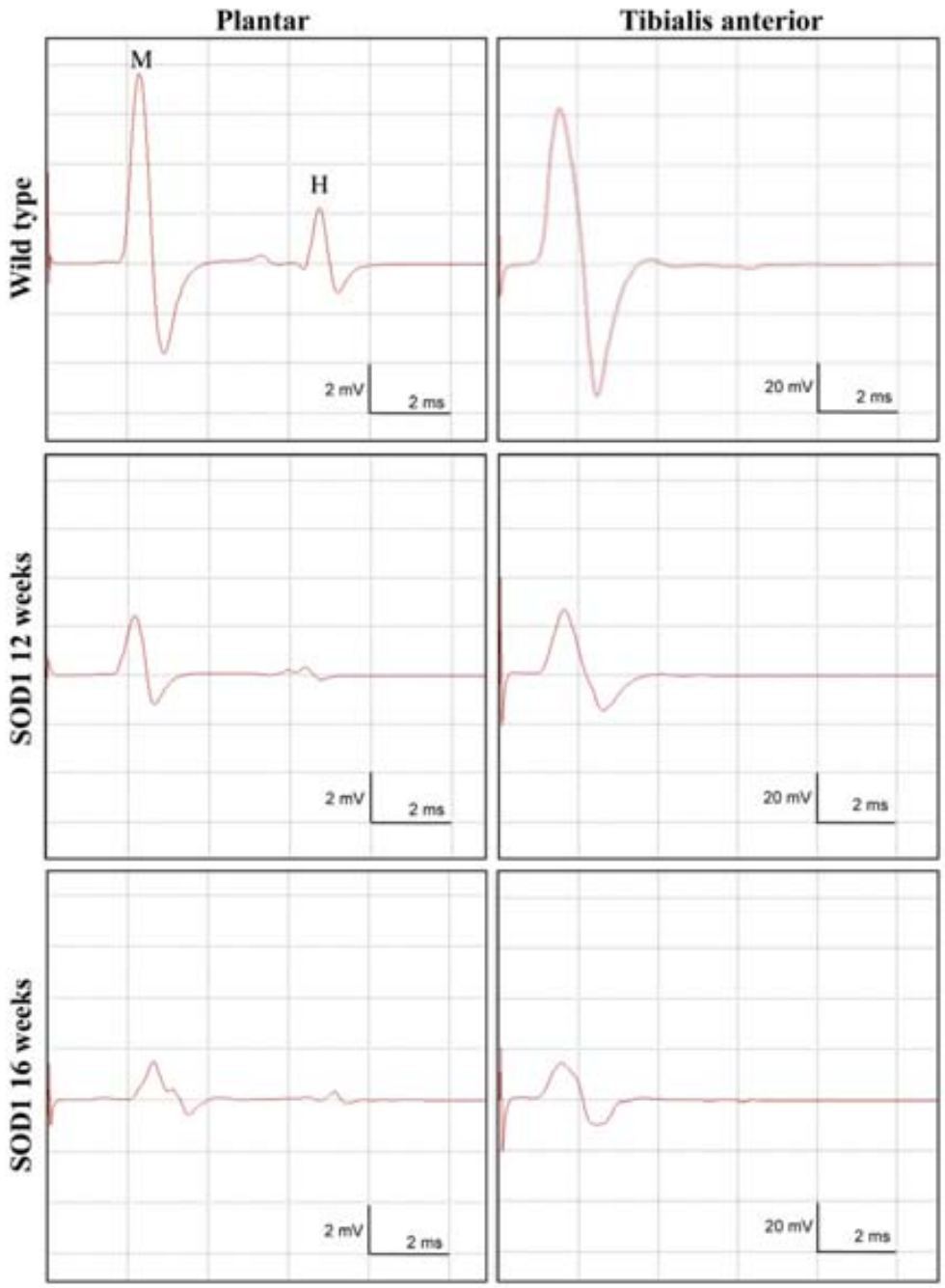

Fig. 2. Representative recordings of CMAPs from plantar and tibialis anterior muscles in wild type and SOD1 animals at 12 and 16 weeks of age. The CMAP recordings present two waveforms: the M wave, pointed by an "M", and the late H reflex response, pointed by an "H". Note the marked decline of the amplitude and the slight increase of the latency of the M wave in SOD1 mice. There is also an increased duration of the M wave in SOD1 animals at 16 weeks of age, demonstrating involvement of all types of motor units.

involvement in clinically silent muscles (Krarup 2010; Wijesekera and Leigh 2009). These techniques have been also applied to evaluate motor function in animal models, such as the SOD1 transgenic mouse (Kennel et al., 1996; Azzouz et al., 1997; Shefner et al., 2006). Kennel et al. (1996) reported the earliest significant decrement in CMAP and loss of motor units in the gastrocnemius muscle of SOD1^{G93A} mice at 47 days of age, which progressed linearly until end-stage disease. Yet with the same methodology from the same muscle, Azzouz et al. (1997) reported a biphasic decline of the CMAP and motor unit number, with a slow decline between 60 and 100 days of age followed by a faster loss. By using surface electrodes to record from all hindlimb muscles simultaneously, Shefner et al. (1999, 2002) found that the CMAP begins to rapidly decline at ~60 days of age, concomitantly with a loss of functional

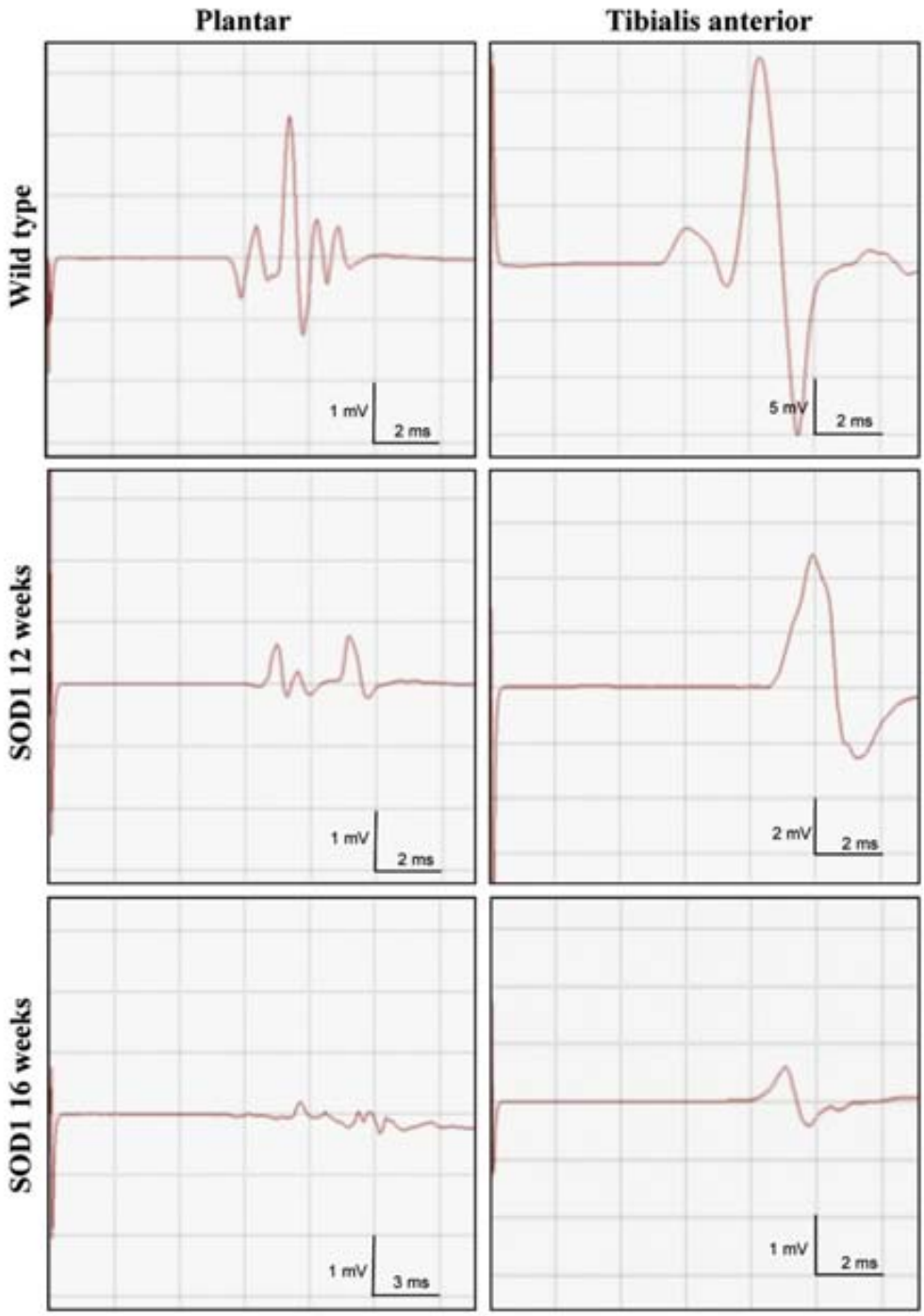

Fig. 3. Representative recordings of MEPs from plantar and tibialis anterior muscles in wild type and SOD1 animals at 12 and 16 weeks of age. Note the marked decline of the amplitude and the slight increase of the latency in SOD1 mice.

motor units. Using more sophisticated and time consuming technique Boërio et al. (2010) have also demonstrated that SOD1^{G93A} mice show abnormalities in axonal excitability that start between 8–10 weeks and stabilize by 11–13 weeks; although these findings do not provide direct information about the loss of lower MN function, they contribute to the understanding of mechanisms that could be altered in the degenerating MN. One of the aims of this study was to provide novel information of the disease course by combining electrophysiological evaluation of TA and plantar muscles from the same animals, during all their life span. Our results showed that, despite human ALS and the SOD1 mice usually present clinical symptoms from distal to proximal muscles (Brown 1995), the first signs of muscle denervation were observed in the TA muscle rather than in the more distal plantar muscles, as

Table 2
Electrophysiological results of central motor conduction comparing SOD1 and wild type (WT) animals at 4, 8, 12 and 16 weeks of age.

		4 weeks		8 weeks		12 weeks		16 weeks	
		WT (n = 14)	SOD (n = 14)	WT (n = 14)	SOD (n = 22)	WT (n = 21)	SOD (n = 22)	WT (n = 16)	SOD (n = 22)
Tibialis ant muscle	Latency MEP (ms)	4.70 ± 0.18	5.06 ± 0.12	4.54 ± 0.31	5.64 ± 0.41	4.38 ± 0.21	5.77 ± 0.37*	4.29 ± 0.26	8.58 ± 0.80*
	Amp MEP (ms)	17.7 ± 1.78	19.0 ± 1.56	14.7 ± 2.21	8.97 ± 1.06*	14.3 ± 1.67	4.84 ± 0.82*	13.4 ± 1.66	1.37 ± 0.21*
	MEP/M ratio (%)	36.2 ± 3.0	36.0 ± 2.84	27.2 ± 3.36	22.5 ± 1.88	27.1 ± 2.93	15.4 ± 1.61*	25.1 ± 2.56	13.5 ± 2.44*
	Latency MEP-M (ms)	3.79 ± 0.18	4.13 ± 0.12	3.62 ± 0.29	4.69 ± 0.40*	3.49 ± 0.22	4.72 ± 0.37*	3.16 ± 0.35	7.53 ± 0.80*
Plantar muscle	Latency MEP (ms)	5.69 ± 0.14	5.81 ± 0.11	5.58 ± 0.03	6.32 ± 0.57	5.37 ± 0.12	6.72 ± 0.23*	4.99 ± 0.14	11.1 ± 1.20*
	Amp MEP (ms)	0.60 ± 0.08	0.56 ± 0.04	0.58 ± 0.09	0.44 ± 0.08	0.75 ± 0.16	0.30 ± 0.05*	0.73 ± 0.15	0.16 ± 0.04*
	MEP/M ratio (%)	8.51 ± 1.46	8.96 ± 0.56	8.96 ± 1.16	8.21 ± 1.48	10.8 ± 1.93	15.6 ± 2.64	11.5 ± 2.42	29.1 ± 9.77
	Latency MEP-M (ms)	3.97 ± 0.14	4.07 ± 0.11	3.72 ± 0.27	4.09 ± 0.57	3.66 ± 0.12	4.19 ± 0.24	3.03 ± 0.34	9.03 ± 1.20*

MEP, motor evoked potential; Amp, amplitude.
* $p < 0.05$ vs. wild type group.

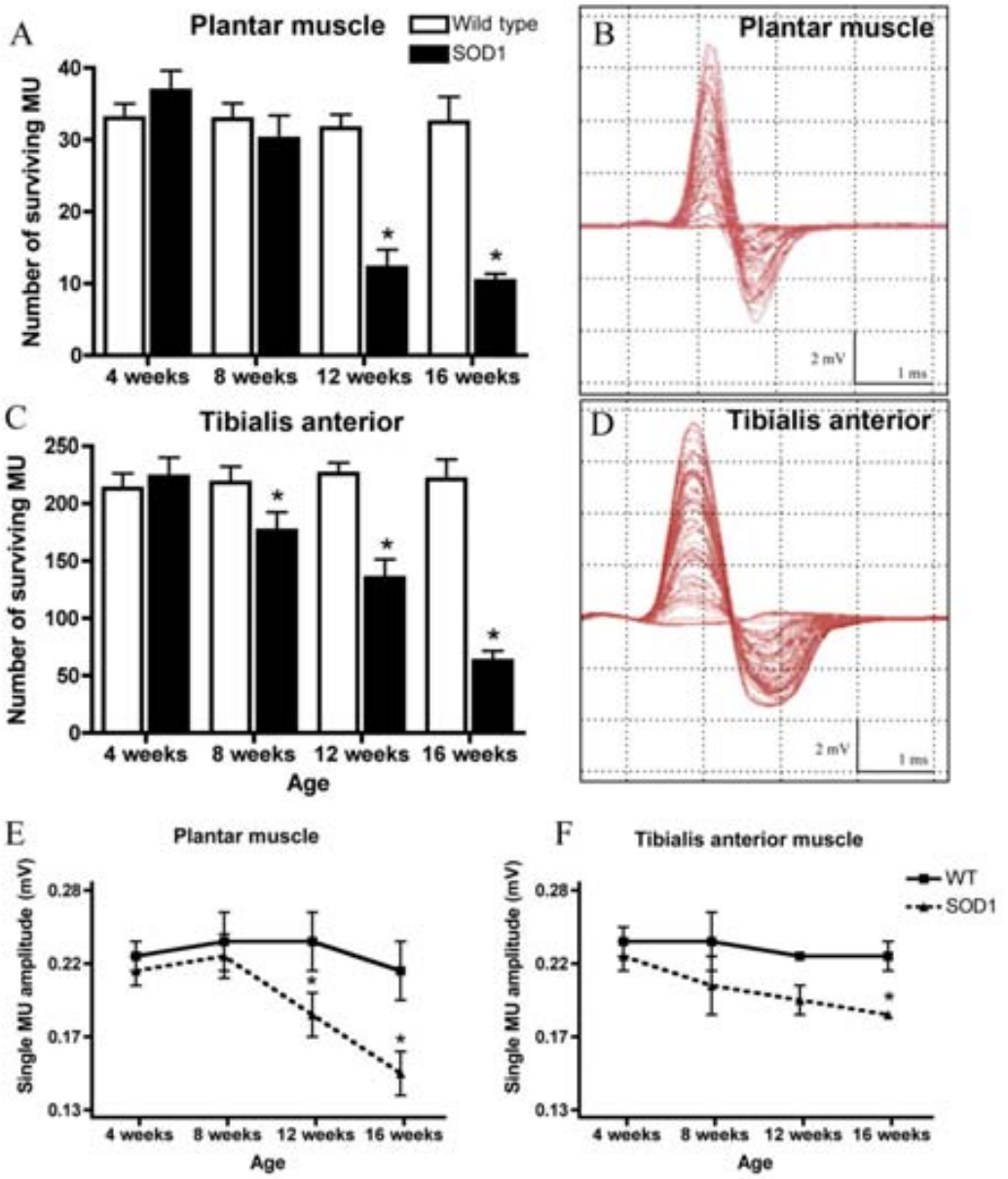

Fig. 4. Evaluation of functional motor units of SOD1 mice. Number of functional motor units (MU) of (A) plantar muscle and (C) tibialis anterior muscle. Representative recordings of motor unit number estimation tests from (B) plantar muscle and (D) tibialis anterior muscle of wild type mice. Mean amplitude of single motor units of SOD1 and wild type mice along follow-up in plantar (E) and tibialis anterior (F) muscles. Values are mean ± SEM; *$p < 0.05$ vs. wild type mice.

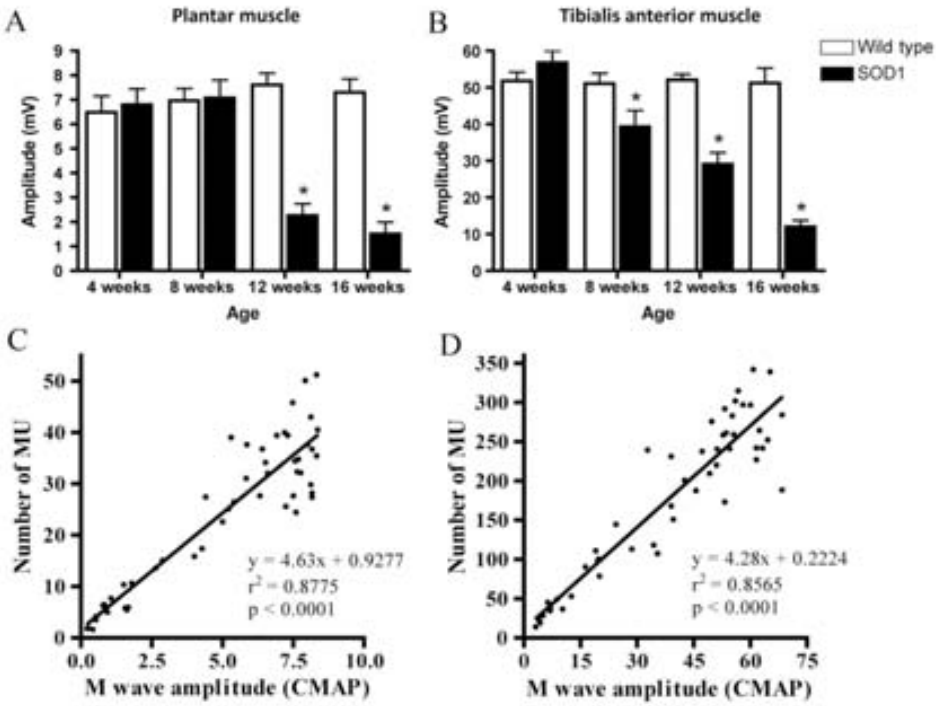

Fig. 5. Amplitude of the M wave of plantar (A) and tibialis anterior (B) muscles obtained in motor nerve conduction tests in the subgroups of mice used for MUNE. Note that the decrease in the CMAP amplitude behaves similarly to the reduction in the number of motor units (see Fig. 4). Values are mean ± SEM; *$p < 0.05$ vs. wild type mice. Significant correlation between the M wave amplitude of the CMAP and the estimated number of motor units (MU) in (C) plantar and (D) tibialis anterior muscles of SOD1 mice.

evidenced by the earlier decrease of M wave amplitude and the more pronounced reduction of number of functioning motor units in the TA muscle at 8 weeks (56 days). Nevertheless, at the beginning of the symptomatic phase by 12 weeks denervation was more pronounced in plantar than in the TA muscle. The CMAP amplitude followed a linear decline in the TA muscle from 4 to 16 weeks of age, whereas in the distal plantar muscle there was a more marked decline from 8 to 12 weeks followed by a mild decrease until 16 weeks of age in the SOD1 mice. The finding of many fibrillation potentials from 12 weeks indicates that an acute ongoing denervation process was taking place (Navarro and Udina 2009). It has been shown that larger (and faster) motor units are the most susceptible to loss in mouse models of ALS (Fischer et al., 2004; Pun et al., 2006) and in human patients (Dengler et al., 1990; Sobue et al., 1983). Considering that TA and plantar muscles have ~90% and ~60% of fast twitch muscle fibers, respectively (Hegedus et al., 2007; Boërio et al., 2010), the especial vulnerability of faster motor units could explain the differences in the onset of manifestations in these two muscles. However, it remains unclear why the TA muscle shows progressive involvement during the disease process while the plantar muscle suffers an acute drop of innervation, with a common final preservation of 25–30% of function by 16 weeks. These findings about progression of motor loss in muscles located at different distance from the spinal cord has not been described before and reveal that, although $SOD1^{G93A}$ mice have been extensively studied, we still need deeper knowledge that may lead to a better understanding of the disease process.

Although the electrophysiological results show clear functional deficits from 8 weeks, the locomotor tests demonstrate that symptoms begin between 12 and 13 weeks, when SOD1 mice start to decline in the rotarod performance, as well as in other strength tests (Miana-Mena et al., 2005; Moreno-Igoa et al., 2010). This means that the animals are able to perform the locomotion tests even if they do not have full motor innervation, and that behavioral symptoms become evident when motor nerve function declines below a critical value, estimated in approximately 50% reduction of the M wave of TA and gastrocnemius (Kennel et al., 1996) muscles.

The histological results indicate that degeneration and loss of spinal MNs follow with delay the abnormalities in motor nerve conduction tests, but are more coincident with locomotion deficits in SOD1 mice. In fact, the first MN cell bodies that degenerate in the spinal cord are those located in the lateral portion of the anterior horn, which are those that innervate hindlimb muscles, whereas MNs in the medial portion that innervate axial muscles are smaller in size and presumably more resistant to the disease (Pun et al., 2006; Hegedus et al., 2008). The decrease in motor unit number before motoneuron loss in the spinal cord is the result of axonal lesion likely taking place distally by detachment at neuromuscular synaptic sites. Analysis of the neuromuscular junction showed that denervation of end-plates was significant by ~7 weeks, and continued to progress until the end stage of the disease (Fischer et al., 2004). These findings agree with the CMAP reduction we observed from 8 weeks in the TA muscle.

It has been noticed in previous studies that large MNs are more vulnerable to disease progression than the small ones (Frey et al., 2000; Pun et al., 2006). These observations are partially supported by our electrophysiological results. First, the large decrease of the M wave amplitude with a comparatively less reduction in number of MNs suggests predominant loss of large motor units. Second, in the TA muscle there was more marked slowing in the initial latency than in the final latency of the CMAP (see Fig. 2B and C), pointing to earlier involvement of the larger (and faster) motor units. According with what happens in ALS patients (Wijesekera and Leigh 2009), sensory nerve conduction was not affected in

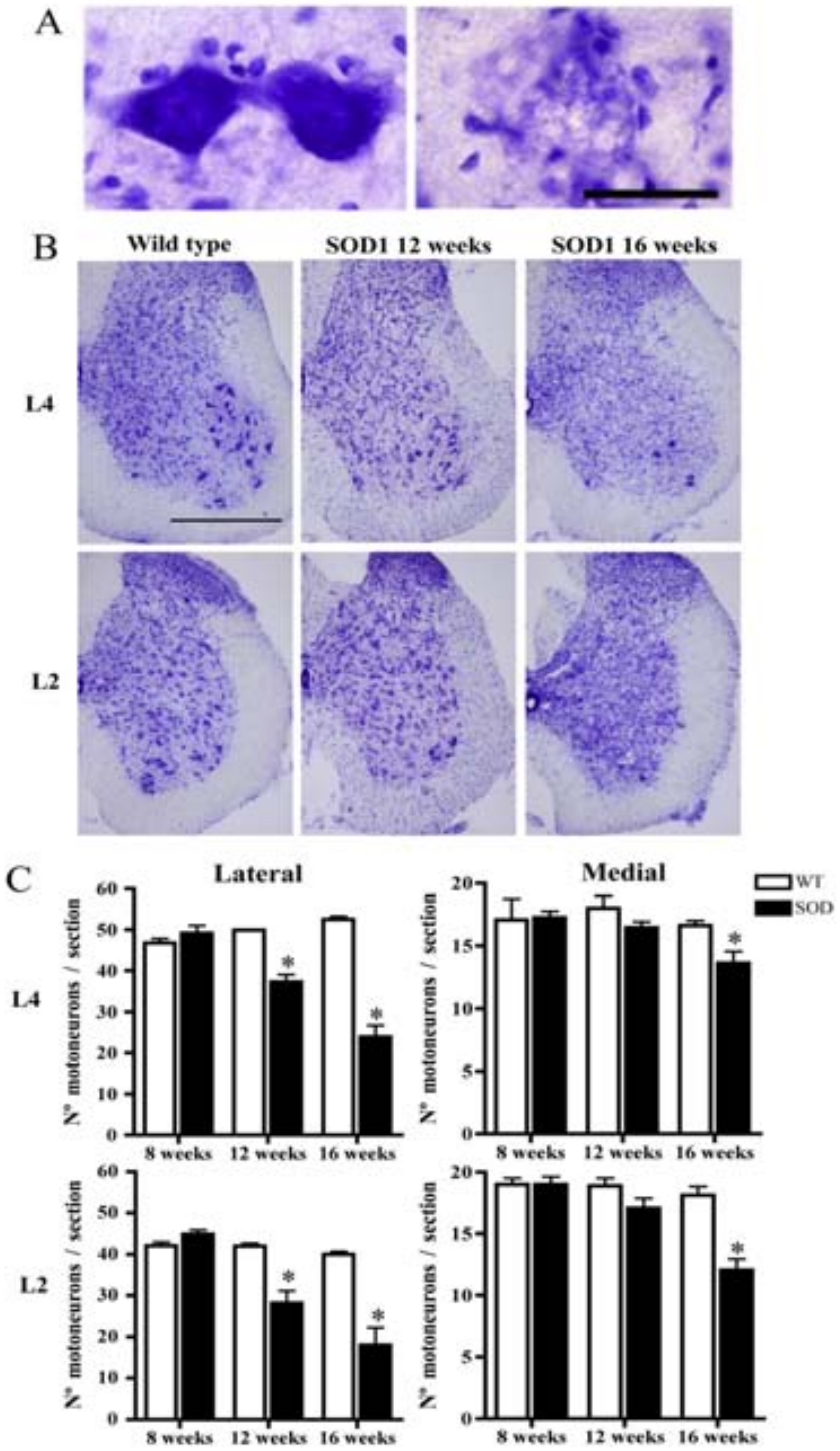

Fig. 6. Motoneuron survival in SOD1 mice. (A) Representative images of MN degeneration. Note the vacuolization and Nissl substance disintegration in SOD1 MN compared with wild type MN; bar = 40 μm. (B) Representative microphotographs of L4 and L2 ventral horns of wild type and SOD1 mice at 12 and 16 weeks of age; bar = 500 μm. (C) Number of surviving lateral (innervating hindlimb muscles) and medial (innervating axial muscles) subpopulations of MNs in SOD1 mice at L4 and L2 spinal cord segments. *$p < 0.05$ vs. wild type mice.

SOD1 transgenic mice. However, it is worth to note that there was a slight but not significant increase in the sensory latency, which may point to a general loss of axonal conduction velocity, likely due to axonal atrophy or to a decrease in metabolic activity and body temperature of the animals. This could also contribute to the decline observed in the motor nerve latency.

Motor unit number estimation is also useful to evaluate lower MN function and to analyze disease progression both in ALS patients and animal models (Hegedus et al., 2008; Shefner et al., 2002, 2006; Wijesekera and Leigh 2009). Methods used for the determination of the number of functioning motor units in vivo, based on electromyographic and tension measurements, give an estimate that does not exactly match but correlates well with the histological counts of alpha-MNs in the spinal cord (Arasaki et al., 1997; McHanwell and Biscoe 1981). Our results demonstrated a progressive reduction in the number of functional motor units, in concordance with previous reports (Azzouz et al., 1997; Hegedus et al., 2008; Shefner et al., 2006). Surviving motor units in SOD1 animals do not have enough sprouting capacity to compensate the loss of their partners, as evidenced by the lack of enlargement, and even reduction, in the mean amplitude of single motor units along time (Hegedus et al., 2008; Shefner et al., 2002, 2006). We also found a significant positive correlation between the number of surviving motor units and the amplitude of the M wave during follow-up. These means that, although other authors suggested that MUNE is the best technique to assess loss of lower MN function in ALS models (Hegedus et al., 2008; Shefner et al., 2002, 2006; Wijesekera and Leigh 2009), the CMAP recorded by motor nerve conduction tests may be a reliable enough and easier to perform measurement to follow up disease progression and evaluate the effects of potential treatments.

4.2. Upper motoneuron contribution to motor dysfunction

Further analysis of lower MN function show that they may become hyperexcitable as MN disease is progressing, as evidenced by the increase in the H/M ratio, especially in the TA muscle. The hyperreflexia is consistent with the spastic paresis that the SOD1 mice present in the symptomatic phase. Actually, this is the first study evidencing abnormalities in the spinal circuits leading to hyperreflexia, similar to what happen in ALS patients (Leigh and Ray-Chaudhuri 1994). The increased H/M ratio may be due to several reasons: first, intrinsic plastic changes or degenerative processes in the spinal cord involving inhibitory interneurons (Chang and Martin 2009); second, changes in intrinsic excitability of MNs (Kuo et al., 2004, Zona et al., 2006) or motor axons (Kuo et al., 2004; Boërio et al., 2010), and third, dysfunction of corticospinal pathways that exert control of lower MNs (Wada et al., 1989).

It has been recently shown that SOD1 alterations are related with sporadic forms of ALS (Bosco et al., 2010). These findings increase the need to better understand if animal models based of SOD1 gene mutations develop a disease process similar to which happens in patients. Although it has been already shown that lower MNs are affected in this mouse models (Kennel et al., 1996; Azzouz et al., 1997; Shefner et al., 2006), a concomitant dysfunction of upper MN, an essential condition for ALS diagnosis in patients (Wijesekera and Leigh 2009) was not demonstrated until now. To our knowledge, this is the first study revealing functional abnormalities of central motor pathways simultaneously to the dysfunction of spinal MNs, demonstrating an upper MN contribution to the disease in the SOD1^{G93A} mouse model. Our results illustrate that central conduction tests showed a decline in the MEP/M ratio and an increase in MEP-M latency from 12 weeks of age, reflecting involvement of brain and brainstem upper MNs (Table 2). By means of the injection of fluorescent retrotracers at the spinal cord it was shown a progressive reduction in corticospinal and brainstem-spinal projections in the SOD1^{G93A} transgenic model that started at 90 days (Zang and Cheema, 2002). Central motor conduction analysis also showed that lower MN dysfunction precedes that of upper MNs, as evidenced by the earlier decline of the M wave amplitude compared with the MEP/M amplitude ratio. This progression fits with that of patients who suffer lumbo-sacral onset ALS, in which the first symptoms are due to lower MN dysfunction (Wijesekera and Leigh, 2009).

4.3. Potential markers of motoneuron disease

In a degenerative disease with so fast evolution, such as ALS, it is presumed that for being effective any therapeutic approach should be started as early as possible in the course of the disease before a significant number of MNs start degenerating. With the advent of specific biological therapies for ALS there is an increasing imperative for early diagnosis. In this work we show that non-invasive electrophysiological studies can be applied in experimental models, as wells as in the clinic, for the early detection of dysfunctions in MN diseases, and as precise markers to assess the functional efficacy of new potential treatments at the experimental level. The diagnosis of ALS is based on the combination of both lower and upper MN dysfunction signs (Wijesekera and Leigh 2009). Interestingly, the results of this study indicate that, at least in the SOD1 mouse model, recording of peripheral CMAPs is an equally reliable functional parameter than MUNE. This may represent an improvement in the repeated evaluation because CMAP acquisition is easier and its variability is lower compared with MUNE, which is a more time-consuming technique. The involvement of central motor pathways also contributes significantly to the progression of ALS not only in patients but also in the animal model. In the search for diagnostic tests to evaluate upper MN involvement, neurophysiological and imaging techniques are used (Iwata 2007), but there is a lack of agreement regarding the sensitivity and specificity of these techniques. The non-invasive recording of MEPs, as performed in this study, is an adequate technique for the study of motor pathways in the experimental model, allowing comparative assessment of lower and upper MN function.

Acknowledgments

This work was supported by Grant PI071133, TERCEL and CIBERNED funds from the Fondo de Investigación Sanitaria of Spain, Grant SAF2009-12495 from the Ministerio de Ciencia e Innovacion of Spain, "Tu eliges, tu decides" of Caja Navarra, FEDER funds, and Action COST-B30 of the EC.

References

Arasaki K, Tamaki M, Hosoya Y, Kudo N. Validity of electromyograms and tension as a means of motor unit number estimation. Muscle Nerve 1997;20:552–60.
Azzouz M, Leclerc N, Gurney M, Warter JM, Poindron P, Borg J. Progressive motor neuron impairment in an animal model of familial amyotrophic lateral sclerosis. Muscle Nerve 1997;20:45–51.
Boërio D, Kalmar B, Greensmith L, Bostock H. Excitability properties of mouse motor axons in the mutant SOD1(G93A) model of amyotrophic lateral sclerosis. Muscle Nerve 2010.
Bosco DA, Morfini G, Karabacak NM, Song Y, Gros-Louis F, Pasinelli P, et al. Wild-type and mutant SOD1 share an aberrant conformation and a common pathogenic pathway in ALS. Nat Neurosci 2010;13:1396–403.
Brown RH. Amyotrophic lateral sclerosis: recent insights from genetics and transgenic mice. Cell 1995;80:687–92.
Bruna J, Udina E, Ale A, Vilches JJ, Vynckier A, Monbaliu J, et al. Neurophysiological, histological and immunohistochemical characterization of bortezomib-induced neuropathy in mice. Exp Neurol 2010;223:599–608.
Chang Q, Martin LJ. Glycinergic innervation of motoneurons is deficient in amyotrophic lateral sclerosis mice. a quantitative confocal analysis. Am J Pathol 2009;174:574–85.
de Carvalho M, Dengler R, Eisen A, England JD, Kaji R, Kimura J, et al. Electrodiagnostic criteria for diagnosis of ALS. Clin Neurophysiol 2008;119:497–503.
Dengler R, Konstanzer A, Kuther G, Hesse S, Wolf W, Struppler A. Amyotrophic lateral sclerosis: macro-EMG and twitch forces of single motor units. Muscle Nerve 1990;13:545–50.
Fischer LR, Culver DG, Tennant P, Davis AA, Wang M, Castellano-Sanchez A, et al. Amyotrophic lateral sclerosis is a distal axonopathy: evidence in mice and man. Exp Neurol 2004;185:232–40.

Frey D, Schneider C, Xu L, Borg J, Spooren W, Caroni P. Early and selective loss of neuromuscular synapse subtypes with low sprouting competence in motoneuron diseases. J Neurosci 2000;20:2534–42.
Garcia-Alias G, Verdu E, Fores J, Lopez-Vales R, Navarro X. Functional and electrophysiological characterization of photochemical graded spinal cord injury in the rat. J Neurotrauma 2003;20:501–10.
Gurney ME, Pu H, Chiu AY, Dal Canto MC, Polchow CY, Alexander DD, et al. Motor neuron degeneration in mice that express a human Cu, Zn superoxide dismutase mutation. Science 1994;264:1772–5.
Hegedus J, Putman CT, Gordon T. Time course of preferential motor unit loss in the SOD1 G93A mouse model of amyotrophic lateral sclerosis. Neurobiol Dis 2007;28:154–64.
Hegedus J, Putman CT, Tyreman N, Gordon T. Preferential motor unit loss in the SOD1 G93A transgenic mouse model of amyotrophic lateral sclerosis. J Physiol (Lond) 2008;586:3337–51.
Iwata NK. Objective markers for upper motor neuron involvement in amyotrophic lateral sclerosis. Brain Nerve 2007;59:1053–64.
Kennel PF, Fonteneau P, Martin E, Schmidt JM, Azzouz M, Borg J, et al. Electromyographical and motor performance studies in the pmn mouse model of neurodegenerative disease. Neurobiol Dis 1996;3:137–47.
Kraemer M, Buerger M, Berlit P. Diagnostic problems and delay of diagnosis in amyotrophic lateral sclerosis. Clin Neurol Neurosurg 2010;112:103–5.
Krarup C. Lower motor neuron involvement examined by quantitative electromyography in amyotrophic lateral sclerosis. Clinical Neurophysiol 2011;122:414–22.
Kuo JJ, Schonewille M, Siddique T, Schults ANA, Fu R, Bär PR, et al. Hyperexcitability of cultured spinal motoneurons from presymptomatic ALS mice. J Neurophysiol 2004;91:571–5.
Lago N, Udina E, Ramachandran A, Navarro X. Neurobiological assessment of regenerative electrodes for bidirectional interfacing injured peripheral nerves. IEEE Trans Biomed Eng 2007;54:1129–37.
Leigh PN, Ray-Chaudhuri K. Motor neuron disease. J Neurol Neurosurg Psychiatry 1994;57:886–96.
Ludolph AC, Jesse S. Review: Evidence-based drug treatment in amyotrophic lateral sclerosis and upcoming clinical trials. Ther Adv Neurol Disord 2009;2:319–26.
McHanwell S, Biscoe TJ. The localization of motoneurons supplying the hindlimb muscles of the mouse. Philos Trans R Soc London B Biol Sci 1981;293:477–508.
Miana-Mena FJ, Muñoz MJ, Yagüe G, Mendez M, Moreno M, Ciriza J, et al. Optimal methods to characterize the G93A mouse model of ALS. Amyotroph Lateral Scler Other Motor Neuron Disord 2005;6:55–62.
Mitsumoto H, Ulug AM, Pullman SL, Gooch CL, Chan S, Tang M-X, et al. Quantitative objective markers for upper and lower motor neuron dysfunction in ALS. Neurology 2007;68:1402–10.
Moreno-Igoa M, Calvo AC, Penas C, Manzano R, Oliván S, Muñoz MJ, et al. Fragment C of tetanus toxin, more than a carrier. Novel perspectives in non-viral ALS gene therapy. J Mol Med 2010;88:297–308.
Navarro X, Udina E. Chapter 6 - Methods and Protocols in Peripheral Nerve Regeneration Experimental Research: Part III-Electrophysiological Evaluation. Int Rev Neurobiol 2009;87:105–26.
Navarro X, Verdu E, Buti M. Comparison of regenerative and reinnervating capabilities of different functional types of nerve fibers. Exp Neurol 1994;129:217–24.
Penas C, Casas C, Robert I, Fores J, Navarro X. Cytoskeletal and activity-related changes in spinal motoneurons after root avulsion. J Neurotrauma 2009;26:763–79.
Pun S, Santos AF, Saxena S, Xu L, Caroni P. Selective vulnerability and pruning of phasic motoneuron axons in motoneuron disease alleviated by CNTF. Nat Neurosci 2006;9:408–19.
Ripps ME, Huntley GW, Hof PR, Morrison JH, Gordon JW. Transgenic mice expressing an altered murine superoxide dismutase gene provide an animal model of amyotrophic lateral sclerosis. Proc Natl Acad Sci USA 1995;92:689–93.
Shefner JM, Cudkowicz M, Brown RH. Motor unit number estimation predicts disease onset and survival in a transgenic mouse model of amyotrophic lateral sclerosis. Muscle Nerve 2006;34:603–7.
Shefner JM, Cudkowicz ME, Brown Jr RH. Comparison of incremental with multipoint MUNE methods in transgenic ALS mice. Muscle Nerve 2002;25:39–42.
Shefner JM, Reaume AG, Flood DG, Scott RW, Kowall NW, Ferrante RJ, et al. Mice lacking cytosolic copper/zinc superoxide dismutase display a distinctive motor axonopathy. Neurology 1999;53:1239–46.
Sobue G, Sahashi K, Takahashi A, Matsuoka Y, Muroga T, Sobue I. Degenerating compartment and functioning compartment of motor neurons in ALS: possible process of motor neuron loss. Neurology 1983;33:654–7.
Turner BJ, Talbot K. Transgenics, toxicity and therapeutics in rodent models of mutant SOD1-mediated familial ALS. Progr Neurobiol 2008;85:94–134.
Udina E, Ceballos D, Gold BG, Navarro X. FK506 enhances reinnervation by regeneration and by collateral sprouting of peripheral nerve fibers. Exp Neurol 2003;183:220–31.
Valero-Cabré A, Navarro X. H reflex restitution and facilitation after different types of peripheral nerve injury and repair. Brain Res 2001;919:302–12.
Verdú E, Vilches JJ, Rodriguez FJ, Ceballos D, Valero A, Navarro X. Physiological and immunohistochemical characterization of cisplatin-induced neuropathy in mice. Muscle Nerve 1999;22:329–40.
Wada N, Yawashima Y, Nakajima Y. Effect of nucleus raphe magnus stimulation on recurrent inhibition of the monosynaptic reflex in the cat. Neurosci Lett 1989;107:94–8.
Wijesekera LC, Leigh PN. Amyotrophic lateral sclerosis. Orphanet J Rare Dis 2009;4:3.
Wegorzewska I, Bell S, Cairns N, Miller T, Baloh R. TDP-43 mutant transgenic mice develop features of ALS and frontotemporal lobar degeneration. Proc Natl Acad Sci USA 2009;106:18809–14.
Worms PM. The epidemiology of motor neuron diseases: a review of recent studies. J Neurol Sci 2001;191:3–9.
Zang DW, Cheema SS. Degeneration of corticospinal and bulbospinal systems in the superoxide dismutase 1(G93A G1H) transgenic mouse model of familial amyotrophic lateral sclerosis. Neurosci Lett 2002;332:99–102.
Zona C, Pieri M, Carunchio I. Voltage-dependent sodium channels in spinal cord motor neurons display rapid recovery from fast inactivation in a mouse model of amyotrophic lateral sclerosis. J Neurophysiol 2006;96:3314–22.

Chapter I: SOD1^{G93A} mouse model characterization

1.2. Evolution of gait abnormalities in SOD1^{G93A} transgenic mice

Mancuso R, Oliván S, Osta R, Navarro X. Evolution of gait abnormalities in SOD1^{G93A} transgenic mice. Brain Res 2011, 1406: 65-73.

BRAIN RESEARCH 1406 (2011) 65–73

available at www.sciencedirect.com

ScienceDirect

www.elsevier.com/locate/brainres

BRAIN RESEARCH

Research Report

Evolution of gait abnormalities in SOD1 ^{G93A} transgenic mice

Renzo Mancuso[a], *Sara Oliván*[b], *Rosario Osta*[b], *Xavier Navarro*[a,*]

[a]*Group of Neuroplasticity and Regeneration, Institute of Neurosciences and Department of Cell Biology, Physiology and Immunology, Universitat Autònoma de Barcelona, and Centro de Investigación Biomédica en Red sobre Enfermedades Neurodegenerativas (CIBERNED), Bellaterra, Spain*

[b]*Laboratory of Genetic Biochemistry (LAGENBIO-I3A), Aragon Institute of Health Sciences, Universidad de Zaragoza, Zaragoza, Spain*

ARTICLE INFO

Article history:
Accepted 12 June 2011
Available online 5 July 2011

Keywords:
Locomotion
Motoneuron disease
Neurodegeneration
SOD1 mouse

ABSTRACT

Amyotrophic lateral sclerosis (ALS) is a neurodegenerative disorder characterized by the loss of upper and lower motoneurons. Clinically, it is manifested by weakness, muscle atrophy and progressive paralysis and ends up with patients' death 2–5 years after diagnosis. Although these symptoms lead in many cases to gait deficits in patients, an exhaustive locomotor profile of animal models mimicking the disease has not been assessed yet. In this work we evaluated the locomotor performance of the SOD1^{G93A} mouse model of ALS using computerized treadmill gait analysis. SOD1^{G93A} mice presented early (8 weeks of age) gait abnormalities, evidenced by an increase in the time of the propulsion phase of hindlimb stance. The alterations progressed during the disease until a complete disturbance of normal gait. This finding is meaningful to the field because the identification of a significant difference in a functional endpoint as early as 8 weeks might be a step forward resolving the debate about treatment of mice prior to the symptomatic phase in efficacy studies. These results also point out that digitizing analysis of treadmill locomotion may be useful to evaluate whether new therapeutic approaches are improving functional outcome of the animals.

1. Introduction

Amyotrophic lateral sclerosis (ALS) is the most common form of motoneuron disease, characterized by degeneration of both upper and lower motoneurons. Clinically, ALS manifests as weakness, muscle atrophy and progressive paralysis, and finishes with patients' death a few years after diagnosis (Wijesekera and Leigh, 2009; Worms, 2001), since there are no effective treatments available (Ludolph and Jesse, 2009). The development of transgenic animal models carrying genetic mutations described in familial ALS cases (Rosen, 1993) has facilitated the study of etiopathogenic factors and therapeutic strategies for the human disease. The most widely used is the SOD1^{G93A} transgenic mouse, whose phenotype recapitulates the clinical and histopathological features of ALS (Miana-Mena et al., 2005; Ripps et al., 1995; Turner and Talbot, 2008). Although animal models carrying SOD1 mutations have been developed based on familial cases of ALS, it has been recently described that alterations of SOD1 protein are also related to sporadic ALS cases (Bosco et al., 2010), thus, increasing the applicability of studies based on these transgenic animals.

Detailed gait analysis applied to common laboratory species has provided valuable information regarding human and quadruped locomotion (Clarke and Still, 1999; Gillette and

* *Corresponding author at:* Unitat de Fisiologia Mèdica, Facultat de Medicina, Universitat Autònoma de Barcelona, E-08193 Bellaterra, Spain. E-mail address: xavier.navarro@uab.cat (X. Navarro).

Abbreviations: ALS, amyotrophic lateral sclerosis; CMAP, compound muscle action potential; CV, coefficient of variation; PL, print length; SOD, superoxide dismutase; TS, toe spreading

0006-8993/$ – see front matter © 2011 Elsevier B.V. All rights reserved.
doi:10.1016/j.brainres.2011.06.033

Angle, 2008; Varejão et al., 2001), and has shown sensitivity to detect disease- or injury-related changes. Until now, the most common behavioral locomotion techniques used in mice have been footprint analysis (mainly used to evaluate recovery from peripheral nerve lesions) (de Medinaceli et al., 1982; Varejão et al., 2001) and the rotarod test (mainly used in peripheral neuropathies and neurodegenerative models including SOD1 mice) (Kaplan and Murphy, 1972; Knippenberg et al., 2010; Miana-Mena et al., 2005; Verdu et al., 1999). However, they are limited by their low sensitivity and specificity.

Historically, the locomotor performance of SOD1^{G93A} mice has been evaluated using the rotarod test (Gurney et al., 1994; Miana-Mena et al., 2005) as one of the primary measures of disease progression and its modification by therapeutical strategies. However, the rotarod test lacks sensitivity, since it only begins to detect motor deficits at 13 weeks of age. These deficits progress rapidly until complete hindlimb paralysis at 16–18 weeks, thus providing a relatively narrow time frame in which to detect possible changes. Thus, rotarod is not sufficiently sensitive to detect motor deficits prior to the onset of overt clinical symptoms, despite histological and electrophysiological evidences demonstrating earlier motor abnormalities in pre-symptomatic SOD1 mice (Azzouz et al., 1997; Fischer et al., 2004; Kennel et al., 1996; Mancuso et al., 2011). Moreover, the rotarod test is not always able to reveal functional improvement, even when the treatment applied improves the condition of the animals or improves the survival of motoneurons (Fischer et al., 2005). For these reasons, in the current study we sought to evaluate locomotor performance of SOD1^{G93A} mice using a digital video system that captures paw placement during treadmill locomotion and calculates standardized gait parameters (DigiGait™, Mouse Specifics Inc.). Our goal was to determine whether locomotor abnormalities could be detected early in the disease, prior to onset of overt symptoms, as well as during symptomatic and end-stage disease. The capability of early detection would likely increase the possibility of demonstrating functional improvement, the primary objective during testing of potential therapeutic approaches.

2. Results

2.1. Rotarod test

The performance of the SOD1 mice in the rotarod test started to decline between 12 and 13 weeks of age, and continued decreasing until the end stage of the disease, when most animals (75%) were paralyzed and completely unable to hold by themselves in the rod (Fig. 1). In contrast, wild type animals maintained performance during the cut-off 180 s time in the rotarod during all the follow up.

2.2. Footprint analysis

The analysis of the footprints recorded in the walking track test did not show significant differences in the print length and in the toe spread between SOD1 and wild type mice (Fig. 2; data not shown). Although other authors have considered the stride length as another parameter for the study of mouse locomotion (Knippenberg et al., 2010), we did not find it as a reliable measurement in this test because mice do not usually perform a regular voluntary walk across the walkway.

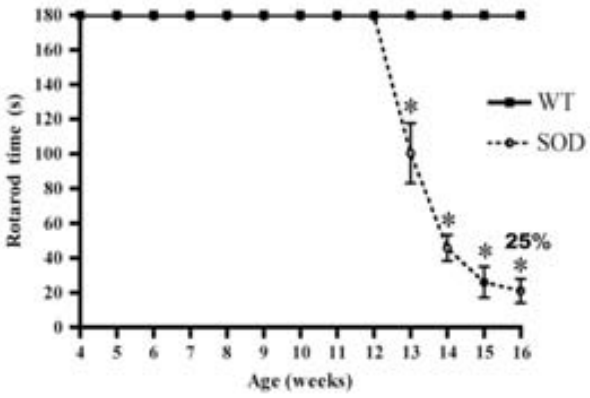

Fig. 1 – Time on the rotarod in SOD1 (n=12) and wild type (n=10) mice: the time declined after 12 weeks of age in transgenic SOD1 mice, whereas wild type mice maintained permanence in the rotarod during 180 s during all the follow up. Values are mean ± SEM; * $p<0.05$ vs. wild type mice. Only 25% of SOD1 mice were able to maintain in the rotarod during at least 5 s to allow for measurement at 16 weeks.

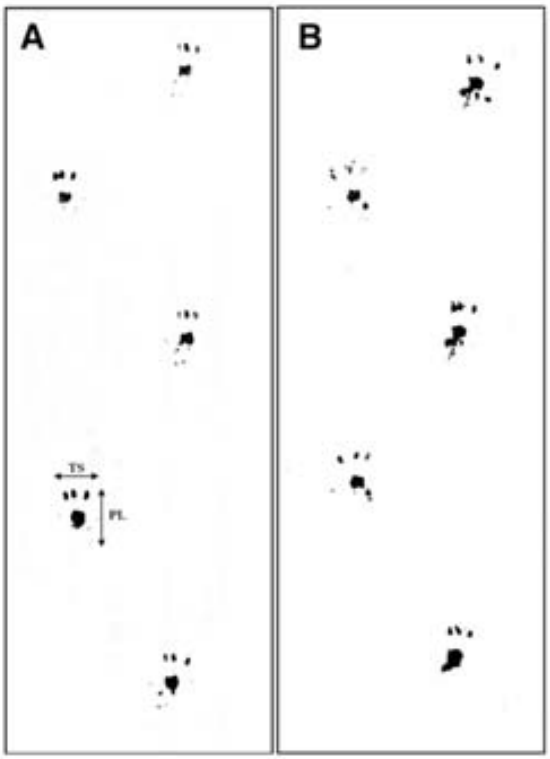

Fig. 2 – Representative images of footprint analysis of (A) wild type and (B) SOD1 mice at 16 weeks of age. The analysis of the footprints did not show any differences in the print length and in the toe spreading between wild type (n=10) and transgenic SOD1 (n=12) animals. TS, toe spread; PL, print length.

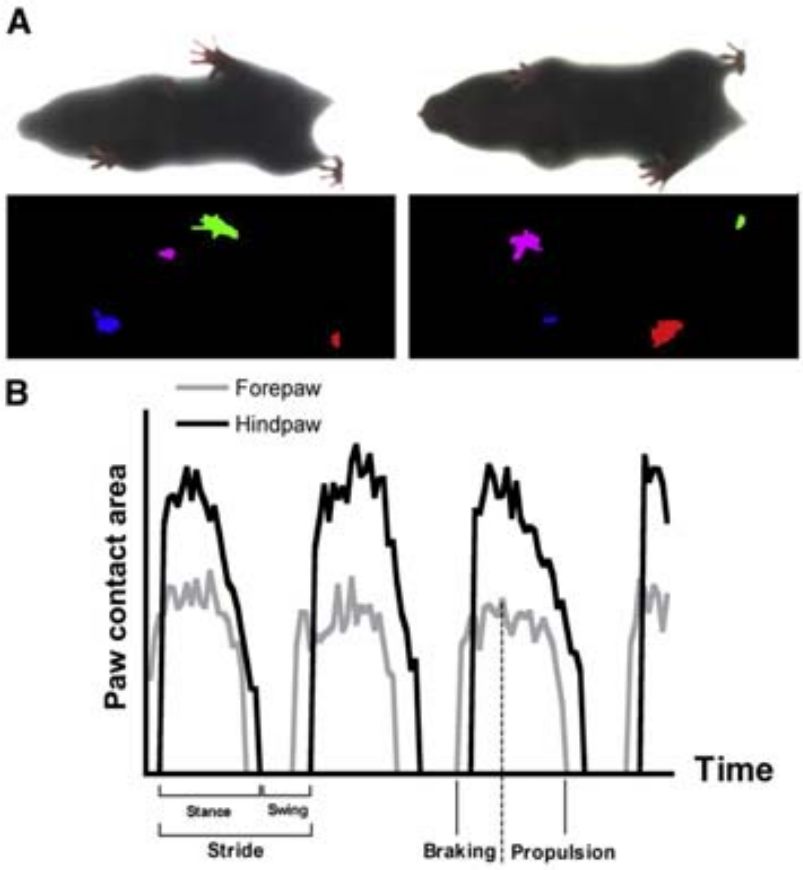

Fig. 3 – A. Images of a mouse walking on the DigiGait, and corresponding software processing (forepaws: right in blue and left in purple; hindpaws: right in red and left in green). B. Representative gait signals for the left forepaw and right hindpaw of a wild type mouse walking at 20 cm/s. Note that gait pattern is qualitatively and quantitatively different in fore- and hindpaws.

2.3. *DigiGait analysis*

Fine analysis of the walking pattern was performed with the DigiGait system (Fig. 3, Tables 1 and 2). To validate the gait analysis performed, we paid attention first to the wild type mice at 8 weeks of age. Previous studies by Clarke and Still (1999) showed that normal mouse locomotion has two main characteristics: on one hand, stride duration of fore- and hindlimbs does not change when velocity is constant and, on the other hand, stride duration decreases and stride frequency increases with increasing velocity. As shown in the Tables 1 and 2, stride duration of fore- and hindlimbs remains unchanged in wild type animals at 20 cm/s. Moreover, stride duration decreases from 320.0 to 251.5 ms and stride frequency increases from 3.38 to 4.12 steps per second when treadmill speed was increased from 15 to 20 cm/s. Thus, our results demonstrate that DigiGait analysis is an adequate method to evaluate locomotion of mice. Then, in order to analyze the repeatability of the gait measurements, wild type mice were subjected to three tests on consecutive days. We calculated

Table 1 – Gait parameters of WT (n = 10) and SOD1^{G93A} (n = 12) mice hindlimbs during disease progression.

	8 weeks		12 weeks		16 weeks	
	WT	SOD1	WT	SOD1	WT	SOD1
Stride (ms)	251.2 ± 9.5	265.2 ± 5.0	257.6 ± 8.9	271.0 ± 8.2*	250.0 ± 8.8	317.7 ± 11.4*
Stance (ms)	153.6 ± 4.8	168.0 ± 4.2*	154.0 ± 5.9	170.3 ± 8.6*	154.5 ± 8.5	196.3 ± 9.6*
Swing (ms)	97.6 ± 6.5	97.3 ± 5.6	103.6 ± 6.3	104.2 ± 7.3	95.5 ± 5.9	121.4 ± 6.0*
Propulsion (ms)	115.8 ± 4.6	126.9 ± 4.6*	112.0 ± 6.2	127.9 ± 7.2*	112.9 ± 7.8	161.4 ± 10.4*
Absolute paw angle (°)	16.10 ± 1.865	14.67 ± 2.203	15.90 ± 2.169	13.45 ± 1.752*	15.33 ± 2.027	5.048 ± 1.443*
Stride freq. (# of steps/s)	4.120 ± 0.155	3.827 ± 0.085	3.940 ± 0.142	3.762 ± 0.111*	4.056 ± 0.165	3.270 ± 0.159*
Stance width (cm)	2.000 ± 0.070	1.918 ± 0.117	2.044 ± 0.079	1.908 ± 0.081	2.100 ± 0.062	1.480 ± 0.107*

Values are mean ± SEM.
*$p < 0.05$ vs. wild type.

Table 2 – Gait parameters of WT (n=10) and SOD1^{G93A} (n=12) mouse forelimbs during disease progression.

	8 weeks		12 weeks		16 weeks	
	WT	SOD1	WT	SOD1	WT	SOD1
Stride (ms)	249.5±8.8	263.8±5.9	251.7±8.7	274.5±8.9*	245.1±9.4	291.5±10.5*
Stance (ms)	160.4±4.6	165.8±5.4	153.0±5.7	166.6±5.7*	145.6±7.8	188.9±6.2*
Swing (ms)	89.2±5.3	98.1±4.6	98.6±4.7	108.1±5.0	99.5±5.5	102.6±7.1
Propulsion (ms)	92.9±6.0	91.5±5.7	88.7±8.2	87.5±6.4	81.8±7.6	83.2±8.8
Absolute paw angle (°)	6.873±1.036	5.550±1.751	6.950±1.194	3.732±0.977*	7.411±1.240	2.075±0.680*
Stride freq. (# of steps/s)	4.095±0.154	3.845±0.072	4.017±0.150	3.686±0.118*	4.144±0.180	3.298±0.139*
Stance width (cm)	1.520±0.078	1.418±0.078	1.344±0.108	1.309±0.107	1.544±0.151	1.117±0.109*

Values are mean±SEM.
*$p<0.05$ vs. wild type.

the coefficient of variation (CV) from 5 to 7 steps of one single recording (intra-test CV) and also from the three different recordings of the same animal (inter-test CV). Intra-test CV of stride, stance, swing and propulsion durations ranged between 9.2 and 16.6%., while inter-test CV was comprised between 7.0 and 14.5%, thus demonstrating enough reproducibility of the results. Furthermore, the mice were divided in two subgroups of wild type (n=5 each subgroup) and SOD1 transgenic (n=6 each subgroup), which were tested on different days. Since we did not find any significant difference in any gait parameter during all the follow up between subgroups (ANOVA for repeated measurements taking the day as a factor; $p>0.05$ in all cases), the results were pooled together for comparisons between wild type and SOD1 animals.

The evaluation of the general motor performance showed that not all SOD1 mice were able to run in the DigiGait test until the end stage of the disease. All the mice were able to walk at the three treadmill speeds assessed (15, 20 and 30 cm/s) at 8 and 12 weeks of age, but their performance significantly (Kaplan–Meir test, $p<0.05$) declined at 16 weeks when only 66.7% (8 of 12) of the mice were able to maintain regular walking at 15 cm/s, 50% (6 of 12) at 20 cm/s and none at 30 cm/s.

A detailed analysis of gait parameters was made for runs at 20 cm/s speed, since this speed is the most adequate for both early detection and evaluation of deficits until the late phase of the disease. When the animals were not able to perform the test at the end stage of the disease (16 weeks), an arbitrary penalization value was attributed consisting on a 10% worse value with respect to the animal that showed the worst performance for each particular parameter.

Gait dynamics of SOD1 mice was significantly different from wild type mice. The most marked differences were related to the hindlimbs' performance, in which SOD1 mice presented a longer stance time compared with wild type mice already at the pre-symptomatic stage (8 weeks). A detailed analysis of the different phases of the stride revealed that this change was due to a significant increase in the propulsion phase, the accelerating part of the stride, whereas the braking phase was not affected (Fig. 4; Table 1).

At 12 weeks of age, gait abnormalities progressed in the hindlimbs and affected also the forelimbs. Stance and propulsion times of the forelimbs were significantly increased, involving relatively more the swing than the propulsion phase, and the global stride time also increased in SOD1 mice compared with wild type mice (Fig. 4, Table 2). In parallel with this increment in the stride time, SOD1 animals showed a significant reduction in the stride frequency. At 16 weeks of age the animals able to perform the test showed pronounced locomotor abnormalities both in forelimbs and hindlimbs. In fact, the only parameter that remained unchanged was the swing time of the forelimbs (Tables 1 and 2).

Finally, SOD1 mice showed a reduction in the paw angle (Fig. 5) that was significant at 12 and 16 weeks, but the stance width showed a significant reduction only at the end stage of the disease (16 weeks) (Tables 1 and 2).

2.4. *Nerve conduction results*

Motor nerve conduction tests were performed to assess whether the repeated battery of locomotion tests applied could somehow affect the disease progression of the animals, thus compromising the reliability of the study. The results did not show any differences between the group of SOD1 mice that were tested and another group not tested (Table 3).

3. Discussion

The results of this study indicate that SOD1 mice suffer early locomotor abnormalities (by 8 weeks of age), mainly evidenced by a significant increase in the time of the propulsion (accelerating) phase of hindlimb stride. These gait abnormalities correlate with previous findings revealing early electrophysiological deficits of peripheral motor function in the hindlimbs of SOD1 mice, also evident at 8 weeks of age (Azzouz et al., 1997; Kennel et al., 1996; Mancuso et al., 2011), and show that these alterations lead to functional deficits. These findings also indicate that computerized analysis of gait parameters may have an important role for the study of the motor system function in mice. Focusing in the ALS model, it is critical to understand functional consequences of the disease process in transgenic mice to determine whether new treatments may not only arrest the disease but also prevent the development of irreversible deficits.

ALS affects the motor system producing muscle weakness and leading in many cases to lower limb paresia and gait deficits in patients (Wijesekera and Leigh, 2009). Despite this fact, there is no exhaustive study evaluating the evolution of

BRAIN RESEARCH 1406 (2011) 65–73

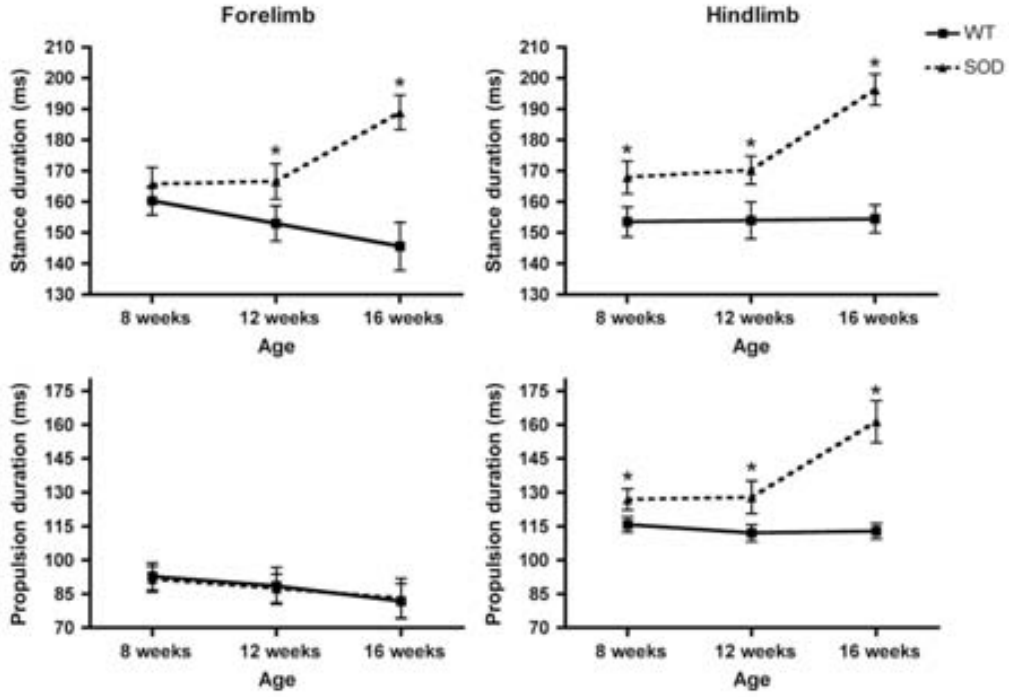

Fig. 4 – Stance and propulsion duration dynamics of fore- and hindlimbs in SOD1 (n = 12) and wild type (n = 10) mice. Note the significant increase in the duration of both parameters in hindlimbs at 8 weeks, pointing out to early abnormalities in locomotion of the transgenic mice. Values are mean ± SEM; * $p < 0.05$ vs. wild type mice.

gait performance during disease progression in SOD1 mice, the most widely used animal model of ALS. Usually, the study of these animals was focused in the detection of the first deficits in motor performance using simple tests such as the hangwire test and the rotarod, with the aim of determining the onset of the symptomatic phase of the disease, (Miana-Mena et al., 2005; Moreno-Igoa et al., 2010). However, these two methods have several limitations, the most important of which is the lack of sensitivity to detect early abnormalities and the short time of dysfunction until complete paralysis.

Our results regarding footprint analysis show that this technique is unable to detect significant deficits in SOD1 mice locomotion, neither in the print length nor in the toe spreading. These findings regarding footprint analysis are in accordance with those from other authors describing abnormalities in locomotion until 17 weeks, when the animals started to show signs of paralysis (Knippenberg et al., 2010). In fact, Knippenberg et al. (2010) have shown a slight reduction in the stride length of SOD1 animals from 15 weeks of age using footprint analysis. However, this reduction might be interpreted as an artifact due to the decline in the runtime of the mice, that increased by 15 weeks. The ability for toe spreading was also reported to occur quite late in the SOD1 mice (Azzouz et al., 1997). It has been shown that electrophysiological deficits of SOD1 mice start earlier in proximal muscles, such as tibialis anterior or gastrocnemius, than in more distal ones,

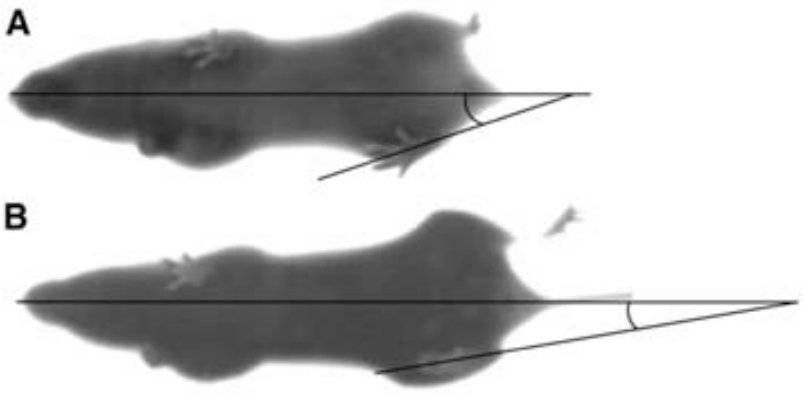

Fig. 5 – Representative images of hindpaws placement angle at maximum contact area of (A) wild type and (B) SOD1 mice. Note the marked decreased in the paw placement angle of SOD1 with respect to wild type animals.

Table 3 – Results of the motor nerve conduction study comparing the disease progression of SOD1^{G93A} mice that were tested (SOD1+DigiGait, n=12) and not tested (SOD1 Control, n=8) on the Digigait. The lack of significant ($p>0.05$) differences points out that DigiGait can be done without affecting the condition of the animals.

	8 weeks		12 weeks		16 weeks	
	SOD1 Control	SOD1+Digigait	SOD1 Control	SOD+Digigait	SOD1 Control	SOD1+Digigait
CMAP amplitude (mV)	36.2±1.22	35.4±1.77	24.7±2.45	25.5±2.57	12.6±2.22	11.7±1.55
Latency (ms)	0.95±0.02	0.94±0.03	1.07±0.04	1.06±0.01	1.06±0.04	1.08±0.03

Values are mean±SEM.

such as plantar interossei muscles (Azzouz et al., 1997; Mancuso et al., 2011). These observations suggest that the first muscles showing functional deficits may be the most proximal and, thus, out of the range of study of the footprint analysis. However, the lack of sensitivity of footprint analysis can also be related to selection bias that arises from the fact that only enough well defined footprints are measured.

Rotarod results showed that SOD1 mice started to decline in performance between 12 and 13 weeks and progressed rapidly to complete lost. In contrast, the first abnormalities in motor nerve conduction tests (Azzouz et al., 1997; Mancuso et al., 2011) and the denervation process of motor end-plates (Fischer et al., 2004) start earlier, at 7–8 weeks of age. Considering that it has also been described that SOD1 mice present marked deficit in the compensatory sprouting capacity of their motoneurons (Hegedus et al., 2008; Mancuso et al., 2011), it is likely that these deficits lead to locomotor manifestations.

This study provides novel information about the start and progression of gait abnormalities in SOD1 mice. Regarding hindlimbs, there was an early (8 weeks of age) enlargement of stance duration mainly due to an increase of the propulsion phase duration of about 10% that progressed over the disease process (Table 1). Wooley et al. (2005) already noticed an increase in the stance duration in SOD1 compared to wild type mice from 8 weeks of age. Our results further demonstrate for the first time that the abnormalities start in the accelerating phase of the stride. In contrast, Guillot et al. (2008) did not find consistent differences regarding SOD1 mice locomotion and concluded that treadmill gait analysis was not able to distinguish SOD1^{G93A} from wild type mice between 6 and 12 weeks. This lack of findings may be related to the small number of animals used by these authors.

The impairments observed in the locomotor performance of SOD1 mice point out to a contribution of muscles that are related with the end of the stance phase and the beginning of the swing phase, such as hamstrings, gastrocnemius and flexor digitorum longus (FDL) muscles (Krouchev et al., 2006). Previous results in our lab suggested that dysfunction of hindlimb muscles progresses proximal to distal, evidenced by earlier significant reduction of compound muscle action potentials (CMAP) in tibialis anterior than in plantar muscles (Mancuso et al., 2011). Azzouz et al. (1997) also found a 15% decline of the gastrocnemius CMAP at 7–8 weeks. However, the loss of 15% muscle function could not be enough by itself to produce overt abnormalities in locomotor activities. We propose that these may be related to a combination of deficits in gastrocnemius and hamstring muscles, both contributing to the lift of the hindlimb (Krouchev et al., 2006), thus producing impairments in the take-off of the paw and delaying the end of the stance phase. The finding of Alves et al. (2011) regarding the impairment of tail elevation at early time points (40 days) could also support the hypothesis of an involvement of proximal muscles at the beginning of the disease process. At 12 weeks, the increase of the stance duration became so evident that it involved also the stride duration. The increase of the stride duration led to significant reduction of the stride frequency, as a compensatory phenomenon. Curiously, the swing duration remained normal, supporting the contribution of the same muscles related to the locomotor abnormalities detected at 8 weeks. Finally, there was a reduction of the paw placement angle possibly due to atrophy of proximal muscles. At 16 weeks, all impairments become more pronounced and swing duration was abnormal, pointing out to involvement of other muscles.

Regarding the forelimbs, SOD1 mice did not show any alteration at 8 weeks. However, at 12 weeks stride and stance duration, paw placement angle and stride frequency started to show abnormalities correlated with hindlimb deficits. Considering that SOD1 animals develop a lumbosacral type of ALS (Ripps et al., 1995), the involvement of forelimb gait could be partially due to compensatory adaptation to the deficits of the hindlimbs.

Since it has been reported that high-intensity exercise exacerbates disease progression in SOD1 animals (Mahoney et al., 2004), we assessed whether locomotion testing could affect the disease progression. We compared the group of locomotion-tested animals with another group of non-tested SOD1 mice by means of motor nerve conduction studies (Mancuso et al., 2011). The results showed that tested and non-tested animals had the same amount of muscle denervation, demonstrating that the locomotor tests applied are not interfering with the disease evolution.

In conclusion, SOD1 mice show significant gait abnormalities, evidenced by increased propulsion phase duration at 8 weeks, indicating an early dysfunction of hindlimb muscles that correlates with early abnormalities of motor nerve conduction. The alterations progressed during the disease until a complete disturbance of normal gait. These findings are meaningful to the field because the identification of significant differences in a functional endpoint as early as 8 weeks may be a step forward resolving the debate about treatment of the mice prior to "symptoms onset" in efficacy studies. Our results also point out that digitizing analysis of treadmill locomotion may be used as a valuable tool to evaluate whether new therapeutic approaches are improving the functional outcome of the animals.

4. Experimental procedures

4.1. Transgenic mice

Transgenic mice with the G93A human SOD1 mutation (B6SJL-Tg [SOD1-G93A]1Gur) were obtained from the Jackson Laboratory (Bar Harbor, ME, USA), and provided from the colony maintained at the Unidad Mixta de Investigacion of the University of Zaragoza. Hemizygotes were maintained by breeding $SOD1^{G93A}$ males with female littermates. The offspring was identified by PCR amplification of DNA extracted from the tail tissue. Analyses were performed in 10 wild type and 12 SOD1 female mice that were tested longitudinally from 8 to 16 weeks of age. These animals were divided into two subgroups (5 wild type and 6 SOD1 each one) tested at different days to ensure the reproducibility of the techniques. The experimental procedures were approved by the Ethics Committee of the Universitat Autònoma de Barcelona.

4.2. Rotarod test

The rotarod test was performed to evaluate motor coordination, strength and balance of the animals (Brooks and Dunnett, 2009; Miana-Mena et al., 2005). Animals were trained three times a week on the rod rotating at 14 rpm, and then tested from 4 to 16 weeks of age, with an arbitrary maximum time of maintenance in the rotating rod of 180 s.

4.3. Footprint analysis

Animals were tested in a confined walkway 3.7 cm wide by 21 cm long, dark at one end. After conditioning runs, the plantar surface of the hindpaws was impregnated with block printing paint (Speedball) and each mouse walked along the walkway with office copier paper on the base. Four prints of each foot were recorded on the length of the paper used. Two measurements were recorded on both left and right prints: the distance of the print length (PL) and the distance of the toe spread (TS) between the first and the fifth toes (Fig. 2). The walking track test was performed at 8, 12 and 16 weeks of age.

4.4. Gait dynamics analysis

Digital video images of the underside of the mouse were collected with a high-speed video camera (80 frames per second) from below the transparent belt of a motorized treadmill (DigiGait™ Imaging System, Mouse Specifics, Boston, MA). The device was located in a normal laboratory room with standard conditions. The compartment of the treadmill in which the mouse walks is ~25 cm long and ~5 cm wide, but it can be adapted to the size of the animal. The mice were introduced to the treadmill belt and testing conditions before the recordings. Each mouse was allowed to explore the treadmill compartment, with the motor speed set to zero, for 5 min. Then, motor speed was set to 15 cm/s, 20 cm/s and 30 cm/s to collect the videos based on previous studies of mice locomotion (Clarke and Still, 1999) and utilization of the same device (Hampton et al., 2004). Based on general performance results (see Section 2.3) further gait analysis was performed from runs at 20 cm/s. A maximum of 3 recording trials at each velocity were needed to obtain the videos for all animals. When necessary, food drops were placed in the front part of the treadmill compartment to encourage the mice to walk. Each animal was allowed to rest a minimum of 2 min between recording trials. After each animal test, the treadmill was carefully cleaned with ethanol 70% in order to avoid a possible effect of urine and feces from previous animal on test results. The time needed to test each animal was less than 15 min. Animals were always tested between 9:00 and 13:00 h to avoid a potential effect of time-of-day on the results.

A minimum of 200 images was collected for each walking mouse so that 5–7 strides were monitored in each run. Only video recordings in which the mouse walked straight ahead, maintaining a constant relative position with respect to the camera were used for measurements and analysis. The researcher was blind to the animals' condition in order to avoid bias in the selection of the recordings for digital analysis. Each video image representing 12.5 ms was digitized and the area (in pixels) of the paws was calculated with the DigiGait software (Amende et al., 2005; Hampton et al., 2004) by means of a computational process that needs to be run during several minutes. Mistakes of the imaging in which a paw area was visible during early swing, after the paw was lifted from the belt and before the next stance, were corrected to improve accuracy in differentiating stance from swing.

Fig. 3 shows representative images of the digitizing process of the video and illustrates how plotting paw area over time of walking provides a dynamic gait signal, indicating the components of each stride. Table 4 provides the definition of each parameter used. Fig. 5 shows representative images of how hindpaw placement angle was calculated.

4.5. Nerve conduction test

For motor nerve conduction tests, the sciatic nerve was stimulated percutaneously by means of single pulses of 0.02 ms duration (Grass S88) delivered through a pair of needle electrodes placed at the sciatic notch. The compound muscle action potential (CMAP, M wave) was recorded from the tibialis anterior (TA) muscle with microneedle electrodes (Mancuso et al., 2011; Udina et al., 2003; Valero-Cabré and Navarro, 2001). The maximal amplitude of the M wave was measured (Mancuso et al., 2011; Valero-Cabré and Navarro, 2001). The potentials were amplified and displayed on a digital oscilloscope (Tektronix 450S) to measure the maximal amplitude of the M wave. During the tests, the mouse body temperature was kept constant between 34 and 36 °C by means of a thermostated heating pad.

4.6. Statistical analysis

Data are presented as mean±SEM and differences were considered significant when $p<0.05$. All data collected from the longitudinal comparison of wild type and SOD1 mice at 8, 12 and 16 weeks of age were analyzed using ANOVA for repeated measurements followed by Bonferroni post-hoc test when necessary. The ability to walk on the treadmill has been analyzed using Kaplan–Meir test. In the case of the DigiGait test, the animals were divided in two groups tested at different days. The data collected from wild type mice was analyzed using ANOVA for repeated measurements to assess for differences between days and to ensure the reproducibility of the technique.

Table 4 – Definition of the parameters used in the DigiGait analysis.

Parameter	Definition
Stride duration (ms)	Time duration of one complete stride for one paw.
Stance duration (ms)	Time duration of the stance phase (paw contact with belt).
Swing duration (ms)	Time duration of the swing phase (no paw contact with the belt).
Propulsion duration (ms)	Time duration of the propulsion phase (maximum paw contact to just before the swing phase).
Absolute paw angle (°)	The angle that the paw makes with the long axis of the direction of motion of the animal.
Stride frequency (# of strides/second)	The number of times that a paw takes a complete stride in each second.
Stance width (cm)	The perpendicular distance between the centroids of forepaws or hindpaws during peak stance.

Acknowledgments

This work was supported by grant PI071133, TERCEL and CIBERNED funds from the Fondo de Investigación Sanitaria of Spain, grant SAF2009-12495 from the Ministerio de Ciencia e Innovación of Spain, FEDER funds, and Action COST-B30 of the EC. We thank the technical help of Jessica Jaramillo and Marta Morell. RM is recipient of a predoctoral fellowship from the Ministerio de Educación of Spain.

REFERENCES

Alves, C.J., de Santana, L.P., Santos, A.J., de Oliveira, G.P., Duobles, T., Scorisa, J.M., Martins, R.S., Maximino, J.R., Chadi, G., 2011. Early motor and electrophysiological changes in transgenic mouse model of amyotrophic lateral sclerosis and gender differences on clinical outcome. Brain Res. 1394, 90–104.

Amende, I., Kale, A., McCue, S., Glazier, S., Morgan, J.P., Hampton, T.G., 2005. Gait dynamics in mouse models of Parkinson's disease and Huntington's disease. J. Neuroeng. Rehabil. 2, 20.

Azzouz, M., Leclerc, N., Gurney, M., Warter, J.M., Poindron, P., Borg, J., 1997. Progressive motor neuron impairment in an animal model of familial amyotrophic lateral sclerosis. Muscle Nerve 20, 45–51.

Bosco, D.A., et al., 2010. Wild-type and mutant SOD1 share an aberrant conformation and a common pathogenic pathway in ALS. Nat. Neurosci. 13, 1396–1403.

Brooks, S.P., Dunnett, S.B., 2009. Tests to assess motor phenotype in mice: a user's guide. Nat. Rev. Neurosci. 10, 519–529.

Clarke, K.A., Still, J., 1999. Gait analysis in the mouse. Physiol. Behav. 66, 723–729.

De Medinaceli, L., Freed, W.J., Wyatt, R.J., 1982. An index of the functional condition of rat sciatic nerve based on measurements made from walking tracks. Exp. Neurol. 77, 634–643.

Fischer, L.R., Culver, D.G., Tennant, P., Davis, A.A., Wang, M., Castellano-Sanchez, A., Khan, J., Polak, M.A., Glass, J.D., 2004. Amyotrophic lateral sclerosis is a distal axonopathy: evidence in mice and man. Exp. Neurol. 185, 232–240.

Fischer, L.R., Culver, D.G., Davis, A.A., Tennant, P., Wang, M., Coleman, M., Asress, S., Adalbert, R., Alexander, G.M., Glass, J.D., 2005. The WldS gene modestly prolongs survival in the SOD1G93A fALS mouse. Neurobiol. Dis. 19, 293–300.

Gillette, R.L., Angle, T.C., 2008. Recent developments in canine locomotor analysis: a review. Vet. J. 178, 165–176.

Guillot, T.S., Asress, S.A., Richardson, J.R., Glass, J.D., Miller, G.W., 2008. Treadmill gait analysis does not detect motor deficits in animal models of Parkinson's disease or amyotrophic lateral sclerosis. J. Mot. Behav. 40, 568–577.

Gurney, M.E., Pu, H., Chiu, A.Y., Dal Canto, M.C., Polchow, C.Y., Alexander, D.D., Caliendo, J., Hentati, A., Kwon, Y.W., Deng, H.X., 1994. Motor neuron degeneration in mice that express a human Cu, Zn superoxide dismutase mutation. Science 264, 1772–1775.

Hampton, T.G., Stasko, M.R., Kale, A., Amende, I., Costa, A.C.S., 2004. Gait dynamics in trisomic mice: quantitative neurological traits of Down syndrome. Physiol. Behav. 82, 381–389.

Hegedus, J., Putman, C.T., Tyreman, N., Gordon, T., 2008. Preferential motor unit loss in the SOD1 G93A transgenic mouse model of amyotrophic lateral sclerosis. J. Physiol. (Lond.) 586, 3337–3351.

Kaplan, M.L., Murphy, S.D., 1972. Effect of acrylamide on rotarod performance and sciatic nerve -glucuronidase activity of rats. Toxicol. Appl. Pharmacol. 22, 259–268.

Kennel, P.F., Finiels, F., Revah, F., Mallet, J., 1996. Neuromuscular function impairment is not caused by motor neurone loss in FALS mice: an electromyographic study. Neuroreport 7, 1427–1431.

Knippenberg, S., Thau, N., Dengler, R., Petri, S., 2010. Significance of behavioural tests in a transgenic mouse model of amyotrophic lateral sclerosis (ALS). Behav. Brain Res. 213, 82–87.

Krouchev, N., Kalaska, J.F., Drew, T., 2006. Sequential activation of muscle synergies during locomotion in the intact cat as revealed by cluster analysis and direct decomposition. J. Neurophysiol. 96, 1991–2010.

Ludolph, A.C., Jesse, S., 2009. Review: evidence-based drug treatment in amyotrophic lateral sclerosis and upcoming clinical trials. Ther. Adv. Neurol. Disord. 2, 319–326.

Mahoney, D.J., Rodriguez, C., Devries, M., Yasuda, N., Tarnopolsky, M.A., 2004. Effects of high-intensity endurance exercise training in the G93A mouse model of amyotrophic lateral sclerosis. Muscle Nerve 29, 656–662.

Mancuso, R., Santos-Nogueira, E., Osta, R., Navarro, X., 2011. Electrophysiological analysis of a murine model of motoneuron disease. Clin Neurophysiol. 122, 1660–1670.

Miana-Mena, F.J., Muñoz, M.J., Yagüe, G., Mendez, M., Moreno, M., Ciriza, J., Zaragoza, P., Osta, R., 2005. Optimal methods to characterize the G93A mouse model of ALS. Amyotroph. Lateral Scler. Other Motor Neuron Disord. 6, 55–62.

Moreno-Igoa, M., Calvo, A.C., Penas, C., et al., 2010. Fragment C of tetanus toxin, more than a carrier. Novel perspectives in non-viral ALS gene therapy. J. Mol. Med. 88, 297–308.

Ripps, M.E., Huntley, G.W., Hof, P.R., Morrison, J.H., Gordon, J.W., 1995. Transgenic mice expressing an altered murine superoxide dismutase gene provide an animal model of amyotrophic lateral sclerosis. Proc. Natl. Acad. Sci. U.S.A. 92, 689–693.

Rosen, D.R., 1993. Mutations in Cu/Zn superoxide dismutase gene are associated with familial amyotrophic lateral sclerosis. Nature 364, 362.

Turner, B.J., Talbot, K., 2008. Transgenics, toxicity and therapeutics in rodent models of mutant SOD1-mediated familial ALS. Prog. Neurobiol. 85, 94–134.

Udina, E., Ceballos, D., Gold, B.G., Navarro, X., 2003. FK506 enhances reinnervation by regeneration and by collateral sprouting of nerve fibers. Exp. Neurol. 183, 220–231.

Valero-Cabré, A., Navarro, X., 2001. H reflex restitution and facilitation after different types of peripheral nerve injury and repair. Brain Res. 919, 302–312.

Varejão, A.S., Meek, M.F., Ferreira, A.J., Patrício, J.A., Cabrita, A.M., 2001. Functional evaluation of peripheral nerve regeneration in the rat: walking track analysis. J. Neurosci. Methods 108, 1–9.
Verdu, E., Vilches, J.J., Rodriguez, F.J., Ceballos, D., Valero, A., Navarro, X., 1999. Physiological and immunohistochemical characterization of cisplatin-induced neuropathy in mice. Muscle Nerve 22, 329–340.
Wijesekera, L.C., Leigh, P.N., 2009. Amyotrophic lateral sclerosis. Orphanet J. Rare Dis. 4, 3.
Wooley, C.M., Sher, R.B., Kale, A., Frankel, W.N., Cox, G.A., Seburn, K.L., 2005. Gait analysis detects early changes in transgenic SOD1(G93A) mice. Muscle Nerve 32, 43–50.
Worms, P.M., 2001. The epidemiology of motor neuron diseases: a review of recent studies. J. Neurol. Sci. 191, 3–9.

Chapter I: SOD1^{G93A} mouse model characterization

1.3. Pre-symptomatic electrophysiological tests predict clinical disease onset and survival in SOD1^{G93A} ALS mice

Mancuso R, Osta R, Navarro X. Pre-symptomatic electrophysiological tests predict clinical onset and survival in SOD1G93A ALS mice. Muscle Nerve, in press.

PRESYMPTOMATIC ELECTROPHYSIOLOGICAL TESTS PREDICT CLINICAL ONSET AND SURVIVAL IN SOD1^{G93A} ALS MICE

RENZO MANCUSO, MS,[1] ROSARIO OSTA, PhD,[2] and XAVIER NAVARRO, PhD, MD[1]

[1]Group of Neuroplasticity and Regeneration, Institute of Neurosciences and Department of Cell Biology, Physiology and Immunology, Universitat Autònoma de Barcelona, and Centro de Investigación Biomédica en Red sobre Enfermedades Neurodegenerativas (CIBERNED), Bellaterra, Spain

[2]Laboratory of Genetic Biochemistry (LAGENBIO-I3A), Aragon Institute of Health Sciences, Universidad de Zaragoza, Zaragoza, Spain

Accepted 6 March 2014

ABSTRACT: *Introduction:* We assessed the predictive value of electrophysiological tests as a marker of clinical disease onset and survival in superoxide-dismutase 1 (SOD1)^{G93A} mice. *Methods:* We evaluated the accuracy of electrophysiological tests in differentiating transgenic versus wild-type mice. We made a correlation analysis of electrophysiological parameters and the onset of symptoms, survival, and number of spinal motoneurons. *Results:* Presymptomatic electrophysiological tests show great accuracy in differentiating transgenic versus wild-type mice, with the most sensitive parameter being the tibialis anterior compound muscle action potential (CMAP) amplitude. The CMAP amplitude at age 10 weeks correlated significantly with clinical disease onset and survival. Electrophysiological tests increased their survival prediction accuracy when evaluated at later stages of the disease and also predicted the amount of lumbar spinal motoneuron preservation. *Conclusions:* Electrophysiological tests predict clinical disease onset, survival, and spinal motoneuron preservation in SOD1^{G93A} mice. This is a methodological improvement for preclinical studies.

Muscle Nerve **000**:000–000, 2014

Amyotrophic lateral sclerosis (ALS) is the most common form of adult motoneuron disease (MND). It is characterized by progressive degeneration of motoneurons (MN) in the motor cortex, brainstem, and spinal cord. Given the lack of biomarkers, diagnosis is based mainly on clinical and electrophysiological findings.[1–3]

Transgenic mice that overexpress the mutant superoxide-dismutase 1 *SOD1*^{G93A} gene[4] constitute the most widely used model of ALS. High copy *SOD1*^{G93A} transgenic mice develop rapidly progressive MN loss, with locomotor deficits beginning at age 12–13 weeks, characterized by hindlimb weakness and muscle atrophy, culminating in paralysis and death between ages 16 and 19 weeks.[5,6] Although *C9ORF72* gene mutations are reported in a higher proportion of ALS and ALS-frontotemporal lobar degeneration (FTLD) patients,[7,8] *SOD1*-based models are still an important tool for basic research and preclinical studies. Alterations in SOD1 protein have also been found in sporadic ALS patients,[9] and accumulation of wild type SOD1 was reported to produce ALS in mice.[10]

A key problem in development of new therapies for ALS is the failure to translate positive experimental results into successful human trials.[11,12] This may raise concerns about the validity of ALS animal models, but it also may be related to methodological shortcomings. Thus, it is important to develop and apply techniques that provide reliable, objective preclinical results. Electrophysiological tests are the most important tool for diagnosis and monitoring of disease progression in human ALS.[13–15] The electrophysiological profile of ALS animal models has been studied by our group and others.[16–18] Although general guidelines have been agreed upon for behavioral and histological evaluation of animal research on ALS/MND,[19,20] few studies have focused on developing new tools that permit the correct interpretation of the findings from preclinical studies. We propose that analysis of lower and upper MN function in presymptomatic animals (ages 8 to 10 weeks) and at late stages of the disease by means of nerve conduction studies and evoked potentials is a reliable, objective biomarker for predicting clinical disease onset and survival in *SOD1*^{G93A} ALS mice.

MATERIAL AND METHODS

Transgenic Mice. Transgenic mice with the G93A human *SOD1* mutation (B6SJL-Tg[SOD1-G93A]1Gur) were obtained from the Jackson Laboratory (Bar Harbor, ME, USA) and maintained at the Animal Service of the Universidad de Zaragoza. Hemizygote B6SJL *SOD1*^{G93A} males were obtained by crossing with B6SJL females from the CBATEG (Barcelona, Spain). The offspring was identified with polymerase chain reaction amplification of DNA extracted from tail tissue. A total of 154 transgenic

Additional supporting information may be found in the online version of this article.

Abbreviations: ALS, amyotrophic lateral sclerosis; CMAP, compound muscle action potential; FTLD, frontotemporal lobar degeneration; MEP, motor evoked potential; MN, motoneuron; MND, motoneuron disease; MUNE, motor unit number estimation; SOD1, superoxide dismutase 1; TA, tibialis anterior

Key words: amyotrophic lateral sclerosis; biomarkers; electrophysiology; motoneuron disease; SOD1

This work was supported by TERCEL and CIBERNED funds and grant PI10/01787 from the Instituto de Salud Carlos III, grant SAF2009-12495 from the Ministerio de Ciencia e Innovación of Spain, and FEDER funds. RM is recipient of a predoctoral fellowship from the Ministerio de Educación of Spain.

Correspondence to: X. Navarro; Unitat de Fisiologia Mèdica, Facultat de Medicina, Universitat Autònoma de Barcelona, E-08193 Bellaterra, Spain; e-mail: xavier.navarro@uab.cat

Published online 00 Month 2014 in Wiley Online Library (wileyonlinelibrary.com). DOI 10.1002/mus.24237

mice were used in this study: 126 for the accuracy assessment, 20 for the correlation with onset and survival, and 8 for the histological analysis. All experimental procedures were approved by the Ethics Committee of the Universitat Autònoma de Barcelona.

Rotarod Test. The rotarod test was performed to assess the onset and progression of motor disability during the course of the disease.[19,21] Animals were trained 3 times per week on a rod rotating at 14 rpm and then were tested weekly from ages 8 to 16 weeks, with an arbitrary maximum time of maintenance on the rotating rod of 180 s. Clinical disease onset was defined as the first week when animals were not able to hold on to the rotating rod for 180 s.

Electrophysiological tests. Electrophysiological tests have previously been described as markers of disease progression in ALS mice.[16,17] Motor nerve conduction tests were performed from ages 8 to 16 weeks based on previous observations.[16,17,22] The sciatic nerve was stimulated percutaneously by means of single 0.02 ms duration pulses (Grass S88) delivered through a pair of needle electrodes placed at the sciatic notch. The compound muscle action potential (CMAP, M wave) and the reflex H wave were recorded from the tibialis anterior (TA) and plantar interosseus muscles with microneedle electrodes. To ensure reproducibility, the recording needles were placed under a microscope to insure the same placement in all animals guided by anatomical landmarks. The active recording electrode was placed subcutaneously in the first third of the distance between knee and ankle when recording from the TA muscle, and in the third metatarsal space when recording from plantar muscle.[16,23,24] The amplitudes of the maximal M and H waves were measured. Because increased MN[16] and motor axon[25] excitability has been described previously in SOD1^{G93A} mice, we calculated the H/M amplitude ratio for assessment of spinal reflex function.[16,23] For evaluation of the central motor pathways, motor evoked potentials (MEPs) were recorded from TA and plantar muscles in response to transcranial electrical stimulation of the motor cortex by single rectangular 0.1 ms duration pulses delivered through needle electrodes inserted subcutaneously, with the cathode over the skull overlaying the sensorimotor cortex and the anode at the nose.[16,26] All potentials were amplified and displayed on a digital oscilloscope (Tektronix 450S) at settings appropriate for amplitude measurement from the baseline to the maximal negative peak. During the tests, mouse body temperature was kept constant between 34 and 36°C by means of a thermostat-controlled heating pad.

Histology. At age 16 weeks, 8 mice (4 of each gender) were transcardially perfused with 4% paraformaldehyde in phosphate buffered saline. The lumbar segment of the spinal cord was removed, post-fixed for 24 h, and cryopreserved in 30% sucrose. Transverse 40-μm-thick sections were cut serially with a cryotome (Leica) between the L2 and L5 segmental levels. For each segment, series of 10 sections each were collected on separate gelatin-coated slides. One slide of each animal was rehydrated for 1 min and stained for 2 h with an acidified solution of 3.1 mM cresyl violet. Then, the slides were washed in distilled water for 1 min, dehydrated, and mounted with DPX (Fluka). MNs were identified by their localization in the ventral horn of the stained spinal cord sections and counted following strict size and morphological criteria; only MNs with diameters larger than 20 μm and with a polygonal shape and prominent nucleoli were counted. The number of MNs present in both ventral horns was counted in 4 serial sections of the L4 and L5 segments.[16,27]

Survival. The end point of the disease was defined as the time when a mouse was unable to right itself within 30 s when placed on its side.

Data Analysis. Data are expressed as mean ± SEM. Electrophysiological test results were analyzed statistically using analysis of variance for repeated measurements, applying a Bonferroni *post hoc* test when necessary. Histological data were analyzed using the Mann-Whitney *U*-test. Survival and clinical disease onset data were analyzed using the Kaplan-Meier test.

The accuracy of the tests was expressed by 2 different parameters. The sensitivity represents the percentage of SOD1^{G93A} mice that were correctly considered to be transgenic animals, whereas the specificity is the percentage of wild-type mice that were correctly considered to be healthy animals. Thus, the maximum accuracy is achieved when both parameters are 100%.

To assess the predictive value of electrophysiological tests, we performed a linear regression analysis between nerve conduction parameters and onset of symptoms and survival of the animals. Furthermore, we calculated the correlation between variables using Pearson and Spearman correlations for quantitative versus quantitative and quantitative versus qualitative variables, respectively.

RESULTS

Classical Disease Progression Markers. SOD1^{G93A} mice of both genders had the same median onset of symptoms, evaluated with rotarod tests, at age

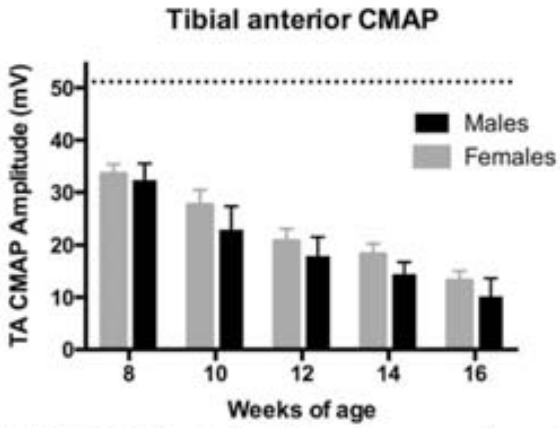

FIGURE 1. Tibialis anterior (TA) muscle compound muscle action potential (CMAP) amplitude. Note the progressive decline between ages 8 and 16 weeks. The dashed line represents the mean value of wild type mice.

84 days. Survival was significantly different between genders ($P < 0.01$), with a median survival of age 132 days for females and 128 for males. MN number counts revealed that the number of surviving MN at age 16 weeks was 23.3 ± 2.5 and 24.5 ± 2.2 in female and male mice, respectively, values which were not different between genders.

Electrophysiological Test Results. Supplementary Tables S1 and S2, which are available online, summarize the main electrophysiological results found during the presymptomatic phase of disease progression between ages 8 and 12 weeks. TA CMAP amplitude showed a progressive decline from presymptomatic (8 weeks) to the end stage of the disease (16 weeks) (Fig. 1), whereas plantar CMAP amplitude dropped dramatically at 12 weeks of age. The MEP/M ratio markedly decreased at 12 weeks of age in the TA muscle but remained unchanged in the plantar muscle. On the contrary, the H/M ratio was increased at 12 weeks of age in the plantar but not in the TA muscle.

Electrophysiological Test Accuracy. Tables 1 and 2 summarize the electrophysiological parameters during the presymptomatic phase, between age 8 and 12 weeks. The TA CMAP latency shows high sensitivity at ages 10 and 12 weeks, and 100% of specificity at all time points. The TA CMAP amplitude shows the highest values for sensitivity among all the considered parameters, reaching 90% and 100% at 10 and 12 weeks, respectively.

Early Electrophysiological Results Predict Clinical Disease Onset and Survival. To assess the potential predictive value of electrophysiological tests on clinical disease onset and survival, we made a set of linear correlations (Table 3). Although some parameters showed significant correlations, the TA CMAP amplitude results most consistently predicted the onset and survival of SOD1^{G93A} mice of both genders. The TA CMAP amplitude recorded at age 10 weeks showed significant correlations with both clinical disease onset and survival in female and male mice, with correlation indices between 0.7 and 0.8 (Fig. 2).

Late Electrophysiological Results Increase Predictive Power. We further investigated the predictive value of the TA CMAP amplitude when it was recorded at a later disease stage (16 weeks), at which time clear signs of motor impairment are observed. The TA CMAP amplitude correlated significantly with survival ($P < 0.01$) (Fig. 3). The correlation coefficient was higher than in earlier disease stages. We also performed linear regression analysis of the TA CMAP amplitude versus the number of MN in the lumbar spinal cord. The relationship was highly significant ($P < 0.01$) with an r^2 value of 0.82 (Fig. 3).

DISCUSSION

The aim of this study was to determine the potential predictive value of electrophysiological tests as a marker of clinical disease onset and

Table 1. Sensitivity of Electrophysiological Tests on 8-, 10-, and 12-Week-Old Animals.*

Muscle	Electrophysiological parameter	8-Weeks-old Sensitivity (%) F	8-Weeks-old Sensitivity (%) M	10-Weeks-old Sensitivity F	10-Weeks-old Sensitivity M	12-Weeks-old Sensitivity F	12-Weeks-old Sensitivity M
Plantar	Initial latency	0	10	10	20	30	20
	Amplitude	0	0	10	0	40	90
	H/M ratio	40	40	80	30	40	60
	MEP/ratio	0	0	0	0	0	0
Tibialis anterior	Initial latency	30	40	50	80	60	90
	Amplitude	80	80	90	90	100	100
	H/M ratio	30	30	60	30	20	30
	MEP/ratio	0	0	10	0	10	40

*Sensitivity is expressed as the percentage of animals that were correctly classified as ALS mice. Plantar cut-off values: initial latency, 1.94 ms; amplitude, 3.82 mV; H/M ratio, 8.30%; MEP/M ratio, 1.83%. Tibialis anterior cut off values: 0.98 ms; 39.66 mV; 6.32% and 6.86%, respectively. Bold characters highlight the most accurate parameter.

Table 2. Specificity of Electrophysiological Tests on 8-, 10-, and 12-Week-Old Animals.*

Muscle	Electrophysiological parameter	8-Weeks-old Specificity (%)		10-Weeks-old Specificity		12-Weeks-old Specificity	
		F	M	F	M	F	M
Plantar	Initial latency	100	100	100	100	100	100
	Amplitude	100	100	100	100	100	100
	H/M ratio	40	40	50	40	30	40
	MEP/Mratio	100	100	100	100	100	100
Tibialis anterior	Initial latency	100	100	100	100	100	100
	Amplitude	100	100	100	100	100	100
	H/M ratio	100	100	100	80	90	80
	MEP/Mratio	100	80	100	100	100	100

Sensitivity is expressed as the percentage of animals that were correctly classified to be ALS mice. Plantar cut-off values: initial latency, 1.94ms; amplitude, 3.82mV; H/M ratio, 8.30% MEP/M ratio, 1.83%. Tibialis anterior cut-off values: 0.98 ms; 39.66 mV; 6.32% and 6.86%, respectively. Bold characters highlight the most accurate parameter.

progression in the SOD1^{G93A} model of ALS. The results indicate that early presymptomatic electrophysiological tests demonstrated great accuracy in differentiating transgenic versus wild type animals, which was especially notable for TA CMAP amplitude. The TA CMAP amplitude recorded at age 10 weeks correlated significantly with both clinical disease onset and survival. Finally, the survival prediction of the electrophysiological results increased at the disease end stage, when it also correlated significantly with the number of preserved MN in the lumbar spinal cord.

The development of new therapies for any disease suggests translation from experimental studies to human trials. In ALS, this issue has raised concerns, because there has been a lack of successful translational findings. Unfortunately, there are several shortcomings in most of the currently existing techniques. Despite consensus efforts to develop agreed-upon guidelines for preclinical studies in ALS/MND animal models,[19] reliable objective markers of clinical disease onset and progression are lacking. Ludolph *et al.*[19] recently summarized the most commonly applied tests in ALS mice. Briefly, they considered that an optimal experimental design must include an onset measure, a quantitative measure of disease progression, a survival analysis, and MN count. Unfortunately, the classical techniques used for these purposes may be inadequate. First, clinical disease onset and progression are analyzed using rotarod and hangwire tests, and sometimes arbitrary neurological scores.[28–30] However, these methods are not sufficiently specific and may be biased due to behavioral effects (*e.g.*, animals need to be trained regularly to learn the task properly, and their performance depends on individual behavior) and researcher objectivity. Second, survival analysis is mandatory for preclinical study publication. However, this raises some concerns given the lack of interlaboratory reproducibility. It has been shown that genetic background affects SOD1^{G93A} mice survival.[31] Moreover, in recent studies we observed that B6SJL SOD1^{G93A} animals bred from animals purchased from different sources showed significantly different life spans.[32] These observations, together with the ethical concerns raised by the survival analysis itself might compromise preclinical studies based on survival.

Electrophysiological tests are widely used to diagnose and monitor disease progression in ALS patients.[13–15] In fact, Maathuis *et al.*[33] recently highlighted the potential predictive value of these techniques to quantify disease progression in human patients. Motor unit number estimation (MUNE) has been proposed to reliably monitor disease progression in ALS patients.[34] Shefner *et al.*[18] found that MUNE can also predict clinical

Table 3. *P*-Values from Linear Correlation between the Electrophysiological Parameters and Onset and Survival of the Animals.*

Muscle	Electrophysiological parameter	Onset		Survival	
		Females	Males	Females	Males
Plantar interosseus	Initial latency	$<0.05r^2 = 0.569$	0.519	0.629	0.544
	Amplitude	0.914	0.733	0.105	0.998
	MEP/M ratio	0.744	0.167	0.326	$<0.05r^2 = 0.655$
Tibialis anterior	Initial latency	0.875	0.059	$<0.05r^2 = -0.636$	0.070
	Amplitude	$<0.01r^2 = 0.783$	$<0.01r^2 = 0.692$	$<0.01r^2 = 0.772$	$<0.01r^2 = 0.742$
	MEP/M ratio	0.626	0.229	0.549	0.091

When $P < 0.05$ (underlined values), r^2 is shown.

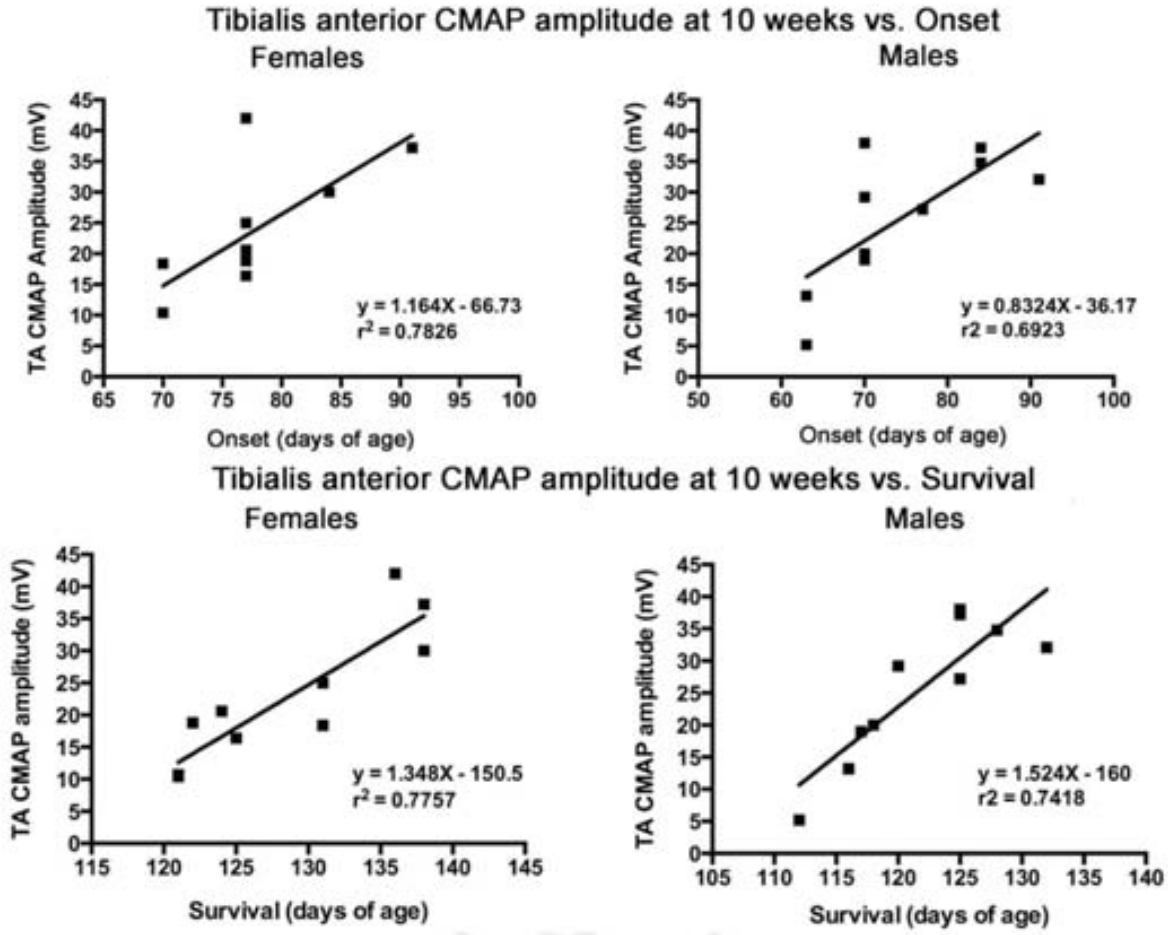

FIGURE 2. Linear regression analysis between tibialis anterior CMAP amplitude at age 10 weeks and clinical disease onset and survival. Results from male and female animals are shown separately. In all 4 plots, there was a significant correlation with Spearman correlation coefficients (r^2) higher than 0.69 for onset comparisons and Pearson correlation indices higher than 0.74 for survival comparisons.

disease onset and survival in SOD1^{G93A} mice. Although some MNs have the ability to generate compensatory collateral sprouts,[35] this capacity seems to be poor,[36] and it is not clear whether it translates into a sustained functional effect. In fact, single motor unit potentials remain unchanged during disease progression in ALS mice,[16,18] suggesting lack of collateral sprouting. As we previously reported,[16] this lack of compensatory sprouting means that recording of CMAPs by nerve conduction tests would be adequate as a marker of muscle innervation. Therefore, we propose the use of CMAP amplitude instead of MUNE as a marker of disease progression in ALS mice, because as shown in this study, CMAP amplitude has good predictive value regarding clinical disease onset and survival. Li *et al.*[37] have recently reported that other electrophysiological measurements, such as the decline of electrical impedance myography also correlated with SOD1^{G93A} mouse survival.

The main goal of this study was to determine whether electrophysiological analysis of upper and lower MN function might serve as an indicator of clinical disease onset and survival of SOD1^{G93A} mice. The correlation analysis of upper MN function (MEP/M ratio) revealed that central motor conduction is not an early predictor, because the first abnormal values were detected from age 12 weeks, coincident with the onset of clinical signs in the rotarod test. These findings are in agreement with previous studies showing that SOD1^{G93A} mice develop a lumbosacral type of ALS in which upper MN contribution is delayed with respect to muscle denervation.[16,38] Regarding lower MN function, our results revealed a different pattern of decline of the CMAP amplitude in TA and plantar muscles, with the first signs of muscle denervation in the TA muscle rather than in the more distal plantar muscle. Nevertheless, coincident with clinical disease onset (12 weeks of age), plantar muscle

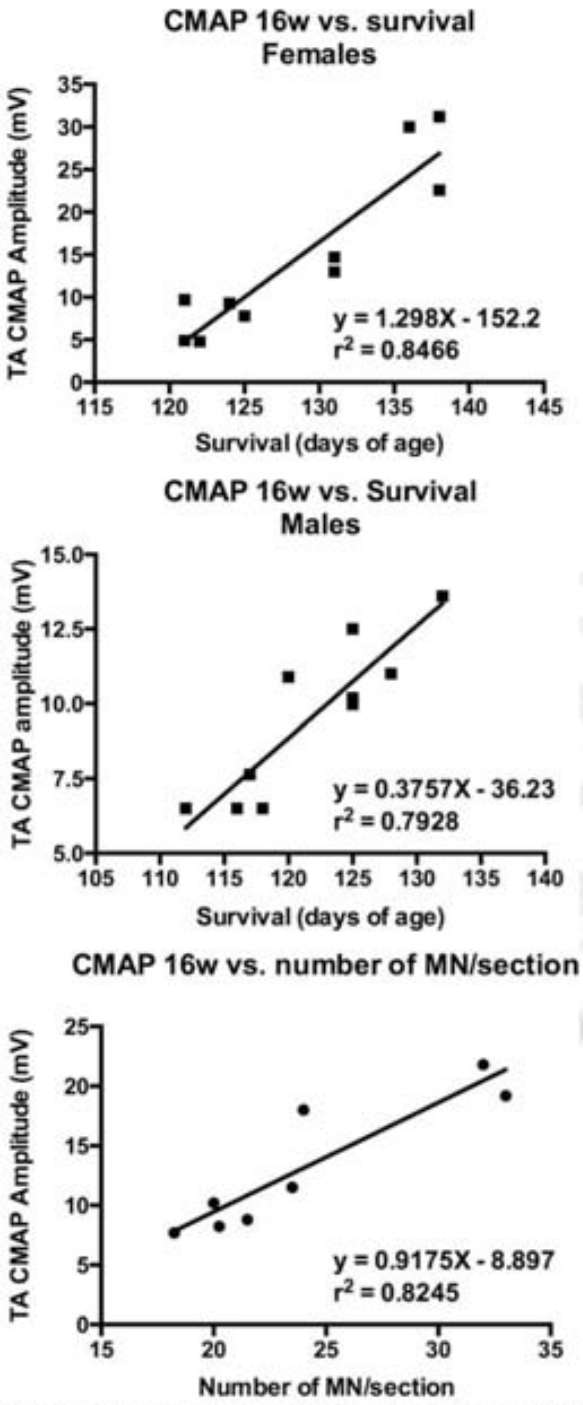

FIGURE 3. Linear correlation between tibialis anterior CMAP amplitude at age 16 weeks and survival and between tibialis anterior CMAP at age 16 weeks and number of surviving motoneurons. For survival comparisons, results from male and female mice are shown separately. For motoneuron preservation comparison, data from male and female animals were pooled. In all cases, there was a significant correlation between parameters with Pearson correlation coefficients (r^2) higher than 0.79. Note that correlation coefficients of survival comparisons are higher than those obtained with CMAPs at age 10 weeks.

CMAP amplitude suffered a marked decrease to comparative values lower than in the TA muscle. These findings suggest that the disease process begins in localized groups of motoneurons and then spreads to neighboring motoneuronal pools, as observed in ALS patients.[39] Although increased MN[16] and motor axon[25] excitability has been described in SOD1^{G93A} mice, our spinal excitability results showed no significant changes in the H/M ratio during the presymptomatic phase of the disease in either tested muscle. Therefore, the H/M ratio is not a good predictor of clinical features in this mouse model.

Diagnostic accuracy defines the ability of a test to discriminate between healthy and sick individuals. We estimated the sensitivity as the percentage of SOD1^{G93A} mice that were correctly considered to be transgenic animals, and the specificity as the proportion of wild type mice that were correctly considered to be healthy animals. Of the various electrophysiological parameters reflecting lower MN function, our findings suggest that the amplitude of the TA CMAP has the highest predictive power, given its progressive decline from early presymptomatic to late stages of the disease. The TA CMAP was the most accurate test result, achieving 90% sensitivity and specificity at age 10 weeks (*i.e.*, it only allows for 10% false negative and 10% false positive "diagnoses"). Further analysis revealed that the TA CMAP amplitude at early stages strongly correlates with both onset of symptoms and survival of SOD1^{G93A} mice. Furthermore, the TA CMAP amplitude at age 16 weeks has even higher correlation with survival, and it was also correlated with the number of preserved spinal MN. These findings represent an improvement in terms of animal testing during preclinical studies, because electrophysiological tests are performed easily, are objective, show small variability, and can be translated directly to human clinical studies.

We are grateful for the technical help of Jessica Jaramillo and Marta Morell and the statistical advice of Dr Albert Navarro (Biostatistics Unit, Faculty of Medicine, Universitat Autònoma de Barcelona).

REFERENCES

1. Wijesekera LC, Leigh PN. Amyotrophic lateral sclerosis. Orphanet J Rare Dis 2009;4:3.
2. Worms PM. The epidemiology of motor neuron diseases: a review of recent studies. J Neurol Sci 2001;191:3–9.
3. Turner MR, Kiernan MC, Leigh PN, Talbot K. Biomarkers in amyotrophic lateral sclerosis. Lancet Neurol 2009;8:94–109.
4. Rosen DR. Mutations in Cu/Zn superoxide dismutase gene are associated with familial amyotrophic lateral sclerosis. Nature 1993;364:362.
5. Ripps ME, Huntley GW, Hof PR, Morrison JH, Gordon JW. Transgenic mice expressing an altered murine superoxide dismutase gene provide an animal model of amyotrophic lateral sclerosis. Proc Natl Acad Sci U S A 1995;92:689–693.
6. Pasinelli P, Brown RH. Molecular biology of amyotrophic lateral sclerosis: insights from genetics. Nat Rev Neurosci 2006;7:710–723.
7. Renton AE, Majounie E, Waite A, Waite A, Simón-Sánchez J, Rollinson S, et al. A Hexanucleotide repeat expansion in C9ORF72 is

the cause of chromosome 9p21-linked ALS-FTD. Neuron 2011;72: 257–268.
8. DeJesus-Hernandez M, Mackenzie IR, Boeve BF, Boxer AL, Baker M, Rutherford NJ, et al. Expanded GGGGCC hexanucleotide repeat in noncoding region of C9ORF72 causes chromosome 9p-linked FTD and ALS. Neuron 2011;72:245–256.
9. Bosco DA, Morfini G, Karabacak NM, Song Y, Gros-Louis F, Pasinelli P, et al. Wild-type and mutant SOD1 share an aberrant conformation and a common pathogenic pathway in ALS. Nat Neurosci 2010;13: 1396–1403.
10. Graffmo KS, Forsberg K, Bergh J, Birve A, Zetterström P, Andersen PM, et al. Expression of wild-type human superoxide dismutase-1 in mice causes amyotrophic lateral sclerosis. Hum Mol Genet 2013;22: 51–60.
11. Rothstein JD. Of mice and men: reconciling preclinical ALS mouse studies and human clinical trials. Ann Neurol 2003;53:423–426.
12. Benatar M. Lost in translation: treatment trials in the SOD1 mouse and in human ALS. Neurobiol Dis 2007;26:1–13.
13. Mitsumoto H, Ulug AM, Pullman SL, Gooch CL, Chan S, Tang MX, et al. Quantitative objective markers for upper and lower motor neuron dysfunction in ALS. Neurology 2007;68:1402–1410.
14. Krarup C. Lower motor neuron involvement examined by quantitative electromyography in amyotrophic lateral sclerosis. Clin Neurophysiol 2011;122:414–422.
15. Hardiman O, van den Berg LH, Kiernan MC. Clinical diagnosis and management of amyotrophic lateral sclerosis. Nat Rev Neurol 2011;7: 639–649.
16. Mancuso R, Santos-Nogueira E, Osta R, Navarro X. Electrophysiological analysis of a murine model of motoneuron disease. Clin Neurophysiol 2011;122:1660–1670.
17. Azzouz M, Leclerc N, Gurney M, Warter JM, Poindron P, Borg J. Progressive motor neuron impairment in an animal model of familial amyotrophic lateral sclerosis. Muscle Nerve 1997;20:45–51.
18. Shefner JM, Cudkowicz M, Brown RH. Motor unit number estimation predicts disease onset and survival in a transgenic mouse model of amyotrophic lateral sclerosis. Muscle Nerve 2006;34:603–607.
19. Ludolph AC, Bendotti C, Blaugrund E, Chio A, Greensmith L, Loeffler JP, et al. Guidelines for preclinical animal research in ALS/MND: a consensus meeting. Amyotroph Lateral Scler 2010;11:38–45.
20. Ludolph AC, Bendotti C, Blaugrund E, Hengerer B, Löffler JP, Martin J, et al. Guidelines for the preclinical in vivo evaluation of pharmacological active drugs for ALS/MND: report on the 142nd ENMC international workshop. Amyotroph Lateral Scler 2007;8:217–223.
21. Brooks SP, Dunnett SB. Tests to assess motor phenotype in mice: a user's guide. Nat Rev Neurosci 2009;10:519–529.
22. Kennel PF, Finiels F, Revah F, Mallet J. Neuromuscular function impairment is not caused by motor neurone loss in FALS mice: an electromyographic study. Neuroreport 1996;7:1427–1431.
23. Valero-Cabré A, Navarro X. H reflex restitution and facilitation after different types of peripheral nerve injury and repair. Brain Res 2001; 919:302–312.
24. Navarro X, Udina E. Chapter 6 - Methods and protocols in peripheral nerve regeneration experimental research: part III-electrophysiological evaluation. Int Rev Neurobiol 2009;87:105–126.
25. Boërio D, Kalmar B, Greensmith L, Bostock H. Excitability properties of mouse motor axons in the mutant SOD1(G93A) model of amyotrophic lateral sclerosis. Muscle Nerve 2010;41:774–784.
26. Garcéa-Alías G, Verdú E, Forés J, López-Vales R, Navarro X. Functional and electrophysiological characterization of photochemical graded spinal cord injury in the rat. J Neurotrauma 2003;20:501–510.
27. Penas C, Casas C, Robert I, Forés J, Navarro X. Cytoskeletal and activity-related changes in spinal motoneurons after root avulsion. J Neurotrauma 2009;26:763–779.
28. Knippenberg S, Thau N, Dengler R, Petri S. Significance of behavioural tests in a transgenic mouse model of amyotrophic lateral sclerosis (ALS). Behav Brain Res 2010;213:82–87.
29. Alves CJ, de Santana LP, dos Santos AJD, Oliveira GP, Duobles T, Scorisa JM, et al. Early motor and electrophysiological changes in transgenic mouse model of amyotrophic lateral sclerosis and gender differences on clinical outcome. Brain Res 2011;1394:90–104.
30. Miana-Mena FJ, Muñoz MJ, Yagüe G, Mendez M, Moreno M, Ciriza J, et al. Optimal methods to characterize the G93A mouse model of ALS. Amyotroph Lateral Scler 2005;6:55–62.
31. Heiman-Patterson TD, Sher RB, Blankenhorn EA, Alexander G, Deitch JD, Kunst CB, et al. Effect of genetic background on phenotype variability in transgenic mouse models of amyotrophic lateral sclerosis: a window of opportunity in the search for genetic modifiers. Amyotroph Lateral Scler 2011;12:79–86.
32. Mancuso R, Oliván S, Rando A, Casas C, Osta R, Navarro X. Sigma-1R agonist improves motor function and motoneuron survival in ALS mice. Neurotherapeutics 2012;9:814–826.
33. Maathuis EM, Drenthen J, van Doorn PA, Visser GH, Blok JH. The CMAP scan as a tool to monitor disease progression in ALS and PMA. Amyotroph Lateral Scler Frontotemporal Degener 2013;14: 217–223.
34. Eisen A, Swash M. Clinical neurophysiology of ALS. Clin Neurophysiol 2001;112:2190–2201.
35. Schaefer AM, Sanes JR, Lichtman JW. A compensatory subpopulation of motor neurons in a mouse model of amyotrophic lateral sclerosis. J Comp Neurol 2005;490:209–219.
36. Frey D, Schneider C, Xu L, Borg J, Spooren W, Caroni P. Early and selective loss of neuromuscular synapse subtypes with low sprouting competence in motoneuron diseases. J Neurosci 2000;20:2534–2542.
37. Li J, Sung M, Rutkove SB. Electrophysiologic biomarkers for assessing disease progression and the effect of riluzole in SOD1 G93A ALS mice. PLoS One 2013;8:e65976.
38. Ozdinler PH, Benn S, Yamamoto TH, Günzel M, Brown R, Macklis JD. Corticospinal motor neurons and related subcerebral projection neurons undergo early and specific neurodegeneration in hSOD1G93A transgenic ALS mice. J Neurosci 2011;31:4166–4177.
39. Brown RH. Amyotrophic lateral sclerosis: recent insights from genetics and transgenic mice. Cell 1995;80:687–692.

Chapter I: SOD1^{G93A} mouse model characterization

1.4. Differences in the disease progression depending on the genetic background of SOD1^{G93A} mice

Mancuso R, Oliván S, Mancera P, Pastén-Zamorano A, Manzano R, Casas C, Osta R, Navarro X. Effect of genetic background on onset and disease progression in the SOD1^{G93A} model of amyotrophic lateral sclerosis. Amyotrophic Lateral Sclerosis 2012, 13:302-310.

Amyotrophic Lateral Sclerosis, 2012; Early Online: 1–9

informa
healthcare

ORIGINAL ARTICLE

Effect of genetic background on onset and disease progression in the SOD1-G93A model of amyotrophic lateral sclerosis

RENZO MANCUSO[1], SARA OLIVÁN[2], PILAR MANCERA[3], ANDREA PASTÉN-ZAMORANO[3], RAQUEL MANZANO[2], CATY CASAS[1], ROSARIO OSTA[2] & XAVIER NAVARRO[1]

[1]*Group of Neuroplasticity and Regeneration, Institute of Neurosciences and Department of Cell Biology, Physiology and Immunology, Universitat Autònoma de Barcelona, and Centro de Investigación Biomédica en Red sobre Enfermedades Neurodegenerativas (CIBERNED), Bellaterra,* [2]*Laboratory of Genetic Biochemistry (LAGENBIO-I3A), Aragon Institute of Health Sciences, Universidad de Zaragoza, Zaragoza, and* [3]*Neurotec Pharma SL, Bioincubadora PCB-Santander, Parc Científic de Barcelona, Barcelona, Spain*

Abstract

Knowledge of the potential effect of genetic background in disease models is important. The SOD1-G93A transgenic mouse is the most widely used model in amyotrophic lateral sclerosis (ALS). Since these animals show considerable variability both in the onset and the progression of the disease, this study aimed to characterize the potential differences between the two most widely used strains, C56BL/6 (B6) and B6SJL. A rotarod test was carried out to assess strength and motor coordination, while electrophysiology tests were performed to evaluate the function of upper and lower motor neurons. Survival of the animals and motor neuron loss were also studied. The results did not show any background effect regarding the rotarod test, despite the differences in the pattern of decline in central and peripheral motor conduction. The onset of motor neuron abnormalities was later in B6SJL mice, but progressed more rapidly. Lifespan was longer for B6 than for B6SJL animals. In conclusion, background differences in disease onset and progression are important. The characteristics of the strain should be taken into account in experimental design of therapeutic studies.

Key words: *Motor neuron disease, neurodegeneration, SOD1-G93A mouse, background, animal model*

Introduction

Amyotrophic lateral sclerosis (ALS), the most common form of motor neuron (MN) disease, is characterized by degeneration of MNs in the motor cortex, brainstem and spinal cord. ALS manifests as weakness, muscle atrophy and progressive paralysis with a life expectancy of three to five years from first symptom (1–3). Although most cases of ALS are sporadic in origin, 10–15% are inherited and related to genetic mutations, such as those in the gene encoding for the superoxide dismutase-1 (SOD1) enzyme or the recently described hexanucleotide expansion in the non-coding region of C9ORF72 (4,5). Interestingly, it has been recently reported that alterations in SOD1 protein also appear in sporadic ALS cases (6). There is limited correlation between phenotype and genotype, as members of families carrying the same mutation have significant differences in the severity of their illness (7,8). The variations in onset and severity of human ALS patients with identical SOD1 mutations suggest that there are other genetic modifiers of the disease.

Based on the genetic mutations described in the familial cases of ALS (9), several animal models mimicking the disease have been developed. The most widely used is the SOD1-G93A transgenic mouse, which overexpresses the G93A human mutant form of SOD1, either in high copy (25 copies of the gene) or low copy (eight or 10 copies) numbers (8–11). High copy SOD1 transgenic mice develop rapidly progressive MN degeneration, which leads to locomotor deficits starting at 12–13 weeks with weakness, dragging of hindlimbs and loss of coordination, and ending up with hindlimb paralysis.

Correspondence: X. Navarro, Unitat de Fisiologia Mèdica, Facultat de Medicina, Universitat Autònoma de Barcelona, E-08193 Bellaterra, Spain. E-mail: xavier.navarro@uab.cat

(Received 11 October 2011; accepted 29 January 2012)

ISSN 1748-2968 print/ISSN 1471-180X online © 2012 Informa Healthcare
DOI: 10.3109/ 17482968.2012.662688

and death between 16 and 19 weeks of age (10–12). However, these animals show considerable variability both in the onset and progression of the clinical signs during the disease process, indicating that genetic variability can modify disease phenotype. It has been observed that SOD1-G93A transgenic mice show significant differences regarding their lifespan depending on the genetic background either in high copy animals (13,14) or low copy animals (15). These differences in lifespan depending on background are also present in other animal models mimicking MN diseases, such as the ALS2/alsin deficient mice (16), and models of neuromuscular disorders (17,18). Moreover, it has been shown also that other animal models not related with neurological disorders are sensitive to genetic background effects (19,20). All these data highlight that the genetic background may be an important factor which modifies the disease characteristics in relevant animal models.

Characterization of the potential differences between strains used to study neurodegenerative diseases, such as ALS, is essential because the potential efficacy of any new therapeutic approach is directly related with the onset of the treatment and, ultimately, with the disease progression in a specific animal model. For this reason, we have studied the background effect on the onset and progression of MN disease by comparing the two most widely used strains of transgenic mice overexpressing mutant SOD1-G93A: C56BL/6J (B6) and B6SJL (21–24).

Material and methods

Transgenic mice

Two different strains expressing G93A human SOD1 mutations were compared. For the development of B6SJL background mice, transgenic animals with the G93A human SOD1 mutation (B6SJL-Tg[SOD1-G93A]1Gur) were obtained from the Jackson Laboratory (Bar Harbor, ME, USA), and provided from the colony maintained at the Unidad Mixta de Investigacion of the University of Zaragoza. Hemizygotes B6SJL SOD1-G93A males were obtained by crossing with B6SJL females obtained from Jackson Laboratory. For the development of C57Bl/6J background mice, transgenic animals with the G93A human SOD1 mutation (B6SJL-Tg[SOD1-G93A]1Gur) were also obtained from Jackson Laboratory, and provided from the colony maintained at the Neurotec Pharma animal facilities located at the University of Barcelona. First generation of hemizygotes carrying the G93A human SOD1 mutation was generated by breeding B6SJL SOD1-G93A males with C57Bl/6J females purchased from Harlan. Animal colony was maintained by consecutive crossbreeds between hSOD1-G93A heterozygotes males and C57Bl/6J females. The offspring was identified by PCR amplification of DNA extracted from the tail tissue. Animals used for these experiments pertained at least to the 12th generation. Wild-type mice of the same strains were used as controls.

In order to determine the human SOD1 transgene (hSOD1) copy number, real-time quantitative PCR (QPCR) analysis was performed following the protocol described by Alexander et al. (25). Two sets of primers were used: primers for the hSOD1 transgene 5′-CATCAGCCCTAATCCATCTGA-3′ (forward) and 5′-CGCGACTAACAATCAAAGTGA-3′ (reverse) that amplify a 236 base pair product, and primers for the reference gene (mouse interleukin-2, mIL-2) 5′-CTAGGCCACAGAATTGAAAGATCT-3′ (forward) and 5′-GTAGGTGGAAATTCTAGCATCATCC-3′ (reverse) that amplify a 324 base pair product. Both primers were obtained from Invitrogen and have been widely used for hSOD1-G93A mice genotyping. Briefly, 5 ng of genomic DNA were added to a reaction mixture containing 15 µl of 2X SYBR Green QPCR Master Mix reagent and 0.6 µl of 20-µM forward and reverse primers for hSOD1 transgene or 0.75 µl of 20-µM primers for IL-2, to a total volume of 30 µl. Amplification was performed with the following thermal cycling parameters: initial incubation of 95°C for 10 min, followed by 40 cycles of 95°C for 30 s, 60°C for 1 min and 72°C for 30 s. Assays were performed in triplicate and 10 animals were analysed from each strain.

Efficiency of amplification for both sets of primers was determined from seven points of four-fold genomic DNA dilution series. Efficiency was calculated from the slope of the linear regression hSOD1 CT vs. DNA standard curve with the expression $E = 10^{(-1/\text{slope})} - 1$, where E is the efficiency of amplification for each corresponding set of primers. Efficiencies were 0.93 for hSOD1 primers and 0.90 for IL-2 primers, respectively. Relative transgene detection was determined using the delta CT method, calculated as the difference between the hSOD1 CT and the mouse IL2 CT.

Functional evaluation

Functional evaluation (rotarod and electrophysiological tests) was performed using 28 animals of each strain: seven female and seven male wild-type, and seven female and seven male transgenic animals. Histological analysis was performed using four samples for each of these subgroups. Survival analysis was made on cohorts of 10 mice of each strain and gender. The experimental procedures were approved by the Ethics Committee of the Universitat Autònoma de Barcelona.

The rotarod test was performed to evaluate general motor coordination, strength and balance of the animals (11,26). Animals were trained three times a week on the rod rotating at 14 rpm, and then tested weekly from six to 16 weeks of age at the same speed

For each test, mice were given three runs in the rotarod and the longest time of maintenance on the rod was measured. An arbitrary maximum time of maintenance in the rotating rod of 180 s was considered.

Motor nerve conduction tests were made by stimulating the sciatic nerve percutaneously at the sciatic notch by means of single pulses delivered through a pair of needle electrodes, and recording the compound muscle action potential (CMAP, M-wave) from the tibialis anterior (TA) and the plantar (interossei) muscles with microneedle electrodes (27,28). For evaluation of motor central pathways, motor evoked potentials (MEP) were recorded from the TA muscle in response to transcranial electrical stimulation of the motor cortex by single electrical pulses, delivered through needle electrodes inserted over the skull over the sensorimotor cortex (28,29). All potentials were amplified and displayed on a digital oscilloscope (Tektronix 450S) at settings appropriate to measure the amplitude from baseline to the maximal negative peak and the latency from stimulus to the onset of the first negative deflection, to the maximal negative peak and to the end of the wave. During the tests, the mice skin temperature was kept between 34 and 36°C by means of a thermostated heating pad.

Histology

Subgroups of four mice of each strain were perfused with 4% paraformaldehyde in PBS at 16 weeks of age. The lumbar segment of the spinal cord was removed, post-fixed for 24 h, and cryopreserved in 30% sucrose. Transverse 40-µm thick sections were serially cut with a cryotome (Leica) at L2, L3 and L4 segmental levels. For each segment, each section of a series of 10 was collected sequentially on separate gelatin-coated slides. One slide was rehydrated for 1 min and stained for 2 h with an acidified solution of 3.1 mM cresyl violet. The slides were then washed in distilled water for 1 min, dehydrated and mounted with DPX (Fluka). MNs were identified by their localization in the ventral horn of the stained spinal cord sections and counted following strict size and morphological criteria: only MNs with diameters larger than 20 µm and with polygonal shape and prominent nucleoli were counted. The number of MNs present in the lateral aspect of both ventral horns was counted in four serial sections of the L4 segment (28,30).

Survival

It was considered that animals reached the endpoint of the disease when they were unable to right themselves for 30 s when placed on their side.

Statistical analysis

Data are expressed as mean ± SEM. For the transgene copy number comparison Student's *t*-test was used. Electrophysiological and locomotion tests results were statistically analysed using repeated measurements ANOVA, applying Bonferroni post hoc test when necessary. Histological data were analysed using the Mann-Whitney non-parametric test. Survival data were analysed using the Kaplan-Meir test.

Results

SOD1 transgene copy number

No significant differences were found in the detection of hSOD1 transgene between mouse strains (Figure 1, $p > 0.05$), suggesting that differences between the strains are due to the genetic background.

Rotarod test

Rotarod test was performed to determine whether B6 and B6SJL SOD1-G93A mice show different onset and/or progression of symptomatic locomotor impairments. The results show clear differences between genders, since male SOD1-G93A mice evidenced the first impairment at 11 weeks, while female SOD1-G93A mice performed like wild-type animals until 12 weeks (Figure 2). Regarding differences between strains, there was no background effect on the time of maintenance in the rotarod, since in both cases locomotor decline of female and male mice achieved statistical differences with respect to wild-type littermates from 13 and 12 weeks, respectively.

Motor nerve conduction

Motor nerve conduction was used to evaluate the function of spinal MNs since the loss of neuromuscular connections is one of the hallmarks of the disease process in this animal model (31). Our results confirm that lower MN abnormalities start early

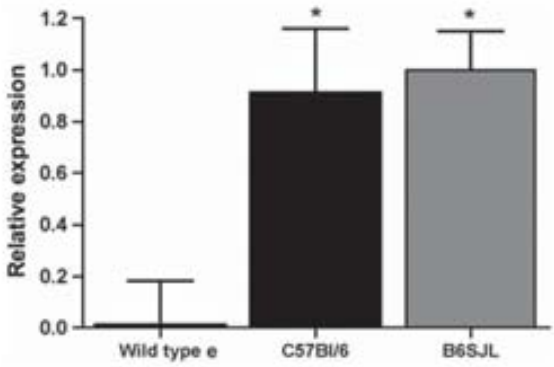

Figure 1. SOD1 transgene expression levels comparing B6-SOD1-G93A, B6SJL-SOD G93A and wild-type animals. Note the lack of differences between both strains ($p > 0.05$). * $p < 0.05$ vs. wild type.

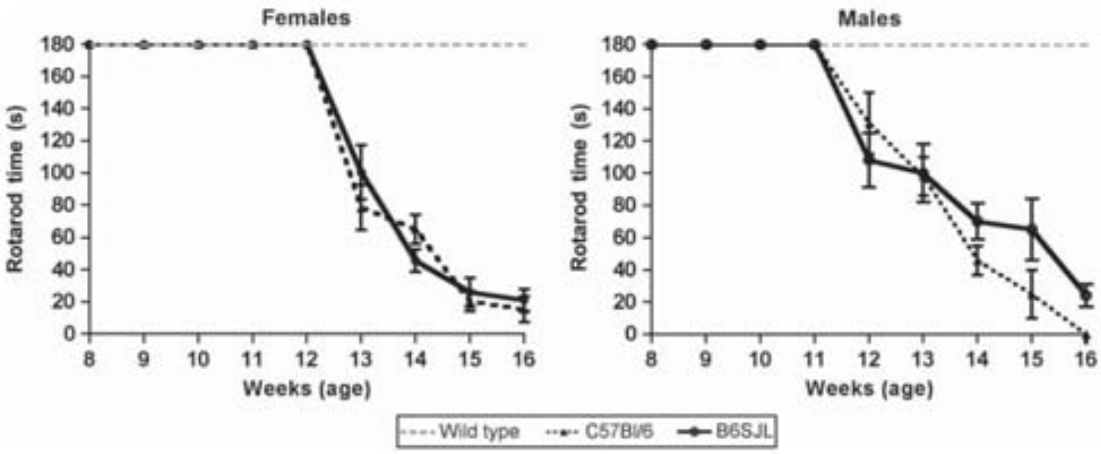

Figure 2. Rotarod test results. Transgenic SOD1 mice performance declined from 12 to 13 weeks of age in both strains. Wild-type mice maintained permanence in the rotarod during 180 s during all the follow-up (grey dashed line). Values are mean ± SEM.

during the disease process, particularly in the TA muscle (between six and eight weeks of age), but also show clear differences between the two strains. While in B6 SOD1-G93A mice the first nerve conduction abnormalities were found at six weeks of age (58% of normal CMAP amplitude in females and 52% in males for the TA muscle), B6SJL mice did not show any deficit until eight weeks (two weeks later), when their CMAP amplitude was 74% of control values in females and 52% in males. From the onset of the abnormalities, there was a similar slope of decline of the CMAP amplitude in both strains. At 16 weeks, the CMAP reached 14% in female and male B6 mice and 26% and 9% in female and male B6SJL mice, respectively (Figure 3). With regard to plantar muscles, the decline in the CMAP amplitude followed a similar pattern in B6 and B6SJL strains regardless of the gender of the animals. In both mouse strains, the abnormalities started at 12 weeks of age, evidenced by a reduction in the amplitude of 50–75% that was maintained until 16 weeks (Figure 3).

Motor evoked potentials

Motor evoked potentials were performed to evaluate the function of the connections that arise from the upper MNs in motor cortex and brainstem, and reach spinal MNs. The evaluation of central motor pathways showed similar results compared with the motor nerve conduction study. Abnormalities in central motor pathways started earlier in the B6 SOD1-G93A mice, evidenced by a reduction of MEP amplitude of 50–60% at six weeks. In turn, in B6SJL SOD1-G93A mice the MEP amplitude was not reduced until eight weeks of age, when it averaged 50–60% of wild-type mice values (Figure 4).

Animal survival

The analysis of survival showed significant differences between the two strains. For both genders, the lifespan was longer in B6 than in B6SJL animals. B6 male mice had a mean survival of 147 ± 1.6 days, whereas B6SJL male mice only reached 138.2 ± 3.2 days ($p < 0.05$, Figure 5). This difference was more evident in female animals in which B6 had a mean survival of 153 ± 1.7 days and B6SJL only reached 138.1 ± 1.9 days ($p < 0.05$, Figure 5). With regard to gender effect on survival, only B6 animals showed significant differences since females lived longer than male mice ($p < 0.05$).

Motor neuron loss

MN degeneration was determined by counting the number of stained MN soma in the lamina IX of the ventral horns of lumbar spinal cord sections of wild-type and SOD1-G93A mice of 12 and 16 weeks of age. The segment analysed was L4, where TA and plantar muscles motor nuclei are partially represented (32). Neurons smaller than 20 µm in diameter were excluded from the count, even if they could be atrophic MNs because they were unlikely to be functional. There were marked differences in the number of surviving MNs between strains. At 12 weeks of age, B6-SOD1-G93A animals showed a lower number of MNs compared to B6SJL (47.5% vs. 67.7%, respectively). However, at 16 weeks of age the percentage of MN loss was similar in both cases (50 – 59% of respective wild-type mice) (Figure 6).

Discussion

The detailed characterization of an animal model of a disease, especially a neurodegenerative disorder such as ALS, is essential for an accurate interpretation of the results obtained in experimental research. The study of the effect of the background on the disease process plays an important role in this characterization. It has been reported that ALS patients expressing SOD1 mutations do not exhibit a uniform

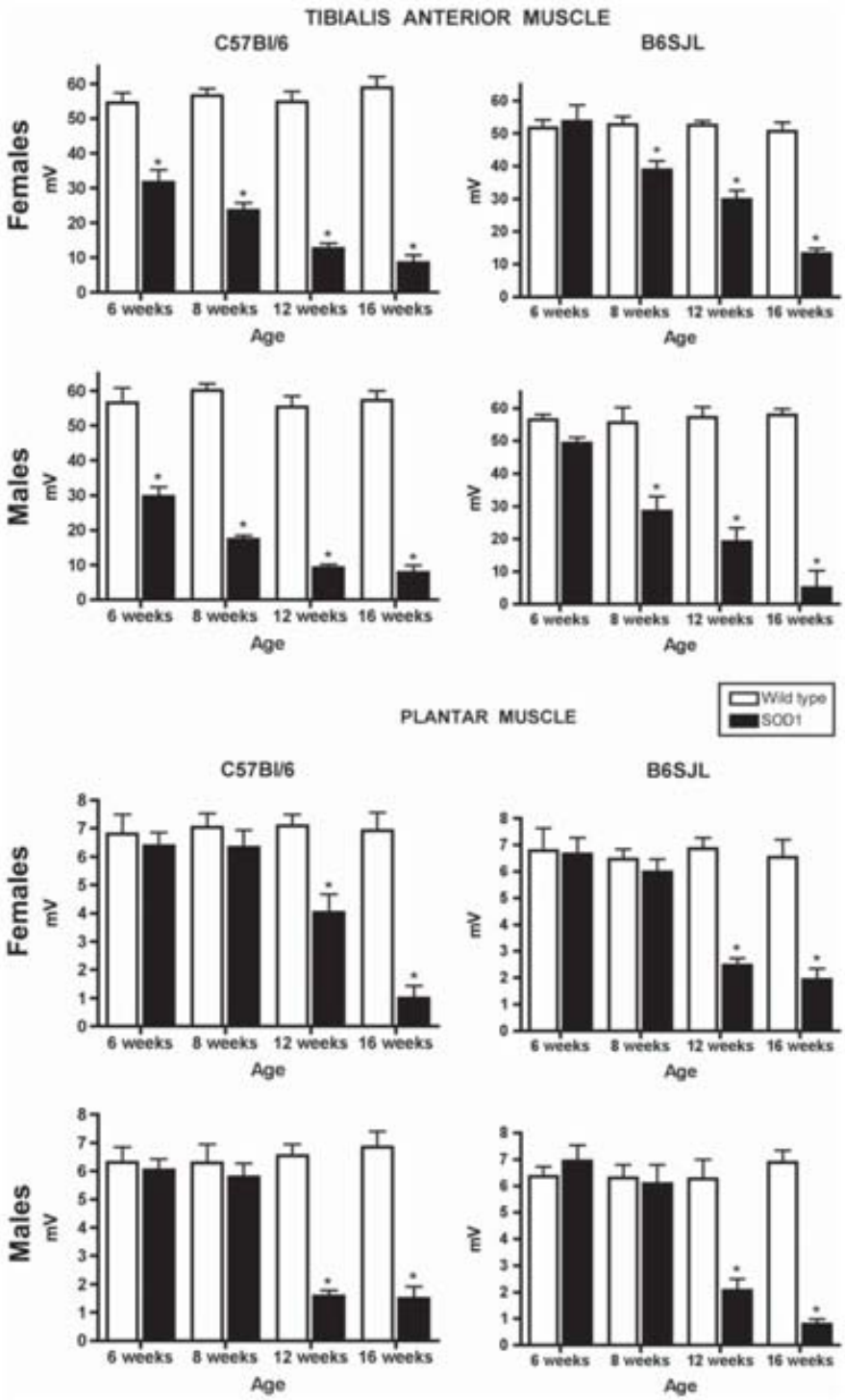

Figure 3. Amplitude of the CMAP of tibialis anterior and plantar muscles comparing SOD1 and wild-type animals of each background (B6 vs. B6SJL) and gender from four to 16 weeks of age. Note that first abnormalities started earlier in the B6 mice. However, at 16 weeks, animals from both backgrounds showed similar decline in the amplitudes, demonstrating that B6SLJ mice suffer a more acute disease progression.

course of disease (7,8). Previous studies regarding background effect on transgenic mutant SOD1 models have shown significant variations in animal survival depending on the genetic background they were expressing (13,14). In this work we have analysed not only survival but also the disease onset and progression in two different genetic background mouse strains. This information is important since variations in these parameters may condition the interpretation of basic studies regarding disease

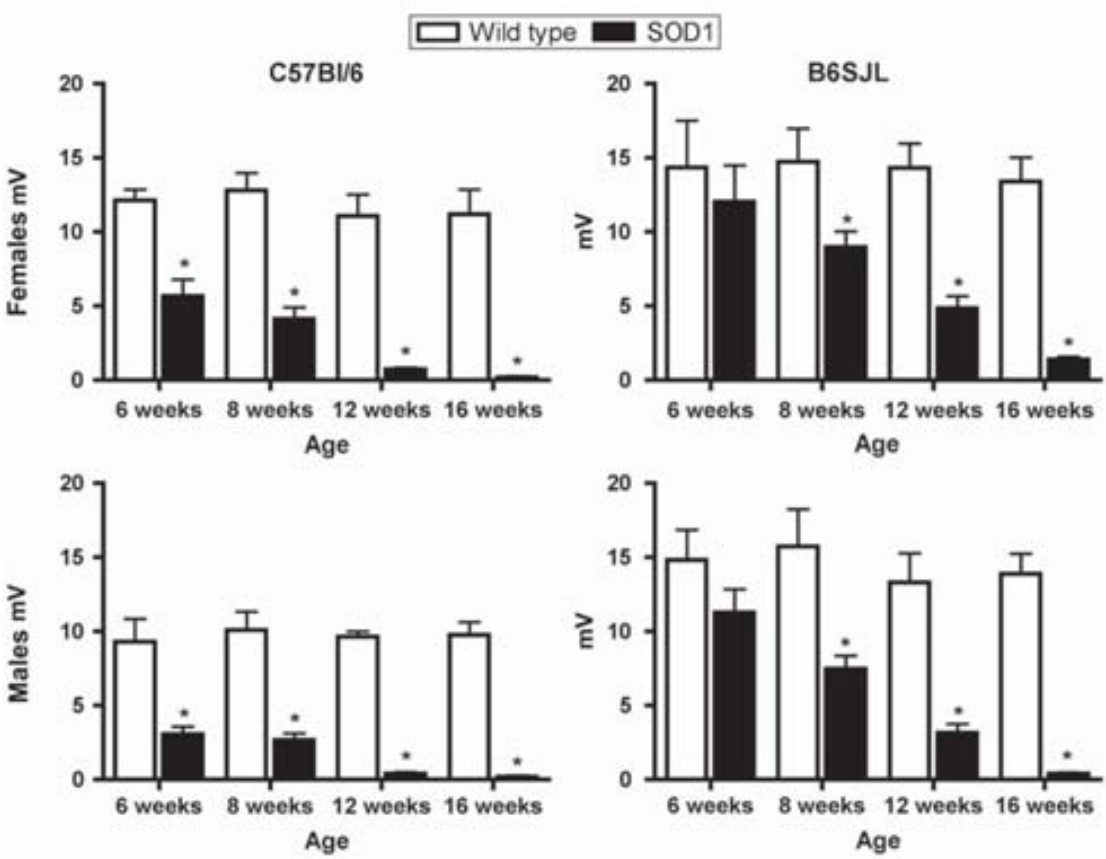

Figure 4. Amplitude of the motor evoked potentials (MEP) comparing SOD1 and wild -type animals of each background (B6 vs. B6SJL) and gender from four to 16 weeks of age. Note that first upper motor neuron abnormalities started earlier in the B6 mice, but at 16 weeks, animals from both backgrounds showed similar decline in MEP amplitude.

aetiopathogenesis, and the evaluation of potential treatments.

Our results demonstrate that the genetic background is a relevant factor that affects both disease onset and progression in the transgenic mutant SOD1 animal model of ALS. Interestingly, the rotarod test did not show any differences in the onset of locomotor impairments between the two strains. Since this test is the most commonly used technique to determine disease onset in SOD1-G93A animals (11,33–35), it would seem that background does not affect the onset of disease 'symptoms'. However, motor nerve conduction studies have been previously demonstrated as a more powerful tool to evaluate motor system impairments in this model (28). Electrophysiological analysis showed that the initial

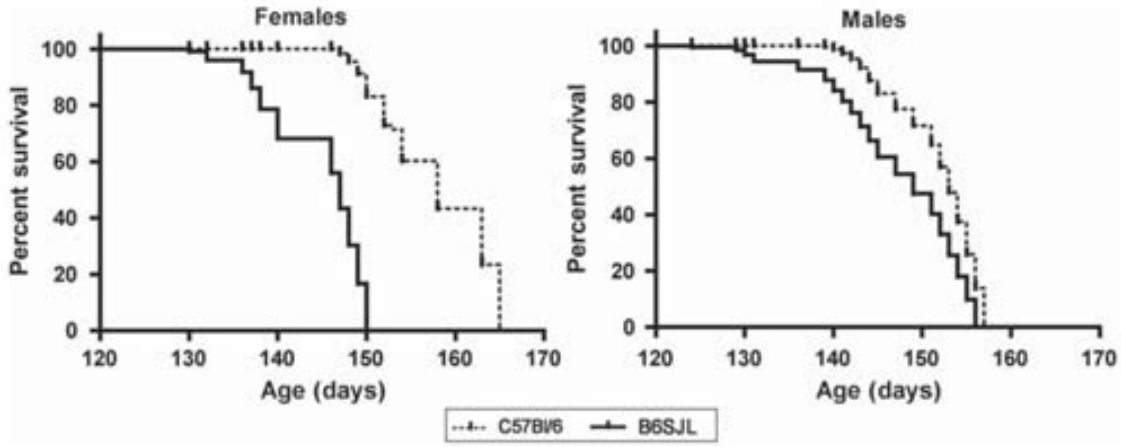

Figure 5. Survival curves comparing each gender of B6 and B6SJL mice. Both female and male B6 lived significantly longer than B6SJL animals (Kaplan-Meir test, $p < 0.05$).

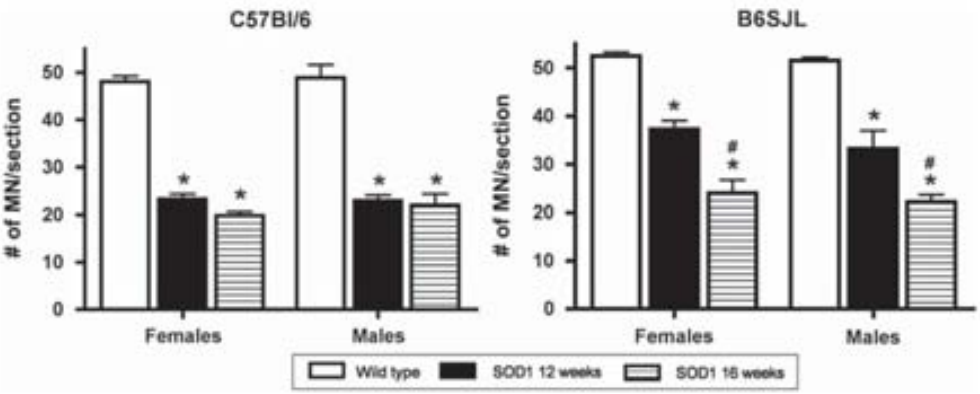

Figure 6. Motor neuron (MN) survival comparing male and female animals of each background strain. Note the differences between backgrounds at 12 weeks of age. At 16 weeks of age there was a similar reduction of approximately 50% in the number of MN/section.

signs of motor impairment are notably different between both strains, since B6 mice showed the first lower and upper MN dysfunctions about two weeks earlier than B6SJL animals. Despite mice of both strains reaching similar values of CMAP at 16 weeks, it appears that B6SJL animals have faster muscle denervation once it has started. These results are confirmed by the histological analysis since the background also affects the progression of MN degeneration in SOD1-G93A transgenic animals. MN counts revealed that B6 animals had a lower number of spinal MNs than B6SJL animals at 12 weeks, indicating that MN degeneration starts earlier in B6 mice, similar to what happens with the first signs of MN dysfunction. These findings should be considered carefully because the timing of application of new treatments and evaluation of consequent improvement depends on the time of disease onset.

The study of upper MN function also indicated clear differences between B6 and B6SJL animals. In the B6, MEP abnormalities started earlier than in B6LSJ animals. These results are in accordance with those from other authors using retrotracers to assess the number of functioning upper MNs. Ozdinler et al. (36) found a significant reduction of labelled cortical MNs before six weeks in B6 SOD1-G93A animals, whereas using the same method Zang and Cheema (37) did not find any significant reduction until 12 weeks of age in B6SJL SOD1-G93A mice. These findings suggest a strong effect of the background on the evolution of the abnormalities in upper MN and central motor pathways in this animal model.

In contrast with the motor conduction impairments in upper and lower MNs, the SOD1-G93A B6 mice showed a more prolonged survival than B6SJL animals. It is also remarkable that only B6 animals show gender differences, suggesting that background might also affect the susceptibility of each gender to the neurodegenerative process. Previous studies regarding survival in these mouse models reported varying results. On the one hand, Heiman-Patterson et al. (13,14) found that B6 animals lived longer than B6SJL ones, but also that only the latter presented gender differences. On the other hand, findings by Miana-Mena et al. (11) support our conclusions about the lack of differences in survival of B6SJL animals between genders. These contradictory findings may be accounted for by differences in animal manipulation that may significantly modify survival in this animal model. This lack of inter-laboratory repeatability highlights that survival analysis may suffer from lack of reliability to evaluate influences of treatments, in addition to ethics concerns (35).

Many reasons could explain the effect of the background in disease onset and progression of SOD1-G93A animal models. Neuroinflammation and, particularly, the role of microglia is a pathological hallmark in ALS. Nikodemova and Watters (20) have recently reported that microglial cells from different mouse strains differ on their pro- and anti-inflammatory properties, pointing out that genetic traits may modify microglial reaction, deeply affecting many CNS pathologies. Since neuromuscular junction destruction is also one of the key pathological events in ALS, muscle disorders could play an important role during the pathological process. It has been reported that ALS pathogenesis produces several muscle abnormalities, such as hypermetabolism, energy deficits and alterations of lipid metabolism (38) that could initiate and/or participate in the loss of neuromuscular junctions. Heydemann et al. (17) have demonstrated that background can modulate muscular dystrophy phenotype in a mouse model with mutations in γ-sarcoglicans. It may be worth also to investigate whether differences in muscle response to denervation and myogenesis occur between strains with SOD1-G93A mutations. Abnormal energy metabolism is another important trait both in ALS patients and animal models of the disease (39). It is known that different mouse strains have important differences regarding their metabolic properties (The Jackson Laboratory, www.jax.org).

Hence, the study of these differences could also be important to determine the background effect of disease onset and progression. Finally, several authors have noted the existence of some so-called 'modifier genes' that might modulate the phenotype of a transgenic mouse depending on the background in which it is maintained (14,19). The comparison of these mouse models will also contribute to the identification of these modifying genes. Understanding genetic modifiers will also improve knowledge of potential mechanisms related to ALS pathogenesis.

Our findings regarding the effects of background differences on disease onset and progression are important in this field because they demonstrate that the experimental design must be adapted to the strain used. With knowledge of these differences, it is also important that all studies on SOD1-G93A animal models include detailed information of mice background in order to correctly interpret the results.

Acknowledgements

This work was supported by grant PI071133, TERCEL and CIBERNED funds from the Fondo de Investigación Sanitaria of Spain, grant SAF2009-12495 from the Ministerio de Ciencia e Innovación of Spain, FEDER funds, and Action COST-B30 of the EC. We thank Jessica Jaramillo and Marta Morell for technical help. RM is recipient of a predoctoral fellowship from the Ministerio de Educación of Spain.

Declaration of interest: The authors report no conflicts of interest. The authors alone are responsible for the content and writing of the paper.

References

1. Wijesekera LC, Leigh PN. Amyotrophic lateral sclerosis. Orphanet Journal of Rare Diseases. 2009;4:3.
2. Worms PM. The epidemiology of motor neuron diseases: a review of recent studies. J Neurol Sci. 2001;191:3–9.
3. Ludolph AC, Jesse S. Review: evidence based drug treatment in amyotrophic lateral sclerosis and upcoming clinical trials. Therapeutic Advances in Neurological Disorders. 2009; 2:319–26.
4. DeJesus-Hernandez M, Mackenzie IR, Boeve BF, Boxer AL, Baker M, Rutherford NJ, et al. Expanded GGGGCC hexanucleotide repeat in non-coding region of C9ORF72 causes chromosome 9p-linked FTD and ALS. Neuron. 2011; 72:245–56.
5. Renton AE, Majounie E, Waite A, Simon-Sanchez J, Rollinson S, Gibbs JR, et al. A hexanucleotide repeat expansion in C9ORF72 is the cause of chromosome 9p21-linked ALS-FTD. Neuron. 2011;72:257–68.
6. Bosco DA, Morfini G, Karabacak NM, Song Y, Gros-Louis F, Pasinelli P, et al. Wild-type and mutant SOD1 share an aberrant conformation and a common pathogenic pathway in ALS. Nat Neurosci. 2010;13:1396–403.
7. Cudkowicz ME, McKenna-Yasek D, Sapp PE, Chin W, Geller B, Hayden DL, et al. Epidemiology of mutations in superoxide dismutase in amyotrophic lateral sclerosis. Ann Neurol. 1997;41:210–21.
8. Andersen PM, Nilsson P, Keranen ML, Forsgren L, Hagglund J, Karlsborg M, et al. Phenotypic heterogeneity in motor neuron disease patients with Cu/Zn superoxide dismutase mutations in Scandinavia. Brain. 1997;120: 1723–37.
9. Rosen DR, Siddique T, Patterson D, Figlewicz DA, Sapp P, Hentati A, et al. Mutations in Cu/Zn superoxide dismutase gene are associated with familial amyotrophic lateral sclerosis. Nature. 1993;364:59–62.
10. Gurney ME, Pu H, Chiu AY, dal Canto MC, Polchow CY, Alexander DD, et al. Motor neuron degeneration in mice that express a human Cu/Zn superoxide dismutase mutation. Science. 1994;264:1772–5.
11. Miana-Mena FJ, Muñoz MJ, Yagüe G, Mendez M, Moreno M, Ciriza J, et al. Optimal methods to characterize the G93A mouse model of ALS. Amyotroph Lateral Scler Other Motor Neuron Disord. 2005;6:55–62.
12. Turner BJ, Talbot K. Transgenics, toxicity and therapeutics in rodent models of mutant SOD1-mediated familial ALS. Prog Neurobiol. 2008;85:94–134.
13. Heiman-Patterson TD, Deitch JS, Blankenhorn EP, Erwin KL, Perreault MJ, Alexander BK, et al. Background and gender effects on survival in the TgN(SOD1-G93A)1Gur mouse model of ALS. J Neurol Sci. 2005;236:1–7.
14. Heiman-Patterson TD, Sher RB, Blankenhorn EA, Alexander G, Deitch JS, Kunst CB, et al. Effect of genetic background on phenotype variability in transgenic mouse models of amyotrophic lateral sclerosis: a window of opportunity in the search for genetic modifiers. Amyotroph Lateral Scler. 2011;12:79–86.
15. Acevedo-Arozena A, Kalmar B, Essa S, Ricketts T, Joyce P, Kent R, et al. A comprehensive assessment of the SOD1-G93A low-copy transgenic mouse, which models human amyotrophic lateral sclerosis. Dis Model Mech. 2011;4: 686–700.
16. Hadano S, Yoshii Y, Otomo A, Kunita R, Suzuki-Utsunomiya K, Pan L, et al. Genetic background and gender effects on gross phenotypes in congenic lines of ALS2/alsin-deficient mice. Neurosci Res. 2010;68:131–6.
17. Heydemann A, Huber JM, Demonbreun A, Hadhazy M, McNally EM. Genetic background influences muscular dystrophy. Neuromuscul Disord. 2005;15:601–9.
18. Achilli F, Bros-Facer V, Williams HP, Banks GT, AlQatari M, Chia R, et al. An ENU-induced mutation in mouse glycyl-tRNA synthetase (GARS) causes peripheral sensory and motor phenotypes creating a model of Charcot-Marie-Tooth type 2D peripheral neuropathy. Dis Model Mech. 2009;2:359–73.
19. Montagutelli X. Effect of genetic background on the phenotype of mouse mutations. J Am Soc Nephrol. 2000;11: S101–5.
20. Nikodemova M, Watters JJ. Outbred ICR/CD1 mice display more severe neuroinflammation mediated by microglial TLR4/CD14 activation than inbred C57Bl/6 mice. Neuroscience. 2011;190:67–74.
21. Moreno-Igoa M, Calvo AC, Penas C, Manzano R, Oliván S, Muñoz MJ, et al. Fragment C of tetanus toxin, more than a carrier. Novel perspectives in non-viral ALS gene therapy. J Mol Med. 2010;88:297–308.
22. Fischer LR, Culver DG, Davis AA, Tennant P, Wang M, Coleman M, et al. The WldS gene modestly prolongs survival in the SOD1-G93A FALS mouse. Neurobiol Dis. 2005;19:293–300.
23. Vercelli A, Mereuta OM, Garbossa D, Muraca G, Mareschi K, Rustichelli D, et al. Human mesenchymal stem cell transplantation extends survival, improves motor performance and decreases neuroinflammation in mouse model of amyotrophic lateral sclerosis. Neurobiol Dis. 2008;31:395–405.
24. Deforges S, Branchu J, Biondi O, Grondard C, Pariset C, Lécolle S, et al. Motor neuron survival is promoted by specific exercise in a mouse model of amyotrophic lateral sclerosis. J Physiol (Lond). 2009;587:3561–72.

25. Alexander GM, Erwin KL, Byers N, Deitch JS, Augelli BJ, Blankenhorn EP, et al. Effect of transgene copy number on survival in the G93A-SOD1 transgenic mouse model of ALS. Brain Res Mol Brain Res. 2004;130:7–15.
26. Brooks SP, Dunnett SB. Tests to assess motor phenotype in mice: a user's guide. Nat Rev Neurosci. 2009;10:519–29.
27. Valero-Cabré A, Navarro X. H reflex restitution and facilitation after different types of peripheral nerve injury and repair. Brain Res. 2001;919:302–12.
28. Mancuso R, Santos-Nogueira E, Osta R, Navarro X. Electrophysiological analysis of a murine model of motor neuron disease. Clin Neurophysiol. 2011;122:1660–70.
29. García-Alías G, Verdú E, Forés J, López-Vales R, Navarro X. Functional and electrophysiological characterization of photochemical graded spinal cord injury in the rat. J Neurotrauma. 2003;20:501–10.
30. Penas C, Casas C, Robert I, Fores J, Navarro X. Cytoskeletal and activity-related changes in spinal motor neurons after root avulsion. J Neurotrauma. 2009;26:763–79.
31. Fischer LR, Culver DG, Tennant P, Davis AA, Wang M, Castellano-Sanchez A, et al. Amyotrophic lateral sclerosis is a distal axonopathy: evidence in mice and man. Exp Neurol. 2004;185:232–40.
32. McHanwell S, Biscoe TJ. The localization of motor neurons supplying the hindlimb muscles of the mouse. Philos Trans R Soc Lond B Biol Sci. 1981;293:477–508.
33. Crosio C, Valle C, Casciati A, Iaccarino C, Carrì MT. Astroglial inhibition of NF-κB does not ameliorate disease onset and progression in a mouse model for amyotrophic lateral sclerosis (ALS). PLoS ONE. 2011;6:e17187.
34. Gould TW, Buss RR, Vinsant S, Prevette D, Sun W, Knudson CM, et al. Complete dissociation of motor neuron death from motor dysfunction by Bax deletion in a mouse model of ALS. J Neurosci. 2006;26:8774–86.
35. Ludolph AC, Bendotti C, Blaugrund E, Chio A, Greensmith L, Loeffler J-P, et al. Guidelines for preclinical animal research in ALS/MND: a consensus meeting. Amyotroph Lateral Scler. 2010;11:38–45.
36. Ozdinler PH, Benn S, Yamamoto TH, Güzel M, Brown RH, Macklis JD. Corticospinal motor neurons and related subcerebral projection neurons undergo early and specific neurodegeneration in hSOD1-G93A transgenic ALS mice. J Neurosci. 2011;31:4166–77.
37. Zang DW, Cheema SS. Degeneration of corticospinal and bulbospinal systems in the superoxide dismutase 1(G93A, G1H) transgenic mouse model of familial amyotrophic lateral sclerosis. Neurosci Lett. 2002;332:99–102.
38. Dupuis L, Loeffler J-P. Neuromuscular junction destruction during amyotrophic lateral sclerosis: insights from transgenic models. Current Op Pharmacol. 2009;9:341–6.
39. Dupuis L, Pradat PF, Ludolph AC, Loeffler JP. Energy metabolism in amyotrophic lateral sclerosis. Lancet Neurol. 2011;10:75–82.

Chapter II: Sigma-1R agonist treatment

Sigma-1R agonist improves motor function and motoneuron survival in ALS mice

Mancuso R, Oliván S, Rando A, Casas C, Osta R, Navarro X. Sigma-1R agonist improves motor function and motoneuron survival in ALS mice. Neurotherapeutics 2012, 9:814-826.

Neurotherapeutics (2012) 9:814–826
DOI 10.1007/s13311-012-0140-y

ORIGINAL ARTICLE

Sigma-1R Agonist Improves Motor Function and Motoneuron Survival in ALS Mice

Renzo Mancuso · Sara Oliván · Amaya Rando · Caty Casas · Rosario Osta · Xavier Navarro

Published online: 31 August 2012

Abstract Amyotrophic lateral sclerosis is a neurodegenerative disorder characterized by progressive weakness, muscle atrophy, and paralysis due to the loss of upper and lower motoneurons (MNs). Sigma-1 receptor (sigma-1R) activation promotes neuroprotection after ischemic and traumatic injuries to the central nervous system. We recently reported that sigma-1R agonist (PRE-084) improves the survival of MNs after root avulsion injury in rats. Moreover, a mutation of the sigma-1R leading to frontotemporal lobar degeneration/amyotrophic lateral sclerosis (ALS) was recently described in human patients. In the present study, we analyzed the potential therapeutic effect of the sigma-1R agonist (PRE-084) in the $SOD1^{G93A}$ mouse model of ALS. Mice were daily administered with PRE-084 (0.25 mg/kg) from 8 to 16 weeks of age. Functional outcome was assessed by electrophysiological tests and computerized analysis of locomotion. Histological, immunohistochemical analyses and Western blot of the spinal cord were performed. PRE-084 administration from 8 weeks of age improved the function of MNs, which was manifested by maintenance of the amplitude of muscle action potentials and locomotor behavior, and preserved neuromuscular connections and MNs in the spinal cord. Moreover, it extended survival in both female and male mice by more than 15 %. Delayed administration of PRE-084 from 12 weeks of age also significantly improved functional outcome and preservation of the MNs. There was an induction of protein kinase C-specific phosphorylation of the NR1 subunit of the N-methyl-D-aspartate (NMDA) receptor in $SOD1^{G93A}$ animals, and a reduction of the microglial reactivity compared with untreated mice. PRE-084 exerts a dual therapeutic contribution, modulating NMDA Ca^{2+} influx to protect MNs, and the microglial reactivity to ameliorate the MN environment. In conclusion, sigma-1R agonists, such as PRE-084, may be promising candidates for a therapeutical strategy of ALS.

Keywords Motoneuron disease · Amyotrophic lateral sclerosis · Sigma-1 receptor · PRE-084 · $SOD1^{G93A}$ mice

R. Mancuso · C. Casas · X. Navarro
Group of Neuroplasticity and Regeneration, Institute of Neurosciences and Department of Cell Biology, Physiology, and Immunology, Universitat Autònoma de Barcelona, Bellaterra 08193, Spain

R. Mancuso · C. Casas · X. Navarro (✉)
Centro de Investigación Biomédica en Red sobre Enfermedades Neurodegenerativas (CIBERNED), Bellaterra 08193, Spain
e-mail: xavier.navarro@uab.es

S. Oliván · A. Rando · R. Osta
Laboratory of Genetic Biochemistry (LAGENBIO-I3A), Aragon Institute of Health Sciences, Universidad de Zaragoza, Zaragoza 50013, Spain

Introduction

Amyotrophic lateral sclerosis (ALS) is an adult onset neurodegenerative disorder characterized by progressive muscle atrophy and paralysis due to death of upper and lower MNs [1]. The majority ALS cases are sporadic with unknown etiology, whereas 10 % of cases correspond to inherited forms of ALS. Among these cases, mutations in the gene encoded for the enzyme Cu/Zn superoxide dismutase 1 (SOD1) are observed in approximately 20 % [2]. Based on these genetic mutations, transgenic animal models have been developed for the study of ALS. The most widely used model is a transgenic mouse with a glycine-to-alanine conversion at the 93rd codon of the SOD1 gene in high copy number ($SOD1^{G93A}$) [3]. The phenotype of this mice recapitulates several clinical and histopathological features of both familial and sporadic forms of the human disease [3]. Moreover, it has been recently reported that alterations of the SOD1 protein are also related to sporadic ALS cases [4], increasing the interest in the study of transgenic animals.

Several studies using ALS animal models have hypothesized that ALS pathogenesis might be related to glutamate excitotoxicity, oxidative stress, protein misfolding, mitochondrial defects, impaired axonal transport, and inflammation, with all of these factors contributing to MN death [5].

The sigma-1R is a transmembrane protein found in the endoplasmic reticulum [6, 7], which is highly expressed in MNs and other cells in the spinal cord [6, 8–10]. This receptor has the ability to translocate from the endoplasmic reticulum to the plasma membrane and mitochondria-associated membranes [7, 11, 12]. In the nervous system, sigma-1R mediates regulation of several processes, such as neuritogenesis, K^+ channels, and N-methyl-D-aspartate (NMDA) receptors activity, Ca^{2+} homeostasis, and microglial activity. Furthermore, it is related to some central nervous system pathologies, including depression, schizophrenia, drug addiction, and Alzheimer disease [13–16]. Several studies have demonstrated potent therapeutic actions of sigma-1R agonists, reducing glutamate-mediated cell death [17, 18] or modulating the inflammatory reaction after stroke in rats [19, 20]. Luty et al. [21] and Al-Saif et al. [22] recently reported a novel mutation of sigma-1R in patients affected by ALS, suggesting that pharmacological interventions targeting this receptor could be a good therapeutic approach.

We have previously reported the role of the selective sigma-1R agonist 2-(4-morpholi-nethyl)1-phenylcyclohexanecarboxylate (PRE-084) in motoneuron death. We demonstrated that PRE-084 administration promotes neuroprotection and neurite elongation through protein kinase C (PKC) on MNs in an *in vitro* organotypic model of excitotoxic lesion [18]. Moreover, administration of PRE-084 prevented spinal MNs death after spinal root avulsion in rats [10]. Therefore, the aim of this study was to assess the potential therapeutic effect of the sigma-1R agonist in the SOD1 mouse model of ALS.

Material and Methods

Transgenic Mice and Drug Administration

Transgenic mice with the G93A human SOD1 mutation (B6SJL-Tg[SOD1-G93A]1Gur) were obtained from the Jackson Laboratory (Bar Harbor, ME), and maintained at the Animal Service of the Universidad de Zaragoza. Hemizygote B6SJL $SOD1^{G93A}$ males were obtained by crossing with B6SJL females from the CBATEG (Barcelona, Spain). The offspring was identified by polymerase chain reaction (PCR) amplification of DNA extracted from the tail tissue. All experimental procedures were approved by the Ethics Committee of the Universitat Autònoma de Barcelona.

Animals were evaluated at 8 weeks (prior to drug administration) by electrophysiological tests to obtain baseline values, and as a diagnostic test to distribute them between the experimental groups. PRE-084 and BD-1036 (Tocris Bioscience, Ellisville, MO) were used as sigma-1R agonist and antagonist, respectively. Both drugs were dissolved in saline and administered daily by intraperitoneal injections at 0.25 mg/kg. The experimental groups included in the study are summarized in Table 1.

Nerve Conduction Tests

Motor nerve conduction tests were performed at 8 weeks of age and then every 2 weeks until 16 weeks in all the animals used in the study (Table 1). The sciatic nerve was percutaneously stimulated by means of single pulses of 0.02 ms duration (grass S88) delivered through a pair of needle electrodes placed at the sciatic notch. The compound muscle action potential (CMAP) (M wave) and the reflex H wave were recorded from the tibialis anterior (TA) and the plantar (interossei) muscles with microneedle electrodes [23, 24]. All potentials were amplified and displayed on a digital oscilloscope (Tektronix 450S; Tektronix, Beaverton OR, USA) at settings appropriate to measure the amplitude from baseline to the maximal negative peak. To ensure reproducibility, the recording needles were placed under the microscope to secure the same placement on all animals guided by anatomical landmarks. During the tests, the mice body temperature was kept constant between 34 and 36ºC by means of a thermostated heating pad.

Treadmill Test

The DigiGait system (DigiGait Imaging System, Mouse Specifics, Boston, MA) was used to assess the locomotor performance of the animals at the end-stage of the disease (at 16 weeks of age). All the animals used in the study (Table 1) were tested. The animals were placed on the treadmill belt and their capacity to run with increasing velocity was recorded. Treadmill speeds used were 5, 10, 15, 20, 25, and 30 cm/s, based on previous studies performed in our laboratory [25].

Table 1 Experimental groups included in the study

Gender	n	Treatment onset	Experimental group
Female	9	—	Wild type
Female	19	8 weeks	SOD1 + saline (SOD1c)
Female	19	8 weeks	SOD1 + PRE (PRE)
Female	9	8 weeks	SOD1 + PRE + BD (PRE + BD)
Female	9	12 weeks	SOD1 + PRE (delayed)
Male	9	—	Wild type
Male	19	8 weeks	SOD1 + saline (SOD1c)
Male	19	8 weeks	SOD1 +PRE (PRE)

BD=BD-1036; PRE=PRE-084; SOD1=superoxide dismutase 1 transgenic; SOD1c=superoxide dismutase 1 transgenic control

Retrotracers Injection

Mice of 15 weeks of age (5 of each group) were anesthetized by an intraperitoneal injection of sodium pentobarbital (50 mg/kg). Their left hind paw was gently shaved and the skin was disinfected with povidone-iodine. A small incision in the skin was performed over the TA muscle and a 30-gauge needle connected to a Hamilton syringe (Hamilton Co, Reno, NV, USA) was inserted in the proximal region of the TA muscle. Two μl of 4 % Fluorogold (Fluorochrome LLC, Denver, CO, USA) were injected directly into the muscle. After the injection, the needle was left in place for 30 s and then slowly withdrawn to avoid liquid from coming out of the muscle.

Histology

One week after retrotracer injection (at 16 weeks of age) mice were transcardially perfused with 4 % paraformaldehyde in phosphate-buffered saline (PBS) and the lumbar segment of the spinal cord was removed, postfixed for 24 h, and cryopreserved in 30 % sucrose. Transverse 40-μm thick sections were serially cut with a cryotome (Leica CM190, Leica Microsystems, Wetzlar, Germany) between L2 and L5 segmental levels. For each segment, each section from a series of 10 was sequentially collected on separate gelatin-coated slides.

One slide of each animal was rehydrated for 1 min and stained for 2 h with an acidified solution of 3.1 mM cresyl violet. Then the slides were washed in distilled water for 1 min, dehydrated and mounted with DPX (Fluka, Buchs, Switzerland). MNs were identified by their localization in the ventral horn of the stained spinal cord sections and counted after strict size and morphological criteria (only MNs with diameters larger than 20 μm and with polygonal shape and prominent nucleoli were counted) [10]. The number of MNs present in both ventral horns was counted in 4 serial sections of each L4 to L5 segments [10, 23].

To estimate the number of MNs innervating the TA muscle, retrograde-labeled MNs were counted under epifluorescence microscopy from slides 1, 3, 5, 7, and 9. The total number of MNs was calculated according to the formula of Abercrombie [26].

Another series of sections was blocked with PBS-Triton-fetal bovine serum (FBS) and incubated overnight at 4 °C with primary antibodies anti-glial fibrillary acidic protein (1:1000, Dako, Glostrup, Denmark), rabbit anti-ionized calcium binding adaptor molecule 1 (1:1000, Wako, Chemicals, Richmond, VA, USA), anti-sigma-1R (1:500, Santa Cruz Biotechnologies, Santa Cruz, CA, USA), anti-phospho-NR1 (Ser896) (1:500, Millipore, Billerica, MA, USA), or anti-phospho-NR1 (Ser897) (1:500, Millipore). After washes, sections were incubated for 1 h at room temperature with Cy2- or Cy3-conjugated secondary antibody (1:200; Jackson Immunoresearch, West Grove, PA, USA), or, in the case of anti-phospho-NR1 antibodies, with biotinilated secondary antibody (1:200, Vector, Burlingame, CA, USA) and then for 2 h at room temperature with Cy3-conjugated streptavidin (1:1000, Vector). For co-localizations, spinal MNs were labeled with Cy2- or Cy3-conjugated fluorotracer Nissl staining (1:200, Life Technologies, Grand Island, NY, USA). To quantify astroglial and microglial immunoreactivity, microphotographs of the grey matter of the ventral horn were taken at ×400 and, after defining the threshold for background correction, the integrated density of glial fibrillary acidic protein (GFAP) or ionized calcium binding adaptor molecule 1 (Iba1) labeling was measured using ImageJ software (National Institutes of Health, Bethesda, MA, USA) [27, 28]. The integrated density is the area above the threshold for the mean density minus the background.

Protein Extraction and Western Blot

For protein extraction, a subset of mice (4 of each experimental group) were anesthetized and decapitated at 16 weeks of age. The lumbar spinal cord was removed and divided into quarters to isolate the ventral parts. One of these parts was prepared for protein extraction and homogenized in modified radioimmunoprecipitation assay buffer (50 mM Tris–HCl pH7.5, 1 % Triton X-100, 0.5 % sodium deoxycholate, 0.2 % sodium dodecyl sulfate (SDS), 100 mM NaCl, 1 mM ethylenediaminetetraacetic acid (EDTA)) adding 10 μl/ml of Protease Inhibitor cocktail (Sigma, St Louis, MO, USA) and 1 mM sodium orthovanadate (phosphatase inhibitor) (Roche, Manheim, Germany). After clearance, protein concentration was measured by bicinchoninic acid assay (BCA Protein Assay Kit, Pierce, Rockford, IL).

To perform the Western blot, 30 μg of protein of each sample were loaded in 7.5 % SDS-poliacrylamide gels. The transfer buffer was 25 mM trizma-base, 192 mM glycine, 20 % (v/v) methanol, pH8.4. The membranes were incubated with 5 % bovine serum albumin in PBS plus 0.05 % Tween-20 for 1 h, and then with primary antibodies at 4 °C overnight. The primary antibodies used were: anti-b-actin (Sigma; 1:10000), anti-sigma-1R (Santa Cruz, 1:500), anti-NMDAR1 (Millipore, 1:500), anti-phospho NR1 (S896) (Millipore, 1:500), or anti-phospho NR1 (S897) (Milllipore, 1:500). Horseradish peroxidase, coupled with secondary antibody incubation was performed for 90 min at room temperature. The membranes were visualized using an enhanced chemiluminiscence method and the images were collected and analyzed with Gene Genome apparatus and Gene Snap and Gene Tolls softwares (Syngene, Cambridge, UK), respectively.

Survival

A subset (of 10 mice of each group and gender) was used to assess the effects of treatment on survival of the animals. It was considered that animals reached the endpoint of the disease when they were unable to stand up for 30 s when placed on their side.

Statistical Analysis

Data are expressed as mean ± SEM. Electrophysiological and locomotion test results were statistically analyzed using repeated measurements and 1-way analysis of variance, applying the Bonferroni post-hoc test when necessary. Histological data were analyzed using the Mann-Whitney *U* test. Survival data was analyzed using the Kaplan-Meir test.

Results

Sigma-1R Expression in SOD1 Animals

We studied the sigma-1R expression levels and localization in the ventral spinal cord of mice aged 16 weeks to assess whether MNs could be directly affected by the PRE-084 administration. Western blot analysis revealed that the expression levels of the receptor were not altered during disease progression because there were no differences in the amount of protein between experimental groups (Fig. 1A). Furthermore, immunohistochemistry revealed co-labeling between Nissl staining (labeling MNs) and sigma-1R (Fig. 1B), indicating that this receptor is expressed in the MNs of both wild-type and transgenic animals.

PRE-084 Administration Improves Spinal Motoneuron Function in SOD1 Animals

The analysis of lower MN functional activity is crucial to assess the effect of new treatments, because the loss of neuromuscular function is 1 of the hallmarks of the disease process in ALS animal models [29–31]. The results showed that PRE-084 administration significantly improved the amplitude of TA and plantar compound muscle action potential (CMAP), both in female and male SOD1^{G93A} mice from 12 weeks of age compared to untreated mice. This effect was sustained until the end of the follow-up (16 weeks of age) when the mean amplitude of the potentials was twice that of the untreated animals. The functional preservation was especially marked in the TA muscle, because at the end of the follow-up its function was 80 % of the baseline values recorded in the pre-treatment 8-weeks test. Coadministration of the sigma-1R antagonist BD-1036 reverted the improvement achieved by the PRE-084 agonist (Fig. 2).

PRE-084 Treatment Improves Locomotor Performance in SOD1 Animals

PRE-084 administration also significantly improved the locomotor performance of SOD1 animals (Kaplan-Meier test; $p<0.05$). Both male and female mice administered with the sigma-1R agonist were able to run at higher speeds compared to untreated mice. The performance of untreated SOD1 animals began to decline from 10 cm/s and none were able to run at 30 cm/s (the maximum speed tested). However, animals treated with PRE-084 did not show locomotor impairments until 25 cm/s, and approximately half of them were able to maintain locomotor performance at 30 cm/s at 16 weeks of age. Again the beneficial effects were blocked when the sigma-1R antagonist was co-administered (Fig. 3).

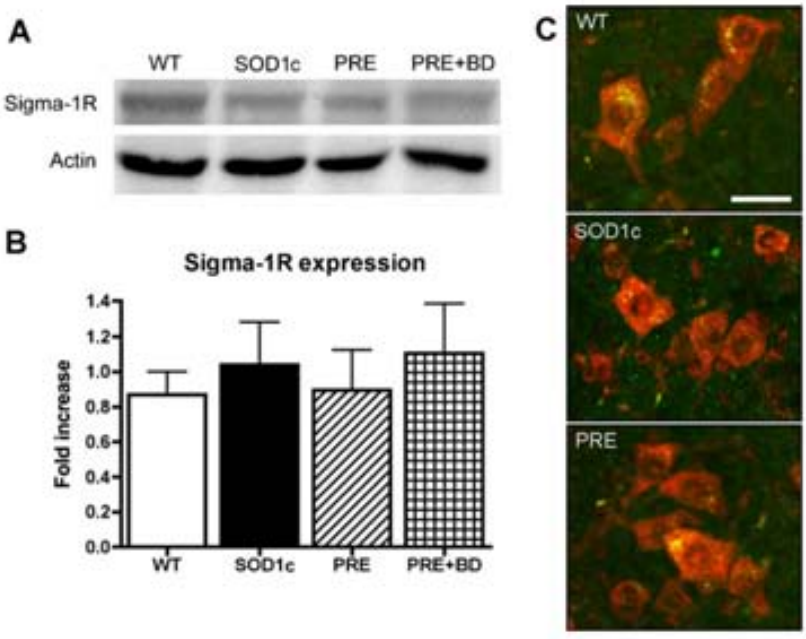

Fig. 1 Sigma-1 receptor (sigma-1R) expression and localization in the lumbar spinal cord. (A) Western blot was used to assess the expression levels of the sigma-1R in the ventral part of the lumbar spinal cord. (B) Quantification of the Western blot evidenced no differences between groups ($F_{3,27}=0.63$; $p=0.6013$). (C) Confocal images of L4-L5 motoneurons (MNs) labeled with fluorescent Nissl staining (red) and anti-sigma-1R (green) to co-localize the receptor into the MNs. Note that the expression pattern is similar in wild-type (WT) mice untreated (SOD1c) and PRE-084 treated (PRE) SOD1^{G93A}. Scale bar, 20 μm

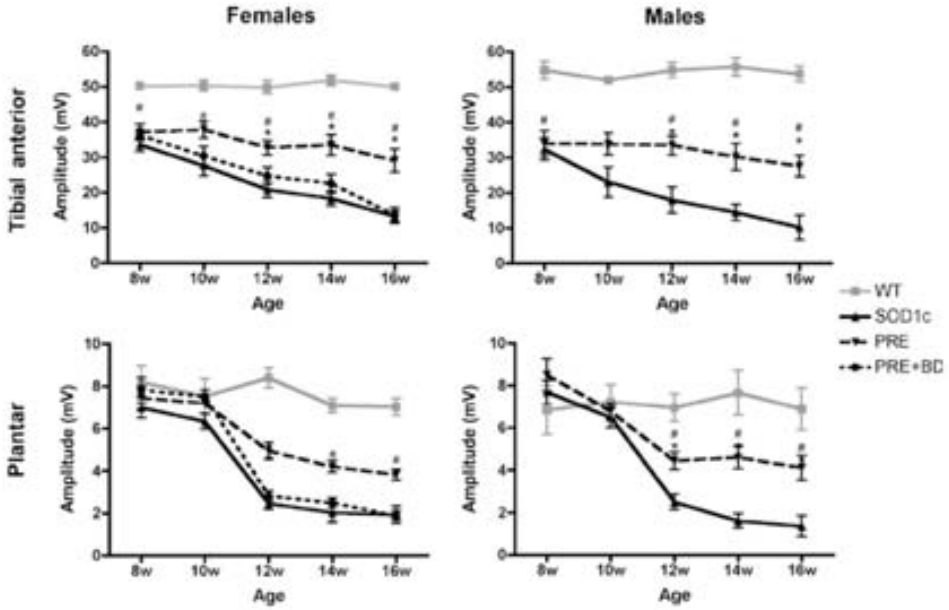

Fig. 2 Electrophysiological tests of male and female animals to evaluate the lower motor function by means of the evoked compound muscle action potential (CMAP). Tibialis anterior (TA) and plantar muscles were evaluated from 8–16 weeks of age in wild-type (WT) mice, SOD1 untreated (SOD1c), treated with PRE-084 (PRE), and co-treated with PRE-084 and BD-1036 (PRE + BD). Daily administration of PRE-084 significantly improved lower motoneuron (MN) function, especially in the case of the TA because its function was almost maintained until the end of the follow-up (TA muscle: $F_{12,208}=5.63$; $p<0.001$ for females; $F_{8,176}=2.27$; $p<0.05$ for males. Plantar muscle: $F_{12,208}=4.71$; $p<0.001$ for females; $F_{8,176}=15.43$; $p<0.001$ for males). Values are mean ± SEM. $^{*}p<0.05$ *vs* WT mice; $^{\#}p<0.05$ *vs* SOD1c

PRE-084 Administration Preserves Neuromuscular Connections in SOD1 Animals

To assess whether PRE-084 administration could maintain the connection between MNs and the skeletal muscles, retrotracers were injected in the TA muscle at 15 weeks and the number of stained MNs in the spinal cord counted 1 week later. The results showed that sigma-1R agonist administration significantly preserved the number of MNs innervating the TA muscle (Fig. 4). PRE-084 treated animals showed 40 % higher number of labeled MNs in the spinal cord with respect to SOD1 untreated mice. This beneficial effect was reverted by coadministration of the sigma-1R antagonist. Figure 4A shows representative images of the cord ventral horns of untreated (SOD1c), treated with PRE-084, and co-treated with PRE-084 and BD-1036 SOD1 transgenic mice.

PRE-084 Administration Preserves Motoneurons in the Anterior Horn of the Lumbar Spinal Cord

The survival of spinal MNs was assessed by counting the number of stained MNs soma in the anterior horns of the lumbar spinal cord in mice of 16 weeks of age, focusing in L4 to L5 segments where the TA and the plantar muscles motor nuclei are represented [32]. MN counts were restricted to the lateral area of the ventral horn lamina IX, because this population innervates the hind-limb muscles. Neurons smaller than 20 μm in diameter were excluded from counting, even if they could be atrophic MNs because they were unlikely to be functional.

PRE-084 administration reduced the neurodegenerative process in SOD1 mice (Fig. 5). Treated animals showed a 30 % increase in the number of MNs present in the ventral spinal horns, without differences between males and females. Alhough SOD1 untreated animals had 16.1±1.6 (male) and 20.1±1.1 (female) MNs per section, PRE-084 treated mice had 34.8±0.9 and 33.9± 2.1, respectively. The coadministration of the sigma-1R antagonist blocked the neuroprotective effect achieved by the agonist (Fig 5B). Figure 5A shows representative images of ventral horns of wild-type, untreated control, treated with PRE-084, and co-treated with PRE-084 and BD-1036 SOD1 mice to illustrate the neuroprotective effect.

PRE-084 Administration Reduces Microglial but Not Astroglial Immunoreactivity in the SOD1 Spinal Cord

It has been extensively reported that glial cells contribute to MN degeneration, both in animal models [33–35] and in ALS patients [36]. Thus, we analyzed both

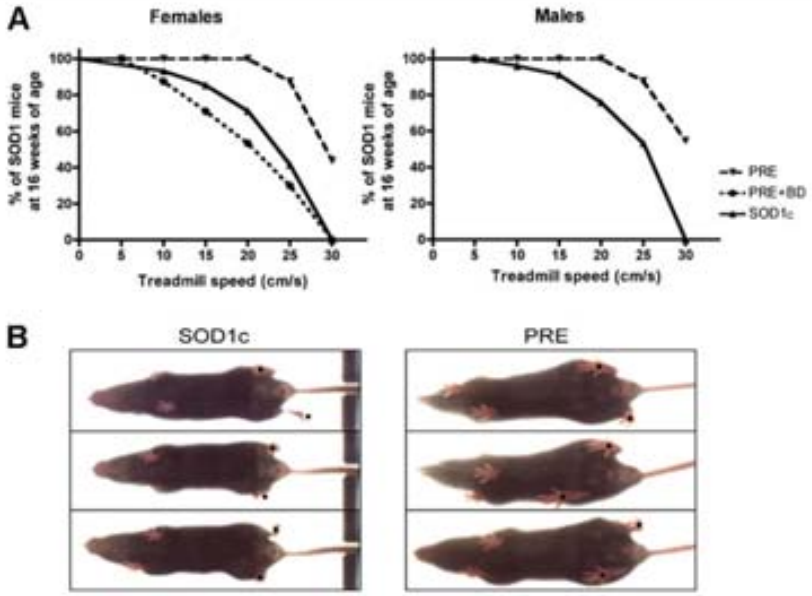

Fig. 3 Locomotor performance of wild-type, SOD1 untreated (SOD1c), treated with PRE-084 and co-treated with PRE-084 and BD-1036 animals at 16 weeks of age. (A) The graphs represent the proportion of animals that were able to run with increasing velocity and evidence the larger proportion of PRE-084 treated animals that were able to run at higher speeds (Kaplan-Meier test; chi-square=17.27, $p<0.001$ for females; chi-square=14.96, $p<0.001$ for males). (B) Representative images of SOD1 untreated animals (SOD1c) and treated animals with PRE-084 (PRE) running at 10 cm/s. Note the misplacement of both paws (black dots) in the untreated SOD1 mouse and the reversion of this sign achieved by PRE-084 administration

astroglial (glial fibrilar acidic protein-positive) and microglial (Iba-1-positive) immunoreactivity in the anterior horns of lumbar spinal cord sections to assess possible modifications of glial cell behavior induced by the treatment.

The results showed that PRE-084 administration significantly reduced microglial, but not astroglial immunoreactivity in the ventral horn of SOD1 animals (Figs. 6 and 7), whereas in both male and female untreated SOD1 mice, Iba-1 immunoreactivity was increased by more than 600 % compared to wild-type mice, PRE-084 treatment reduced it to approximately 300 %. This improvement was reverted when the sigma-1R antagonist was coadministered.

PRE-084 Delayed Treatment Also Produces Functional Improvement in SOD1 Animals

Considering the important effect achieved by the sigma-1R agonist administered from 8 weeks of age (i.e., a presymptomatic stage), we studied that if a more delayed treatment (i.e., from the 12th week) could also ameliorate the animals condition. Electrophysiological tests revealed that PRE-084 treatment produced a

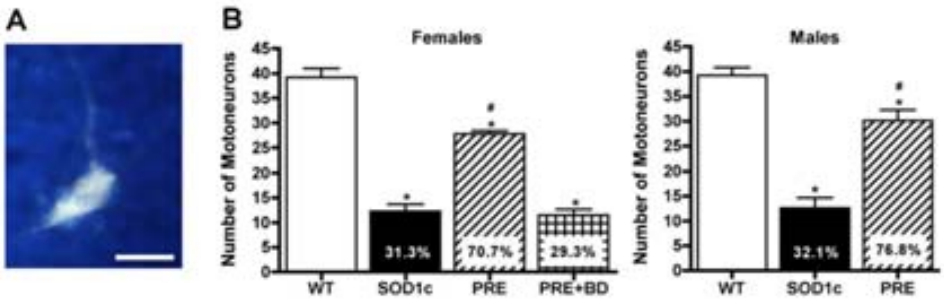

Fig. 4 Retrotracer injection performed to assess the proportion of lumbar motoneurons (MNs) that were still connected to the tibialis anterior (TA) muscle in wild-type (WT) animals, SOD1 untreated animals (SOD1c), animals treated with PRE-084 and co-treated with PRE-084 and BD-1036 at 16 weeks of age. (A) Representative image of a Fluorogold-labeled MN in the lumbar spinal cord. Scale bar, 20 μm. (B) The quantification of the total number of Fluorogold-stained MNs revealed a 40 % preservation of neuromuscular connections in the PRE-084 compared to SOD1c untreated mice ($F_{3,19}=105.4$, $p<0.001$ for females; $F_{2,14}=86.68$, $p<0.001$ for males). Values are mean ± SEM. *$p<0.05$ *vs* WT mice; #$p<0.05$ *vs* SOD1c

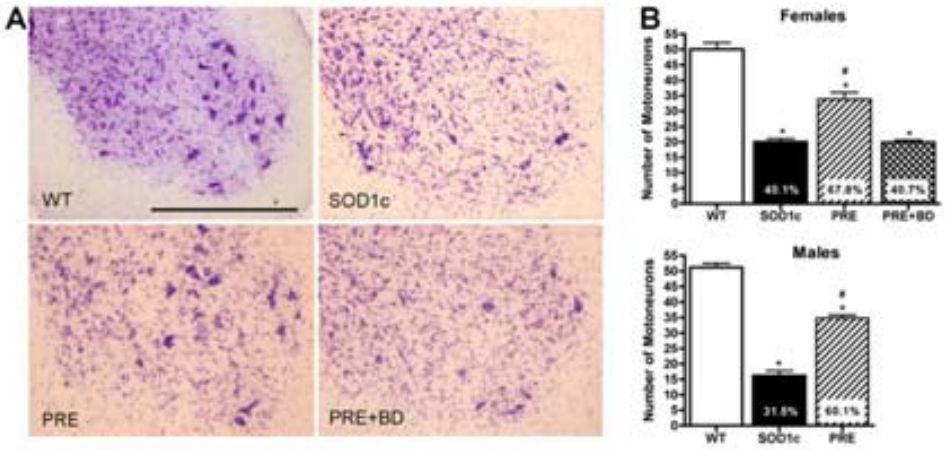

Fig. 5 Motoneurons (MN) survival in SOD1 animals. (A) Representative images of Nissl stained L4 spinal cord sections from wild-type mice, SOD1 untreated (SOD1c), treated with PRE-084 (PRE), and co-treated with PRE-084 and BD-1036 (PRE + BD). Note the evident improvement after PRE-084 treatment. Scale bar, 500 µm. (B) The quantification of MNs per sections in female and male mice showed a 30 % significant improvement in MN preservation ($F_{3,19}$=95.53, p< 0.001 for females; $F_{2,14}$=197.9, p<0.001 for males). Values are mean ± SEM. *p<0.05 *vs* WT mice; #p<0.05 *vs* SOD1c

significant increase of the TA CMAP from 14 weeks, with a maximum effect at the end of the follow-up, when the mean amplitude was 25 % higher than in untreated SOD1 mice (Fig. 8A). The delayed treatment also improved the locomotor performance of the animals (Kaplan-Meier test, p<0.05), whereas SOD1 untreated animals performance declined from 10 cm/seconds to all treated mice supported until 15 cm/seconds. At 30 cm/seconds, when SOD1 controls were completely unable to perform the test, 42 % of the treated animals were able to run (Fig. 8B). MN counts revealed that delayed administration of the sigma-1R agonist produced a significant 13 % increase in the number of stained MN in the anterior horns of spinal cord sections compared to SOD1 untreated mice (Fig. 8C).

Sigma-1R Agonist Significantly Extends Survival of SOD1 Transgenic Mice

The administration of PRE-084 from 8 weeks of age significantly prolonged survival of both female and male SOD1 mice (Kaplan-Meir analysis, p<0.001), whereas untreated female and male SOD1 mice lived 124.1±0.96 and 122.6± 3.06 days, respectively, and treated animals survived for 140.5±1.77 and 133.1±3.91 days (approximately 15 and 10 % longer) (Fig. 9).

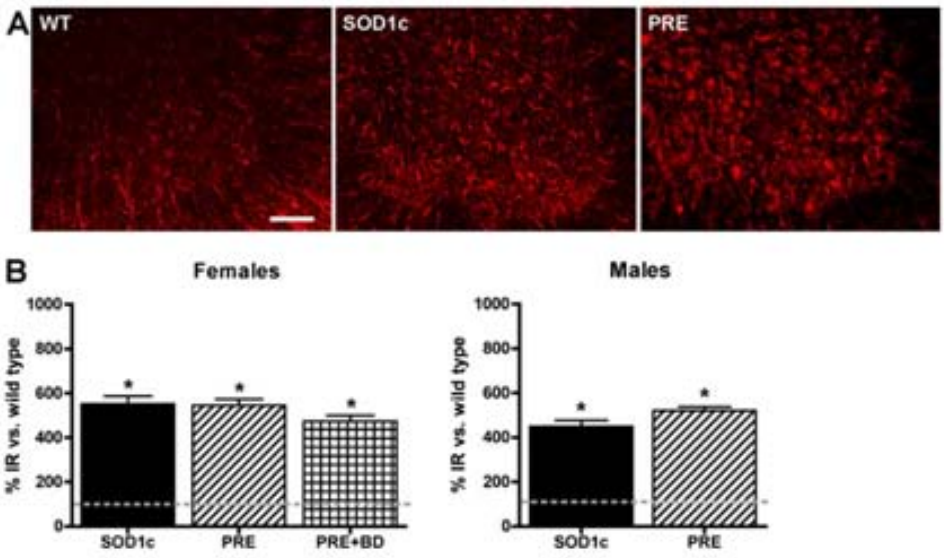

Fig. 6 Analysis of astroglial reactivity. (A) Representative microphotographs of wild-type (WT) mice, SOD1 untreated (SOD1c) and treated with PRE-084 (PRE) mice immunolabeled for astrocytes (glial fibrilar acidic protein). Scale bar, 125 µm. (B) Quantification of glial fibrilar acidic protein immunoreactivity in female and male mice. There were no differences between treated and untreated animals ($F_{3,19}$=38.52, p<0.001 for females; $F_{2,14}$= 106.1, p<0.001 for males). Values are mean ± SEM. *p< 0.05 *vs* WT; #p<0.05 *vs* SOD1c

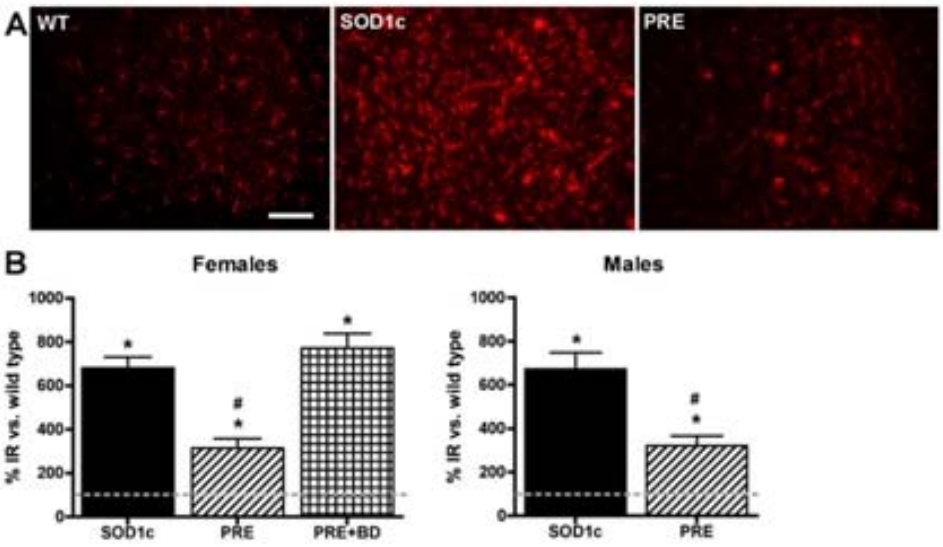

Fig. 7 Analysis of microglial reactivity. (A) Representative microphotographs of wild-type (WT) mice, SOD1 untreated (SOD1c) and treated mice with PRE-084 (PRE) immunolabeled for microglial cells (Iba-1). Scale bar, 125 µm. (B) Quantification of Iba-1 immunoreactivity in female and male mice. Note the marked reduction of the microglial reactivity after the PRE-084 treatment ($F_{3,19}$=17.91, p<0.001 for females; $F_{2,14}$=85.7, p<0.001 for males). Values are mean ± SEM. *p<0.05 *vs* WT; #p<0.05 *vs* SOD1c

Sigma-1R Exerts Modulation of NMDA Receptors through the PKC Pathway

Previously reported, *in vitro* studies indicate that the sigma-1R agonist suppresses NMDA currents in rat retinal ganglion cells [14] and rescues MNs from excitotoxic-induced death mediated by PKC activation [18]. Thus, we assessed if PRE-084 might exert its therapeutic effect *in vivo* through modulation of NMDA receptors via PKC. To assess this hypothesis, we analyzed the phosphorylation state of 2 PKC-specific

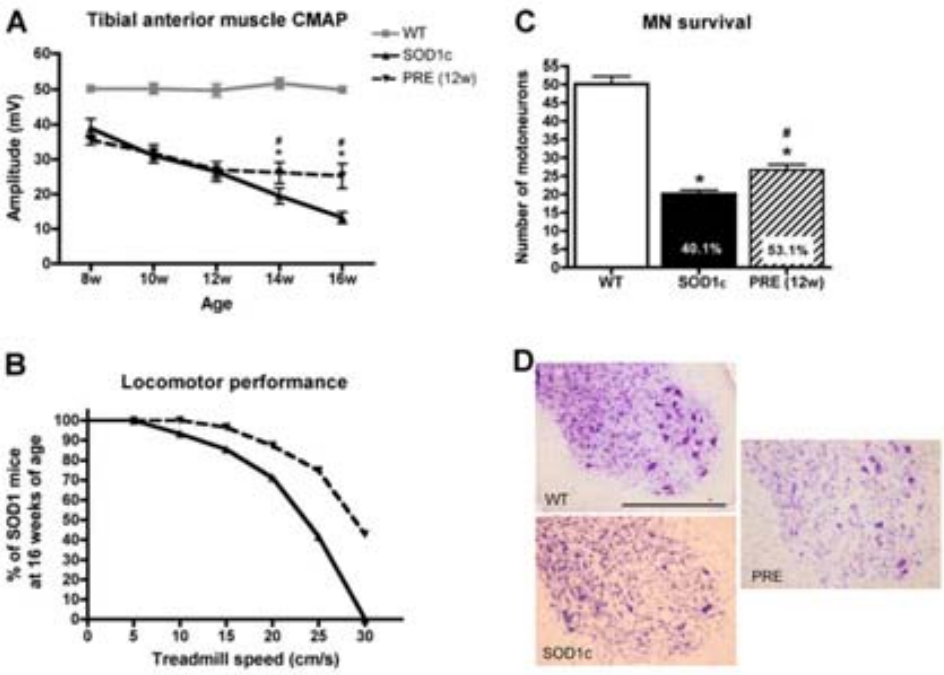

Fig. 8 Effect of delayed administration of PRE-084 from 12 weeks of age. (A) Lower motoneuron (MN) function evaluated by the compound muscle action potential (CMAP) of the tibialis anterior muscle. PRE-084 treatment prevents the decline in spinal MN function ($F_{8,136}$= 6.71; p<0.001). (B) Locomotor performance of the animals at 16 weeks of age. The graph represents the proportion of animals that were able to run with increasing velocity. Note the greater proportion of PRE-084-treated animals that were able to run at higher speeds (Kaplan-Meier test, chi-square=8.21, p<0.05). (C) Quantification of MNs per sections evidenced a 13 % significant improvement in MN preservation ($F_{2,14}$= 138.7, p<0.001). (D) Representative images of wild-type (WT) mice, SOD1 untreated (SOD1c) and treated with PRE-084 mice from 12 weeks of age (PRE 12w). Values are mean ± SEM. *p<0.05 *vs* WT; #p<0.05 *vs* SOD1c

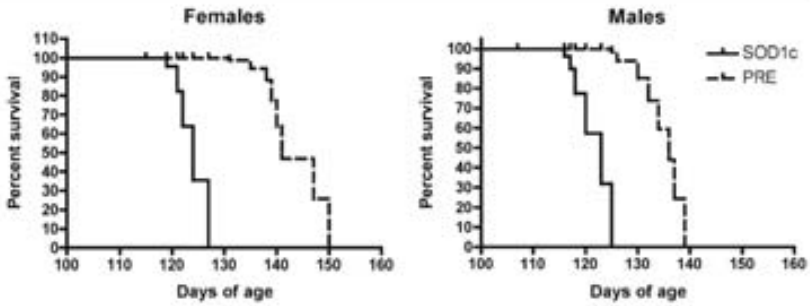

Fig. 9 PRE-084 administration significantly extended SOD1 mice survival. Sigma-1 receptor (sigma-1R) agonist treatment prolonged SOD1 animals life-span for (A) 16 days in females (chi-square=165.3, $p<0.001$) and (B) 11 days in males (chi-square=141.2, $p<0.001$)

serines (Ser896 and Ser897) in the NR1 subunits of NMDA receptors. Because there were no differences between males and females in the functional and histological results, data from both genders was pooled. The results showed a significant increase in the phosphorylation of PKC-specific Ser896 and Ser897 of the NMDA-NR1 subunit in mice treated with the sigma-1R agonist, by 4.3- and 5.5-fold with respect to SOD1 untreated animals, respectively. The coadministration of the sigma-1R antagonist reduced the amount of phosphorylated NR1 to control values (Fig. 10A). To assess whether the phosphorylation was affecting the receptors expressed in MNs, we performed immunohistochemical co-localization of the phopho-NR1 subunits and the MNs in the lumbar spinal cord. Results revealed that both PKC-specific NR1 phosphorylations were exclusively present in MNs of PRE-084-treated SOD1 animals (Fig. 10B).

Discussion

In this study we have analyzed the effect of the sigma-1R agonist, PRE-084, as a treatment for the SOD1^{G93A} mouse

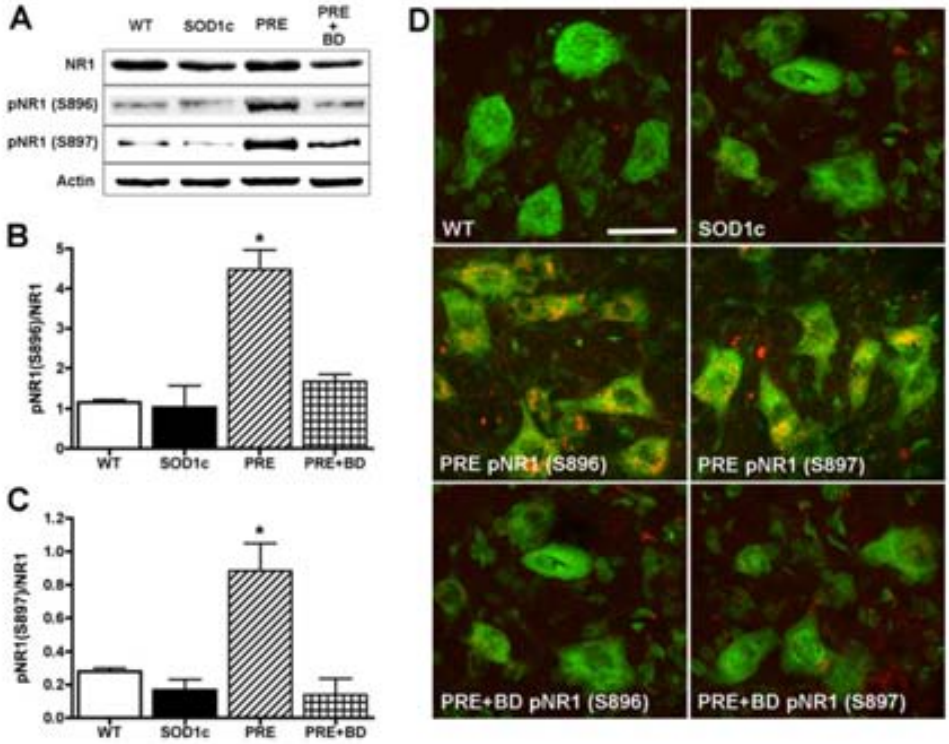

Fig. 10 Protein kinase C (PKC)-dependent phosphorylation in S897 and S897 of NMDA-NR1 subunits in the anterior horn of lumbar spinal cord of SOD1 animals at 16 weeks of age. (A) Western blots to assess the degree of phosphorylation of the NMDA-NR1 subunits in the anterior horn of lumbar spinal cord. PRE-084 increased the PKC-specific phosphorylation of NR1 subunits. (B, C) Quantification of Western blots revealed a 4.3- and 5.5-fold increase in phospho-NR1 subunits after the treatment with PRE-084 for (B) S896 and (C) S897, respectively ($F_{3,27}=15.91$, $p<0.001$ for females; $F_{3,27}=11.47$, $p<0.001$ for males). Values are mean ± SEM. *$p<0.05$. (D) Confocal images of L4 to L5 motoneurons (MNs) labeled with fluorescent Nissl staining (green) and anti-phospho-NR1 (red) to co-localize the phopho-NR1 into the MNs. Note that phosphorylation of the NMDA-NR1 subunit is only visible in the MNs of animals treated with PRE-084. Scale bar, 20 μm

model of ALS. The results indicate that daily administration of PRE-084 from 8 weeks of age significantly improved spinal MN function, manifested by maintenance of the amplitude of muscle action potentials and improved locomotion behavior, and preserved both neuromuscular connections and MNs survival in the spinal cord. Moreover, sigma-1R agonist prolonged survival in female and male SOD1 animals. Delayed administration of PRE-084 starting at 12 weeks of age also significantly improved functional outcome and MN preservation of $SOD1^{G93A}$ animals. Among other possible effects, further analyses revealed that PRE-084-induced PKC-specific phosphorylation of 2 serines (Ser896 and 897) of the NMDA-NR1 subunit in MNs, and a reduction of the microglial reactivity in the spinal cord of $SOD1^{G93A}$-treated animals compared with $SOD1^{G93A}$-untreated mice.

We previously reported the beneficial role of PRE-084 in terms of neuroprotection on both *in vitro* and *in vivo* models of MN death. First we demonstrated that PRE-084 promotes MN survival and neurite outgrowth in an organotypic model of excitotoxic insult [18]. We have also shown a potent neuroprotective effect of PRE-084 treatment on spinal MNs after L4 to L5 root avulsion injury in adult rats [10]. Focusing on ALS, it has been recently described a causative relation of mutations in the *SIGMA-R1* gene in human patients developing juvenile ALS and frontotemporal lobar degeneration-ALS pathology [21, 22], suggesting that this receptor may be a good target for the treatment of ALS. First we assessed the expression levels and localization of the sigma-1R in the ventral part of the lumbar spinal cord of $SOD1^{G93A}$ mice. Despite a slight reduction compared to wild-type mice, the results showed that sigma-1R was present in spinal MNs of $SOD1^{G93A}$ animals, even at 16 weeks of age, pointing out that agonist administration can directly affect MNs. To confirm that the effects of the selective agonist PRE-084 were due to modulation of the sigma-1R, a selective antagonist (BD1036) was coadministered in another group of animals. This coadministration blocked all the beneficial effects, demonstrating that the therapeutic action can be attributed to the activation of the sigma-1R.

Abnormal function of spinal MNs, loss of neuromuscular junctions, and subsequent death of the MNs are key elements of the pathology in human patients and animal models of ALS [1, 29, 37]. Recently, we characterized the pattern of lower and upper MN dysfunction electrophysiologically [23] during disease progression in the $SOD1^{G93A}$ mouse model, revealing that this is a reliable test to monitor the animal model, as well as human patients. In the present work, we found that daily sigma-1R agonist administration from 8 weeks of age, a time when signs of paresis are not present, yet but when nerve conduction tests clearly identify motor dysfunction, greatly improves the function of lower MN in both male and female $SOD1^{G93A}$ mice, as evidenced by the amplitude of the CMAPs, especially in the TA muscle,which functioned at 16 weeks of age and was maintained compared to baseline values. This improved function correlated with the preservation of more than 70 % of spinal MNs, still innervating the TA muscle, twice as many as in the untreated $SOD1^{G93A}$ animals (32 %). Gait abnormalities and progressive paralysis are also 2 main characteristics of ALS in human [1] and animal models [25]. We found a significant improvement in the locomotor capacity of $SOD1^{G93A}$ mice treated with PRE-084 because they were able to run at higher speeds on a treadmill than untreated $SOD1^{G93A}$ mice. This fact demonstrates that sigma-1R agonist administration preserves muscle strength and reduces signs of paralysis. Furthermore, it resulted in a significant prolongation for 16 and 11 days in survival of female and male $SOD1^{G93A}$ mice, respectively. Therefore, sigma-1R modulation produces important functional benefits in terms of spinal MN function, locomotion, and survival in the $SOD1^{G93A}$ mouse model, even comparatively better than silencing the mutant SOD1 expression [38] or other pharmacological treatments previously reported [39], such as riluzole [40].

Once demonstrated that daily PRE-084 administration from 8 weeks of age significantly improves functional performance and preserves MN in the spinal cord, we performed a second study in which PRE-084 was administered from 12 weeks, the beginning of the classical symptomatic phase in $SOD1^{G93A}$ mice, to mimic the time point at which patients might start the treatment. The results showed that delayed administration was also able to improve spinal MN function and locomotion performance, and significantly preserved MN cell bodies in the spinal cord compared to $SOD1^{G93A}$ untreated animals.

Sigma-1R ligands have been shown to promote neuroprotection in several types of insults [15]. *In vitro* studies revealed potent neuroprotective effects of sigma-1R agonists after excitotoxic damage [18], hypoxia-mediated neurotoxicity [41], oxidative stress-induced cell death [17], or glucose deprivation [42]. *In vivo* studies demonstrated that sigma-1R agonists exert therapeutic actions in rats after stroke [19, 20], after selective cholinergic lesions [43], and after spinal root avulsion [10]. The results found in this study also reveal a potent neuroprotective effect of PRE-084 administration on spinal MNs in the neurodegenerative $SOD1^{G93A}$ mice model. At 16 weeks of age, there was a 30 % increase in the number of surviving MNs in the spinal cord of both male and female SOD1 animals treated with PRE-084 with respect to untreated animals. We have previously described the progression of spinal MN degeneration of $SOD1^{G93A}$ mice, showing that the number of surviving MNs per lumbar cord section averaged 37±2 and 33±3 in male and female mice, respectively, at 12 weeks of age, and 16±2 and 20±1 in male and female mice at 16 weeks of age

[23, 44], respectively. In the present study, we found that PRE-084 treated animals had a mean of 35±1 (males) and 34±2 (females) MNs per section at 16 weeks of age. Thus, sigma-1R agonist administration slows down the degenerative process so that treated animals have the same number of MNs per section at 16 weeks than untreated animals at 12 weeks.

It has been extensively described that calcium dysregulation and excitotoxicity are 2 main pathogenic mechanisms of ALS pathology [45, 46]. ALS-vulnerable spinal and brainstem MNs display low endogenous Ca^{2+} buffering capacity, that is 5 to 6 times lower than that found in ALS-resistant MNs (i.e., oculomotor MNs), making them more susceptible to excitotoxic insults [47]. NMDA receptor is considered to be 1 of the key elements in excitotoxiciy [46]. It has been reported that sera from ALS patients induces abnormal NMDA receptor activation [48]. Moreover, Sunico et al. [49] showed an excitation/inhibition imbalance in MNs of $SOD1^{G93A}$ mice with an increased density of glutamatergic synapses, which could lead to an enhancement of Ca^{2+} influx into the cells. Thus, NMDA receptor modulation might be a good target to reduce MN damage. Sigma-1R agonists, such as SKF10097 and PRE-084, suppress NMDA currents in rat retinal ganglion cells through a PKC-dependent mechanism, leading to a reduction of calcium influx into the cytoplasm [14]. Furthermore, sigma-1R agonists prevent Ca^{2+} dysregulation and promote neuroprotection in rat cortical neurons by modulating Ca^{2+} influx through NMDA receptors [41], and also protect MNs in organotypic cultures against excitotoxicity [18]. Our novel results show that sigma-1R agonist administration led to increased PKC-specific phosphorylation of NR1 subunits present in spinal MNs, demonstrating a direct effect of the treatment in these cells. These changes in the NMDA receptor might reduce its permeability and, thus, the calcium influx into the MNs, attenuating excitotoxicity. Further experiments should be performed to assess whether PRE-084 modifies the NMDA channel properties in SOD1 MNs.

Neuroinflammation, and particularly the role of microglia is another pathological hallmark of ALS [50]. In resting conditions, SOD1 transgenic microglia shows reduced neuroprotective properties [51]. Moreover, phagocytic microglia adjacent to MNs is present at the very early stages of the disease in the transgenic rat model of ALS [35], suggesting that abnormal microglial function could play an active role in MN degeneration. Our results revealed a reduction of microglial immunoreactivity in the ventral spinal cord of PRE-084-treated $SOD1^{G93A}$ mice compared to untreated $SOD1^{G93A}$ mice. *In vitro* assays performed by Hall et al. [13], in 2009, showed that the activation of sigma-1R suppresses adenosine triphosphate-induced Ca^{2+} influx and attenuates microglial activation. Both findings point out that sigma-1R could directly modulate microglial activation in $SOD1^{G93A}$ animals acting through a complementary non-neuronal pathway to ameliorate the MNs environment and promote their survival. This effect may add to the reduction of neuroinflammatory response, secondary to the prevention of motoneuron degeneration.

Our results demonstrate for the first time that a sigma-1R agonist has potent beneficial actions in the $SOD1^{G93A}$ model of ALS. We show that PRE-084 may exert, at least, a dual therapeutic contribution, modulating the NMDA Ca^{2+} influx to reduce excitotoxic damage to MNs, and the microglial reactivity to ameliorate the MNs environment. Such a pluri-functional target may provide better translational outcomes than drugs that act only on 1 of the multiple physiopathological mechanisms involved in ALS. These findings have increased importance because sigma-1R alterations have been reported in human patients, opening a novel perspective for the study of the potential role of sigma-1R agonists as therapeutic agents for ALS.

Acknowledgments This work was supported by Red de Terapia Celular (TERCEL) and Centro de Investigación Biomédica en Red sobre Enfermedades Neurodegenerativas (CIBERNED) funds, the Fondo de Investigación Sanitaria of Spain (grant no. PI1001787); the Ministerio de Ciencia e Innovación of Spain (grant SAF2009-12495), FEDER funds, and Action COST-B30 of the EC. We thank the technical help of Jessica Jaramillo and Marta Morell. RM is recipient of a predoctoral fellowship from the Ministerio de Educación of Spain.

Required Author Forms Disclosure forms provided by the authors are available with the online version of this article.

Conflict of interest The authors report no conflicts of interest.

References

1. Wijesekera LC, Leigh PN. Amyotrophic lateral sclerosis. Orphanet J Rare Dis 2009;4:3.
2. Rosen DR. Mutations in Cu/Zn superoxide dismutase gene are associated with familial amyotrophic lateral sclerosis. Nature 1993;364:362.
3. Ripps ME, Huntley GW, Hof PR, Morrison JH, Gordon JW. Transgenic mice expressing an altered murine superoxide dismutase gene provide an animal model of amyotrophic lateral sclerosis. Proc Natl Acad Sci USA 1995;92:689-693.
4. Bosco DA, Morfini G, Karabacak NM, et al. Wild-type and mutant SOD1 share an aberrant conformation and a common pathogenic pathway in ALS. Nat Neurosci 2010;13:1396-1403.
5. Pasinelli P, Brown RH. Molecular biology of amyotrophic lateral sclerosis: insights from genetics. Nature Rev Neurosci 2006;7:710-723.
6. Alonso G, Phan V-L, Guillemain I, et al. Immunocytochemical localization of the sigma1 receptor in the adult rat central nervous system. Neuroscience 2000;97:155-170.
7. Hayashi T, Su T-P. Sigma-1 receptor chaperones at the ER-mitochondrion interface regulate Ca(2+) signaling and cell survival. Cell 2007;131:596-610.

8. Gekker G, Hu S, Sheng WS, Rock RB, Lokensgard JR, Peterson PK. Cocaine-induced HIV-1 expression in microglia involves sigma-1 receptors and transforming growth factor-beta1. Int Immunopharmacol 2006;6:1029-1033.
9. Palacios G, Muro A, Vela JM, et al. Immunohistochemical localization of the sigma1-receptor in oligodendrocytes in the rat central nervous system. Brain Res 2003;961:92-99.
10. Penas C, Pascual-Font A, Mancuso R, Forés J, Casas C, Navarro X. Sigma receptor agonist 2-(4-morpholinethyl)1 phenylcyclohexanecarboxylate (Pre084) increases GDNF and BiP expression and promotes neuroprotection after root avulsion injury. J Neurotrauma 2011;28:831-840.
11. Morin-Surun MP, Collin T, Denavit-Saubié M, Baulieu EE, Monnet FP. Intracellular sigma1 receptor modulates phospholipase C and protein kinase C activities in the brainstem. Proc Natl Acad Sci USA 1999;96:8196-8199.
12. Mavlyutov TA, Ruoho AE. Ligand-dependent localization and intracellular stability of sigma-1 receptors in CHO-K1 cells. J Mol Signal 2007;2:8.
13. Hall AA, Herrera Y, Ajmo CT Jr., Cuevas J, Pennypacker KR. Sigma receptors suppress multiple aspects of microglial activation. Glia 2009;57:744-754.
14. Zhang X-J, Liu L-L, Jiang S-X, Zhong Y-M, Yang X-L. Activation of the ζ receptor 1 suppresses NMDA responses in rat retinal ganglion cells. Neuroscience 2011;177:12-22.
15. Maurice T, Su T-P. The pharmacology of sigma-1 receptors. Pharmacol Therap 2009;124:195-206.
16. Aydar E, Palmer CP, Klyachko VA, Jackson MB. The sigma receptor as a ligand-regulated auxiliary potassium channel subunit. Neuron 2002;34:399-410.
17. Tuerxun T, Numakawa T, Adachi N, et al. SA4503, a sigma-1 receptor agonist, prevents cultured cortical neurons from oxidative stress-induced cell death via suppression of MAPK pathway activation and glutamate receptor expression. Neurosci Lett 2010;469:303-308.
18. Guzmán-Lenis M-S, Navarro X, Casas C. Selective sigma receptor agonist 2-(4-morpholinethyl)1-phenylcyclohexanecarboxylate (PRE084) promotes neuroprotection and neurite elongation through protein kinase C (PKC) signaling on motoneurons. Neuroscience 2009;162:31-38.
19. Allahtavakoli M, Jarrott B. Sigma-1 receptor ligand PRE-084 reduced infarct volume, neurological deficits, pro-inflammatory cytokines and enhanced anti-inflammatory cytokines after embolic stroke in rats. Brain Res Bull 2011;85:219-224.
20. Ajmo CT, Vernon DOL, Collier L, Pennypacker KR, Cuevas J. Sigma receptor activation reduces infarct size at 24 hours after permanent middle cerebral artery occlusion in rats. Curr Neurovasc Res 2006;3:89-98.
21. Luty AA, Kwok JBJ, Dobson-Stone C, et al. Sigma nonopioid intracellular receptor 1 mutations cause frontotemporal lobar degeneration-motor neuron disease. Ann Neurol 2010;68:639-649.
22. Al-Saif A, Al-Mohanna F, Bohlega S. A mutation in sigma-1 receptor causes juvenile amyotrophic lateral sclerosis. Ann Neurol 2011;70:913-919.
23. Mancuso R, Santos-Nogueira E, Osta R, Navarro X. Electrophysiological analysis of a murine model of motoneuron disease. Clin Neurophysiol 2011;122:1660-1670.
24. Valero-Cabré A, Navarro X. H reflex restitution and facilitation after different types of peripheral nerve injury and repair. Brain Res 2001;919:302-312.
25. Mancuso R, Oliván S, Osta R, Navarro X. Evolution of gait abnormalities in SOD1(G93A) transgenic mice. Brain Res 2011;1406:65-73.
26. Abercrombie M. Estimation of nuclear population from microtome sections. Anat Rec 1946;94:239-247.
27. Moreno-Igoa M, Calvo AC, Penas C, et al. Fragment C of tetanus toxin, more than a carrier. Novel perspectives in non-viral ALS gene therapy. J Mol Med 2010;88:297-308.
28. Penas C, Casas C, Robert I, Forés J, Navarro X. Cytoskeletal and activity-related changes in spinal motoneurons after root avulsion. J Neurotrauma 2009;26:763-779.
29. Fischer LR, Culver DG, Tennant P, et al. Amyotrophic lateral sclerosis is a distal axonopathy: evidence in mice and man. Exp Neurol 2004;185:232-240.
30. Mohajeri MH, Figlewicz DA, Bohn MC. Selective loss of alpha motoneurons innervating the medial gastrocnemius muscle in a mouse model of amyotrophic lateral sclerosis. Exp Neurol 1998;150:329-336.
31. Wegorzewska I, Bell S, Cairns NJ, Miller TM, Baloh RH. TDP-43 mutant transgenic mice develop features of ALS and frontotemporal lobar degeneration. Proc Natl Acad Sci USA 2009;106:18809-18814.
32. McHanwell S, Biscoe TJ. The localization of motoneurons supplying the hindlimb muscles of the mouse. Philos Trans R Soc Lond B Biol Sci 1981;293:477-508.
33. Diaz-Amarilla P, Olivera-Bravo S, Trias E, et al. Phenotypically aberrant astrocytes that promote motoneuron damage in a model of inherited amyotrophic lateral sclerosis. Proc Natl Acad Sci USA 2011;108:18126-18131.
34. Yamanaka K, Boillee S, Roberts EA, et al. Mutant SOD1 in cell types other than motor neurons and oligodendrocytes accelerates onset of disease in ALS mice. Proc Natl Acad Sci USA 2008;105:7594-7599.
35. Sanagi T, Yuasa S, Nakamura Y, et al. Appearance of phagocytic microglia adjacent to motoneurons in spinal cord tissue from a presymptomatic transgenic rat model of amyotrophic lateral sclerosis. J Neurosci Res 2010;88:2736-2746.
36. Haidet-Phillips AM, Hester ME, Miranda CJ, et al. Astrocytes from familial and sporadic ALS patients are toxic to motor neurons. Nat Biotechnol 2011;29:824-828.
37. Azzouz M, Leclerc N, Gurney M, Warter JM, Poindron P, Borg J. Progressive motor neuron impairment in an animal model of familial amyotrophic lateral sclerosis. Muscle Nerve 1997;20:45-51.
38. Raoul C, Abbas-Terki T, Bensadoun J-C, et al. Lentiviral-mediated silencing of SOD1 through RNA interference retards disease onset and progression in a mouse model of ALS. Nat Med 2005;11:423-428.
39. Turner B, Talbot K. Transgenics, toxicity and therapeutics in rodent models of mutant SOD1-mediated familial ALS. Prog Neurobiol 2008;85:94-134.
40. Gurney ME, Cutting FB, Zhai P, et al. Benefit of vitamin E, riluzole, and gababapentin in a transgenic model of familial amyotrophic lateral sclerosis. Ann Neurol 1996;39:147-157.
41. Lockhart BP, Soulard P, Benicourt C, Privat A, Junien JL. Distinct neuroprotective profiles for sigma ligands against N-methyl-D-aspartate (NMDA), and hypoxia-mediated neurotoxicity in neuronal culture toxicity studies. Brain Res 1995;675:110-120.
42. Katnik C, Guerrero WR, Pennypacker KR, Herrera Y, Cuevas J. Sigma-1 receptor activation prevents intracellular calcium dysregulation in cortical neurons during in vitro ischemia. J Pharmacol Exp Ther 2006;319:1355-1365.
43. Antonini V, Marrazzo A, Kleiner G, et al. Anti-amnesic and neuroprotective actions of the sigma-1 receptor agonist (-)-MR22 in rats with selective cholinergic lesion and amyloid infusion. J Alzheimers Dis 2011;24:569-586.
44. Mancuso R, Oliván S, Mancera P, et al. Effect of genetic background on onset and disease progression in the SOD1-G93A model of amyotrophic lateral sclerosis. Amyotroph Lateral Scler 2012;13:302-310.

45. Grosskreutz J, Van Den Bosch L, Keller BU. Calcium dysregulation in amyotrophic lateral sclerosis. Cell Calcium 2010;47:165-174.
46. Van Den Bosch L, Van Damme P, Bogaert E, Robberecht W. The role of excitotoxicity in the pathogenesis of amyotrophic lateral sclerosis. Biochimica Biophysica Acta 2006;1762:1068-1082.
47. Alexianu ME, Ho BK, Mohamed AH, La Bella V, Smith RG, Appel SH. The role of calcium-binding proteins in selective motoneuron vulnerability in amyotrophic lateral sclerosis. Ann Neurol 1994;36:846-858.
48. Texidó L, Hernández S, Martín-Satué M, et al. Sera from amyotrophic lateral sclerosis patients induce the non-canonical activation of NMDA receptors "in vitro." Neurochem Int 2011;59:954-964.
49. Sunico CR, Dominguez G, García-Verdugo JM, Osta R, Montero F, Moreno-López B. Reduction in the motoneuron inhibitory/excitatory synaptic ratio in an early-symptomatic mouse model of amyotrophic lateral sclerosis. Brain Pathol 2011;21:1-15.
50. Henkel JS, Beers DR, Zhao W, Appel SH. Microglia in ALS: the good, the bad, and the resting. J Neuroimmune Pharmacol 2009;4:389-398.
51. Sargsyan SA, Blackburn DJ, Barber SC, et al. A comparison of in vitro properties of resting SOD1 transgenic microglia reveals evidence of reduced neuroprotective function. BMC Neuroscience 2011;12:91.

Chapter III: Resveratrol treatment

Resveratrol improves motoneuron function and extends survival in SOD1^{G93A} ALS mice

Mancuso R, Del Valle J, Mòdol L, Martinez A, Granado-Serrano AB, Ramírez-Nuñez O, Pallás M, Portero-Otín M, Osta R, Navarro X. Neurotherapeutics 2014; 11:419-432.

Neurotherapeutics
DOI 10.1007/s13311-013-0253-y

ORIGINAL ARTICLE

Resveratrol Improves Motoneuron Function and Extends Survival in SOD1^{G93A} ALS Mice

Renzo Mancuso · Jaume del Valle · Laura Modol · Anna Martinez · Ana B Granado-Serrano · Omar Ramirez-Núñez · Mercé Pallás · Manel Portero-Otin · Rosario Osta · Xavier Navarro

Abstract Amyotrophic lateral sclerosis (ALS) is an adult onset neurodegenerative disease that causes progressive paralysis and death due to degeneration of motoneurons in spinal cord, brainstem and motor cortex. Nowadays, there is no effective therapy and patients die 2–5 years after diagnosis. Resveratrol (trans-3,4′,5-trihydroxystilbene) is a natural polyphenol found in grapes, with promising neuroprotective effects since it induces expression and activation of several neuroprotective pathways involving Sirtuin1 and AMPK. The objective of this work was to assess the effect of resveratrol administration on SOD1^{G93A} ALS mice. We determined the onset of symptoms by rotarod test and evaluated upper and lower motoneuron function using electrophysiological tests. We assessed the survival of the animals and determined the number of spinal motoneurons. Finally, we further investigated resveratrol mechanism of action by means of western blot and immunohistochemical analysis. Resveratrol treatment from 8 weeks of age significantly delayed disease onset and preserved lower and upper motoneuron function in female and male animals. Moreover, resveratrol significantly extended SOD1^{G93A} mice lifespan and promoted survival of spinal motoneurons. Delayed resveratrol administration from 12 weeks of age also improved spinal motoneuron function preservation and survival. Further experiments revealed that resveratrol protective effects were associated with increased expression and activation of Sirtuin 1 and AMPK in the ventral spinal cord. Both mediators promoted normalization of the autophagic flux and, more importantly, increased mitochondrial biogenesis in the SOD1^{G93A} spinal cord. Taken together, our findings suggest that resveratrol may represent a promising therapy for ALS.

Keywords Motoneuron disease · Amyotrophic lateral sclerosis · Resveratrol · Sirtuin 1 · AMPK · SOD1^{G93A} mice

Electronic supplementary material The online version of this article (doi:10.1007/s13311-013-0253-y) contains supplementary material, which is available to authorized users.

R. Mancuso · J. del Valle · L. Modol · A. Martínez · X. Navarro
Institute of Neurosciences and Department of Cell Biology, Physiology and Immunology, Universitat Autònoma de Barcelona, and Centro de Investigación Biomédica en Red sobre Enfermedades Neurodegenerativas (CIBERNED), Bellaterra, Spain

A. B. Granado-Serrano · O. Ramirez-Núñez · M. Portero-Otin
Department of Experimental Medicine, Faculty of Medicine, Universitat de Lleida-IRBLleida, Lleida, Spain

M. Pallás
Unitat de Farmacologia i Farmacognòsia, Facultat de Farmàcia, Institut de Biomedicina (IBUB), Universitat de Barcelona, and CIBERNED, Barcelona, Spain

R. Osta
Laboratory of Genetic Biochemistry (LAGENBIO-I3A), Aragon Institute of Health Sciences, Universidad de Zaragoza, Zaragoza, Spain

X. Navarro (✉)
Unitat de Fisiologia Mèdica, Facultat de Medicina, Universitat Autònoma de Barcelona, E-08193 Bellaterra, Spain
e-mail: xavier.navarro@uab.cat

Introduction

Amyotrophic lateral sclerosis (ALS) is a fatal neurodegenerative disease characterized by the death of upper and lower motoneurons (MN) that clinically manifests by progressive muscle atrophy and paralysis [1]. Although the majority of ALS cases are sporadic with unknown etiology, 10 % of them are inherited forms, caused by genetic mutations. Among these, mutations in the gene encoding for the enzyme Cu/Zn superoxide dismutase 1 (SOD1) are observed in about 20 % of the patients [2]. The study of these genetic mutations led to the development of several transgenic animal models of ALS. The most widely used is a transgenic mouse that over-

Published online: 11 January 2014

expresses the human mutated form of the SOD1 gene with a glycine to alanine conversion at the 93rd codon [3]. This model recapitulates most relevant clinical and histopathological features of both familial and sporadic forms of the human disease [3]. It is also of relevance that alterations of the SOD1 protein have been reported in sporadic ALS patients [4], increasing the interest of this murine model. Several mechanisms have been implicated as contributors to MN death in ALS, such as glutamate excitotoxicity, oxidative stress, protein misfolding, mitochondrial defects, impaired axonal transport, and inflammation [5, 6]. Nevertheless, positive experimental results targeting some of these abnormalities have failed to translate into successful human trials [7, 8].

Resveratrol (3,5,4'-trihydroxy-trans-stilbene), a polyphenol found in grapes and red wine, has been reported to exert age-delaying and neuroprotective effects [9, 10]. Despite these well-documented beneficial effects, the mechanisms of action of resveratrol remain controversial. However, it has been recently described that resveratrol can trigger a cascade of intracellular events that converge on Sirtuin 1 (Sirt1), AMP-activated protein kinase (AMPK) and PGC-1α, as important energy-sensing regulators [11, 12]. Sirt1 is a NAD^+-dependent deacetylase that has emerged as an important element of the cellular metabolic network. Its activation has been shown to protect against neurodegeneration in several neurodegenerative disorders [13]. In fact, Sirt1 may promote neuroprotection by the modulation of several cellular pathways, such as autophagy [14, 15] and mitochondrial biogenesis [16]. On the other hand, it is also accepted that resveratrol benefits may be mediated through AMPK activation [16, 17]. It has been proposed that resveratrol works primarily by activating AMPK, which then activates Sirt1 indirectly by elevating intracellular levels of its cosubstrate NAD+[18, 19]. Alternatively, resveratrol may first activate Sirt1, leading to AMPK activation via deacetylation and activation of the AMPK kinase LKB1 [20, 21].

Resveratrol administration has been shown to provide beneficial effects on several neurodegenerative disease models, such as Alzheimer's disease [10] and Parkinson's disease [22] and in traumatic [23] and ischemic injuries to the central nervous system [24]. Since previous studies showed that resveratrol administration protects MN on *in vitro* ALS models [25, 26], the main goal of the present work was to assess the potential therapeutic effect of a resveratrol-enriched diet in the $SOD1^{G93A}$ mouse model of ALS.

Material and Methods

Transgenic Mice and Drug Administration

Transgenic mice with the G93A human SOD1 mutation (B6SJL-Tg[SOD1-G93A]1Gur) were obtained from the Jackson Laboratory (Bar Harbor, ME, USA) and maintained at the Animal Service of the Universidad de Zaragoza. Hemizygotes B6SJL $SOD1^{G93A}$ males were obtained by crossing with B6SJL females from the CBATEG (Bellaterra, Spain). The offspring was identified by PCR amplification of DNA extracted from the tail tissue. Mice were kept in standard conditions of temperature (22±2 °C) and a 12:12 light:dark cycle with access to food and water *ad libitum*. All experimental procedures were approved by the Ethics Committee of the Universitat Autònoma de Barcelona, where the animal experiments were performed.

Animals were evaluated at 8 weeks (prior to starting resveratrol administration) by rotarod and electrophysiological tests to obtain baseline values. Animals were distributed, according to their progenitors, weight and electrophysiological baseline values, in balanced experimental groups. All functional and survival assessments were performed by researchers blinded with respect to the group treatment. A resveratrol-enriched diet [10] was given to the groups of treated mice from 8 weeks of age and from 12 weeks of age for the delayed treatment group. Assuming a normal food intake of 4 g/animal/day, resveratrol was given at a daily dose of 160 mg/kg. The control groups received a standard diet, with no differences in manipulations during the study. The experimental groups included in the study are summarized in Table 1.

Nerve Conduction Tests

Motor nerve conduction tests were performed at 8 weeks of age and then every two weeks until 16 weeks in all the animals used in the study. The sciatic nerve was stimulated percutaneously by means of single pulses of 0.02 ms duration (Grass S88) delivered through a pair of needle electrodes placed at the sciatic notch. The compound muscle action potential (CMAP, M wave) was recorded from the tibialis anterior (TA) and the plantar (interossei) muscles with microneedle electrodes [27, 28]. For evaluation of the motor central pathways, motor evoked potentials (MEP) were recorded from the TA and plantar muscles in response to transcranial electrical stimulation of the motor cortex by single rectangular pulses of 0.1 ms duration, delivered through needle electrodes inserted subcutaneously, the cathode over the skull overlaying the sensorimotor cortex and the anode at the nose [27, 29]. All potentials were amplified and displayed on a digital oscilloscope (Tektronix 450S) at settings appropriate to measure the amplitude from baseline to the maximal negative peak. To ensure reproducibility, the recording needles were placed under microscope to secure the same placement on all animals guided by anatomical landmarks. During the tests, the mice body temperature was kept constant by means of a thermostated heating pad.

Table 1 Experimental groups included in the study.

Experimental group	Gender	n	Treatment onset
Wild type	Females	10	–
SOD1 untreated	Females	20	–
SOD1 + Resveratrol	Females	23	8 weeks
Wild type	Males	10	–
SOD1 untreated	Males	16	–
SOD1 + Resveratrol	Males	22	8 weeks
SOD1 untreated	Females	8	–
SOD1 + Resveratrol	Females	8	12 weeks
SOD1 untreated	Males	8	–
SOD1 + Resveratrol	Males	8	12 weeks

Locomotion Tests

The rotarod test was performed to evaluate motor coordination, strength and balance [30, 31] in all the animals used in the study (Table 1). Mice were trained three times a week on the rod rotating at 14 rpm, and then tested from 8 to 16 weeks of age, with an arbitrary maximum time of maintenance in the rotating rod of 180 seconds. Clinical disease onset was defined as the first day when an animal was not able to complete the 180 seconds on the rotating rod.

The DigiGait system (Mouse Specifics, Boston, MA) was used to assess the locomotor performance of the animals at the end stage of the disease (16 weeks of age). The animals were placed over the treadmill belt and their capacity to run with increasing treadmill velocity was recorded. Treadmill speeds used were 5, 10, 15, 20, 25 and 30 cm/s, based on previous studies performed in our laboratory [32, 33].

Survival

For survival assessment, 23 female (10 untreated and 13 resveratrol administered) and 20 male (10 untreated and 10 resveratrol administered) $SOD1^{G93A}$ mice were used. It was considered that animals reached the end point of the disease when they were unable to right themselves in 30s when placed on their side.

Histology

At 16 weeks of age, 4–5 mice from each group were transcardially perfused with 4 % paraformaldehyde in PBS and the lumbar segment of the spinal cord was harvested, post-fixed for 24 h, and cryopreserved in 30 % sucrose. Transverse 40-µm thick sections were serially cut with a cryotome (Leica) between L2–L5 segmental levels. For each segment, each section of a series of ten was collected sequentially on separate gelatin-coated slides or free-floating in Olmos medium.

One slide of each animal was rehydrated for 1 min and stained for 2 h with an acidified solution of 3.1 mM cresyl violet. Then, the slides were washed in distilled water for 1 min, dehydrated and mounted with DPX (Fluka). MNs were identified by their localization in the ventral horn of the spinal cord sections and counted following strict size and morphological criteria; only MNs with diameters larger than 20 µm, polygonal shape and prominent nucleoli were counted. The number of MNs present in both ventral horns was counted in four serial sections of each L4 and L5 segments [27, 34].

Another series of sections was blocked with PBS-Triton-FBS and incubated overnight at 4 °C with primary antibodies anti-glial fibrilary acidic protein (GFAP, 1:1000, Dako), rabbit anti-ionized calcium binding adaptor molecule 1 (Iba1, 1:1000, Wako), or anti-sirtuin 1 (Sirt1, 1:200, Abcam). After several washes, sections were incubated for 1 hour at room temperature with Alexa 488 or Alexa 594-conjugated secondary antibody (1:200; Life Science), or, for anti-Sirt antibody, with biotinilated secondary antibody (1:200, Vector) and then for 1 hour with Alexa 594-conjugated streptavidin (1:1000, Vector). For co-localizations, spinal MNs were labeled with 435/455-Neurotrace fluorescent Nissl staining (1:200, Life Science). To quantify astroglial and microglial immunoreactivity, microphotographs of the ventral horn grey matter were taken at×400 and, after defining the threshold for background correction, the integrated density of GFAP or Iba1 labeling was measured using ImageJ software [33]. The integrated density represents the area above the threshold for the mean density minus the background.

Protein Extraction and Western Blot

For protein extraction, another subset of mice (4–5 from each experimental group) were anesthetized and decapitated at 16 weeks of age. The lumbar spinal cord was removed and divided into quarters to isolate the ventral quadrants. One of them was prepared for protein extraction and homogenized in modified RIPA buffer (50 mM Tris–HCl pH 7.5, 1 % Triton X-100, 0.5 % sodium deoxycholate, 0.2 % SDS, 100 mM NaCl, 1 mM EDTA) adding 10 µl/ml of Protease Inhibitor cocktail (Sigma) and PhosphoSTOP phosphatase inhibitor cocktail (Roche). After clearance, protein concentration was measured by Lowry assay (Bio-Rad Dc protein assay).

To perform western blots, 20 µg of protein of each sample were loaded in SDS-poliacrylamide gels. The transfer buffer was 25 mM trizma-base, 192 mM glycine, 20 % (v/v) methanol, pH 8.4. The membranes were blocked with 5 % BSA in PBS plus 0.1 % Tween-20 for 1 hour, and then incubated with primary antibodies at 4 °C overnight. The primary antibodies used were: anti-b-actin (Sigma; 1:10000), anti-GAPDH (Millipore, 1:20000), anti-Sirt1 (Abcam, 1:1000), anti-p53 (Abcam, 1:500), anti-acetyl p53 (L382) (Millipore, 1:500), anti-AMPK (Cell Signaling, 1:1000), anti-pAMPK (Cell

Signaling, 1:1000), anti-LC3b (Abcam, 1:200), anti-Beclin 1 (Cell signaling, 1:1000), anti-Fis-1 (ThermoScientific, 1:1000), anti mitofusin 2 (Sigma, 1:1000), anti-porin, (Abcam, 1:1000), anti-complex I subunit 39 kDa (Invitrogen, 1:1000), anti-complex II Fp subunit (Invitrogen, 1:1000), anti-complex III subunit Core 2 (Invitrogen, 1:1000), anti-complex IV subunit I (Invitrogen, 1:1000), and anti-complex V subunit α (Molecular Probes, 1:1000). Horseradish peroxidase–coupled secondary antibody (1:5000, Vector) incubation was performed for 60 min at room temperature. The membranes were visualized using enhanced chemiluminiscence method and the images were collected and analyzed with Gene Genome apparatus and Gene Snap and Gene Tolls software (Syngene, Cambridge, UK), respectively.

Statistical Analysis

Data are expressed as mean±SEM. Electrophysiological and locomotion test results were statistically analyzed using repeated measurements and one-way ANOVA, applying Turkey post-hoc test when necessary. Histological data were analyzed using Mann-Whitney U test. Onset and survival data were analyzed using the Mantel-Cox test.

Results

Resveratrol Treatment Delays the Onset of Symptoms and Improves Locomotion Impairment in SOD^{G93A} Mice

The beginning of symptoms for each animal was considered when it showed the first deficits in locomotor performance in the rotarod test [35]. Results revealed a significant delay of symptoms onset (Mantel-Cox test, $p<0.05$) in both female and male treated SOD1^{G93A} mice of 1 and 2 weeks, respectively, compared to untreated mice (Fig. 1a).

Locomotor performance was assessed with rotarod and DigiGait tests [27, 32]. Rotarod performance was significantly higher in both female and male resveratrol treated mice than in control SOD1^{G93A} mice (Fig. 1b). Moreover, we explored the ability of animals to run on a treadmill that induced forced locomotion. The proportion of 16-week-old mice that were able to run at increasing velocities revealed a significant improvement of locomotor performance (Mantel-Cox test, $p<0.001$) in resveratrol treated mice (Fig. 1c).

Resveratrol Administration Preserves Lower and Upper Motoneuron Function in SOD1^{G93A} Mice

Upper and lower MN function impairment is the main feature of ALS pathology both in human patients [1] and animal models [27, 36, 37]. We analyzed the amplitude of plantar and TA CMAP and MEP as a measure of lower and upper MN functional state, respectively. The CMAP amplitude ranged between 49 and 51 mV for TA muscle and between 6 and 9 mV for plantar muscles in wild type mice, and remained unaltered during all the follow-up. In contrast, there was a progressive decline in CMAP amplitude of SOD1^{G93A} mice from 8 to 16 weeks of age in TA and plantar muscles, as previously reported [27]. The results revealed a significant preservation of plantar and TA CMAP amplitude in resveratrol treated mice of both sexes (Fig. 2). Central motor pathways were also protected by the treatment, since the amplitude of MEP was also significantly preserved at the end of the follow-up. Central motor conduction preservation was also evidenced by an increased proportion of animals with recorded MEP responses in resveratrol treated groups at the end stage of the disease (16 weeks of age) (Fig. 2).

Resveratrol Administration Reduces Spinal Motoneuron Degeneration of SOD1^{G93A} Mice

The survival of spinal MNs was assessed by evaluating the number of stained MN cell bodies in the anterior horns of the lumbar spinal cord in 16-week-old mice. We focused the analysis on L4–L5 segments where the motor nuclei of TA and plantar muscles are represented [38]. MN counts were restricted to the lateral part of the lamina IX, since this population of MN innervates the hindlimb muscles. Neurons smaller than 20 μm in diameter were excluded from counting, even if they could be atrophic MNs because they were unlikely to be functional. MN counts of female and male animals were pooled since there were no significant differences between genders. Resveratrol administration significantly reduced MN degeneration in SOD1^{G93A} mice. While SOD1^{G93A} untreated animals had 18.2±1.3 (35.9 % vs. wild type) MNs per section, resveratrol treated mice had 35.2±1.1 (63.6 % vs. wild type), representing an increase of almost two-fold in surviving MNs (Fig. 3). Figure 3 also shows representative images of ventral horns of wild type, untreated and resveratrol treated SOD1^{G93A} mice illustrating the neuroprotective effect.

Resveratrol Administration Reduces Microglial Immunoreactivity in the SOD1^{G93A} Mice Spinal Cord

It has been extensively reported that glial cells contribute to MN degeneration both in ALS patients [39] and animal models [40–42]. We evaluated astroglial (GFAP labeled cells) and microglial (Iba-1 labeled cells) immunoreactivity in the anterior horns of lumbar spinal cord sections in order to assess whether resveratrol treatment influenced the response of glial cells. As in the MN counts, female and male animals were pooled due to the lack of differences between them. Results revealed that resveratrol administration significantly reduced microglial but not astroglial immunoreactivity in the anterior horn of SOD1^{G93A} mice. Whereas in untreated SOD1^{G93A}

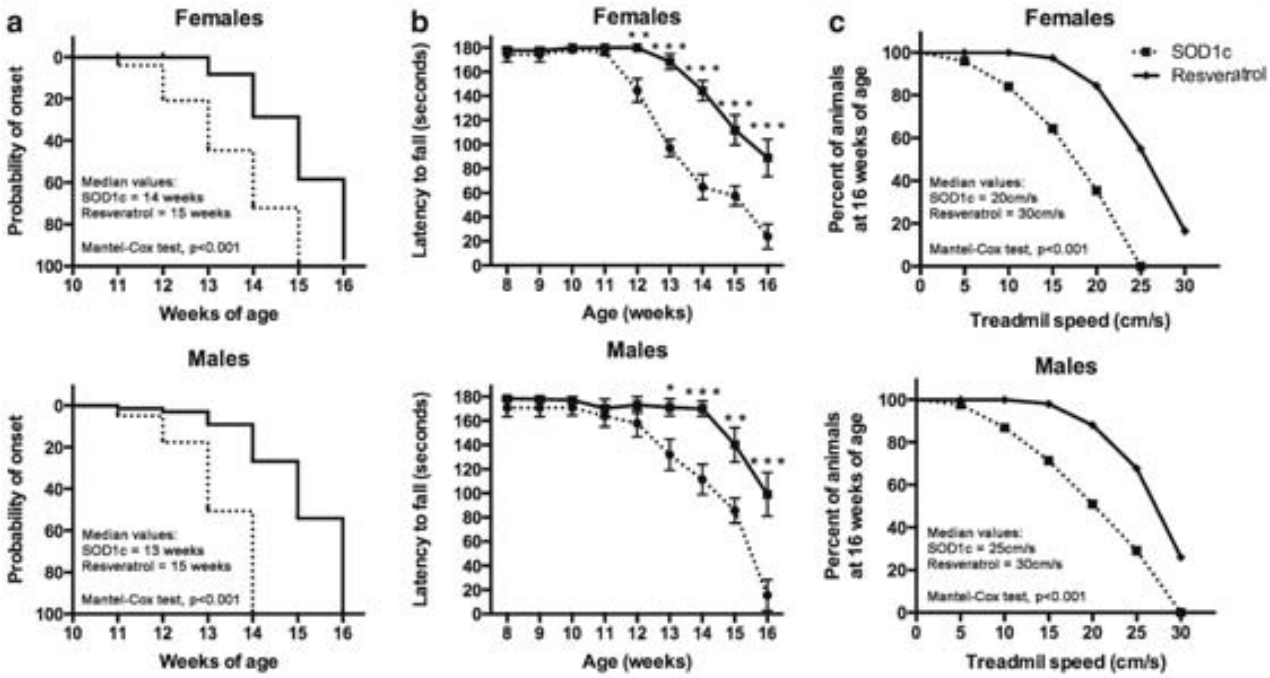

Fig. 1 Resveratrol administration delays disease onset and improves locomotor performance in SOD1^{G93A} mice. Continuous lines represent resveratrol SOD1^{G93A} treated animals (n=23 females; 22 males) while dashed lines represent SOD1^{G93A} untreated mice (n=20 females; 16 males). **a** Disease onset assessed by means of rotarod test revealed a significant delay of symptoms appearance of 1 and 2 weeks for male and female SOD1^{G93A} mice, respectively. **b** Locomotor performance evaluated with rotarod test showed significant improvement with resveratrol administration. Values are expressed as mean±SEM. *p<0.05, **p<0.01, ***p<0.001 vs. SOD1^{G93A} untreated mice. **c** Locomotor performance evaluated by the Digigait test and expressed as the proportion of 16-week-old SOD1^{G93A} mice that were able to run at increasing treadmill velocities. Results revealed significantly increased locomotor capacity in animals treated with resveratrol (p<0.05, Mantel-Cox test)

mice Iba-1 immunoreactivity was increased over 1152 % compared to wild type mice, resveratrol treatment reduced it to 649 %. GFAP immunoreactivity remained unchanged after the treatment, since untreated and resveratrol treated animals showed similar values of 673 % and 614 % over wild type levels, respectively (Fig. 4).

Resveratrol Treatment Significantly Extends Survival of SOD1^{G93A} Mice

The administration of resveratrol from 8 weeks of age significantly prolonged survival of both female and male SOD1^{G93A} mice (Mantel-Cox test, p<0.001). While untreated female and male SOD1^{G93A} mice lived a median of 134 (mean ±SEM=130.7±1.32) and 127 (121.6±2.07) days, treated animals survived for 148 (142±2.76) and 139 (131±2.37) days, respectively (Fig. 5).

Resveratrol Treatment from 12 Weeks of Age also Produces Motor Functional Improvement and Neuroprotection in SOD1^{G93A} Mice

Considering the important effect achieved by resveratrol administered from 8 weeks of age, a pre-symptomatic stage of SOD1^{G93A} mice, we wondered if a delayed treatment from the 12th week, when signs of the disease are clearly present, could also ameliorate the animals' condition. Electrophysiological analysis revealed that resveratrol treatment led to preservation of spinal MN function, evidenced by increased TA and plantar muscle CMAP amplitudes that became statistically significant at 16 weeks of age with respect to values of untreated mice (Fig. 6a,b). This functional effect was accompanied by significant preservation of the number of surviving MNs in L4–L5 spinal cord segments (Fig. 6c), along with a mild reduction of microglial reactivity (p=0.15, Fig. 6d).

Resveratrol Administration Induces Sirtuin1 Expression and Activation

It has been extensively described that, among other effects, resveratrol promotes neuroprotection by increasing Sirt1 activity [9, 43]. To assess whether Sirt1 was overexpressed, we analyzed Sirt1 levels in the lumbar spinal cord by western blot analysis. Results showed a marked increase in Sirt1 expression in resveratrol treated animals (Fig. 7a). Moreover, immunohistochemistry of the ventral spinal cord revealed that Sirt1 expression was localized in the MNs (Fig. 7b). To check the activity state of Sirt1 we evaluated the acetylation degree of

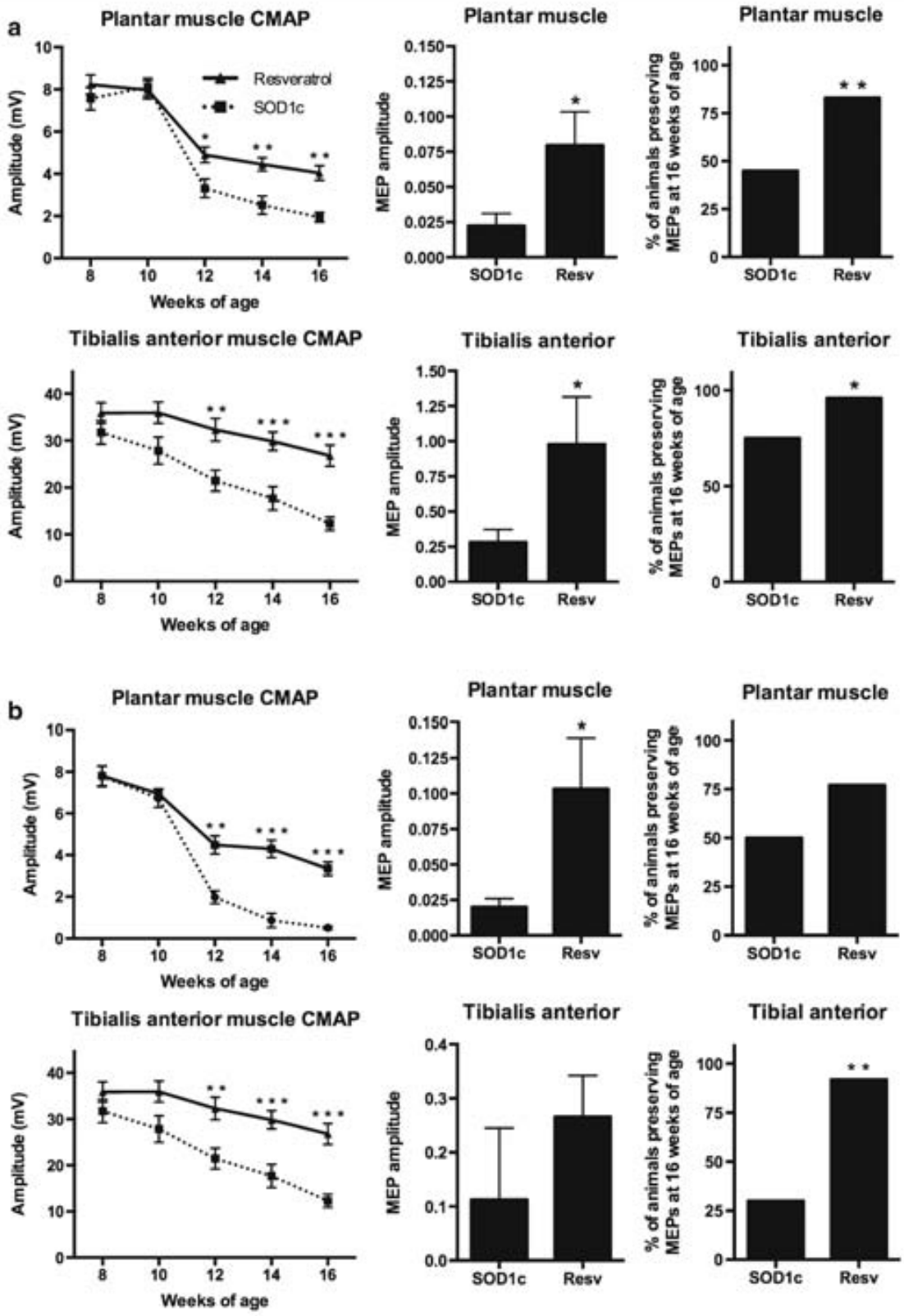
a
Plantar muscle CMAP
Amplitude (mV)
Weeks of age
Resveratrol
SOD1c
Plantar muscle
MEP amplitude
SOD1c
Resv
Plantar muscle
% of animals preserving MEPs at 16 weeks of age
SOD1c
Resv
Tibialis anterior muscle CMAP
Amplitude (mV)
Weeks of age
Tibialis anterior
MEP amplitude
SOD1c
Resv
Tibialis anterior
% of animals preserving MEPs at 16 weeks of age
SOD1c
Resv
b
Plantar muscle CMAP
Amplitude (mV)
Weeks of age
Plantar muscle
MEP amplitude
SOD1c
Resv
Plantar muscle
% of animals preserving MEPs at 16 weeks of age
SOD1c
Resv
Tibialis anterior muscle CMAP
Amplitude (mV)
Weeks of age
Tibialis anterior
MEP amplitude
SOD1c
Resv
Tibial anterior
% of animals preserving MEPs at 16 weeks of age
SOD1c
Resv

◀ **Fig. 2** Resveratrol treatment preserves upper and lower motoneuron function. **a** Electrophysiological tests performed in female mice (n=20 untreated vs. 23 resveratrol treated SOD1^{G93A} mice). **b** Electrophysiological tests performed in male mice (n=16 untreated vs. 22 resveratrol treated SOD1^{G93A} mice). Results in both sexes revealed significant preservation of compound muscle action potentials (CMAP) and motor evoked potential (MEP) amplitudes, and an increased proportion of animals maintaining MEPs at 16 weeks of age. Values are mean±SEM. *p<0.05, **p<0.01, ***p<0.001 vs. SOD1^{G93A} untreated mice

one of its most important downstream targets, p53. Indeed, we found a significant reduction in the acetylation of p53, indicating increased Sirt1 activation in the resveratrol treated group (Fig. 7c).

Resveratrol Treatment Restores Autophagic Flux

Increasing evidence suggests that autophagic abnormalities may contribute to ALS physiopathology [44] and resveratrol has been reported as a modulator of autophagia through Sirt1 activation [45]. Thus, we examined the autophagic state of the animals after resveratrol treatment. The results showed normalization of the early markers of autophagy LC3II and Beclin 1 after resveratrol administration (Fig. 8), suggesting that resveratrol treatment normalizes autophagic flux in the SOD1^{G93A} mouse spinal cord.

Resveratrol Restores Mitochondrial Function and Promotes Mitochondrial Biogenesis through AMPK Pathway

Recent evidence has demonstrated that resveratrol promotes mitochondrial biogenesis through the activation of AMPK [16]. Thus, we first assessed the expression and activation of AMPK by analyzing the active phospho-AMPK and total AMPK forms. Results revealed a significant increase of the pAMPK/AMPK ratio (p<0.01) in the ventral part of the lumbar spinal cord in SOD1^{G93A} mice treated with resveratrol (Fig. 9c). Next, we analyzed whether resveratrol treatment led to changes of mitochondrial behavior. We found that SOD1^{G93A} untreated mice had an increased expression of the respiratory chain mitochondrial complexes compared to wild-type mice. In contrast, resveratrol treatment reduced the expression of these mitochondrial complexes, with levels similar to wild type mice (Fig. 9a, b). Finally, we evaluated mitochondrial fission and fusion in the ventral spinal cord. Results revealed a significant increase of Fis-1 expression, a marker of mitochondrial fission without alterations of mitofusin 2, an indicator of mitochondrial fusion. Taken together, these results suggest that the activation of AMPK by resveratrol likely leads to a switch of the mitochondrial response to energetic stress from the upregulation of respiratory chain complexes to a more adaptive increase of mitochondrial biogenesis.

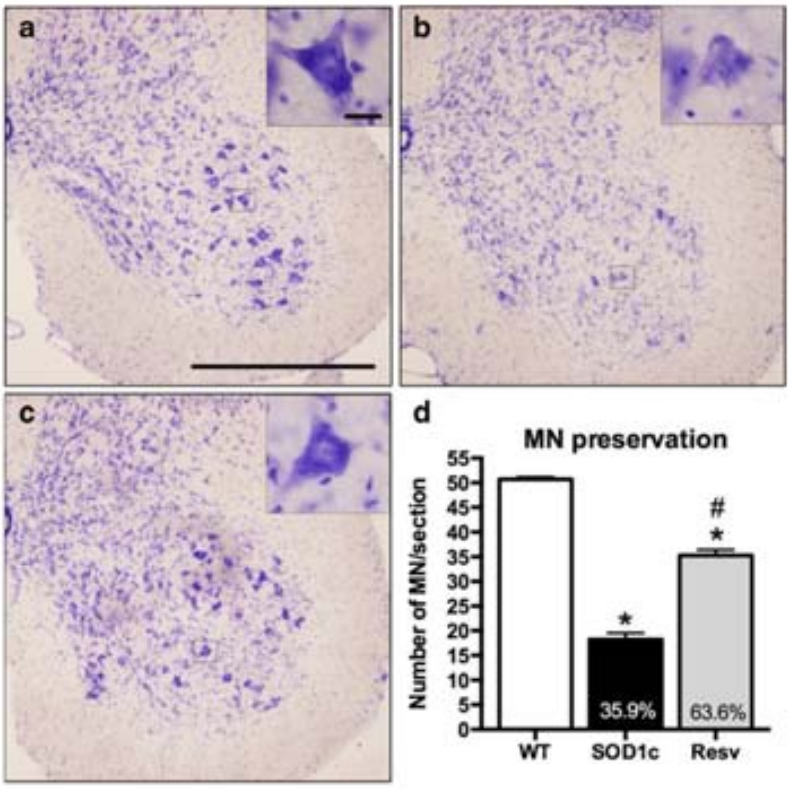

Fig. 3 Resveratrol administration significantly preserves spinal motoneurons from degeneration. Representative images of L4 spinal cord at x200 of (**a**) wild type, (**b**) SOD1^{G93A} untreated and (**c**) resveratrol SOD1^{G93A} treated mice (n=5 animals per each gender and treatment). Scale bar, 500 μm. *Inset boxes* show detail of single motoneurons at×1000. Scale bar, 20 μm (**d**) L4–L5 spinal cord motoneurons quantification revealed significant neuroprotection exerted by resveratrol administration (n=5 per group). Values are mean ±SEM. *p<0.05 vs. wild type, # p<0.05 vs. untreated SOD1^{G93A} mice

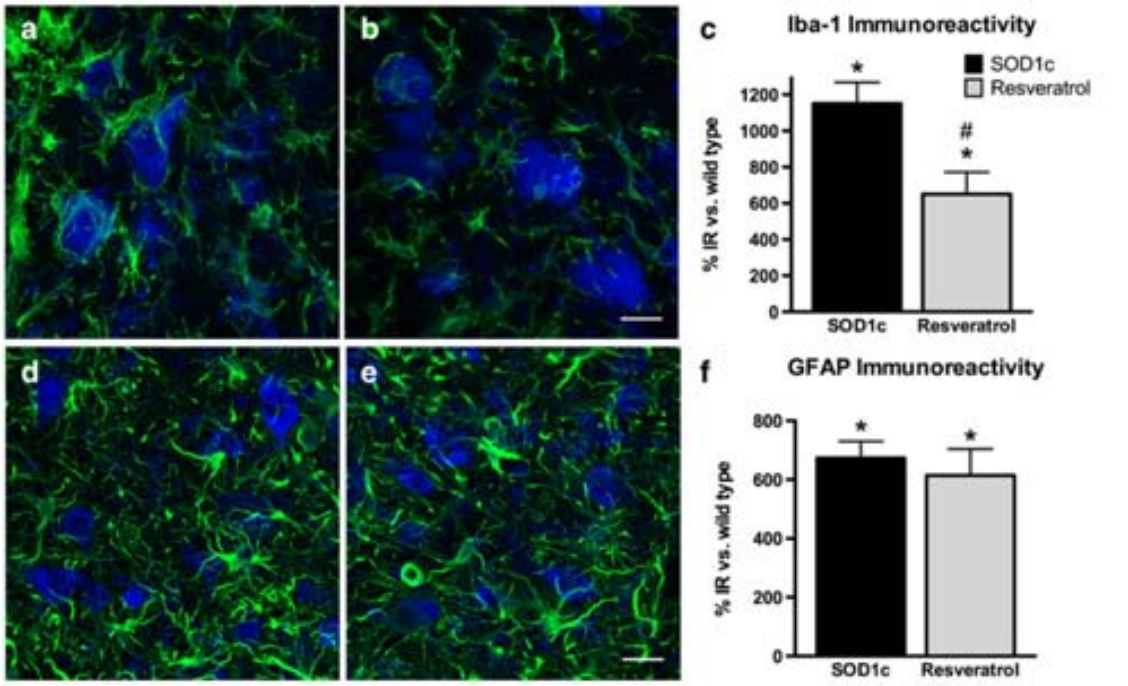

Fig. 4 Resveratrol treatment reduces microglial reactivity. Representative confocal images of microglial cells (Iba-1, *green*) and motoneurons (fluoronissl staining, *blue*) in (**a**) untreated SOD1^{G93A} and (**b**) resveratrol treated SOD1^{G93A} mice (n=5 animals per gender and treatment). (**c**) Quantification of Iba-1 immunoreactivity revealed a significant reduction after resveratrol administration. Representative confocal images of astroglial cells (GFAP, *green*) and motoneurons (fluoronissl staining, *blue*) in (**a**) untreated SOD1^{G93A} and (**b**) resveratrol treated SOD1^{G93A} mice. (**c**) Quantification of GFAP immunoreactivity did not show differences between groups. Scale bars, 20 μm. *p<0.05 vs. wild type, #p<0.05 vs. untreated SOD1^{G93A} mice. *IR* immunoreactivity

Discussion

The physiopathological complexity that characterizes ALS [5, 6] is one of the most limiting factors for the development of successful therapies. Several works have been conducted targeting one or more of the physiopathological mechanisms linked to the disease, but even if they achieved positive experimental results they have failed to translate into successful human therapies [7, 8]. It is conceivable that successful treatments should not only fight pathogenic elements of the disease but also promote cellular neuroprotective pathways providing surviving tools to the MNs. The main goal of the present study was to assess the potential therapeutic effect of resveratrol in the SOD1^{G93A} model of ALS, since it has been reported to produce beneficial neuroprotective effects on other neuropathologies through the modulation of several cellular pathways [9]. Our results reveal that resveratrol significantly delayed disease symptoms onset by 1–2 weeks and importantly improved the locomotor performance of the SOD1^{G93A} animals. Moreover, electrophysiological tests showed maintenance of spinal MN function and, by the first time, a significant improvement of upper MN function. These effects were accompanied by an increased preservation of lower MNs cell bodies in the lumbar spinal cord. Resveratrol administration was also able to significantly extend both female and male SOD1^{G93A} lifespan. Furthermore, delayed resveratrol administration from the beginning of evident locomotor impairments (12 weeks of age) still produced a significant preservation of spinal MN function and cell bodies in the spinal cord. Further experiments revealed that these therapeutic effects were mediated by the increased expression and activation of Sirt1 and AMPK in the spinal cord, both well-known effectors of resveratrol. Moreover, we observed significant restoration of the autophagic flux normal values and, more importantly, increased mitochondrial biogenesis in the spinal cord of resveratrol treated animals.

It has been previously shown that resveratrol and its downstream effectors Sirt1 and AMPK promote protective effects both in neurodegenerative and traumatic injury models. Indeed, potent therapeutic effects of resveratrol administration were reported in animal models of Alzheimer's disease and accelerated ageing [10, 26, 46], multiple sclerosis [47, 48], Huntington's disease [9, 49], Parkinson's disease [22, 50], and even reducing peripheral axonal degeneration [51] or promoting functional recovery after traumatic spinal cord injury [23]. In this sense, resveratrol has been also reported to exert neuroprotection on *in vitro* models of ALS. Thus, Kim et al. [26] showed that resveratrol reduces cell death on primary cultures of neurons overexpressing the SOD1^{G93A} mutant protein, and Yáñez et al. [52] demonstrated that this

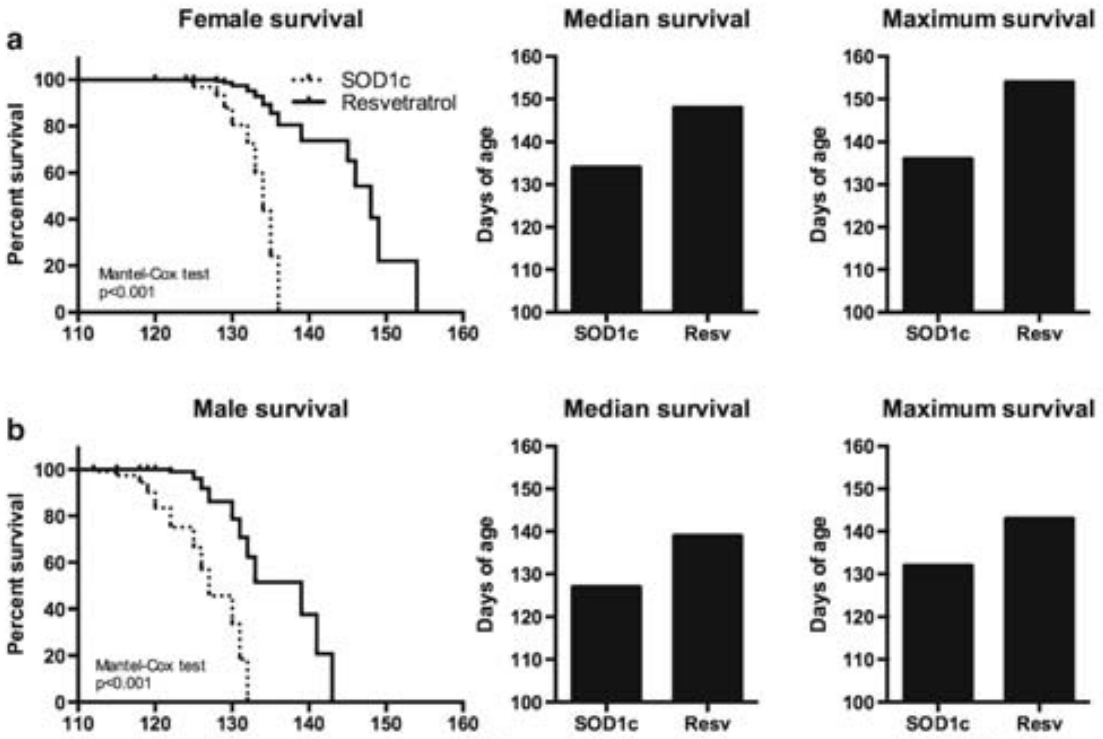

Fig. 5 Resveratrol administration significantly extended SOD1^{G93A} mice survival. Resveratrol treatment prolonged SOD1^{G93A} animals median and maximum life span in (**a**) female (n=13 treated, 10 untreated) and (**b**) male (n=11 treated, 10 untreated) SOD1^{G93A} mice

compound protects from neuronal death triggered by CSF of ALS patients. There is some controversy about the *in vivo* effect of resveratrol administration in SOD1^{G93A} mice. Markert et al. [53] reported that dietary resveratrol given at 25 mg/kg did not produce functional effects, whereas Han et al. [54] showed that intraperitoneal administration of resveratrol at 20 mg/kg led to improved functional outcome although less important than found in our study. A likely explanation of such discrepancies would be the differences in the dose and the route of administration. Resveratrol

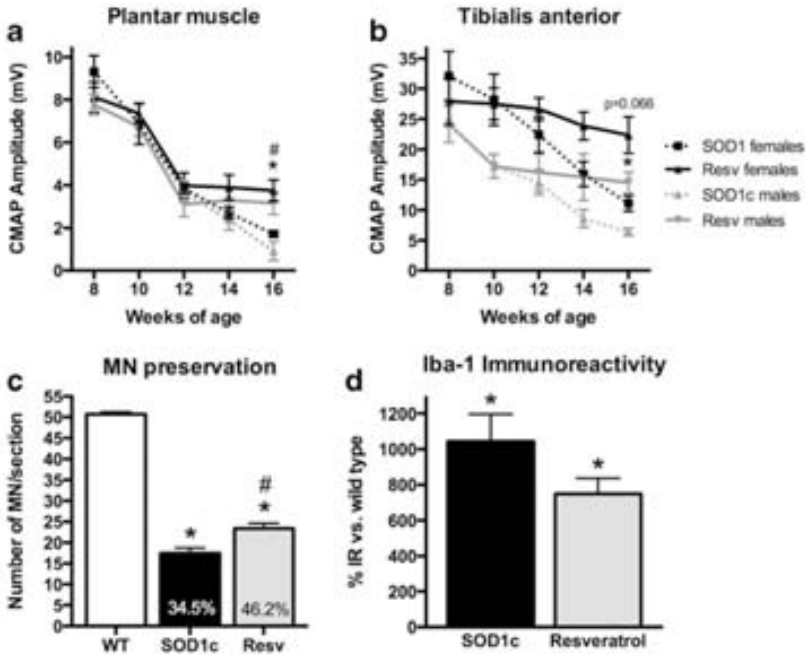

Fig. 6 (**a**–**b**) Delayed resveratrol administration from 12 weeks of age significantly preserved lower motoneuron function. Compound muscle action potential (CMAP) amplitude of plantar and tibialis anterior muscles in female and male SOD1^{G93A} mice (n=8 treated and 8 untreated for each sex). Resveratrol administration from 12 weeks of age (**c**) significantly protects spinal motoneurons in L4–L5 spinal cord segments and (**d**) slightly reduces microglial reactivity (p=0.15). Values are mean±SEM. *p<0.05 vs. wild type, #p<0.05 vs. corresponding untreated SOD1^{G93A} mice

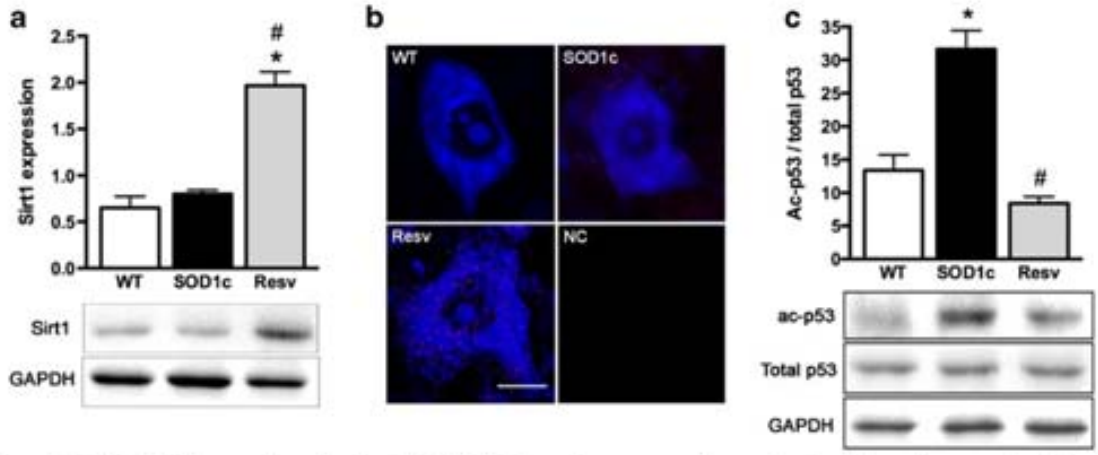

Fig. 7 Increased sirtuin 1 (Sirt1) expression and activation in SOD1^{G93A} spinal motoneurons after resveratrol treatment. **a** Sirt1 expression was significantly increased in the ventral part of the lumbar spinal cord of resveratrol treated animals. **b** Confocal microphotoghraps of L4 spinal cord confirmed that this expression was localized inside spinal motoneurons. Scale bar, 20 μm. *WT* wild type, *SOD1c* untreated SOD1^{G93A} mice, *Resv* resveratrol treated mice, *NC* negative control without Sirtuin 1 primary antibody or Fluoronissl staining. **c** Evaluation of Sirt1 activity by measuring the acetylation levels of p53 revealed significant deacetylation and thus, an increased activity of Sirt1 in SOD1^{G93A} mice treated with resveratrol. *$p<0.05$ vs. wild type, #$p<0.05$ vs. untreated SOD1^{G93A} mice

pharmacokinetics have been extensively studied, revealing that enteric absorption is up to 80 % after oral administration, while up to 98 % of the compound is excreted 7–15 h after administration [55]. Accordingly, resveratrol treatment should be performed either dietary at high doses or intraperitoneally but with more frequent injections than made in the above-mentioned studies.

Although many studies have been conducted to elucidate the mechanisms of action of resveratrol, they still remain controversial. It is known that resveratrol acts through some specific effector molecules, such as Sirt1 or AMPK [11, 12]. Sirt1 is a NAD^+-dependent deacetylase that plays an important role regulating cell metabolism and has recently been postulated as a neuroprotective element in several neurodegenerative disorders [13]. Sirt1 induces protective effects since it is upstream of multiple effectors that participate in several cell processes, such as inflammation [43], autophagy [45] and mitochondrial function [16, 46], all of them related to ALS physiopathology [5, 56]. In the present work, we found that Sirt1 was overexpressed in spinal MNs of SOD1^{G93A} mice after resveratrol administration. Then, we assessed Sirt1 activity by evaluating the deacetylation degree of one of the most important Sirt1 substrates, p53. Indeed, we found significantly reduced acetylation of p53, evidencing an increased activity of Sirt1.

Autophagy serves multiple physiological functions, such as protein degradation, organelle turnover and response to stress. Dysregulation of autophagy has been reported to contribute to ALS pathology both in human patients and animal models [44, 57]. Li et al. [58] reported a progressive increase of the relative amount of LC3b II from 90 to 140 days of age in SOD1^{G93A} mice, accompanied by accumulation of autophagic vesicles. These findings could be the result of autophagic flux impairment. Since it has been hypothesized that Sirt1

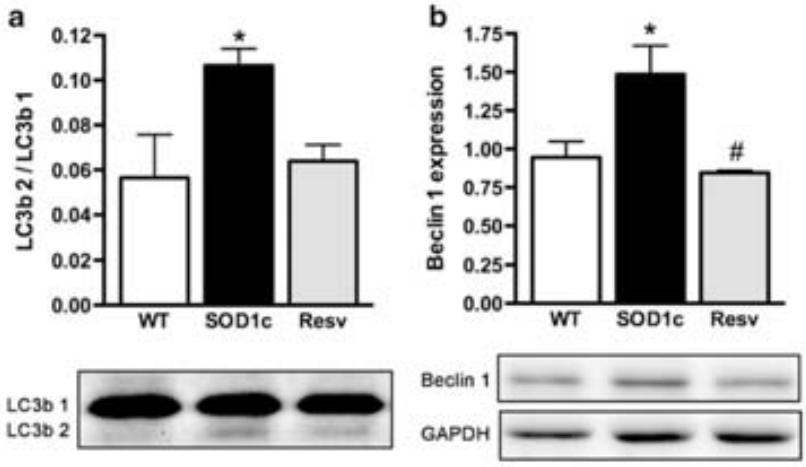

Fig. 8 Recovery of normal autophagic flux after resveratrol treatment. **a** LC3b2 / LC3b1 ratio. **b** Beclin 1 expression were normalized by resveratrol administration to SOD1^{G93A} mice. *$p<0.05$ vs. wild type, #$p<0.05$ vs. untreated SOD1^{G93A} mice

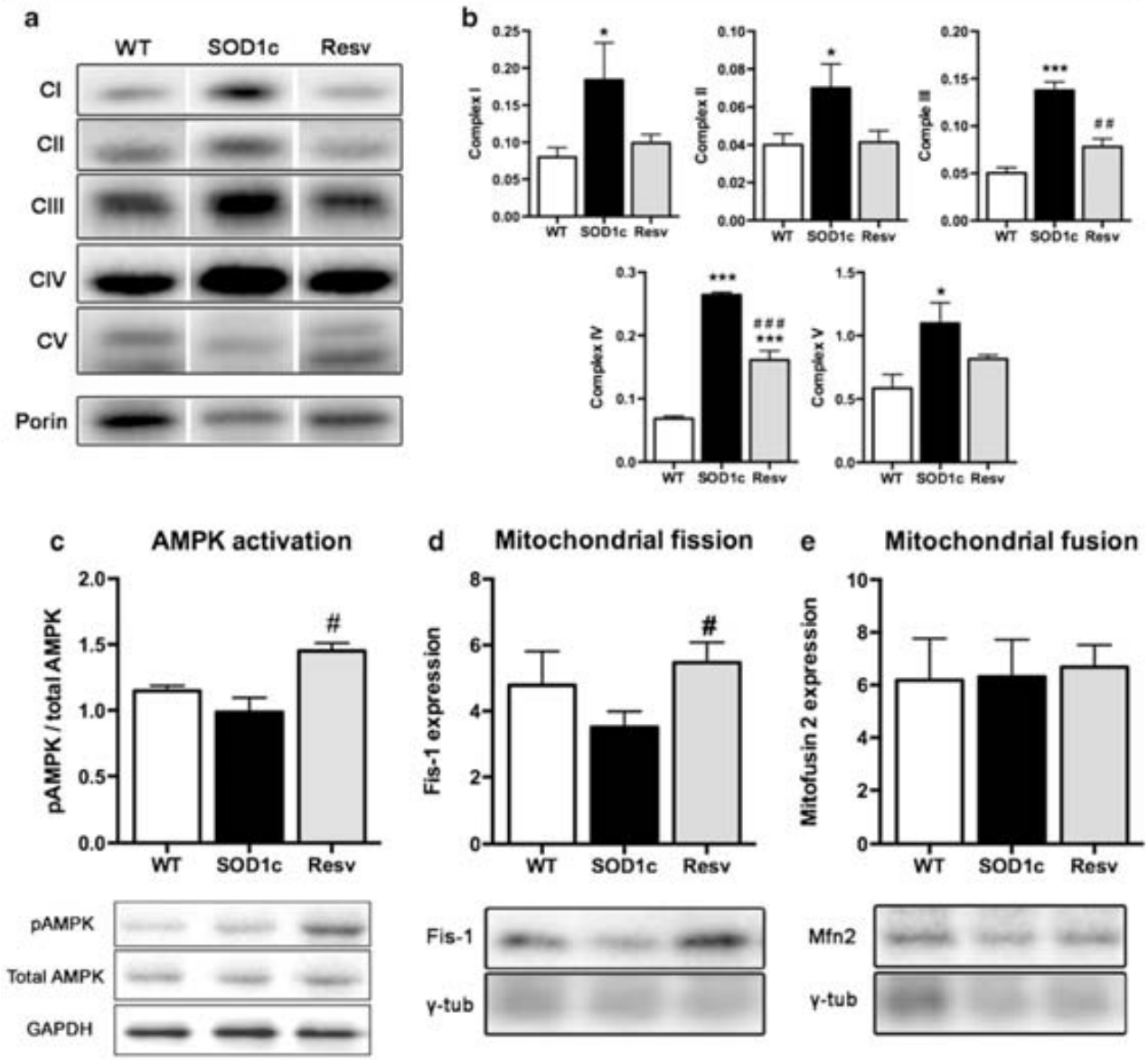

Fig. 9 Resveratrol administration normalized mitochondrial function and increased mitochondrial biogenesis. **a** Representative western blot of the five different mitochondrial respiratory chain complexes. **b** Quantification revealed significant increase of all complexes expression in control SOD1^{G93A} mice, whereas in resveratrol administered SOD1^{G93A} mice the levels were close to normal. **c** Enhanced AMPK activation after resveratrol treatment, evidenced by an increased pAMPK/AMPK ratio. **d** Increased mitochondrial biogenesis in resveratrol administered SOD1^{G93A} animals. **e** Mitochondrial fusion was not altered by the treatment. Values are mean±SEM. *p<0.05, *** p<0.001 vs. wild type; # p<0.05, ## p<0.01, ### p<0.001 vs. untreated SOD1^{G93A} mice

plays its protective role through the modulation of autophagy [45, 59], we evaluated the expression of two of the most typical markers of autophagy, LC3 and Beclin-1. Our results revealed that both Beclin-1 and the LC3bII/LC3bI ratio were significantly increased in SOD1^{G93A} mice compared to wild type littermates, evidencing impairment of the autophagic flux. In contrast, after resveratrol administration, both markers were normalized to wild type values. Though the restoration of the autophagic flux may be a direct effect downstream of resveratrol-induced Sirt1 activation, it is also possible that it could be an indirect consequence derived from the general improvement of the mice condition and, thus, of restoration of MN homeostasis.

On the other hand, recent evidence suggests that the resveratrol-induced Sirt1 activation works through AMPK activation [18]. According to this view, Park et al. [12] recently described that resveratrol promotes AMPK phosphorilation through the inhibition of cAMP phosphodiesterase, thus increasing the amount of cAMP. AMPK then activates Sirt1 indirectly by elevating intracellular levels of its cosubstrate,

NAD+[18, 19]. Alternatively, other authors proposed that resveratrol may first activate Sirt1, leading to AMPK activation via deacetylation and activation of the AMPK kinase LKB1 [20, 21]. In any case, resveratrol administration leads to direct or indirect activation of AMPK, as evidenced in our results by the increased pAMPK/totalAMPK ratio in SOD1^{G93A} treated animals.

Numerous studies have highlighted the common role of mitochondria in the pathogenesis of neurodegenerative diseases [60]. Although there is no consensus about the exact role of mitochondrial abnormalities [61], it is accepted that mitochondrial dysfunction is an important hallmark of ALS pathogenesis [5, 62, 63]. Several authors have shown deficits in mitochondrial function in the spinal cord and muscles of both human patients [64] and animal models of ALS [65–67]. Resveratrol improves mitochondrial function and induces biogenesis, although there is some controversy about whether this effect is mediated by AMPK activation [18] or by Sirt1 [16, 68]. Since both Sirt1 and AMPK were found over-activated in SOD1^{G93A} animals treated with resveratrol, we performed a detailed analysis on mitochondria. Contrary to what was expected, we found a significant increase of all the respiratory chain complexes in SOD1^{G93A} mice compared to wild-type littermates, but complete normalization following resveratrol treatment. Then, we found an increased expression of the fission protein Fis-1 in resveratrol treated SOD1^{G93A} mice, evidencing an active process of mitochondrial biogenesis. Our hypothesis is that resveratrol may promote a switch of mitochondrial response to cellular stress from the overexpression of respiratory chain complexes and the consequent increased production of harmful oxidative mediators, to a more adaptive response by increasing mitochondrial biogenesis. It has also been reported that resveratrol administration promotes mitochondrial biogenesis in skeletal muscles [12, 16] through AMPK activation. Further studies are needed to assess whether resveratrol benefits in SOD1^{G93A} mice could be partially explained by its effect on skeletal muscles.

Neuroinflammation is another common pathological hallmark of neurodegenerative disorders [69] and its modulation has been proposed as a potential therapeutic target [70]. In ALS, the inflammatory response is characterized by the activation and proliferation of microglia, and the infiltration of T cells into the spinal cord. Although it is still unknown whether it is a cause or a consequence of the MN degeneration, some evidence suggested that its manipulation could ameliorate the disease progression. Resveratrol has been found to modulate neuroinflammation in both *in vivo* and *in vitro* models, specifically targeting activated micloglial cells [71]. Actually, resveratrol suppresses the activation of the NF-kB pathway in LPS-activated microglia by reducing the phosphorylation and consequent degradation of its inhibitor, IkB [72–75]. Our results demonstrate that microglial, but not astroglial reactivity, was significantly diminished with resveratrol administration compared to untreated SOD1^{G93A} mice. Although further studies should be performed to assess the exact effect, resveratrol modulates microglia activity, thus contributing to the neuroprotection observed in resveratrol administered SOD1^{G93A} mice.

The results of this work demonstrate that resveratrol exerts potent therapeutic actions in the SOD1^{G93A} model of ALS. Here, we show for the first time a treatment that combines significant preservation of both lower and upper MN function, translating into significantly delayed disease onset and extended animal survival. These effects were associated with an important preservation of MN and a significant reduction of microglial reactivity in the spinal cord. Molecular analyses revealed that the beneficial effects of reseveratrol were accompanied by an activation of Sirt1 and AMPK. Such pluri-functional targets that combine the inhibition of detrimental processes and the promotion of neuroprotective pathways may provide better translational outcomes than drugs with more restricted targets. These findings strongly suggest that resveratrol may be a promising therapy for motoneuron diseases.

Acknowledgments This work was supported by grants PI1001787 and PI1111532, TERCEL and CIBERNED funds from the Fondo de Investigación Sanitaria of Spain, grant SAF2009-12495 from the Ministerio de Ciencia e Innovación of Spain, FEDER funds, and Action COST-B30 of the EC. We thank the technical help of Jessica Jaramillo and Marta Morell. RM is the recipient of a predoctoral fellowship from the Ministerio de Educación of Spain.

Conflict of interest The authors report no conflicts of interest. The authors alone are responsible for the content and writing of the paper.

Required Author Forms Disclosure forms provided by the authors are available with the online version of this article.

References

1. Wijesekera LC, Leigh PN. Amyotrophic lateral sclerosis. Orphanet J Rare Dis 2009;4:3.
2. Rosen DR. Mutations in Cu/Zn superoxide dismutase gene are associated with familial amyotrophic lateral sclerosis. Nature 1993;364:362.
3. Ripps ME, Huntley GW, Hof PR, Morrison JH, Gordon JW. Transgenic mice expressing an altered murine superoxide dismutase gene provide an animal model of amyotrophic lateral sclerosis. Proc Natl Acad Sci USA 1995;92:689–93.
4. Bosco DA, Morfini G, Karabacak NM, Song Y, Gros-Louis F, Pasinelli P, et al. Wild-type and mutant SOD1 share an aberrant conformation and a common pathogenic pathway in ALS. Nat Neurosci 2010;13:1396–403.
5. Pasinelli P, Brown RH. Molecular biology of amyotrophic lateral sclerosis: insights from genetics. Nat Rev Neurosci 2006;7:710–23.
6. Ferraiuolo L, Higginbottom A, Heath PR, Barber SC, Greenald D, Kirby J, et al. Dysregulation of astrocyte-motoneuron cross-talk in mutant superoxide dismutase 1-related amyotrophic lateral sclerosis. Brain 2011;134:2627–41.

7. Rothstein JD. Of mice and men: reconciling preclinical ALS mouse studies and human clinical trials. Ann Neurol 2003;53:423–6.
8. Benatar M. Lost in translation: treatment trials in the SOD1 mouse and in human ALS. Neurobiol Dis 2007;26:1–13.
9. Albani D, Polito L, Signorini A, Forloni G. Neuroprotective properties of resveratrol in different neurodegenerative disorders. BioFactors 2010;36:370–6.
10. Porquet D, Casadesús G, Bayod S, Vicente A, Canudas AM, Vilaplana J, et al. Dietary resveratrol prevents Alzheimer's markers and increases life span in SAMP8. Age (Dordr) 2013;35:1851-1865.
11. Tennen RI, Michishita-Kioi E, Chua KF. Finding a target for resveratrol. Cell 2012;148:387–389.
12. Park S-J, Ahmad F, Philp A, Baar K, Williams T, Luo H, et al. Resveratrol ameliorates aging-related metabolic phenotypes by inhibiting cAMP phosphodiesterases. Cell 2012;148:421–433.
13. Donmez G. The neurobiology of sirtuins and their role in neurodegeneration. Trends Pharmacol Sci 2012;33:494–501.
14. Jeong J-K, Moon M-H, Bae B-C, Lee Y-J, Seol J-W, Kang H-S, et al. Autophagy induced by resveratrol prevents human prion protein-mediated neurotoxicity. Neurosci Res 2012;73:99–105.
15. Jeong JK, Moon MH, Lee YJ, Seol JW, Park SY. Autophagy induced by the class III histone deacetylase Sirt1 prevents prion peptide neurotoxicity. Neurobiol Aging 2013;34:146–56.
16. Price NL, Gomes AP, Ling AJY, Duarte FV, Martin-Montalvo A, North BJ, et al. SIRT1 is required for AMPK activation and the beneficial effects of resveratrol on mitochondrial function. Cell Metabolism 2012;15:675–90.
17. Baur JA. Biochemical effects of SIRT1 activators. Biochimica Biophysica Acta 2010;1804:1626–34.
18. Cantó C, Gerhart-Hines Z, Feige JN, Lagouge M, Noriega L, Milne JC, et al. AMPK regulates energy expenditure by modulating NAD+ metabolism and SIRT1 activity. Nature 2009;458:1056–1060.
19. Fulco M, Cen Y, Zhao P, Hoffman EP, McBurney MW, Sauve AA, et al. Glucose restriction inhibits skeletal myoblast differentiation by activating SIRT1 through AMPK-mediated regulation of Nampt. Dev Cell 2008;14:661–673.
20. Hou X, Xu S, Maitland-Toolan KA, Sato K, Jiang B, Ido Y, et al. SIRT1 regulates hepatocyte lipid metabolism through activating AMP-activated protein kinase. J Biol Chem 2008;283:20015–20026.
21. Lan F, Cacicedo JM, Ruderman N, Ido Y. SIRT1 modulation of the acetylation status, cytosolic localization, and activity of LKB1. Possible role in AMP-activated protein kinase activation. J Biol Chem 2008;283:27628–35.
22. Wu Y, Li X, Zhu JX, Xie W, Le W, Fan Z, et al. Resveratrol-activated AMPK/SIRT1/autophagy in cellular models of Parkinson's disease. Neurosignals 2011;19:163–174.
23. Liu C, Shi Z, Fan L, Zhang C, Wang K, Wang B. Resveratrol improves neuron protection and functional recovery in rat model of spinal cord injury. Brain Res 2011;1374:100–109.
24. Wang L-M, Wang Y-J, Cui M, Luo W-J, Wang X-J, Barber PA, et al. A dietary polyphenol resveratrol acts to provide neuroprotection in recurrent stroke models by regulating AMPK and SIRT1 signaling, thereby reducing energy requirements during ischemia. Eur J Neurosci 2013;37:1669–1681.
25. Wang J, Zhang Y, Tang L, Zhang N, Fan D. Protective effects of resveratrol through the up-regulation of SIRT1 expression in the mutant hSOD1-G93A-bearing motor neuron-like cell culture model of amyotrophic lateral sclerosis. Neurosci Lett 2011;503:250–255.
26. Kim D, Nguyen MD, Dobbin MM, Fischer A, Sananbenesi F, Rodgers JT, et al. SIRT1 deacetylase protects against neurodegeneration in models for Alzheimer's disease and amyotrophic lateral sclerosis. The EMBO Journal 2007;26:3169–3179.
27. Mancuso R, Santos-Nogueira E, Osta R, Navarro X. Electrophysiological analysis of a murine model of motoneuron disease. Clin Neurophysiol 2011;122:1660–1670.
28. Valero-Cabré A, Navarro X. H reflex restitution and facilitation after different types of peripheral nerve injury and repair. Brain Res 2001;919:302–312.
29. García-Alías G, Verdú E, Forés J, López-Vales R, Navarro X. Functional and electrophysiological characterization of photochemical graded spinal cord injury in the rat. J Neurotrauma 2003;20:501–510.
30. Brooks SP, Dunnett SB. Tests to assess motor phenotype in mice: a user's guide. Nat Rev Neurosci 2009;10:519–529.
31. Miana-Mena FJ, Muñoz MJ, Yagüe G, Mendez M, Moreno M, Ciriza J, et al. Optimal methods to characterize the G93A mouse model of ALS. Amyotroph Lateral Scler 2005;6:55–62.
32. Mancuso R, Oliván S, Osta R, Navarro X. Evolution of gait abnormalities in SOD1(G93A) transgenic mice. Brain Res 2011;1406:65–73.
33. Mancuso R, Oliván S, Rando A, Casas C, Osta R, Navarro X. Sigma-1R agonist improves motor function and motoneuron survival in ALS mice. Neurotherapeutics 2012;9:814–826.
34. Penas C, Pascual-Font A, Mancuso R, Forés J, Casas C, Navarro X. Sigma receptor agonist 2-(4-morpholinethyl)1 phenylcyclohexanecarboxylate (Pre084) increases GDNF and BiP expression and promotes neuroprotection after root avulsion injury. J Neurotrauma 2011;28:831–840.
35. Ralph GS, Radcliffe PA, Day DM, Carthy JM, Leroux MA, Lee DCP, et al. Silencing mutant SOD1 using RNAi protects against neurodegeneration and extends survival in an ALS model. Nat Med 2005;11:429–433.
36. Fischer LR, Culver DG, Tennant P, Davis AA, Wang M, Castellano-Sanchez A, et al. Amyotrophic lateral sclerosis is a distal axonopathy: evidence in mice and man. Exp Neurol 2004;185:232–240.
37. Ozdinler PH, Benn S, Yamamoto TH, Güzel M, Brown RH, Macklis JD. Corticospinal motor neurons and related subcerebral projection neurons undergo early and specific neurodegeneration in hSOD1G93A transgenic ALS mice. J Neurosci 2011;31:4166–4177.
38. McHanwell S, Biscoe TJ. The localization of motoneurons supplying the hindlimb muscles of the mouse. Philos Trans R Soc Lond, B, Biol Sci 1981;293:477–508.
39. Haidet-Phillips AM, Hester ME, Miranda CJ, Meyer K, Braun L, Frakes A, et al. Astrocytes from familial and sporadic ALS patients are toxic to motor neurons. Nat Biotechnol 2011;29:824–828.
40. Diaz-Amarilla P, Olivera-Bravo S, Trias E, Cragnolini A, Martinez-Palma L, Cassina P, et al. Phenotypically aberrant astrocytes that promote motoneuron damage in a model of inherited amyotrophic lateral sclerosis. Proc Natl Acad Sci USA 2011;108:18126–18131.
41. Yamanaka K, Boillee S, Roberts EA, Garcia ML, McAlonis-Downes M, Mikse OR, et al. Mutant SOD1 in cell types other than motor neurons and oligodendrocytes accelerates onset of disease in ALS mice. Proc Natl Acad Sci USA 2008;105:7594–7599.
42. Sanagi T, Nakamura Y, Suzuki E, Uchino S, Aoki M, Warita H, et al. Involvement of activated microglia in increased vulnerability of motoneurons after facial nerve avulsion in presymptomatic amyotrophic lateral sclerosis model rats. Glia 2012;60:782–793.
43. Han S-H. Potential role of sirtuin as a therapeutic target for neurodegenerative diseases. J Clin Neurol 2009;5:120.
44. Song C-Y, Guo J-F, Liu Y, Tang B-S. Autophagy and its comprehensive impact on ALS. Int J Neurosci 2012;122:695–703.
45. Lee IH, Cao L, Mostoslavsky R, Lombard DB, Liu J, Bruns NE, et al. A role for the NAD-dependent deacetylase Sirt1 in the regulation of autophagy. Proc Natl Acad Sci USA 2008;105:3374–3379.
46. Herskovits AZ, Guarente L. Sirtuin deacetylases in neurodegenerative diseases of aging. Cell Res 2013;23:746–758.
47. Fonseca-Kelly Z, Nassrallah M, Uribe J, Khan RS, Dine K, Dutt M, et al. Resveratrol neuroprotection in a chronic mouse model of multiple sclerosis. Front Neurol 2012;3:84.
48. Nimmagadda VK, Bever CT, Vattikunta NR, Talat S, Ahmad V, Nagalla NK, et al. Overexpression of SIRT1 protein in neurons protects against experimental autoimmune encephalomyelitis

through activation of multiple SIRT1 targets. J Immunol 2013;190: 4595–4607.
49. Maher P, Dargusch R, Bodai L, Gerard PE, Purcell JM, Marsh JL. ERK activation by the polyphenols fisetin and resveratrol provides neuroprotection in multiple models of Huntington's disease. Hum Mol Genet 2010;20:261–270.
50. Jin F, Wu Q, Lu Y-F, Gong Q-H, Shi J-S. Neuroprotective effect of resveratrol on 6-OHDA-induced Parkinson's disease in rats. Euro J Pharmacol 2008;600(1-3):78–82.
51. Araki T, Sasaki Y, Milbrandt J. Increased nuclear NAD biosynthesis and SIRT1 activation prevent axonal degeneration. Science 2004;305:1010–1013.
52. Yáñez M, Galán L, Matías-Guiu J, Vela A, Guerrero A, García AG. CSF from amyotrophic lateral sclerosis patients produces glutamate independent death of rat motor brain cortical neurons: Protection by resveratrol but not riluzole. Brain Res 2;1423:77–86.
53. Markert CD, Kim E, Gifondorwa DJ, Childers MK, Milligan CE. A single-dose resveratrol treatment in a mouse model of amyotrophic lateral sclerosis. J Med Food 2010;13:1081–1085.
54. Han S, Choi JR, Shin KS, Kang SJ. Resveratrol upregulated heat shock proteins and extended the survival of G93A-SOD1 mice. Brain Res 2012;1483:112–117.
55. Amri A, Chaumeil JC, Sfar S, Charrueau C. Administration of resveratrol: what formulation solutions to bioavailability limitations?. J Control Release 2012;158:182–193.
56. Robberecht W, Philips T. The changing scene of amyotrophic lateral sclerosis. Nat Rev Neurosci 2013;14:248–264.
57. Chen S, Zhang X, Song L, Le W. Autophagy dysregulation in amyotrophic lateral sclerosis. Brain Pathology 2011;22:110–116.
58. Li L, Zhang X, Le W. Altered macroautophagy in the spinal cord of SOD1 mutant mice. Autophagy 2008;4:290–293.
59. Morselli E, Maiuri MC, Markaki M, Megalou E, Pasparaki A, Palikaras K, et al. Caloric restriction and resveratrol promote longevity through the Sirtuin-1-dependent induction of autophagy. Cell Death Dis 2010;1:e10.
60. Lin MT, Beal MF. Mitochondrial dysfunction and oxidative stress in neurodegenerative diseases. Nature 2006;443:787–795.
61. Boillee S, Vandevelde C, Cleveland D. ALS: a disease of motor neurons and their nonneuronal neighbors. Neuron 2006;52:39–59.
62. Shi P, Gal J, Kwinter DM, Liu X, Zhu H. Mitochondrial dysfunction in amyotrophic lateral sclerosis. Biochimica Biophysica Acta 2010; 1802:45–51.
63. Ferraiuolo L, Kirby J, Grierson AJ, Sendtner M, Shaw PJ. Molecular pathways of motor neuron injury in amyotrophic lateral sclerosis. Nat Rev Neurol 2011;7:616–630.
64. Wiedemann FR, Winkler K, Kuznetsov AV, Bartels C, Vielhaber S, Feistner H, et al. Impairment of mitochondrial function in skeletal muscle of patients with amyotrophic lateral sclerosis. J Neurol Sci 1998;156:65–72.
65. Fuchs A, Kutterer S, Mühling T, Duda J, Schütz B, Liss B, et al. Selective mitochondrial Ca2+ uptake deficit in disease endstage vulnerable motoneurons of the SOD1G93A mouse model of amyotrophic lateral sclerosis. J Physiol (Lond) 2013;591: 2723–2745.
66. Jung C, Higgins CMJ, Xu Z. Mitochondrial electron transport chain complex dysfunction in a transgenic mouse model for amyotrophic lateral sclerosis. J Neurochem 2002;83:535–545.
67. Kong J, Xu Z. Massive mitochondrial degeneration in motor neurons triggers the onset of amyotrophic lateral sclerosis in mice expressing a mutant SOD1. J Neurosci 1999;18:3241–250.
68. Lagouge M, Argmann C, Gerhart-Hines Z, Meziane H, Lerin C, Daussin F, et al. Resveratrol improves mitochondrial function and protects against metabolic disease by activating SIRT1 and PGC-1α. Cell 2006;127:1109–1122.
69. Khandelwal PJ, Herman AM, Moussa CEH. Inflammation in the early stages of neurodegenerative pathology. J Neuroimmunol 2011;238:1–11.
70. Yong VW, Rivest S. Taking advantage of the systemic immune system to cure brain diseases. Neuron 2009;64:55–60.
71. Zhang F, Liu J, Shi J-S. Anti-inflammatory activities of resveratrol in the brain: role of resveratrol in microglial activation. Euro J Pharmacol 2010;636:1–7.
72. Bi XL, Yang JY, Dong YX, Wang JM, Cui YH, Ikeshima T, et al. Resveratrol inhibits nitric oxide and TNF-alpha production by lipopolysaccharide-activated microglia. Int Immunopharmacol 2005;5:185–193.
73. Candelario-Jalil E, de Oliveira A, Gräf S, Bhatia HS, Hüll M, Muñoz E, et al. Resveratrol potently reduces prostaglandin E2 production and free radical formation in lipopolysaccharide-activated primary rat microglia. J Neuroinflamm 2007;4:25.
74. Heynekamp JJ, Weber WM, Hunsaker LA, Gonzales AM, Orlando RA, Deck LM, et al. Substituted trans-stilbenes, including analogues of the natural product resveratrol, inhibit the human tumor necrosis factor alpha-induced activation of transcription factor nuclear factor kappaB. J Med Chem 2006;49:7182–7189.
75. Meng X-L, Yang JY, Chen G-L, Wang L-H, Zhang L-J, Wang S, et al. Effects of resveratrol and its derivatives on lipopolysaccharide-induced microglial activation and their structure-activity relationships. Chem Biol Interact 2008;174:51–59.

Chapter IV: Combined treatment

Lack of synergistic effect of resveratrol and sigma-1 receptor agonist (PRE-084) in SOD1^{G93A} ALS mice: an indication of limited therapeutic opportunity?

Mancuso R, Del Valle J, Morell M, Pallás M, Osta R, Navarro X Lack of synergistic effect of resveratrol and sigma-1 receptor agonist (PRE-084) in SOD1^{G93A} ALS mice: an indication of limited therapeutic opportunity? Orphanet J Rare Dis, submitted

I

Lack of synergistic effect of resveratrol and sigma-1 receptor agonist (PRE-084) in SOD1^{G93A} ALS mice: overlapping effects or an indication of limited therapeutic opportunity?

Renzo Mancuso[1], Jaume del Valle[1], Marta Morell[1], Mercé Pallás[2], Rosario Osta[3], Xavier Navarro[1]

[1] Institute of Neurosciences and Department of Cell Biology, Physiology and Immunology, Universitat Autònoma de Barcelona, and Centro de Investigación Biomédica en Red sobre Enfermedades Neurodegenerativas (CIBERNED), Bellaterra, Spain.

[2] Unitat de Farmacologia i Farmacognòsia, Facultat de Farmàcia, Institut de Biomedicina (IBUB), Universitat de Barcelona, and CIBERNED, Barcelona, Spain.

[3] Laboratory of Genetic Biochemistry (LAGENBIO-I3A), Aragon Institute of Health Sciences, Universidad de Zaragoza. Zaragoza, Spain.

Abstract

Background: Amyotrophic lateral sclerosis (ALS) is an adult onset neurodegenerative disease characterized by the loss of motoneurons (MNs) in the spinal cord, brainstem and motor cortex, causing progressive paralysis and death. Nowadays, there is no effective therapy and most patients die 2-5 years after diagnosis. Sigma-1R is a transmembrane protein highly expressed in the CNS and specially enriched in MNs. Mutations on the Sigma-1R leading to frontotemporal lobar degeneration-ALS were recently described in human patients. We previously reported the therapeutic role of the selective sigma-1R agonist 2-(4-morpholi-nethyl)1-phenylcyclohexanecarboxylate (PRE-084) in SOD1^{G93A} ALS mice, that promoted spinal MN preservation and extended animal survival by controlling NMDA receptor calcium influx. Resveratrol (RSV, trans-3,4′,5-trihydroxystilbene) is a natural polyphenol with promising neuroprotective effects. We recently found that RSV administration to SOD1^{G93A} mice preserves spinal MN function and increases mice survival. These beneficial effects were associated to activation of Sirtuin 1 (Sirt1) and AMP-activated protein kinase (AMPK) pathways, leading to the modulation of autophagy and an increase of mitochondrial biogenesis. The main goal of this work was to assess the effect of combined RSV and PRE-084 administration in SOD1^{G93A} ALS mice.

Methods: We determined the locomotor performance of the animals by rotarod test and evaluated spinal motoneuron function using electrophysiological tests.

Results: RSV plus PRE-084 treatment from 8 weeks of age significantly improved locomotor performance and spinal motoneuron function, accompanied by a significant reduction of motoneuron degeneration and an extension of mice lifespan. In agreement with our previous findings, there was an induction of PKC-specific phosphorylation of the NMDA-NR1 subunit and an increased expression and activation of Sirt1 and AMPK in the ventral spinal cord of treated SOD1^{G93A} animals.

Conclusions: Although combined PRE and RSV treatment significantly ameliorated SOD1^{G93A} mice, it did not show a synergistic effect compared to RSV-only and PRE-084-only treated groups.

Corresponding author: Dr. Xavier Navarro, Unitat de Fisiologia Mèdica, Facultat de Medicina, Universitat Autònoma de Barcelona, E-08193 Bellaterra, Spain. E-mail: xavier.navarro@uab.cat

Introduction

Amyotrophic lateral sclerosis (ALS) is an adult onset neurodegenerative disease characterized by the loss of motoneurons (MN) in the spinal cord, brainstem and motor cortex. It clinically manifests by progressive weakness, muscle atrophy and paralysis [1,2]. The majority of ALS cases are sporadic with unknown etiology but 10% of them are inherited forms, linked to genetic mutations. Mutations in the gene encoding for the enzyme Cu/Zn superoxide dismutase 1 (SOD1) are observed in about 20% of the familial cases of ALS [3]. The transgenic mouse that over-expresses the human mutated form of the SOD1 gene with a glycine to alanine conversion at the 93rd codon is the most studied model [4-6] and recapitulates the main features of both sporadic and familial ALS forms [5]. SOD1 protein alterations have also been reported in sporadic ALS patients [7].

The sigma-1 receptor (sigma-1R) is an endoplasmic reticulum (ER) transmembrane protein [8] highly expressed in spinal MNs [9-11], and specially enriched in postsynaptic sites of C-terminals [12]. Sigma-1R participates in several cellular processes including neuritogenesis, ionic channels conductance, calcium homeostasis and microglial activity [13-16]. It has been implicated in diverse neuropathologies, such as depression, schizophrenia and Alzheimer's disease [17]. A novel mutation of the sigma-1R has been recently described in patients affected by juvenile ALS [18]. Sigma-1R agonists have demonstrated to promote protective effects reducing glutamate-mediated cell death [19,20] or modulating inflammatory reaction following stroke in rats [21]. Indeed, we have previously reported the therapeutic role of the selective sigma-1R agonist 2-(4-morpholi-nethyl)1-phenylcyclohexanecarboxylate (PRE-084) in SOD1^{G93A} ALS mice, that promoted spinal MN preservation and extended animal survival by controlling NMDA receptor calcium influx [22].

Resveratrol (RSV, 3,5,4'-trihydroxy-trans-stilbene) is a polyphenol naturally present in grapes and red wine that has been reported to exert neuroprotective effects on neurodegenerative disease models of Alzheimer's disease [23] and Parkinson's disease [24], and in traumatic [25] and ischemic injuries to the CNS [26]. Previous studies showed protective effects after resveratrol administration on in vitro ALS models [27,28]. We recently found that RSV administration to SOD1^{G93A} mice preserves spinal MN function and increases their survival. These beneficial effects were associated to activation of Sirtuin 1 (Sirt1) and AMP-activated protein kinase (AMPK) pathways, modulation of autophagy and an increase of mitochondrial biogenesis [29-32].

The pathophysiology of ALS is complex, with several processes contributing to MN death, including glutamate excitotoxicity, oxidative stress, protein misfolding, mitochondrial defects, impaired axonal transport and inflammation [33,34]. In this context, it is likely that combined therapies targeting several pathophysiological mechanisms could lead to stronger effects and better functional outcomes, potentially resulting in successful clinical translation. Thus, the main goal of this study is to assess if the combination of PRE-084 and RSV treatments may have synergistic effects in the SOD1^{G93A} ALS mice.

Material and methods

Transgenic mice and drug administration

Transgenic mice with the G93A human SOD1 mutation (B6SJL-Tg[SOD1-G93A]1Gur) were obtained from the Jackson Laboratory (Bar Harbor, ME, USA), and maintained at the Animal Service of the Universidad de Zaragoza. Hemizygotes B6SJL SOD1^{G93A} males were obtained by crossing with B6SJL females from the CBATEG (Bellaterra, Spain). The offspring was identified by PCR amplification of DNA extracted from the tail tissue. Mice were kept in standard conditions of temperature (22±2 °C) and a 12:12 light:dark cycle with access to food and water *ad libitum*. All experimental procedures were approved by the Ethics Committee of the Universitat Autònoma de Barcelona, where the animal experiments were performed.

Animals were evaluated at 8 weeks (prior to starting treatments) by rotarod and electrophysiological tests to obtain baseline values. Animals were distributed, according to their progenitors, weight and electrophysiological baseline values, in balanced experimental groups. A resveratrol-enriched diet [23] was given to groups of treated mice from 8 weeks of age. It has been previously demonstrated that RSV do not affect food intake of the animals [35], thereby assuming a normal food intake of 4 g/animal/day, then resveratrol was

given at a daily dose of 160 mg/kg. PRE-084 (Tocris Bioscience, Ellisville, MO), a Sigma-1R agonist, was dissolved in saline and administered daily by single intraperitoneal injections at 0.25 mg/kg. The experimental groups included in the study are summarized in Table 1.

Nerve conduction tests

Motor nerve conduction tests were performed at 8 weeks of age and then every two weeks until 16 weeks in all the animals used in the study. The sciatic nerve was stimulated percutaneously by means of single pulses of 0.02 ms duration (Grass S88) delivered through a pair of needle electrodes placed at the sciatic notch. The compound muscle action potential (CMAP, M wave) was recorded from the tibialis anterior (TA) and the plantar (interossei) muscles with microneedle electrodes [36,37]. All potentials were amplified and displayed on a digital oscilloscope (Tektronix 450S) at settings appropriate to measure the amplitude from baseline to the maximal negative peak. To ensure reproducibility, the recording needles were placed under microscope to secure the same placement on all animals guided by anatomical landmarks. During the tests, mouse body temperature was kept constant by means of a thermostated-controlled heating pad.

Locomotion tests and clinical disease onset

The rotarod test was performed to evaluate motor coordination, strength and balance [38,39] in all the animals used in the study (Table 1). Mice were trained three times a week on the rod rotating at 14 diameters larger than 20 µm, polygonal shape and prominent nucleoli were counted. The number of MNs present in both ventral horns was counted in four serial sections of each L4 and L5 segments [36,40], where motor nuclei innervating TA and plantar muscles are located [41].

Protein extraction and western blot

For protein extraction, another subsets of mice (4-5 of each experimental group) were anesthetized and decapitated at 16 weeks of age. The lumbar spinal cord was removed and divided into quarters to isolate the ventral quadrants. One of them was prepared for protein extraction and homogenized in modified RIPA buffer (50 mM Tris–HCl pH 7.5, 1% Triton X-100, rpm, and then tested from 8 to 16 weeks of age, with an arbitrary maximum time of maintenance in the rotating rod of 180s. Clinical disease onset was defined as the first day when an animal was not able to complete the 180 seconds on the rotating rod.

Survival

The mice were inspected daily until the standard end point or death. It was considered that animals reached the end point of the disease when they were unable to right themselves in 30s when placed on their side.

Histology

At 16 weeks of age 4-5 mice of each group were transcardially perfused with 4% paraformaldehyde in PBS and the lumbar segment of the spinal cord was harvested, post-fixed for 24 h, and cryopreserved in 30% sucrose. Transverse 40 µm thick sections were serially cut with a cryotome (Leica) between L2-L5 segmental levels. For each segment, each section of a series of 10 was collected sequentially on separate gelatin-coated slides or free-floating in Olmos medium.

One slide of each animal was rehydrated for 1 min and stained for 2 h with an acidified solution of 3.1 mM cresyl violet. Then, the slides were washed in distilled water for 1 min, dehydrated and mounted with DPX (Fluka). MNs counts were made for neuronal soma present in the lateral part of lamina IX of the ventral horn in the spinal cord sections and following strict size and morphological criteria: only MNs with 0.5% sodium deoxycholate, 0.2% SDS, 100 mM NaCl, 1 mM EDTA) adding 10 µl/ml of Protease Inhibitor cocktail (Sigma) and PhosphoSTOP phosphatase inhibitor cocktail (Roche). After clearance, protein concentration was measured by Lowry assay (Bio-Rad Dc protein assay).

To perform western blots, 20-30 µg of protein of each sample were loaded in SDS-poliacrylamide gels. The transfer buffer was 25 mM trizma-base, 192 mM glycine, 20% (v/v) methanol, pH 8.4. The membranes were blocked with 5% BSA in TBS plus 0.1% Tween-20 for 1 hour, and then incubated with primary antibodies at 4°C overnight. The primary antibodies used were: anti-GAPDH (MAB374, Millipore, 1:20000), anti-Sirt1 (ab50517, Abcam,

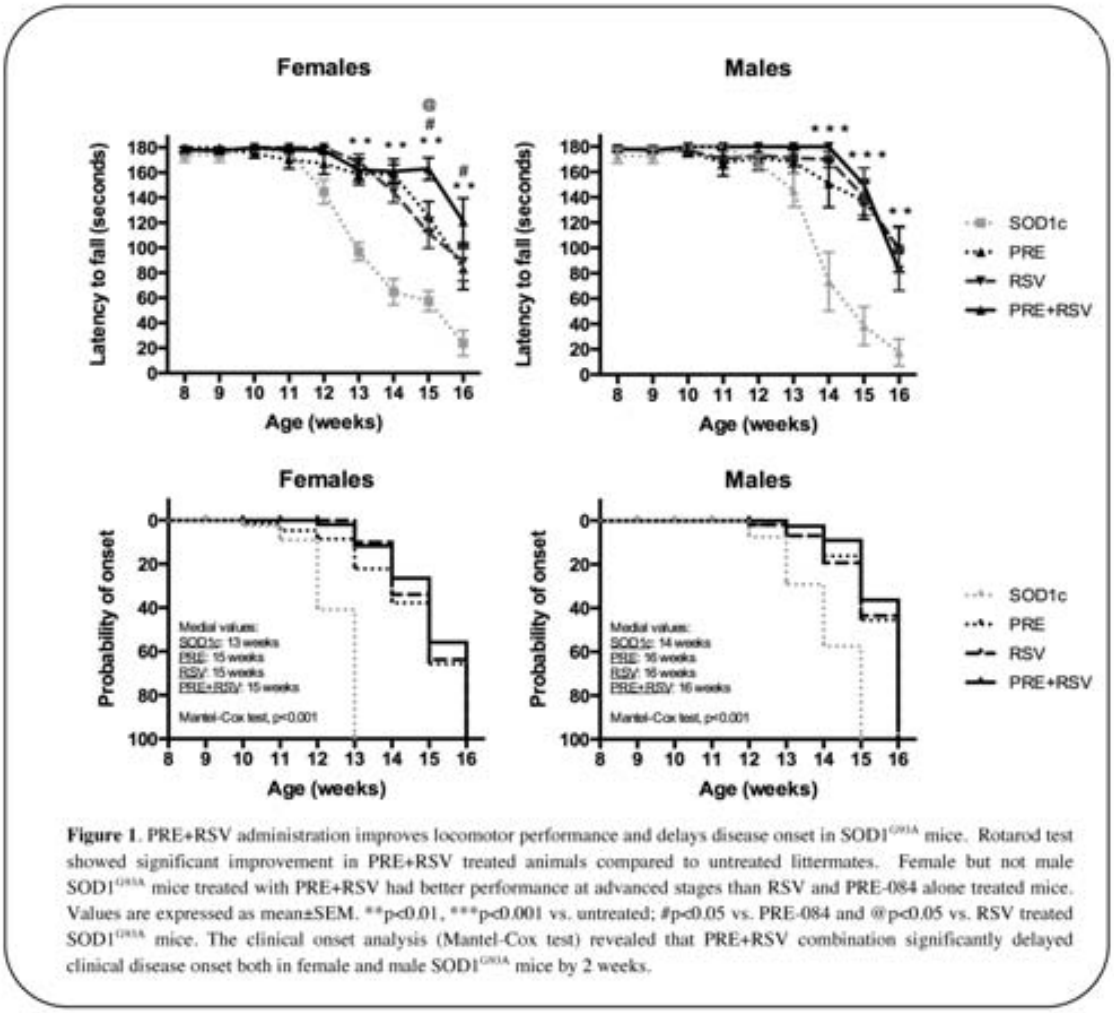

Figure 1. PRE+RSV administration improves locomotor performance and delays disease onset in SOD1^{G93A} mice. Rotarod test showed significant improvement in PRE+RSV treated animals compared to untreated littermates. Female but not male SOD1^{G93A} mice treated with PRE+RSV had better performance at advanced stages than RSV and PRE-084 alone treated mice. Values are expressed as mean±SEM. **p<0.01, ***p<0.001 vs. untreated; #p<0.05 vs. PRE-084 and @p<0.05 vs. RSV treated SOD1^{G93A} mice. The clinical onset analysis (Mantel-Cox test) revealed that PRE+RSV combination significantly delayed clinical disease onset both in female and male SOD1^{G93A} mice by 2 weeks.

1:1000), anti-p53 (#2524, Cell Signaling, 1:500), anti-acetyl p53 (L382) (06-758, Millipore, 1:500), anti-AMPK (#2532, Cell Signaling, 1:1000), anti-pAMPK (#2531, Cell Signaling, 1:1000), anti-NMDAR1 (AB9864, Millipore, 1:500) and anti-phospho NR1 (S896) (ABN88, Millipore, 1:500). Horseradish peroxidase–coupled secondary antibody (1:5000, Vector) incubation was performed for 60 min at room temperature. The membranes were visualized by enhanced chemiluminiscence method and the images were collected and analyzed with a Gene Genome apparatus using Gene Snap and Gene Tools software (Syngene, Cambridge, UK), respectively.

Statistical analysis

Data are expressed as mean±SEM. Electrophysiological and locomotion test results were statistically analyzed using repeated measurements and one-way ANOVA, applying Turkey post-hoc test when necessary. Histological data were analyzed using Mann-Whitney U test. Onset and survival data were analyzed using the Mantel-Cox test.

Results

Combined resveratrol and PRE-084 reduces locomotor impairments and delays clinical disease onset in SOD1^{G93A} mice

We assessed locomotor performance with the rotarod test [38,39]. Rotarod performance was significantly higher in both female and male PRE+RSV treated mice than in control SOD1^{G93A} mice (Fig. 1). Furthermore, the combined treatment significantly improved motor outcome of female animals with respect to single RSV or PRE-084 mice at 15 and 16 weeks of age. However, in male mice

5

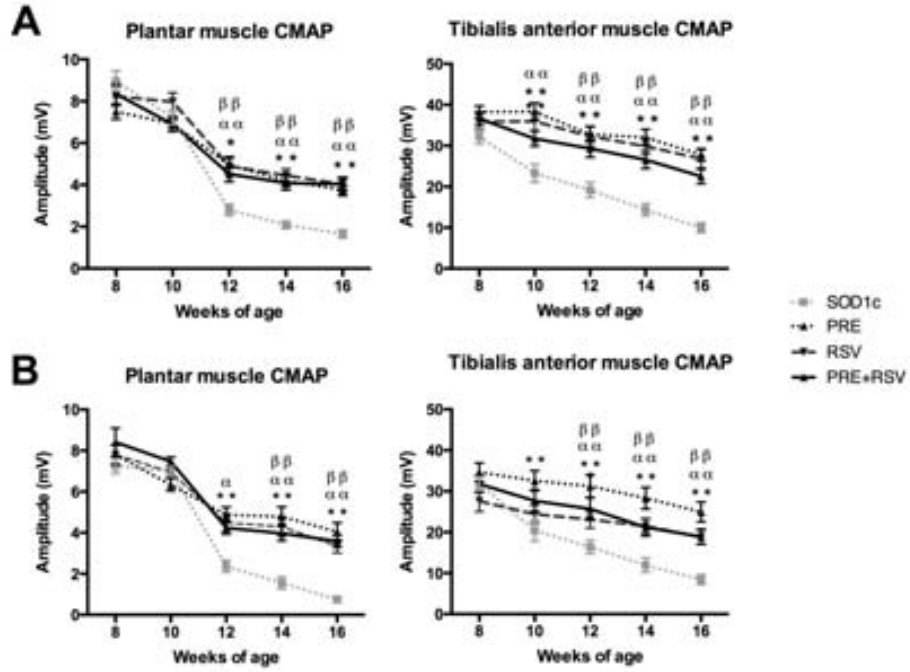

Figure 2. PRE+RSV treatment preserves lower motoneuron function. Electrophysiological tests performed in (A) female and (B) male SOD1G93A mice revealed significant preservation of compound muscle action potentials (CMAP) amplitude in treated groups. Values are mean±SEM. *p<0.05, **p<0.01 PRE-084 vs. untreated; α p<0.05, αα p<0.01 PRE+RSV vs. untreated; ββ p<0.01 RSV vs. untreated.

PRE+RSV did not produce additional benefits regarding single treatments. Regarding clinical disease onset, although PRE+RSV combination significantly delayed first locomotor signs compared to untreated SOD1c mice, it not represented an improvement in comparison to single treated groups (Fig. 1).

Combined resveratrol and PRE-084 preserves spinal motoneuron function in SOD1^{G93A} mice

Lower MN dysfunction is one the main clinical signs of ALS pathology both in animal models [36,41] and human patients [1]. We assessed the functional state of spinal MN by evaluating the amplitude of plantar and TA CMAPs. As previously reported [36] there was a progressive decline in CMAP amplitudes in both muscles along disease progression in SOD1^{G93A} untreated mice. The results revealed that PRE+RSV administration significantly preserves spinal MN function compared to SOD1^{G93A} untreated animals, although it did not promote a better outcome than separated RSV and PRE-084 treatments (Fig. 2).

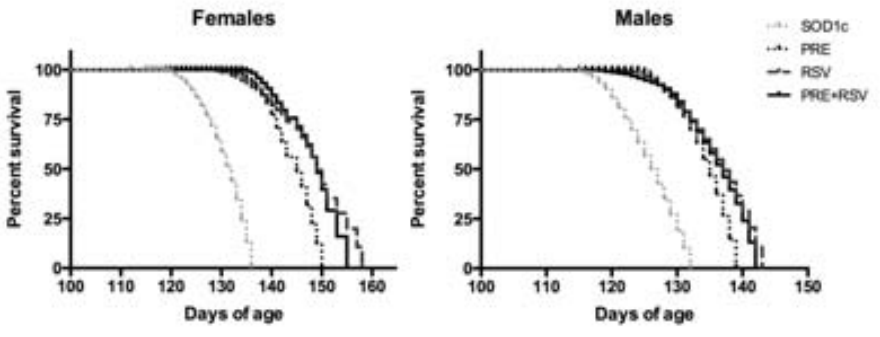

Figure 3. PRE+RSV administration significantly extended SOD1^{G93A} mice survival (Mantel-Cox test, p<0.001). PRE+RSV treatment also increased animals survival compared to PRE-084-only treated group (Mantel-Cox test, p<0.05).

6

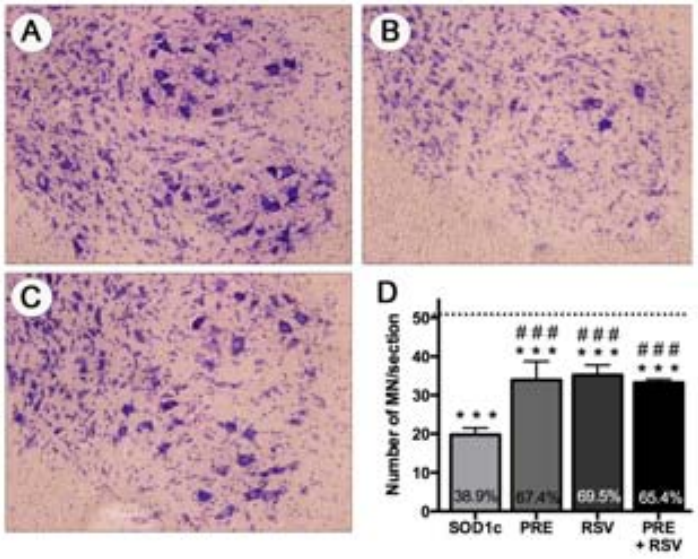

Figure 4. Resveratrol administration significantly preserves spinal motoneurons from degeneration. Representative images of L4 spinal cord of (**A**) wild type, (**B**) SOD1^{G93A} untreated and (**C**) PRE+RSV SOD1^{G93A} treated mice. Scale bar, 500μm. (**D**) L4-L5 spinal cord motoneuron counts revealed significant neuroprotection exerted by PRE+RSV co-administration compared to untreated SOD1^{G93A} but not to RSV-only or PRE-084-only treatments. Dashed line respresent the mean number of motoneurons per section of wild type mice. Values are mean±SEM. ***p<0.05 vs. wild type, ### p<0.05 vs. untreated SOD1^{G93A} mice.

Combined resveratrol and PRE-084 extends survival of SOD1^{G93A} mice

RSV and PRE-084 combined administration from 8 weeks of age significantly extended both female (12.9%) and male (8.7%) lifespan compared to SOD1^{G93A} untreated mice (Mantel-Cox test, p<0.001). The combined treatment also prolonged mice survival with respect to PRE-084 (Mantel-Cox test, p<0.01) but not to RSV only treated SOD1^{G93A} mice (Fig. 3).

Combined resveratrol and PRE-084 administration reduces spinal motoneuron degeneration and reduces microglial reactivity in SOD1^{G93A} mice

Spinal MN preservation was assessed by evaluating the number of Nissl stained MN cell bodies in the ventral horns of lumbar L4-L5 spinal segments in 16 weeks old SOD1^{G93A} mice. Figure 4 shows representative images of Nissl stained anterior horns to illustrate the differences between experimental groups. MN counts of female and male animals were pooled since there were no significant differences between genders. PRE-084 and RSV co-administration from 8 weeks of age significantly increased the number of preserved MNs in SOD1^{G93A} mice. PRE+RSV treated mice had 33.3±1.74 MNs (65.4% vs. wild type) per section whereas SOD1^{G93A} untreated animals had 19.8±0.79 (38.9% vs. wild type), almost a two-fold increase in surviving MNs. However, the combinatory treatment did not represent improvement in terms of neuronal preservation compared to single RSV or PRE-084 administered animals (Fig. 4).

Combined resveratrol and PRE-084 increases Sirt1 and AMPK activation, and promotes specific PKC-depended phosphorylation of NMDA-NR1 subunits

We have previously shown that RSV treatment induced an increased expression and activation of Sirt1 and AMPK and a consequent modulation of autophagy and mitochondrial biogenesis [32]. On the other hand, PRE-084 administration leads to specific PKC-dependent NMDA-NR1 subunit phosphorylation that may protect MN from degeneration by reducing NMDA calcium currents and thus preventing excitotoxicity [14,22,42]. Therefore, we further analyzed whether RSV and PRE-084 co-administration similarly promotes the activation of the same downstream cellular pathways or there was any interference between drugs.

To assess RSV effects in the combinatory treated SOD1^{G93A} mice we first analyzed Sirt1 levels and activation in the ventral part of the lumbar spinal cord by western blot analysis. Results revealed a pronounced increase in Sirt1 expression after PRE+RSV co-administration (Fig. 5A). To check whether this augmented expression was translated into an enhanced function we analyzed the acetylation

7

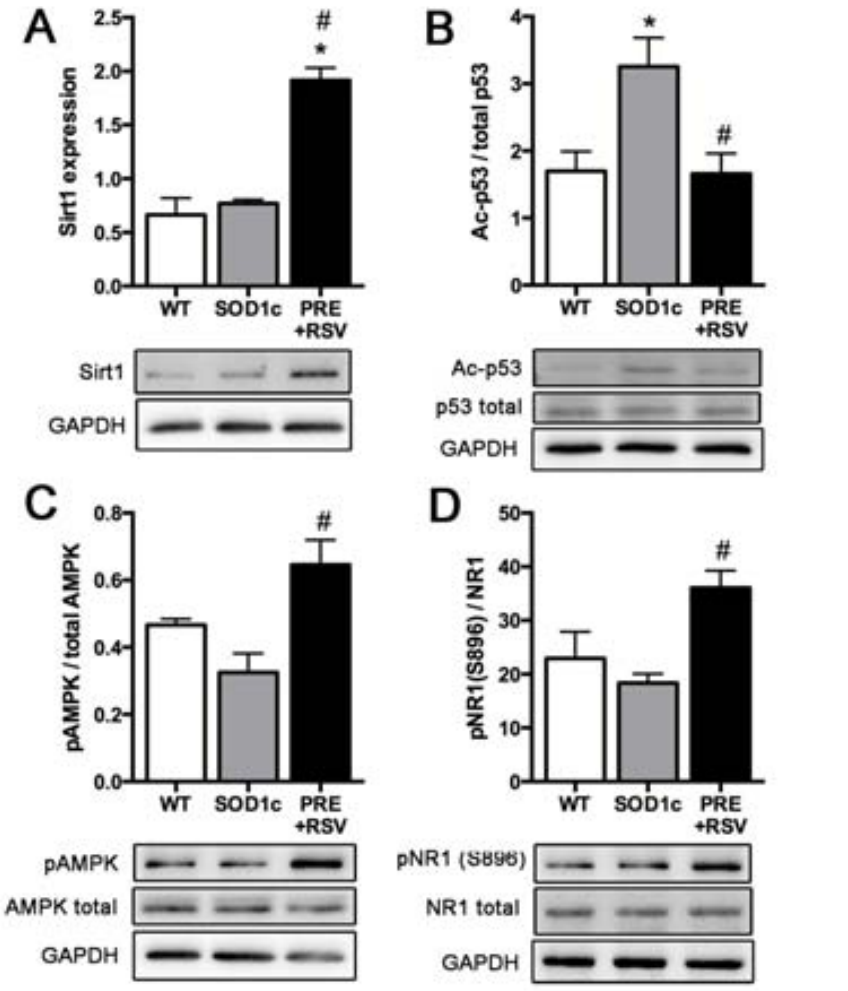

Figure 5. Western blot analysis on the ventral lumbar spinal cord of animals co-administered with PRE+RSV. (**A**) Increased sirtuin 1 expression in SOD1^{G93A} spinal motoneurons after PRE+RSV treatment. (**B**) Evaluation of Sirt1 activity by measuring the acetylation levels of p53 revealed significant deacetylation and thus, increased activity of Sirt1 in SOD1^{G93A} mice treated with PRE+RSV. (**C**) Enhanced AMPK activation after PRE+RSV treatment, evidenced by an increased pAMPK/AMPK ratio. (**D**) Increased Ser896 PKC-specific phosphorylation in NMDA-NR1subunits of animals treated with PRE+RSV. Values are mean±SEM, *p<0.05 vs. wild type, #p<0.05 vs. untreated SOD1^{G93A} mice.

state of one the most important Sirt1 targets, p53. We found a significant reduction of acetyl-p53 proportion indicating that Sirt1 was also over-activated (Fig. 5B). Secondly, we assessed the activation of AMPK by evaluating active phospho-AMPK fraction. Results showed a marked increase in the pAMPK/AMPK ratio after PRE+RSV co-administration (Fig. 5C). These changes were similar to those previously reported after treatment with RSV alone [32].

On the other hand, we evaluated the molecular effects of PRE-084 by analyzing the phosphorylation state of a PKC-specific serine (Ser896) in the NMDA-NR1 subunit. Western blot results showed increased Ser896 phosphorylation of the NMDA-NR1 subunit in the animals administered with PRE+RSV (Fig. 5D).

Discussion

The main goal of this study was to assess the effect of a novel therapeutic approach combining a

Sigma-1R agonist, PRE-084, and RSV in the SOD1^{G93A} mouse model of ALS, since separate administration of the two compounds had resulted in significant improvement of disease progression and survival of these mice [22,32]. Our results indicate that co-administration of PRE-084 and RSV from 8 weeks of age significantly preserved spinal MNs function and reduced MN degeneration together with a reduction of microglial immunoreactivity in the lumbar spinal cord lamina IX. This effect was accompanied by improvement in the locomotor performance and significant extension of the animals survival. Western blot analyses revealed that, as we previously described, PRE-084 induced PKC-specific phosphorylation of Ser896 of the NMDA-NR1 subunit, whereas RSV increased the expression and activation of Sirt1 and AMPK in the ventral part of the lumbar spinal cord of SOD1^{G93A} mice. Unfortunately, the combinatory therapy did not represent a clear improvement compared to RSV-only or PRE-084-only treated animals.

Mechanisms of neuroprotection and possible overlapping effects

As we previously described, PRE-084 promotes potent neuroprotective effects to MNs both *in vitro* after excitotoxic insults [43], and *in vivo* after spinal root avulsion [11] and in the SOD1^{G93A} mouse model accompanied by a significant extension of animals survival [22]. Calcium dysregulation and excitotoxicity are two pathophysiological mechanisms contributing to ALS pathology [44,45]. In fact, spinal ALS-vulnerable MNs have an endogenous calcium buffering capacity 5-6 times lower than that found in ALS-resistant MNs, increasing their susceptibility to excitotoxic insults [46]. NMDA receptor plays an important role during excitotoxicity [45] and Sigma-1R agonists have been shown to suppress calcium influx to the cells by modulating NMDA receptor through PKC activation. Consistent with our previous observations that PRE-084 administration promotes PKC-specific NMDA-NR1 subunit phosphorylation [22], we have found that PRE+RSV combined treatment also increased Ser896 phosphorylation of the NDMA-NR1 subunit in the ventral part of the spinal cord. Interestingly, increased NMDA-NR1 phosphorylation was only present in the treated group, maybe suggesting that the treatment is activating compensatory protective pathways rather than counteracting a pre-existent pathological event. Although it has been demonstrated that Sigma-1R physically interacts with NMDA-NR1 subunits [47], it has been also reported that Sigma-1R agonists can modulate ionic flow through calcium, sodium and potassium channels, thus modifying cells excitability properties [14,48,49]. In fact, recent findings by Mavlutov et al. [50] indicate that the lack of Sigma-1R is detrimental in SOD1^{G93A} mice probably because it acts by reducing the excitability of spinal MNs. Moreover, Sigma-1R is found associated to ER chaperones (such as BiP) and plays a role in clearance of misfolded proteins by the ERAD response [51,52]. Sigma-1R is enriched in the so-called mitochondrial-associated ER membrane (MAM) and its activation can also modulate mitochondrial metabolism [8,53].

It has been reported that RSV promotes protective effects both in neurodegenerative and traumatic injury models, including Alzheimer's disease and accelerated aging [23,28,54], multiple sclerosis [55,56], Huntington's disease [57,58], Parkinson's disease [24,59], and reducing peripheral axonal degeneration [60] or promoting functional improvements after spinal cord injury [25]. We have recently found that RSV administration significantly delays clinical symptoms onset, improves spinal MNs function and survival, and extends SOD1^{G93A} mice lifespan. We also determined that the therapeutic effect was mediated by the increased expression and activation of both Sirt1 and AMPK, leading to normalization of the autophagic flux and enhanced mitochondrial biogenesis [32]. Although there is some controversy about the exact molecular mechanisms underlying RSV effect, it has been established that Sirt1 or AMPK activation are upstream of pathways that participate in several cellular processes, including inflammation [61-64], autophagy [32] and mitochondrial function [29,54]. Consistent with our previous findings, PRE+RSV treated animals also presented higher expression and activation of both Sirt1 and AMPK compared to SOD1^{G93A} untreated mice. As we previously observed regarding the increased NMDA-NR1 phosphorylation, Sirt1 and AMPK overactivation was only present in the treated

group, suggesting again that the treatment is activating compensatory protective pathways rather than counteracting a pre-existent pathological condition. This fact might increase the interest of these treatments since the potentiation of endogenous protective mechanisms can be translated to other non-SOD1 ALS situations.

Although the absence of summative effect in the PRE+RSV treated group may be due to an insufficient dose of any of both compounds, a possible overlapping in the pathways activated by both compounds may underlie the lack of synergy. As above mentioned, RSV protective effect is likely related to normalization of the autophagic flux and increased mitochondrial biogenesis [32]. Although PRE-084 main therapeutic effects have been considered associated to modulation of calcium influx and MNs excitability [14,48,49], it also participates on the response to misfolded protein accumulation [8,52] and the modulation of mitochondrial metabolism [53]. Considering this action, RSV effects on autophagy and mitochondrial biogenesis may mask those of PRE-084 administration thus explaining the lack of summative effect of the combined treatment. Alternatively, both compounds may exert opposite effects on some pathways. For example, it has been reported that Sigma-1R stabilize IRE1α and increase cell survival through the transcriptional activity of X Box binding Protein 1 (XBP1) which in turn regulates genes responsible for protein folding and degradation during the Unfolded Protein Response (UPR) [51]. In contrast, RSV has been shown to suppress the transcriptional activity of XBP1 through Sirt1 [65], therefore promoting an opposite effect that could contribute to the lack of synergistic effect of the combinatory treatment.

Another explanation for the lack of summative effect of the combined treatment lies in the pathology state of the animals in the moment we began the drug administration. SOD1^{G93A} mice at 8 weeks of age present 25-30% loss of CMAP amplitude in proximal muscles (TA and gastrocnemius) [36,66], due to early neuromuscular junction retraction and motor axons degeneration [41]. Thus, although MN cell bodies in the anterior spinal cord are intact, up 30% of them are already under a degenerative process that may be irreversible. Since our treatment is focused on the preservation of remaining functional MNs, it is likely that we are acting on the still functioning population of MNs and thus, the maximum effect that can be reached would be limited.

Does the SOD1^{G93A} mouse model present a limited therapeutic capacity?

An alterative explanation for the lack of summative effect after combining PRE-084 and RSV could be that the SOD1^{G93A} mouse model has a limit in terms of MN function and survival that cannot be overpassed by therapeutic interventions. To address this possibility, we made a review of successful preclinical trials using both single and combinatorial treatments in SOD1^{G93A} mice. Supplementary table 1 shows a summary of the therapies performed and the percentage of increased survival compared to untreated mice. It is worth noting that no replication of the positive results was achieved for several of the drugs initially reported to provide efficacy when re-tested using a careful study design [67]. Up to our knowledge and without considering those works showing negative or null results, only 4 of 48 studies reported an extension of survival longer than 25% with just few showing a synergistic effect after combinatory approaches. Although deeper analyses must be performed, such observations may reflect an endogenous limitation for the therapeutical benefits that can be achieved using the SOD1^{G93A} mouse model.

Conclusions

The main goal of the present work was to assess the therapeutic potential of a combinatory strategy using RSV and PRE-084 in the SOD1^{G93A} mouse model of ALS. Our results revealed that RSV and PRE-084 co-administration significantly improved MN functional preservation and neuroprotection, accompanied by an improvement of the locomotor performance and survival extension. However, this effect was not comparatively better than that achieved by administration of RSV alone.

Author's contribution

RM designed the study, performed functional tests and histological studies, collected and analyzed the data, made the figures and prepared the manuscript; JdV performed molecular biology analyses; MM

performed the locomotion evaluation; RO breaded and genotyped the animals; MP contributed to set the treatment diet and to prepare the manuscript, XN conceived and designed the study, supervised data analysis and prepared the manuscript.

Acknowledgment

This work was supported by TERCEL and CIBERNED funds from the Fondo de Investigación Sanitaria of Spain, grant SAF2009-12495 from the Ministerio de Ciencia e Innovación of Spain, FEDER funds, and Action COST-B30 of the EC. We thank the technical help of Jessica Jaramillo and Mónica Espejo. RM is recipient of a predoctoral fellowship from the Ministerio de Educación of Spain.

Conflict of interest

The authors declare that they have not competing interests.

Reference

1. Wijesekera LC, Leigh PN. **Amyotrophic lateral sclerosis**. *Orphanet J Rare Dis* 2009;**4**:3.
2. Kiernan MC, Vucic S, Cheah BC, Turner MR, Eisen A, Hardiman O, et al. **Amyotrophic lateral sclerosis**. *The Lancet* 2011;**377**:942–55.
3. Rosen DR. **Mutations in Cu/Zn superoxide dismutase gene are associated with familial amyotrophic lateral sclerosis**. *Nature* 1993;**364**:362.
4. McGoldrick P, Joyce PI, Fisher EMC, Greensmith L. **Rodent models of amyotrophic lateral sclerosis**. *BBA - Molecular Basis of Disease* 2013;**1832**:1421–1436.
5. Ripps ME, Huntley GW, Hof PR, Morrison JH, Gordon JW. **Transgenic mice expressing an altered murine superoxide dismutase gene provide an animal model of amyotrophic lateral sclerosis**. *Proc Natl Acad Sci USA* 1995;**92**:689–93.
6. Gurney ME, Pu H, Chiu AY, Dal Canto MC, Polchow CY, Alexander DD, Caliendo J, Hentati A, Kwon YW, Deng HX. **Motor neuron degeneration in mice that express a human Cu,Zn superoxide dismutase mutation**. *Science* 1994;**264**:1772–5.
7. Bosco DA, Morfini G, Karabacak NM, Song Y, Gros-Louis F, Pasinelli P, Goolsby H, Fontaine BA, Lemay N, McKenna-Yasek D, Frosch MP, Agar JN, Julien JP, Brady ST, Brown RH. **Wild-type and mutant SOD1 share an aberrant conformation and a common pathogenic pathway in ALS**. *Nat Neurosci* 2010;**13**:1396–403.
8. Hayashi T, Su T-P. **Sigma-1 receptor chaperones at the ER-mitochondrion interface regulate Ca(2+) signaling and cell survival**. *Cell* 2007;**131**:596–610.
9. Alonso G, Phan V-L, Guillemain I, Saunier M, Legrand A, Anoal M, Maurice T. **Immunocytochemical localization of the sigma1 receptor in the adult rat central nervous system**. *Neuroscience* 2000;**97**:155–70.
10. Palacios G, Muro A, Vela JM, Molina-Holgado E, Guitart X, Ovalle S, Zamanillo D. **Immunohistochemical localization of the sigma1-receptor in oligodendrocytes in the rat central nervous system**. *Brain Res* 2003;**961**:92–9.
11. Penas C, Pascual-Font A, Mancuso R, Forés J, Casas C, Navarro X. **Sigma receptor agonist 2-(4-morpholinethyl)1 phenylcyclohexanecarboxylate (Pre084) increases GDNF and BiP expression and promotes neuroprotection after root avulsion injury**. *J Neurotrauma* 2011;**28**:831–40.
12. Mavlyutov TA, Epstein ML, Andersen KA, Ziskind-Conhaim L, Ruoho AE. **The sigma-1 receptor is enriched in postsynaptic sites of C-terminals in mouse motoneurons. An anatomical and behavioral study**. *Neuroscience* 2010;**167**:247–55.
13. Hall AA, Herrera Y, Ajmo CT Jr., Cuevas J, Pennypacker KR. **Sigma receptors suppress multiple aspects of microglial activation**. *Glia* 2009;**57**:744–54.
14. Zhang X-J, Liu L-L, Jiang S-X, Zhong Y-M, Yang X-L. **Activation of the ζ receptor 1 suppresses NMDA responses in rat retinal ganglion cells**. *Neuroscience* 2011;**177**:12–22.
15. Aydar E, Palmer CP, Klyachko VA, Jackson MB. **The sigma receptor as a ligand-regulated auxiliary potassium channel subunit**. *Neuron* 2002;**34**:399–410.
16. Zhang H, Cuevas J. **σ Receptor activation blocks potassium channels and depresses neuroexcitability in rat intracardiac neurons**. *J Pharmacol Exp Ther* 2005;**313**:1387–96.
17. Maurice T, Su T-P. **The pharmacology of sigma-1 receptors**. *Pharmacol Ther* 2009;**124**:195–206.
18. Al-Saif A, Al-Mohanna F, Bohlega S. **A mutation in sigma-1 receptor causes juvenile amyotrophic lateral sclerosis**. *Ann Neurol*

2011;**70**:913–9.

19. Allahtavakoli M, Jarrott B. **Sigma-1 receptor ligand PRE-084 reduced infarct volume, neurological deficits, pro-inflammatory cytokines and enhanced anti-inflammatory cytokines after embolic stroke in rats**. *Brain Res Bull* 2011;**85**:219–24.
20. Tuerxun T, Numakawa T, Adachi N, Kumamaru E, Kitazawa H, Kudo M, et al. **SA4503, a sigma-1 receptor agonist, prevents cultured cortical neurons from oxidative stress-induced cell death via suppression of MAPK pathway activation and glutamate receptor expression**. *Neurosci Lett* 2010;**469**:303–8.
21. Ajmo CT Jr., Vernon DOL, Collier L, Pennypacker KR, Cuevas J. **Sigma receptor activation reduces infarct size at 24 hours after permanent middle cerebral artery occlusion in rats**. *Curr Neurovasc Res* 2006;**3**:89–98.
22. Mancuso R, Oliván S, Rando A, Casas C, Osta R, Navarro X. **Sigma-1R Agonist Improves Motor Function and Motoneuron Survival in ALS Mice**. *Neurotherapeutics* 2012;**9**:814–26.
23. Porquet D, Casadesús G, Bayod S, Vicente A, Canudas AM, Vilaplana J, Pelegrí C, Sanfeliu C, Camins A, Pallás M, del Valle J. **Dietary resveratrol prevents Alzheimer's markers and increases life span in SAMP8**. *Age (Dordr)* 2013;**35**:1851–65.
24. Wu Y, Li X, Zhu JX, Xie W, Le W, Fan Z, Jankovic J, Pan T. **Resveratrol-activated AMPK/SIRT1/Autophagy in cellular models of parkinson's disease**. *Neurosignals* 2011;**19**:163–74.
25. Liu C, Shi Z, Fan L, Zhang C, Wang K, Wang B. **Resveratrol improves neuron protection and functional recovery in rat model of spinal cord injury**. *Brain Res* 2011;**1374**:100–9.
26. Wang L-M, Wang Y-J, Cui M, Luo W-J, Wang X-J, Barber PA, et al. **A dietary polyphenol resveratrol acts to provide neuroprotection in recurrent stroke models by regulating AMPK and SIRT1 signaling, thereby reducing energy requirements during ischemia**. *Eur J Neurosci* 2013;**37**:1669–81.
27. Wang J, Zhang Y, Tang L, Zhang N, Fan D. **Protective effects of resveratrol through the up-regulation of SIRT1 expression in the mutant hSOD1-G93A-bearing motor neuron-like cell culture model of amyotrophic lateral sclerosis**. *Neurosci Lett* 2011;**503**:250–5.
28. Kim D, Nguyen MD, Dobbin MM, Fischer A, Sananbenesi F, Rodgers JT, Delalle I, Baur JA, Sui G, Armour SM. **SIRT1 deacetylase protects against neurodegeneration in models for Alzheimer's disease and amyotrophic lateral sclerosis**. *EMBO J* 2007;26:3169–79.
29. Price NL, Gomes AP, Ling AJY, Duarte FV, Martin-Montalvo A, North BJ, Agarwal B, Ye L, Ramadori G, Teodoro JD, Hubbard BP, Varela AT, Davis JG, Veramini B, Hafner A, Moaddel R, Rolo AP, Coppari R, Palmeira CM, del Cabo R, Baur JA, Sinclair DA. **SIRT1 is required for AMPK activation and the beneficial effects of resveratrol on mitochondrial function.** *Cell Metabolism* 2012;**15**:675–90.
30. Park S-J, Ahmad F, Philp A, Baar K, Williams T, Luo H, Ke H, Rehmann H, Taussing R, Brown AL, Kim MK, Beaven MA, Burgin AB, Manganiello V, Chung JH. **Resveratrol ameliorates aging-related metabolic phenotypes by inhibiting cAMP phosphodiesterases**. *Cell* 2012;**148**:421–33.
31. Lee IH, Cao L, Mostoslavsky R, Lombard DB, Liu J, Bruns NE, Tsokos M, Alt FW, Finkel T. **A role for the NAD-dependent deacetylase Sirt1 in the regulation of autophagy**. *Proc Natl Acad Sci USA* 2008;**105**:3374–9.
32. Mancuso R, del Valle J, Modol L, Martinez A, Granado-Serrano AB, Ramirez-Núñez O, Pallás M, Portero-Otin M, Osta R, Navarro X. **Resveratrol improves motoneuron function and extends survival in SOD1^{G93A} ALS mice**. *Neutotherapeutics* 2014; in press.
33. Ferraiuolo L, Higginbottom A, Heath PR, Barber SC, Greenald D, Kirby J, Shaw PJ. **Dysregulation of astrocyte-motoneuron cross-talk in mutant superoxide dismutase 1-related amyotrophic lateral sclerosis**. *Brain* 2011;**134**:2627–41.
34. Pasinelli P, Brown RH. **Molecular biology of amyotrophic lateral sclerosis: insights from genetics**. *Nat Rev Neurosci* 2006;**7**:710–23.
35. Rege SD, Kumar S, Wilson DN, Tamura L, Geetha T, Mathews ST, Huggins KW, Broderick TL, Babu JR. **Resveratrol protects the brain of obese mice from oxidative damage**. *Oxid Med Cell Long* 2013; **4**;1-7.
36. Mancuso R, Santos-Nogueira E, Osta R, Navarro X. **Electrophysiological analysis of a murine model of motoneuron disease**. *Clin Neurophysiol* 2011;**122**:1660–70.
37. Navarro X, Krueger TB, Lago N, Micera S, Stieglitz T, Dario P. **A critical review of interfaces with the peripheral nervous system for the control of neuroprostheses and hybrid bionic systems**. *J Peripher Nerv Syst* 2005;**10**:229–58.
38. Brooks SP, Dunnett SB. **Tests to assess motor**

phenotype in mice: a user's guide. *Nat Rev Neurosci* 2009;**10**:519–29.

39. Mancuso R, Oliván S, Osta R, Navarro X. **Evolution of gait abnormalities in SOD1(G93A) transgenic mice**. *Brain Res* 2011;**1406**:65–73.
40. Penas C, Casas C, Robert I, Forés J, Navarro X. **Cytoskeletal and activity-related changes in spinal motoneurons after root avulsion**. *J Neurotrauma* 2009;**26**:763–79.
41. Fischer LR, Culver DG, Tennant P, Davis AA, Wang M, Castellano-Sanchez A, Khan J, Polak MA, Glass JD. **Amyotrophic lateral sclerosis is a distal axonopathy: evidence in mice and man**. *Exp Neurol* 2004;**185**:232–40.
42. McHanwell S, Biscoe TJ. **The localization of motoneurons supplying the hindlimb muscles of the mouse**. *Philos Trans R Soc Lond, B, Biol Sci* 1981;**293**:477–508.
43. Guzmán-Lenis M-S, Navarro X, Casas C. **Selective sigma receptor agonist 2-(4-morpholinethyl)1-phenylcyclohexanecarboxylate (PRE084) promotes neuroprotection and neurite elongation through protein kinase C (PKC) signaling on motoneurons**. *Neuroscience* 2009;**162**:31–8.
44. Grosskreutz J, Van Den Bosch L, Keller BU. **Calcium dysregulation in amyotrophic lateral sclerosis**. *Cell Calcium* 2010;**47**:165–74.
45. Van Den Bosch L, Van Damme P, Bogaert E, Robberecht W. **The role of excitotoxicity in the pathogenesis of amyotrophic lateral sclerosis**. *BBA - Molecular Basis of Disease* 2006;**1762**:1068–82.
46. Alexianu ME, Ho BK, Mohamed AH, La Bella V, Smith RG, Appel SH. **The role of calcium-binding proteins in selective motoneuron vulnerability in amyotrophic lateral sclerosis**. *Ann Neurol* 1994;**36**:846–58.
47. Balasuriya D, Stewart AP, Edwardson JM. **The σ-1 receptor interacts directly with GluN1 but not GluN2A in the GluN1/GluN2A NMDA receptor**. *J Neurosci* 2013;**33**:18219–24.
48. Amer MS, McKeown L, Tumova S, Liu R, Seymour VAL, Wilson LA, Naylor J, Greenhalgh K, Hou B, Majeed Y, Turner P, Sedo A, O'Regan DJ, Li J, Bon RS, Porter KE, Beech DJ. **Inhibition of endothelial cell Ca^{2+} entry and transient receptor potential channels by Sigma-1 receptor ligands**. *British J Pharmacol* 2013;**168**:1445–55.
49. Kourrich S, Hayashi T, Chuang J-Y, Tsai S-Y, Su T-P, Bonci A. **Dynamic interaction between sigma-1 receptor and Kv1.2 shapes neuronal and behavioral responses to cocaine**. *Cell* 2013;**152**:236–47.
50. Mavlyutov TA, Epstein ML, Verbny YI, Huerta MS, Zaitoun I, Ziskind-Conhaim L, Ruoho AE. **Lack of sigma-1 receptor exacerbates ALS progression in mice**. *Neuroscience* 2013;**240**:129–34.
51. Mori T, Hayashi T, Hayashi E, Su T-P. **Sigma-1 receptor chaperone at the ER-mitochondrion interface mediates the mitochondrion-ER-nucleus signaling for cellular survival**. *PLoS ONE* 2013;**8**:e76941.
52. Hayashi T, Hayashi E, Fujimoto M, Sprong H, Su T-P. **The lifetime of UDP-galactose:ceramide galactosyltransferase is controlled by a distinct endoplasmic reticulum-associated degradation (ERAD) regulated by sigma-1 receptor chaperones**. *J Biol Chem* 2012;**287**:43156–69.
53. Marriott K-SC, Prasad M, Thapliyal V, Bose HS. **σ-1 receptor at the mitochondrial-associated endoplasmic reticulum membrane is responsible for mitochondrial metabolic regulation**. *J Pharmacol Exp Ther* 2012;**343**:578–86.
54. Herskovits AZ, Guarente L. **Sirtuin deacetylases in neurodegenerative diseases of aging**. *Cell Res* 2013;**23**:746–58.
55. Fonseca-Kelly Z, Nassrallah M, Uribe J, Khan RS, Dine K, Dutt M, Shindler KS. **Resveratrol neuroprotection in a chronic mouse model of multiple sclerosis**. *Front Neurol* 2012;**3**:84.
56. Nimmagadda VK, Bever CT, Vattikunta NR, Talat S, Ahmad V, Nagalla NK, Trisler D, Judge SIV, Royal W, Chandrasekaran K, Russel JW, Makar TP. **Overexpression of SIRT1 protein in neurons protects against experimental autoimmune encephalomyelitis through activation of multiple SIRT1 targets**. *J Immunol* 2013;**190**:4595–607.
57. Maher P, Dargusch R, Bodai L, Gerard PE, Purcell JM, Marsh JL. **ERK activation by the polyphenols fisetin and resveratrol provides neuroprotection in multiple models of Huntington's disease**. *Hum Mol Genet* 2010;**20**:261–70.
58. Albani D, Polito L, Signorini A, Forloni G. **Neuroprotective properties of resveratrol in different neurodegenerative disorders**. *BioFactors* 2010;**36**:370–6.
59. Jin F, Wu Q, Lu Y-F, Gong Q-H, Shi J-S. **Neuroprotective effect of resveratrol on 6-OHDA-induced Parkinson's disease in rats**. *Eur J Pharmacol* 2008;**600**:78–82.
60. Araki T, Sasaki Y, Milbrandt J. **Increased**

nuclear NAD biosynthesis and SIRT1 activation prevent axonal degeneration. *Science* 2004;**305**:1010–3.

61. Zhang F, Liu J, Shi J-S. **Anti-inflammatory activities of resveratrol in the brain: role of resveratrol in microglial activation**. *Eur J Pharmacol* 2010;**636**:1–7.
62. Bi XL, Yang JY, Dong YX, Wang JM, Cui YH, Ikeshima T, Zhao YQ, Wu CF. **Resveratrol inhibits nitric oxide and TNF-alpha production by lipopolysaccharide-activated microglia**. *Int Immunopharmacol* 2005;**5**:185–93.
63. Candelario-Jalil E, de Oliveira A, Gräf S, Bhatia HS, Hüll M, Muñoz E, Fiebich BL. **Resveratrol potently reduces prostaglandin E2 production and free radical formation in lipopolysaccharide-activated primary rat microglia**. *J Neuroinflamm* 2007;**4**:25.
64. Meng X-L, Yang JY, Chen G-L, Wang L-H, Zhang L-J, Wang S, Li J, Wu CF. **Effects of resveratrol and its derivatives on lipopolysaccharide-induced microglial activation and their structure-activity relationships**. *Chem Biol Interact* 2008;**174**:51–9.
65. Wang FM, Galson DL, Roodman GD, Ouyang H. **Resveratrol triggers the pro-apoptotic endoplasmic reticulum stress response and represses pro-survival XBP1 signaling in human multiple myeloma cells**. *Exp Hematol* 2011;**39**:999-1006.
66. Azzouz M, Leclerc N, Gurney M, Warter JM, Poindron P, Borg J. **Progressive motor neuron impairment in an animal model of familial amyotrophic lateral sclerosis**. *Muscle Nerve* 1997;**20**:45–51.
67. Scott S, Kranz JE, Cole J, Lincecum JM, Thompson K, Kelly N, Bostrom A, Theodoss J, Al Nakhala BM, Vieira FG, Ramasubbu J, Heywood JA. **Design, power, and interpretation of studies in the standard murine model of ALS**. *Amyotroph Lateral Scler* 2008;**9**:4–15.

Discussion

General discussion

Motoneuron vulnerability in ALS

ALS, the most frequent form of MND in adult humans, consists in a degenerative process in which lower and upper MNs are selectively vulnerable, but interestingly some groups of MNs are relatively resistant to the disease process. A consistent clinical feature of ALS is the preservation of eye movements and external sphincters function. Pathological studies confirmed that there is relative sparing of the cranial motor nuclei of the oculomotor, trochlear and abducens nerves, and of Onuf's nucleus in the sacral spinal cord, which innervates the external sphincters of the pelvic floor (Mannen et al., 1977). Although neuronal numbers are relatively well-preserved in these resistant motor nuclei, some pathological changes resembling those observed in anterior spinal cord cells are present, but to a lesser degree (Okamoto et al., 1993a; 1991). In fact, in mSOD1 overexpressing mouse models oculomotor nuclei are also relatively spared (Nimchinsky et al., 2000). The oculomotor nucleus innervates four of the six extraocular muscles, which display a distinct phenotype, gene expression profile (Porter et al., 2001) and disease responsiveness (Porter and Baker, 1996). They have a unique composition of six fiber types, distinct from other skeletal muscles, some with very high mitochondrial content and marked fatigue resistance. Such differences may be determined by their distinct embryonic origin, or by demands imposed by the relative complexity of oculomotor control systems, and the specific discharge patterns of oculomotor neurons (Porter, 2002). Motor unit discharge patterns are a key determinant of skeletal muscle properties, and extraocular muscles and oculomotor neurons interact in a highly specific manner: explants of neonatal extraocular muscle grown in co-culture with incorrect spinal MNs die faster than those grown with oculomotor neurons (Porter and Hauser, 1993). The pattern of innervation of extraocular muscles is different from other skeletal muscles. Neuromuscular junctions are distributed throughout the fiber length at a higher density (Harrison et al., 2007), and show some structural peculiarities (Khanna et al., 2003). About 20% of the extraocular muscles fibers are innervated by multiple neuromuscular junctions (Pachter, 1983). Oculomotor motor units are amongst the smallest seen in any skeletal muscle (Porter et al., 2001), with high MN discharge rates. Even in the primary position of gaze, 70% oculomotor neurons are active, commonly discharging at 100 Hz (Robinson, 1970). This level of activity would be predicted to require a significant metabolic demand on the neuron. It is likely that understanding the differences in properties of vulnerable vs. resistant MNs may provide insights into the mechanisms of neuronal

degeneration, and identify targets for therapeutic manipulation.

Why some MNs are particularly affected is not completely understood. One proposed explanation of their specific vulnerability could lie in aspects of their structural and metabolic specialization (Shaw and Eggett, 2000). MNs are unusually large neurons, with cell bodies of approximately 50–60 μm and axons of up to 1 m long in humans, which requires a high metabolic input. These demands may leave the MNs more prone to oxidative stress because of the high-energy demand that is met by the mitochondria, with the side effect of increased ROS production. This could result in a vicious cycle of increased ROS generation and decreased mitochondrial efficiency (Barber and Shaw, 2010). MNs express lower levels of cytosolic calcium-binding proteins compared to other neuronal populations, with MN populations that are typically lost earlier during the disease course showing the lowest expression levels, suggesting that reduced cytosolic calcium buffering contributes to the selective vulnerability of MNs (Appel et al., 2001; Reiner et al., 1995). In fact, ALS-vulnerable spinal and brainstem MNs display low endogenous Ca^{2+} buffering capacity, that is 5-6 times lower than that found in ALS-resistant MNs (i.e. oculomotor MNs), making them more susceptible to excitotoxic insults (Alexianu et al., 1994). However, this view may not agree with above mentioned oculomotor motor units properties since although this MN population is highly active it is not vulnerable to ALS disease process.

In a recent publication, Brockington et al. (2012) performed a microarray analysis to compare the gene expression profile of isolated MNs from the ALS-resistant oculomotor nuclei and ALS-vulnerable spinal cord MNs from post-mortem ALS patients tissue. They found nearly 2,000 genes differentially expressed by the two MNs subtypes, participating in synaptic transmission, ubiquitin-dependent proteolysis, mitochondrial function, transcriptional regulation, immune system functions and the extracellular matrix. They further focused on glutamate and GABA neurotransmission. The AMPA glutamate receptor consists of four subunits, GluR1–GluR4, and the presence of the GluR2 subunit determines the calcium permeability of the receptor. In the absence of GluR2, the AMPA receptor–ion channel complex becomes permeable to calcium. Gene array results showed up-regulation of the GluR2 subunit in resistant oculomotor MNs relative to the vulnerable lumbar apinal MN population, thus reducing calcium influx into the cells. On the other hand, GABA is the most widely distributed inhibitory neurotransmitter in the CNS and acts through the interaction with GABA-A (ligand-gated chloride channels) and GABA-B (metabotropic) receptors. In oculomotor MNs, there is up-regulation of six GABA-A receptor subunits and of

GABA-B receptor subunit 2 relative to spinal MNs, leading to an increased inhibition. Other studies performed in mSOD1 models confirmed these findings, revealing an excitatory/inhibitory imbalance affecting spinal MN (Sunico et al., 2011).

Interestingly, Saxena et al. (2013) have recently hypothesized that the increased excitation and reduced inhibition of MNs is a protective compensatory reaction rather a detrimental phenomenon. As above mentioned, oculomotor nucleus MNs are strongly resistant to ALS degenerative process, but have particular physiological characteristics, including high discharge rates of about 100Hz (Robinson, 1970). In turn, it has been shown that vulnerable fast-fatigable spinal MNs are those with larger cell bodies and more phasic activity pattern. Surprisingly, Saxena et al. (2013) demonstrated that early administration of AMPA receptor agonist protects spinal MNs whereas AMPA receptor antagonist enhances MNs pathology in $SOD1^{G93A}$ mice. Furthermore, the authors propose that gephyrin (inhibitory synapse marker) reduction, increased serotonin labeled area in the ventral spinal cord and increased c-buttons size and number that have been extensively described are a protective compensatory reaction in order to promote MN survival.

It is also remarkable that MNs are not the only cell type affected by ALS. Recent studies performed on mSOD1 mice have shown an important loss of oligocendrocytes from early pre-symptomatic phases of disease process, together with a compensatory enhanced oligodendrocyte biogenesis (Kang et al., 2013). In contrast, there are no evidences of astrocytes and microglial cells death during ALS disease progression probably because these cell populations present strong proliferation that translate into a gain in number of cells. Focusing on neuronal populations, other kind of neurons have been also reported to degenerate during ALS, such as spinal calbindin positive Renshaw cells. Renshaw cells are glycinergic inhibitory interneurons localized in the spinal lamina VII that play an important role in the recurrent inhibition. Loss of glycinergic synaptic contacts onto MNs and posterior Renshaw cells death have been described in $mSOD1^{G93A}$ mice (Chang and Martin, 2009; 2011; Mòdol et al., 2014).

$SOD1^{G93A}$ mouse model characterization: developing reliable, objective disease markers

One of the most important problems regarding the development of new therapies for ALS is the failure to translate positive experimental results into successful human trials (Benatar, 2007; Rothstein, 2003). This fact may raise concerns about the validity of ALS animal models but it also may be related to methodological shortcomings. Thus, it is of importance to develop and apply

techniques that provide reliable, objective preclinical results. However, few studies have focused on developing new tools that permit the correct interpretation of the findings from preclinical studies. General guidelines have been agreed through international consensus for the behavioral and histological evaluation of animal research on ALS/MND (Ludolph et al., 2010; 2007). Briefly, an optimal experimental design must include an onset measure, a quantitative measure of disease progression, a survival analysis and MN counts. Unfortunately, the classical techniques used for these purposes might not be up to the task. First, clinical disease onset and progression are usually analyzed using rotarod and hangwire tests, and sometimes, arbitrary neurological scores. However, these methods are not specific enough and may be biased due to behavioral effects (e. g. animals need to be trained regularly to learn the task properly and their performance depends on individual behavior) and researcher's subjectivity. Second, survival analysis is mandatory for preclinical study publication. However, there is lack of inter-laboratory reproducibility. It has been shown how genetic background affects $SOD1^{G93A}$ mice survival (Heiman-Patterson et al., 2005; 2011; Mancuso et al., 2012a). These observations, together with the ethical concerns raised by the survival analysis itself might compromise preclinical studies based on survival. The main goal of the chapter 1 of this thesis was to characterize the $SOD1^{G93A}$ mouse model of ALS to develop reliable, objective markers of disease progression and to evaluate the potential usefulness of new therapies.

In the first part of chapter I we focused on the electrophysiological characterization of $SOD1^{G93A}$ mice since electrophysiological tests are the most clinically relevant for diagnosis and monitoring of ALS patients (Inghilleri and Iacovelli, 2011; Wijesekera and Leigh, 2009). Several authors have used these techniques in the $SOD1^{G93A}$ rodents but, in most cases, only focusing on the analysis of lower MN function (Azzouz et al., 1997; Kennel et al., 1996; Shefner et al., 2006) and on several occasions using methods that do not allow a time follow-up of the same animal (Gordon et al., 2010; Hegedus et al., 2009; 2008). We provided a detailed electrophysiological profile of the $SOD1^{G93A}$ transgenic mouse model of ALS by evaluating both lower and upper MN function from early pre-symptomatic (4 weeks) to end stage of the disease (16 weeks) by means of nerve conduction and evoked potential tests. The results revealed dysfunction of lower MNs that progresses from proximal to distal muscles, evidenced by deficits in motor nerve conduction from 8 weeks of age. Moreover, the MUNE demonstrated that lower MNs lose muscle innervation and had a deficit in their sprouting capacity. The study of MEPs showed that, in parallel to peripheral deficits, there is a dysfunction in central motor conduction in $SOD1^{G93A}$ mice starting later, at 12 weeks. In parallel, we demonstrated that locomotor impairments assessed by rotarod began at 12-13

weeks, coincident with noticeable MN loss in the anterior lumbar spinal cord. These results provide important information about the SOD1^{G93A} transgenic mouse, as they demonstrate for the first time that dysfunction of central motor pathways is coexisting with spinal motor deficits, and both are detected well before the loss of spinal MN cell bodies or the first functional evidences appear (by 12-13 weeks of age). The finding of a concomitant dysfunction of upper and lower MNs contributes to the validation of the SOD1^{G93A} mouse as a useful model of ALS, because this double contribution is an essential condition for ALS diagnosis in patients. We also demonstrated that non-invasive electrophysiological studies can be applied in experimental models, as wells as in the clinic, for the early detection of dysfunctions in MNDs, and as precise markers to assess the functional efficacy of new potential treatments at the experimental level.

In the second part of chapter I, we focused on the characterization of SOD1^{G93A} mice locomotion to investigate whether loss of neuromuscular connections evidenced by electrophysiological recordings was translated to impairments of locomotor performance. Historically, locomotor performance of SOD1^{G93A} mice has been evaluated using the rotarod test as one of the primary measures of disease progression and its modification by therapeutical strategies (Alves et al., 2011; Gurney et al., 1994; Klivenyi et al., 1999; Miana-Mena et al., 2005; Ralph et al., 2005). Motor deficits detected by rotarod begin at 12-13 weeks of age and progress rapidly until complete hindlimb paralysis at 16-18 weeks, thus providing a relatively narrow time frame for detecting possible changes. In fact, the rotarod test is not sufficiently sensitive to detect motor deficits in SOD1^{G93A} mice despite histological and electrophysiological evidences demonstrating earlier motor abnormalities (Azzouz et al., 1997; Fischer et al., 2004; Kennel et al., 1996; Mancuso et al., 2011). Moreover, the rotarod test is not always able to reveal treatment-derived functional improvements, even when the treatment applied improves the condition of the animals or increases the survival of MNs (Fischer et al., 2005). For these reasons, in this part of the study we evaluated fine locomotor performance of SOD1^{G93A} mice by using a digital video system that captures paw placement during treadmill locomotion and calculates standardized gait parameters (DigiGait^{TM}, Mouse Specifics Inc.). Our goal was to determine whether locomotor abnormalities could be detected early in the disease, prior to onset of overt symptoms, as well as during symptomatic and end-stage disease. Our results provide novel information about the onset and progression of gait abnormalities in SOD1^{G93A} mice. Focusing on hindlimbs, there was an early (8 weeks of age) enlargement of stance duration mainly due to an increase of the propulsion phase duration of about 10% that progressed along the course of the disease. These findings agree with previous

observations by Wooley et al. (2005) who already noticed an increase in the stance duration in 8-weeks-old SOD1^{G93A} compared to wild type mice. Locomotor alterations progressed during the disease until complete disturbance of the normal gait pattern. Interestingly, the early dysfunction of hindlimb function correlates with early abnormalities of motor nerve conduction that we observed in the electrophysiological characterization (Mancuso et al., 2011). These findings are meaningful to the field because the identification of significant differences in a functional endpoint as early as 8 weeks may be a step forward resolving the debate about treating the mice prior to "symptoms onset" in efficacy studies. Our results also point out that digitizing analysis of treadmill locomotion may be used as a valuable tool to evaluate whether new therapeutic approaches are improving the functional outcome of the animals.

We then performed an analysis of the potential predictive value of electrophysiological tests as a marker of clinical disease onset and progression in the SOD1^{G93A} model of ALS. As previously commented, the development of new therapies for any disease implies the translation from experimental studies to human trials. In ALS, this issue has raised concerns since there has been lack of success of numerous translational findings (Benatar, 2007; Rothstein, 2003), that may be due to shortcomings in most of the currently existing techniques used in preclinical studies. To address this objective we first evaluated the accuracy of electrophysiological tests in differentiating transgenic vs. wild-type mice and then, we made a correlation analysis of electrophysiological parameters and the clinical onset of symptoms, survival and number of spinal MNs. The results from this part of the present thesis indicate that early pre-symptomatic electrophysiological tests demonstrated great accuracy in differentiating transgenic vs. wild type animals, which was especially notable for the TA CMAP amplitude. The TA CMAP amplitude recorded from 10 weeks of age correlated significantly with both clinical disease onset and survival. The survival prediction of the electrophysiological results increased at the end stage of the disease, when it was also correlated significantly with the number of preserved MNs in the lumbar spinal cord. These findings represent an improvement in terms of animal testing during preclinical studies, since electrophysiological tests are easily performed, they are objective, they show small variability and they can be directly translated to the clinical field.

As a proof of concept that nerve conduction studies and locomotion tests were capable of detecting significant differences between variations in the MN dysfunction and the evolution of the disease, we made a comparative study of SOD1^{G93A} mice bread on two different genetic backgrounds. The rotarod test results did not show any differences in the onset of locomotor

impairments between the two strains. However, electrophysiological results showed that the initial signs of motor impairment are notably different between strains, since B6 mice showed the first lower and upper MN dysfunctions about 2 weeks earlier than B6SJL mice. In contrast, B6SJL mice have faster course of muscle denervation once it has started than B6 mice. Our results were also useful to demonstrate that the genetic background is a relevant factor that affects both disease onset and progression in the transgenic SOD1^{G93A} animal model of ALS, as previously revised (Heiman-Patterson et al., 2011). Therefore, the timing of application of treatments and evaluation of consequent improvement should be different depending on the mouse strain used. From these results, the following studies on new therapeutic approaches made in this thesis were performed on B6SJL SOD1^{G93A} mice (Mancuso et al., 2012a).

Sigma-1R therapeutic effect on SOD1^{G93A} ALS mice

The Sigma-1R is a transmembrane protein found in the ER (Alonso et al., 2000; Hayashi and Su, 2007), highly expressed in MNs and other cells in the spinal cord (Alonso et al., 2000; Gekker et al., 2006; Palacios et al., 2003; Penas et al., 2011). In the nervous system, Sigma-1R mediates regulation of several processes, such as neuritogenesis, K^+ channels and NMDA receptors activity, Ca^{2+} homeostasis, and microglial activity. Furthermore, it is related to some CNS pathologies, including depression, schizophrenia, drug addiction, and Alzheimer's disease (Aydar et al., 2002; Hall et al., 2009; Maurice and Su, 2009; Zhang et al., 2011). Several studies have demonstrated potent therapeutic actions of Sigma-1R agonists, reducing glutamate-mediated cell death (Guzmán-Lenis et al., 2009; Tuerxun et al., 2010) or modulating the inflammatory reaction following stroke in rats (Ajmo et al., 2006; Allahtavakoli and Jarrott, 2011). Luty et al. (2010) and Al-Saif et al. (2011) recently reported a novel mutation of Sigma-1R in patients affected by ALS, suggesting that pharmacological interventions targeting this receptor could be a good therapeutic approach.

It was previously demonstrated in our laboratory that PRE-084 administration promotes neuroprotection and neurite elongation through protein kinase C (PKC) on MNs in an *in vitro* organotypic model of excitotoxic lesion (Guzmán-Lenis et al., 2009). Moreover, administration of PRE-084 prevented spinal MN death following spinal root avulsion in rats (Penas et al., 2011). Based on these previous works, the aim of chapter 2 of this thesis was to assess the potential therapeutic effect of the Sigma-1R agonist in the SOD1^{G93A} mouse model of ALS. The results indicate that daily administration of PRE-084 from 8 weeks of age significantly improved spinal

MN function, manifested by maintenance of the amplitude of muscle action potentials, improved locomotion behavior, and preserved both neuromuscular connections and MNs survival in the spinal cord. Moreover, Sigma-1R agonist prolonged survival in female and male $SOD1^{G93A}$ animals. Delayed administration of PRE-084 starting at 12 weeks of age also significantly improved functional outcome and MN preservation. Further analysis revealed that, among other possible effects, PRE-084 induced PKC-specific phosphorylation of two serines (Ser896 and 897) of the NMDA-NR1 subunit in MNs of $SOD1^{G93A}$ treated animals, and a reduction of the microglial reactivity in the spinal cord compared with untreated mice. Based on previous observations (Hall et al., 2009; Zhang et al., 2011), we hypothesized that PRE-084 may exert, at least, a dual therapeutic contribution, modulating the NMDA Ca^{2+} influx to reduce excitotoxic damage to MNs, and the microglial reactivity to ameliorate the MNs environment. Such a pluri-functional target may provide better translational outcomes than drugs that act only on one of the multiple pathophysiological mechanisms involved in ALS.

Resveratrol effect on $SOD1^{G93A}$ ALS mouse

Resveratrol (RSV, 3,5,4′-trihydroxy-trans-stilbene), a polyphenol found in grapes and red wine, has been reported to exert age-delaying and neuroprotective effects (Albani et al., 2010) in several contexts including Alzheimer's disease (Porquet et al., 2013), Parkinson's disease (Wu et al., 2011) and in traumatic (Liu et al., 2011) and ischemic injuries to the CNS (Wang et al., 2011a). It has been recently described that RSV can trigger a cascade of intracellular events that converge on Sirtuin 1 (Sirt1), AMP-activated protein kinase (AMPK) and PGC-1α, as important energy-sensing regulators (Donmez, 2012; Tennen et al., 2012). Sirt1 is a NAD^+-dependent deacetylase that has emerged as an important element of the cellular metabolic network. Its activation protects against neurodegeneration in several neurodegenerative disorders (Donmez, 2012). In fact, Sirt1 may promote neuroprotection by the modulation of several cellular pathways, such as autophagy (Jeong et al., 2013; 2012) and mitochondrial biogenesis (Price et al., 2012). On the other hand, it has been proposed that RSV works primarily by activating AMPK, which then activates Sirt1 indirectly by elevating intracellular levels of its co-substrate NAD+ (Cantó et al., 2009; Fulco et al., 2008). Alternatively, RSV may first activate Sirt1, leading to AMPK activation via deacetylation and activation of the AMPK kinase LKB1 (Hou et al., 2008; Lan et al., 2008). Previous studies showed that RSV administration protects MNs on *in vitro* ALS models (Kim et al., 2007; Wang et al., 2011a), thus the main goal of the chapter III of this thesis was to assess the potential therapeutic

effect of a RSV-enriched diet in the SOD1^{G93A} mouse model of ALS. The results of this work demonstrate that RSV exerts potent therapeutic actions in the SOD1^{G93A} model of ALS. In fact, we show for the first time a treatment that combines significant preservation of both lower and upper MN function, translating into significantly delayed disease onset and extended animal survival. These effects were associated to an important preservation of MNs and a significant reduction of microglial reactivity in the spinal cord. Molecular analyses revealed that the beneficial effects of RSV were accompanied by an enhanced activation of Sirt1 and AMPK. Such pluri-functional targets that combine the inhibition of detrimental processes and the promotion of neuroprotective pathways may provide better translational outcomes than drugs with more restricted targets.

Lack of synergistic effect of Sigma-1R and resveratrol co-administration

The main goal of the last chapter of this thesis was to assess the effect of combining the Sigma-1R agonist PRE-084 and RSV in the SOD1^{G93A} mouse model of ALS, since separate administration of the two compounds had resulted in significant improvement of disease progression and survival of these mice (chapters II and III). The co-administration of PRE-084 and RSV from 8 weeks of age significantly preserved spinal MN function and reduced MN degeneration. This effect was accompanied by an improvement in the locomotor performance and a significant extension of animals survival. According with what we previously described in chapters II and III, PRE-084 induced PKC-specific phosphorylation of Ser896 of the NMDA-NR1 subunit, whereas RSV increased the expression and activation of Sirt1 and AMPK in the ventral part of the lumbar spinal cord of SOD1^{G93A} mice (Mancuso et al., 2012b; 2014). Unfortunately, the combinatory therapy did not represent a clear improvement compared to RSV-only or PRE-084-only treated animals.

Mechanisms underlying neuroprotection and possible overlapping effects

Consistent with our previous observations in chapter II (Mancuso et al., 2012b), we have found that PRE+RSV combined treatment also increased Ser896 phosphorylation of the NDMA-NR1 subunit in the ventral part of the spinal cord, thus modulating calcium influx into MNs (Zhang et al., 2011). Although it has been demonstrated that Sigma-1R physically interacts with NMDA-NR1 subunits (Balasuriya et al., 2013) and promote a reduction of NMDA calcium conductance (Zhang et al., 2011), it has been also reported that Sigma-1R agonists can modulate ionic flow through calcium, sodium and potassium channels, thus modifying cells excitability properties (Amer et al., 2013;

Kourrich et al., 2013; Zhang et al., 2011). In fact, recent findings by Mavlyutov et al. (2013) indicate that the lack of Sigma-1R is detrimental in SOD1^{G93A} mice probably because it acts by reducing the excitability of spinal MNs. Moreover, Sigma-1R is found associated to ER chaperones (such as BiP) and plays a role in clearance misfolded proteins by the ERAD response (Hayashi et al., 2012; Mori et al., 2013b). Sigma-1R is enriched in the so-called mitochondrial-associated ER membrane (MAM) and its activation can also modulate mitochondrial metabolism (Hayashi and Su, 2007; Marriott et al., 2012). As above mentioned, it has been reported that RSV promotes protective effects both in neurodegenerative and traumatic injury models, including Alzheimer's disease and accelerated aging (Herskovits and Guarente, 2013; Kim et al., 2007; Porquet et al., 2013), multiple sclerosis (Fonseca-Kelly et al., 2012; Nimmagadda et al., 2013), Huntington's disease (Albani et al., 2010; Maher et al., 2010), Parkinson's disease (Jin et al., 2008; Wu et al., 2011), and reducing peripheral axonal degeneration (Araki et al., 2004) or promoting functional improvements after spinal cord injury (Liu et al., 2011). In the chapter III we described how RSV administration significantly delays clinical symptoms onset, improves spinal MNs function and survival, and extends SOD1^{G93A} mice lifespan. We also determined that the therapeutic effect was mediated by the increased expression and activation of both Sirt1 and AMPK, leading to normalization of the autophagic flux and enhanced mitochondrial biogenesis (Mancuso et al., 2014a). Although there is some controversy about the exact molecular mechanisms underlying RSV effect, it has been established that Sirt1 or AMPK activation are upstream of pathways that participate in several cellular processes, including inflammation (Bi et al., 2005; Candelario-Jalil et al., 2007; Meng et al., 2008; Zhang et al., 2010), autophagy (Lee et al., 2008) and mitochondrial function (Herskovits and Guarente, 2013; Price et al., 2012). Consistent with our previous findings, PRE+RSV treated animals also presented higher expression and activation of both Sirt1 and AMPK compared to SOD1^{G93A} untreated mice.

The lack of summative effect in the PRE+RSV treated group may be due to a possible overlapping in the pathways activated by both compounds. As above mentioned (chapter III), RSV protective effect is likely related to normalization of the autophagic flux and increased mitochondrial biogenesis (Mancuso et al., 2014a). Although PRE-084 main therapeutic effects have been considered associated to modulation of calcium influx and MNs excitability (Amer et al., 2013; Kourrich et al., 2013; Mavlyutov et al., 2011; Zhang et al., 2011), it also participates on the response to misfolded protein accumulation (Hayashi and Su, 2007; Hayashi et al., 2012) and the modulation of mitochondrial metabolism (Marriott et al., 2012). Considering these actions, RSV

effects on autophagy and mitochondrial biogenesis may mask those of PRE-084 administration thus explaining the lack of summative effect of the combined treatment.

Another explanation for the lack of summative effect of the combined treatment lies in the pathology state of the animals in the moment we began the drug administration. SOD1^{G93A} mice at 8 weeks of age present 25-30% loss of CMAP amplitude in proximal muscles (TA and gastrocnemius) (Azzouz et al., 1997; Mancuso et al., 2011), due to early neuromuscular junction retraction and motor axons degeneration (Fischer et al., 2004). Thus, although MN cell bodies in the anterior spinal cord are intact, up 30% of them are already under a degenerative process that may be irreversible. Since our treatment is focused on the preservation of remaining functional MNs, it is likely that we are acting on the still functioning population of MNs and thus, the maximum effect that can be reached would be limited.

Does the SOD1^{G93A} mouse model present a limited therapeutic capacity?

An alterative explanation for the lack of summatory effect of combining PRE-084 and RSV could be that the SOD1^{G93A} mouse model has a limit in terms of MN function and survival that cannot be overpassed by therapeutic interventions. To address this possibility, we made a review of successful preclinical trials using both single and combinatorial treatments in SOD1^{G93A} mice. The following table (Table 2) summarizes the successful therapies performed on SOD1^{G93A} mice and the percentage of increased survival compared to untreated mice. It is worth noting that no replication of the positive results was achieved for several of the drugs initially reported to provide efficacy when re-tested using a careful study design (Scott et al., 2008). Up to our knowledge and without considering those works showing negative or null results, only 4 of 48 studies reported an extension of survival longer than 25%. Although further analyses must be performed, such observations may reflect an endogenous limitation for the therapeutical benefits that can be achieved using the SOD1^{G93A} mouse model.

Table 2. Summary of recent therapeutic trials performed in the SOD1^{G93A} mouse model. When dose-dependent or gender effects were described, the greatest improvement was selected.

Compound	Treatment onset	Survival extension	Reference
Oxidative stress			
M30	Pre-symptomatic	6%	(Kupershmidt et al., 2009)
Metallothionein-III	Onset	10%	(Hashimoto et al., 2011)
VK-28	Pre-symptomatic	10%	(Wang et al., 2011b)
Dispocynin	Post-symptomatic	8%	(Trumbull et al., 2012)
Apocynin		2.3%	(Trumbull et al., 2012)
Mitochondrial dysfunction			
Uridine	Pre-symptomatic	17%	(Amante et al., 2010)
Dichloroacetate	Pre-symptomatic	9%	(Miquel et al., 2012)
Excitotoxicity			
Methionine sulfoximine	Pre-symptomatic	8%	(Ghoddoussi et al., 2010)
Protein missfolding			
Immunization against mSOD1	Pre-symptomatic	6.5%	(Gros-Louis et al., 2010)
Ariloxanyl	Pre-symptomatic	16%	(Chen et al., 2012)
Cyclohexane	Pre-symptomatic	18%	(Zhang et al., 2012)
Salubrinal	Early pre-symptomatic	21.6%	(Saxena et al., 2009)
Trophic support			
Lead	Pre-symptomatic	10%	(Barbeito et al., 2010)
VEGF (AVV4-mediated)	Onset	16%	(Dodge et al., 2010)
IGF-1 (AVV4-mediated)	Onset	10%	(Dodge et al., 2010)
BDNF-TTC	Pre-symptomatic	14%	(Calvo et al., 2011)
Non-cell autonomous /inflammation			
Revlimid	Onset	12%	(Neymotin et al., 2009)
GCSF (AAV1/2-mediated)	Pre-symptomatic	10%	(Henriques et al., 2011)
Monoclonal antibodies	Pre-symptomatic	7%	(Lincecum et al., 2010)

antiCD40L			
Minocycline	Early Pre-symptomatic	8.8%	(Zhu et al., 2002)
Pegfilgastrim	Pre-symptomatic	6%	(Pollari et al., 2011)
Anti-Ly6C monoclonal antibodies	Onset	16%	(Butovsky et al., 2012)
Caffeic acid	Post-symptomatic	7%	(Fontanilla et al., 2012)
Other			
L-arginine	Early pre-symptomatic	20%	(Lee et al., 2009)
	Pre-symptomatic	9%	(Lee et al., 2009)
Activated protein C	Onset	22%	(Zhong et al., 2009)
SUN N8075	Pre-symptomatic	11%	(Shimazawa et al., 2010)
TTC	Pre-symptomatic	12%	(Moreno-Igoa et al., 2010)
Diallyl trisulfide	Onset	5%	(Guo et al., 2011)
CDDO ethylamide	Early pre-symptomatic	16%	(Neymotin et al., 2011)
	Onset	13%	(Neymotin et al., 2011)
CDDO trifluoroethylamide	Early pre-symptomatic	14%	(Neymotin et al., 2011)
	Onset	13%	(Neymotin et al., 2011)
Trichostatin A	Onset	7%	(Eitan et al., 2012)
AGS-499	Pre-symptomatic	16%	(Eitan et al., 2012)
PRE-084	Pre-symptomatic	16%	(Mancuso et al., 2012b)
Dihydrotestosterona	Pre-symptomatic	5%	(Yoo and Ko, 2012)
Bromocriptine methylase	Onset	2%	(Tanaka et al., 2011)
CPN-9	Onset	16%	(Kanno et al., 2012)
Arimoclomol	Early pre-symptomatic	22%	(Kieran et al., 2004)
	Pre-symptomatic	18%	(Kieran et al., 2004)
Multiple pathways			
Resveratrol	Pre-symptomatic	10.5%	(Mancuso et al., 2014a)
Lithium chloride	Pre-symptomatic	8%	(Ferrucci et al., 2010)
Combinatorial strategies			

VEGF+IGF-1 (AAV4-mediated)	Onset	8%	(Dodge et al., 2010)
IGF-1 (AVV2-mediated) + exercise	Early pre-symptomatic	**69.7%**	(Kaspar et al., 2005)
	Onset	**31%**	(Kaspar et al., 2005)
Minocycline + Creatine	Early pre-symptomatic	25%	(Zhang et al., 2003)
NEU2000 + Lithium chloride	Pre-symptomatic	21.5%	(Shin et al., 2007)
PBA + AEOL 10150	Onset	19%	(Petri et al., 2006)
Creatine + calecoxib	Early pre-symptomatic	**28.5%**	(Klivenyi et al., 2003)
Creatine + rafecoxib	Early pre-symptomatic	**30.5%**	(Klivenyi et al., 2003)
Resveratrol + PRE-084	Pre-symptomatic	10.8%	(Mancuso et al., 2014b)

Bold letter labels those strategies that resulted in more than 25% increased survival.

Conclusions

The main conclusions of the present thesis are:

Chapter I – SOD1^{G93A} ALS mouse model characterization:

1. In the SOD1^{G93A} transgenic mouse model, there is a dysfunction of spinal motoneurons beginning with muscle denervation and ending up with cell death. Lower motoneuron dysfunction coexists with alterations of upper motoneurons. The electrophysiological tests for peripheral and central motor conduction are useful for early detecting and temporal monitoring motor dysfunctions in the ALS mouse model.

2. The functional abnormalities of lower and upper motoneurons evidenced by conduction studies are accompanied by a significant alteration of locomotion in the SOD1^{G93A} mice. Fine locomotor disturbances are detectable by using the computerized DigiGait system from 8 weeks of age in SOD1^{G93A} mice, representing a step forward resolving the debate about treatment of the mice prior to "symptoms onset" in efficacy studies.

3. The early electrophysiological tests can predict clinical disease onset, animal survival and motoneuron preservation in SOD1^{G93A} ALS mice. Moreover, they can detect disease progression differences on distinct SOD1^{G93A} mice strains. Thereby, electrophysiological tests can be used both as early markers of the disease and to evaluate the potential influences of neuroprotective treatments.

Chapter II: Sigma-1R treatment in SOD1^{G93A} ALS mice

4. The Sigma-1R agonist, PRE-084, improves spinal motoneuron function and prevents motoneuron degeneration in SOD1^{G93A} mice, exerting, at least, a dual therapeutic contribution:

- modulation of Ca^{2+} influx through NMDA receptors to reduce excitotoxic damage to MNs, and
- reduction of microglial reactivity to ameliorate the motoneurons environment.

5. Such a pluri-functional target may provide better translational outcomes than drugs acting only on one of the multiple pathophysiological mechanisms involved in ALS. These findings have increased importance since Sigma-1R alterations have been reported in human patients, opening a novel perspective for the use of Sigma-1R agonists as new therapeutic agents for ALS.

Chapter III: Resveratrol treatment in SOD1^{G93A} ALS mice.

6. Resveratrol improves spinal motoneuron function, prevents motoneuron degeneration and extends survival in SOD1^{G93A} mice by activating Sirt1 and AMPK in the ventral spinal cord of SOD1^{G93A} mice.

7. AMPK and Sirt1 activation induces the recovery of mitochondrial function and promotes an active process of mitochondrial biogenesis.

Chapter IV: Sigma-1R modulation and resveratrol combinatory therapy

8. There is a lack of synergistic effect of PRE-084 and resveratrol co-administration that may be due to:

- possible overlapping in the pathways activated by both compounds,
- the time point when the treatment begun given that a high proportion of motoneurons were already suffering from the degenerative process, or
- intrinsic limitations of the SOD1^{G93A} mouse model itself.

References

Abe, K., Fujimura, H., Kobayashi, Y., Fujita, N., and Yanagihara, T. (1997). Degeneration of the pyramidal tracts in patients with amyotrophic lateral sclerosis. A premortem and postmortem magnetic resonance imaging study. J Neuroimaging *7*, 208–212.

Ajmo, C.T., Jr., Vernon, D.O.L., Collier, L., Pennypacker, K.R., and Cuevas, J. (2006). Sigma receptor activation reduces infarct size at 24 hours after permanent middle cerebral artery occlusion in rats. Curr Neurovasc Res *3*, 89–98.

Al-Saif, A., Al-Mohanna, F., and Bohlega, S. (2011). A mutation in sigma-1 receptor causes juvenile amyotrophic lateral sclerosis. Ann Neurol *70*, 913–919.

Albani, D., Polito, L., Signorini, A., and Forloni, G. (2010). Neuroprotective properties of resveratrol in different neurodegenerative disorders. BioFactors *36*, 370–376.

Alexander, G.M., Erwin, K.L., Byers, N., Deitch, J.S., Augelli, B.J., Blankenhorn, E.P., and Heiman-Patterson, T.D. (2004). Effect of transgene copy number on survival in the G93A SOD1 transgenic mouse model of ALS. Mol Brain Res. *130*, 7–15.

Alexianu, M.E., Ho, B.K., Mohamed, A.H., La Bella, V., Smith, R.G., and Appel, S.H. (1994). The role of calcium-binding proteins in selective motoneuron vulnerability in amyotrophic lateral sclerosis. Ann Neurol *36*, 846–858.

Allahtavakoli, M., and Jarrott, B. (2011). Sigma-1 receptor ligand PRE-084 reduced infarct volume, neurological deficits, pro-inflammatory cytokines and enhanced anti-inflammatory cytokines after embolic stroke in rats. Brain Res Bull *85*, 219–224.

Allen, M.J., Lacroix, J.J., Ramachandran, S., Capone, R., Whitlock, J.L., Ghadge, G.D., Arnsdorf, M.F., Roos, R.P., and Lal, R. (2011). Mutant SOD1 forms ion channel: Implications for ALS pathophysiology. Neurobiol Dis 1–8.

Alonso, G., Phan, V.-L., Guillemain, I., Saunier, M., Legrand, A., Anoal, M., and Maurice, T. (2000). Immunocytochemical localization of the sigma1 receptor in the adult rat central nervous system. Neuroscience *97*, 155–170.

Alves, C.J., de Santana, L.P., Santos, dos, A.J.D., de Oliveira, G.P., Duobles, T., Scorisa, J.M., Martins, R.S., Maximino, J.R., and Chadi, G. (2011). Early motor and electrophysiological changes in transgenic mouse model of amyotrophic lateral sclerosis and gender differences on clinical outcome. Brain Res *1394*, 90–104.

Amante, D.J., Kim, J., Carreiro, S.T., Cooper, A.C., Jones, S.W., Li, T., Moody, J.P., Edgerly, C.K., Bordiuk, O.L., Cormier, K., et al. (2010). Uridine ameliorates the pathological phenotype in transgenic G93A-ALS mice. Amyotroph Lateral Scler *11*, 520–530.

Amer, M.S., McKeown, L., Tumova, S., Liu, R., Seymour, V.A.L., Wilson, L.A., Naylor, J., Greenhalgh, K., Hou, B., Majeed, Y., et al. (2013). Inhibition of endothelial cell Ca^{2+} entry and transient receptor potential channels by Sigma-1 receptor ligands. British J Pharmacol *168*, 1445–1455.

Angelov, D.N., Waibel, S., Guntinas-Lichius, O., Lenzen, M., Neiss, W.F., Tomov, T.L., Yoles, E., Kipnis, J., Schori, H., Reuter, A., et al. (2003). Therapeutic vaccine for acute and chronic motor neuron diseases: implications for amyotrophic lateral sclerosis. Proc Natl Acad Sci USA *100*, 4790–4795.

Appel, S.H., Beers, D.R., Siklos, L., Engelhardt, J.I., and Mosier, D.R. (2001). Calcium: the Darth Vader of ALS. Amyotroph Lateral Scler Other Motor Neuron Disord *2 Suppl 1*, S47–S54.

Araki, T., Sasaki, Y., and Milbrandt, J. (2004). Increased nuclear NAD biosynthesis and SIRT1 activation prevent axonal degeneration. Science *305*, 1010–1013.

Arundine, M., and Tymianski, M. (2003). Molecular mechanisms of calcium-dependent neurodegeneration in excitotoxicity. Cell Calcium *34*, 325–337.

Ash, P.E.A., Bieniek, K.F., Gendron, T.F., Caulfield, T., Lin, W.-L., DeJesus-Hernandez, M., van Blitterswijk, M.M., Jansen-West, K., Paul, J.W., Rademakers, R., et al. (2013). Unconventional translation of C9ORF72 GGGGCC expansion generates insoluble polypeptides specific to

c9FTD/ALS. Neuron *77*, 639–646.
Atkin, J.D., Farg, M.A., Turner, B.J., Tomas, D., Lysaght, J.A., Nunan, J., Rembach, A., Nagley, P., Beart, P.M., Cheema, S.S., et al. (2006). Induction of the unfolded protein response in familial amyotrophic lateral sclerosis and association of protein-disulfide isomerase with superoxide dismutase 1. J Biol Chem *281*, 30152–30165.
Atkin, J.D., Farg, M.A., Walker, A.K., McLean, C., Tomas, D., and Horne, M.K. (2008). Endoplasmic reticulum stress and induction of the unfolded protein response in human sporadic amyotrophic lateral sclerosis. Neurobiol Dis *30*, 400–407.
Aydar, E., Palmer, C.P., Klyachko, V.A., and Jackson, M.B. (2002). The sigma receptor as a ligand-regulated auxiliary potassium channel subunit. Neuron *34*, 399–410.
Azzouz, M., Hottinger, A., Paterna, J.C., Zurn, A.D., Aebischer, P., and Büeler, H. (2000). Increased motoneuron survival and improved neuromuscular function in transgenic ALS mice after intraspinal injection of an adeno-associated virus encoding Bcl-2. Hum Mol Genet *9*, 803–811.
Azzouz, M., Leclerc, N., Gurney, M., Warter, J.M., Poindron, P., and Borg, J. (1997). Progressive motor neuron impairment in an animal model of familial amyotrophic lateral sclerosis. Muscle Nerve *20*, 45–51.
Azzouz, M., Ralph, G.S., Storkebaum, E., Walmsley, L.E., Mitrophanous, K.A., Kingsman, S.M., Carmeliet, P., and Mazarakis, N.D. (2004). VEGF delivery with retrogradely transported lentivector prolongs survival in a mouse ALS model. Nature *429*, 413–417.
Balasuriya, D., Stewart, A.P., and Edwardson, J.M. (2013). The σ-1 receptor interacts directly with GluN1 but not GluN2A in the GluN1/GluN2A NMDA receptor. J Neurosci *33*, 18219–18224.
Barbeito, A.G., Martinez-Palma, L., Vargas, M.R., Pehar, M., Mañay, N., Beckman, J.S., Barbeito, L.H., and Cassina, P. (2010). Lead exposure stimulates VEGF expression in the spinal cord and extends survival in a mouse model of ALS. Neurobiol Dis *37*, 574–580.
Barber, S.C., and Shaw, P.J. (2010). Oxidative stress in ALS: key role in motor neuron injury and therapeutic target. Free Rad Biol Med *48*, 629–641.
Benatar, M. (2007). Lost in translation: treatment trials in the SOD1 mouse and in human ALS. Neurobiol Dis *26*, 1–13.
Bi, X.L., Yang, J.Y., Dong, Y.X., Wang, J.M., Cui, Y.H., Ikeshima, T., Zhao, Y.Q., and Wu, C.F. (2005). Resveratrol inhibits nitric oxide and TNF-alpha production by lipopolysaccharide-activated microglia. Int Immunopharmacol *5*, 185–193.
Blanquer, M., Moraleda, J.M., Iniesta, F., Gómez Espuch, J., Meca Lallana, J., Villaverde, R., Pérez Espejo, M.Á., Ruíz López, F.J., García Santos, J.M., and Bleda, P. (2012). Neurotrophic bone marrow cellular nests prevent spinal motoneuron degeneration in amyotrophic lateral sclerosis patients: a pilot safety study. Stem Cells *30*, 1277–1285.
Bogdanov, M., Brown, R.H., Jr, Matson, W., Smart, R., Hayden, D., O'Donnell, H., Flint Beal, M., and Cudkowicz, M. (2000). Increased oxidative damage to DNA in ALS patients. Free Rad Biol Med *29*, 652–658.
Boillee, S., VANDEVELDE, C., and CLEVELAND, D. (2006a). ALS: A Disease of Motor Neurons and Their Nonneuronal Neighbors. Neuron *52*, 39–59.
Boillee, S., Yamanaka, K., Lobsiger, C.S., Copeland, N.G., Jenkins, N.A., Kassiotis, G., Kollias, G., and Cleveland, D.W. (2006b). Onset and progression in inherited ALS determined by motor neurons and microglia. Science *312*, 1389–1392.
Borasio, G.D., Robberecht, W., Leigh, P.N., Emile, J., Guiloff, R.J., Jerusalem, F., Silani, V., Vos, P.E., Wokke, J.H., and Dobbins, T. (1998). A placebo-controlled trial of insulin-like growth factor-I in amyotrophic lateral sclerosis. European ALS/IGF-I Study Group. Neurology *51*, 583–586.
Bosco, D.A., Lemay, N., Ko, H.K., Zhou, H., Burke, C., Kwiatkowski, T.J., Sapp, P., McKenna-

Yasek, D., Brown, R.H., and Hayward, L.J. (2010a). Mutant FUS proteins that cause amyotrophic lateral sclerosis incorporate into stress granules. Hum Mol Genet *19*, 4160–4175.

Bosco, D.A., Morfini, G., Karabacak, N.M., Song, Y., Gros-Louis, F., Pasinelli, P., Goolsby, H., Fontaine, B.A., Lemay, N., McKenna-Yasek, D., et al. (2010b). Wild-type and mutant SOD1 share an aberrant conformation and a common pathogenic pathway in ALS. Nat Neurosci *13*, 1396–1403.

Braun, R.J., Sommer, C., Carmona-Gutierrez, D., Khoury, C.M., Ring, J., Büttner, S., and Madeo, F. (2011). Neurotoxic 43-kDa TAR DNA-binding protein (TDP-43) triggers mitochondrion-dependent programmed cell death in yeast. J Biol Chem *286*, 19958–19972.

Brettschneider, J., Van Deerlin, V.M., Robinson, J.L., Kwong, L., Lee, E.B., Ali, Y.O., Safren, N., Monteiro, M.J., Toledo, J.B., Elman, L., et al. (2012). Pattern of ubiquilin pathology in ALS and FTLD indicates presence of C9ORF72 hexanucleotide expansion. Acta Neuropathol *123*, 825–839.

Breuer, A.C., Lynn, M.P., Atkinson, M.B., Chou, S.M., Wilbourn, A.J., Marks, K.E., Culver, J.E., and Fleegler, E.J. (1987). Fast axonal transport in amyotrophic lateral sclerosis: an intra-axonal organelle traffic analysis. Neurology *37*, 738–748.

Bristol, L.A., and Rothstein, J.D. (1996). Glutamate transporter gene expression in amyotrophic lateral sclerosis motor cortex. Ann Neurol *39*, 676–679.

Brockington, A., Ning, K., Heath, P.R., Wood, E., Kirby, J., Fusi, N., Lawrence, N., Wharton, S.B., Ince, P.G., and Shaw, P.J. (2012). Unravelling the enigma of selective vulnerability in neurodegeneration: motor neurons resistant to degeneration in ALS show distinct gene expression characteristics and decreased susceptibility to excitotoxicity. Acta Neuropathol *125*, 95–109.

Bromberg, M.B., and Brownell, A.A. (2008). Motor unit number estimation in the assessment of performance and function in motor neuron disease. Phys Med Rehabil Clin N Am *19*, 509–32–ix.

Brooks, B.R., Miller, R.G., Swash, M., Munsat, T.L., World Federation of Neurology Research Group on Motor Neuron Diseases (2003). El Escorial revisited: revised criteria for the diagnosis of amyotrophic lateral sclerosis. pp. 293–299.

Browne, S.E., Yang, L., DiMauro, J.-P., Fuller, S.W., Licata, S.C., and Beal, M.F. (2006). Bioenergetic abnormalities in discrete cerebral motor pathways presage spinal cord pathology in the G93A SOD1 mouse model of ALS. Neurobiol Dis *22*, 599–610.

Bruijn, L.I., Houseweart, M.K., Kato, S., Anderson, K.L., Anderson, S.D., Ohama, E., Reaume, A.G., Scott, R.W., and Cleveland, D.W. (1998). Aggregation and motor neuron toxicity of an ALS-linked SOD1 mutant independent from wild-type SOD1. Science *281*, 1851–1854.

Buratti, E., and Baralle, F.E. (2008). Multiple roles of TDP-43 in gene expression, splicing regulation, and human disease. Front Biosci *13*, 867–878.

Burghes, A.H.M., and Beattie, C.E. (2009). Spinal muscular atrophy: why do low levels of survival motor neuron protein make motor neurons sick? Nature Reviews Neuroscience *10*, 597–609.

Butovsky, O., Siddiqui, S., Gabriely, G., Lanser, A.J., Dake, B., Murugaiyan, G., Doykan, C.E., Wu, P.M., Gali, R.R., Iyer, L.K., et al. (2012). Modulating inflammatory monocytes with a unique microRNA gene signature ameliorates murine ALS. J Clin Invest *122*, 3063–3087.

Calvo, A.C., Moreno-Igoa, M., Mancuso, R., Manzano, R., Oliván, S., Muñoz, M.J., Penas, C., Zaragoza, P., Navarro, X., and Osta, R. (2011). Lack of a synergistic effect of a non-viral ALS gene therapy based on BDNF and a TTC fusion molecule. Orphanet J Rare Dis *6*, 10.

Candelario-Jalil, E., de Oliveira, A., Gräf, S., Bhatia, H.S., Hüll, M., Muñoz, E., and Fiebich, B.L. (2007). Resveratrol potently reduces prostaglandin E2 production and free radical formation in lipopolysaccharide-activated primary rat microglia. J Neuroinflamm *4*, 25.

Cantó, C., Gerhart-Hines, Z., Feige, J.N., Lagouge, M., Noriega, L., Milne, J.C., Elliott, P.J.,

Puigserver, P., and Auwerx, J. (2009). AMPK regulates energy expenditure by modulating NAD+ metabolism and SIRT1 activity. Nature *458*, 1056–1060.

Cappellari, A., Ciammola, A., and Silani, V. (2008). The pseudopolyneuritic form of amyotrophic lateral sclerosis (Patrikios' disease). Electromyogr Clin Neurophysiol *48*, 75–81.

Carriedo, S.G., Yin, H.Z., and Weiss, J.H. (1996). Motor neurons are selectively vulnerable to AMPA/kainate receptor-mediated injury in vitro. J Neurosci *16*, 4069–4079.

Chang, Q., and Martin, L.J. (2009). Glycinergic innervation of motoneurons is deficient in amyotrophic lateral sclerosis mice: a quantitative confocal analysis. Am J Pathol *174*, 574–585.

Chang, Q., and Martin, L.J. (2011). Glycine receptor channels in spinal motoneurons are abnormal in a transgenic mouse model of amyotrophic lateral sclerosis. J Neurosci *31*, 2815–2827.

Chang, Y., Kong, Q., Shan, X., Tian, G., Ilieva, H., Cleveland, D.W., Rothstein, J.D., Borchelt, D.R., Wong, P.C., and Lin, C.-L.G. (2008). Messenger RNA Oxidation Occurs Early in Disease Pathogenesis and Promotes Motor Neuron Degeneration in ALS. PLoS ONE *3*, e2849.

Chen, T., Benmohamed, R., Kim, J., Smith, K., Amante, D., Morimoto, R.I., Kirsch, D.R., Ferrante, R.J., and Silverman, R.B. (2012). ADME-guided design and synthesis of aryloxanyl pyrazolone derivatives to block mutant superoxide dismutase 1 (SOD1) cytotoxicity and protein aggregation: potential application for the treatment of amyotrophic lateral sclerosis. J Med Chem *55*, 515–527.

Chen, Y.-Z., Bennett, C.L., Huynh, H.M., Blair, I.P., Puls, I., Irobi, J., Dierick, I., Abel, A., Kennerson, M.L., Rabin, B.A., et al. (2004). DNA/RNA helicase gene mutations in a form of juvenile amyotrophic lateral sclerosis (ALS4). Am J Hum Genet *74*, 1128–1135.

Choudry, R.B., and Cudkowicz, M.E. (2005). Clinical trials in amyotrophic lateral sclerosis: the tenuous past and the promising future. J Clin Pharmacol *45*, 1334–1344.

Clement, A.M., Nguyen, M.D., Roberts, E.A., Garcia, M.L., Boillee, S., Rule, M., McMahon, A.P., Doucette, W., Siwek, D., Ferrante, R.J., et al. (2003). Wild-type nonneuronal cells extend survival of SOD1 mutant motor neurons in ALS mice. Science *302*, 113–117.

Cornblath, D.R., Kuncl, R.W., Mellits, E.D., Quaskey, S.A., Clawson, L., Pestronk, A., and Drachman, D.B. (1992). Nerve conduction studies in amyotrophic lateral sclerosis. Muscle Nerve *15*, 1111–1115.

Crozat, A., Aman, P., Mandahl, N., and Ron, D. (1993). Fusion of CHOP to a novel RNA-binding protein in human myxoid liposarcoma. Nature *363*, 640–644.

Damiano, M., Starkov, A.A., Petri, S., Kipiani, K., Kiaei, M., Mattiazzi, M., Flint Beal, M., and Manfredi, G. (2006). Neural mitochondrial Ca2+ capacity impairment precedes the onset of motor symptoms in G93A Cu/Zn-superoxide dismutase mutant mice. J Neurochem *96*, 1349–1361.

de Carvalho, M., Johnsen, B., and Fuglsang-Frederiksen, A. (2001). Medical technology assessment. Electrodiagnosis in motor neuron diseases and amyotrophic lateral sclerosis. Neurophysiol Clin *31*, 341–348.

de Carvalho, M., and Swash, M. (2000). Nerve conduction studies in amyotrophic lateral sclerosis. Muscle Nerve *23*, 344–352.

de Carvalho, M., Dengler, R., Eisen, A., England, J.D., Kaji, R., Kimura, J., Mills, K., Mitsumoto, H., Nodera, H., Shefner, J.M., et al. (2008). Electrodiagnostic criteria for diagnosis of ALS. Clin Neurophysiol *119*, 497–503.

De Vos, K.J., Grierson, A.J., Ackerley, S., and Miller, C.C.J. (2008). Role of Axonal Transport in Neurodegenerative Diseases*. Annu Rev Neurosci *31*, 151–173.

DeJesus-Hernandez, M., Mackenzie, I.R., Boeve, B.F., Boxer, A.L., Baker, M., Rutherford, N.J., Nicholson, A.M., Finch, N.A., Flynn, H., Adamson, J., et al. (2011). Expanded GGGGCC Hexanucleotide Repeat in Noncoding Region of C9ORF72 Causes Chromosome 9p-Linked FTD and ALS. Neuron *72*, 245–256.

Deng, H.-X., Chen, W., Hong, S.-T., Boycott, K.M., Gorrie, G.H., Siddique, N., Yang, Y., Fecto, F., Shi, Y., Zhai, H., et al. (2011). Mutations in UBQLN2 cause dominant X-linked juvenile and adult-onset ALS and ALS/dementia. Nature 1–7.

Dengler, R., Konstanzer, A., K ther, G., Hesse, S., Wolf, W., and Strupplerdr, A. (1990). Amyotrophic lateral sclerosis: Macro-EMG and twitch forces of single motor units. Muscle Nerve *13*, 545–550.

Diaz-Amarilla, P., Olivera-Bravo, S., Trias, E., Cragnolini, A., Martinez-Palma, L., Cassina, P., Beckman, J.S., and Barbeito, L.H. (2011). Phenotypically aberrant astrocytes that promote motoneuron damage in a model of inherited amyotrophic lateral sclerosis. Proc Natl Acad Sci USA *108*, 18126–18131.

Doble, A. (1996). The pharmacology and mechanism of action of riluzole. Neurology *47*, S233–S241.

Dodge, J.C., Treleaven, C.M., Fidler, J.A., Hester, M., Haidet, A., Handy, C., Rao, M., Eagle, A., Matthews, J.C., Taksir, T.V., et al. (2010). AAV4-mediated expression of IGF-1 and VEGF within cellular components of the ventricular system improves survival outcome in familial ALS mice. Mol Ther *18*, 2075–2084.

Donmez, G. (2012). The neurobiology of sirtuins and their role in neurodegeneration. Trends Pharmacol Sci *33*, 494–501.

Dormann, D., Rodde, R., Edbauer, D., Bentmann, E., Fischer, I., Hruscha, A., Than, M.E., Mackenzie, I.R.A., Capell, A., Schmid, B., et al. (2010). ALS-associated fused in sarcoma (FUS) mutations disrupt Transportin-mediated nuclear import. Embo J. *29*, 2841–2857.

Eisen, A.A., and Shtybel, W. (1990). AAEM minimonograph #35: Clinical experience with transcranial magnetic stimulation. Muscle Nerve *13*, 995–1011.

Eitan, E., Tichon, A., Gazit, A., Gitler, D., Slavin, S., and Priel, E. (2012). Novel telomerase-increasing compound in mouse brain delays the onset of amyotrophic lateral sclerosis. EMBO Mol Med *4*, 313–329.

Estes, P.S., Boehringer, A., Zwick, R., Tang, J.E., Grigsby, B., and Zarnescu, D.C. (2011). Wild-type and A315T mutant TDP-43 exert differential neurotoxicity in a Drosophila model of ALS. Hum Mol Genet *20*, 2308–2321.

Federici, T., and Boulis, N.M. (2006). Gene-based treatment of motor neuron diseases. Muscle Nerve *33*, 302–323.

Ferraiuolo, L., Higginbottom, A., Heath, P.R., Barber, S.C., Greenald, D., Kirby, J., and Shaw, P.J. (2011). Dysregulation of astrocyte-motoneuron cross-talk in mutant superoxide dismutase 1-related amyotrophic lateral sclerosis. Brain *134*, 2627–2641.

Ferraiuolo, L., Heath, P.R., Holden, H., Kasher, P., Kirby, J., and Shaw, P.J. (2007). Microarray analysis of the cellular pathways involved in the adaptation to and progression of motor neuron injury in the SOD1 G93A mouse model of familial ALS. J Neurosci *27*, 9201–9219.

Ferrucci, M., Spalloni, A., Bartalucci, A., Cantafora, E., Fulceri, F., Nutini, M., Longone, P., Paparelli, A., and Fornai, F. (2010). A systematic study of brainstem motor nuclei in a mouse model of ALS, the effects of lithium. Neurobiol Dis *37*, 370–383.

Fischer, L.R., Culver, D.G., Davis, A.A., Tennant, P., Wang, M., Coleman, M., Asress, S., (null), Alexander, G.M., and Glass, J.D. (2005). The WldS gene modestly prolongs survival in the SOD1G93A fALS mouse. Neurobiol Dis *19*, 293–300.

Fischer, L.R., Culver, D.G., Tennant, P., Davis, A.A., Wang, M., Castellano-Sanchez, A., Khan, J., Polak, M.A., and Glass, J.D. (2004). Amyotrophic lateral sclerosis is a distal axonopathy: evidence in mice and man. Exp Neurol *185*, 232–240.

Fonseca-Kelly, Z., Nassrallah, M., Uribe, J., Khan, R.S., Dine, K., Dutt, M., and Shindler, K.S. (2012). Resveratrol neuroprotection in a chronic mouse model of multiple sclerosis. Front Neurol *3*, 84.

Fontanilla, C.V., Wei, X., Zhao, L., Johnstone, B., Pascuzzi, R.M., Farlow, M.R., and Du, Y. (2012). Caffeic acid phenethyl ester extends survival of a mouse model of amyotrophic lateral sclerosis. Neuroscience *205*, 185–193.

Foran, E., and Trotti, D. (2009). Glutamate transporters and the excitotoxic path to motor neuron degeneration in amyotrophic lateral sclerosis. Antioxid Redox Signal *11*, 1587–1602.

Fuchs, A., Kutterer, S., Mühling, T., Duda, J., Schütz, B., Liss, B., Keller, B.U., and Roeper, J. (2013). Selective mitochondrial Ca2+ uptake deficit in disease endstage vulnerable motoneurons of the SOD1G93A mouse model of amyotrophic lateral sclerosis. J Physiol (Lond) *591*, 2723–2745.

Fulco, M., Cen, Y., Zhao, P., Hoffman, E.P., McBurney, M.W., Sauve, A.A., and Sartorelli, V. (2008). Glucose restriction inhibits skeletal myoblast differentiation by activating SIRT1 through AMPK-mediated regulation of Nampt. Dev Cell *14*, 661–673.

Gal, J., Zhang, J., Kwinter, D.M., Zhai, J., Jia, H., Jia, J., and Zhu, H. (2011). Nuclear localization sequence of FUS and induction of stress granules by ALS mutants. Neurobiol Aging *32*, 2323.e27–.e40.

Gekker, G., Hu, S., Sheng, W.S., Rock, R.B., Lokensgard, J.R., and Peterson, P.K. (2006). Cocaine-induced HIV-1 expression in microglia involves sigma-1 receptors and transforming growth factor-beta1. Int Immunopharmacol *6*, 1029–1033.

Ghoddoussi, F., Galloway, M.P., Jambekar, A., Bame, M., Needleman, R., and Brusilow, W.S.A. (2010). Methionine sulfoximine, an inhibitor of glutamine synthetase, lowers brain glutamine and glutamate in a mouse model of ALS. J Neurol Sci *290*, 41–47.

Giordano, A., Galderisi, U., and Marino, I.R. (2007). From the laboratory bench to the patient's bedside: An update on clinical trials with mesenchymal stem cells. J Cell Physiol *211*, 27–35.

Godena, V.K., Romano, G., Romano, M., Appocher, C., Klima, R., Buratti, E., Baralle, F.E., and Feiguin, F. (2011). TDP-43 regulates Drosophila neuromuscular junctions growth by modulating Futsch/MAP1B levels and synaptic microtubules organization. PLoS ONE *6*, e17808.

Gong, Y.H., Parsadanian, A.S., Andreeva, A., Snider, W.D., and Elliott, J.L. (2000). Restricted Expression of G86R Cu/Zn Superoxide Dismutase in Astrocytes Results in Astrocytosis But Does Not Cause Motoneuron Degeneration. J Neurosci *20*, 660-665.

Goodin, D.S., Rowley, H.A., and Olney, R.K. (1988). Magnetic resonance imaging in amyotrophic lateral sclerosis. Ann Neurol *23*, 418–420.

Gordon, P.H., Moore, D.H., Miller, R.G., Florence, J.M., Verheijde, J.L., Doorish, C., Hilton, J.F., Spitalny, G.M., MacArthur, R.B., Mitsumoto, H., et al. (2007). Efficacy of minocycline in patients with amyotrophic lateral sclerosis: a phase III randomised trial. Lancet Neurol *6*, 1045–1053.

Gordon, T., Tyreman, N., Li, S., Putman, C.T., and Hegedus, J. (2010). Functional over-load saves motor units in the SOD1-G93A transgenic mouse model of amyotrophic lateral sclerosis. Neurobiol Dis *37*, 412–422.

Gould, T.W., Buss, R.R., Vinsant, S., Prevette, D., Sun, W., Knudson, C.M., Milligan, C.E., and Oppenheim, R.W. (2006). Complete dissociation of motor neuron death from motor dysfunction by Bax deletion in a mouse model of ALS. J Neurosci *26*, 8774–8786.

Gowing, G., Philips, T., Van Wijmeersch, B., Audet, J.N., Dewil, M., Van Den Bosch, L., Billiau, A.D., Robberecht, W., and Julien, J.P. (2008). Ablation of Proliferating Microglia Does Not Affect Motor Neuron Degeneration in Amyotrophic Lateral Sclerosis Caused by Mutant Superoxide Dismutase. J Neurosci *28*, 10234–10244.

Graffmo, K.S., Forsberg, K., Bergh, J., Birve, A., Zetterström, P., Andersen, P.M., Marklund, S.L., and Brännström, T. (2013). Expression of wild-type human superoxide dismutase-1 in mice causes amyotrophic lateral sclerosis. Hum Mol Genet *22*, 51–60.

Greenway, M.J., Andersen, P.M., Russ, C., Ennis, S., Cashman, S., Donaghy, C., Patterson, V., Swingler, R., Kieran, D., Prehn, J., et al. (2006). ANG mutations segregate with familial and "sporadic" amyotrophic lateral sclerosis. Nat Genet *38*, 411–413.

Groen, E.J.N., van Es, M.A., van Vught, P.W.J., Spliet, W.G.M., van Engelen-Lee, J., de Visser, M., Wokke, J.H.J., Schelhaas, H.J., Ophoff, R.A., Fumoto, K., et al. (2010). FUS mutations in familial amyotrophic lateral sclerosis in the Netherlands. Arch Neurol *67*, 224–230.

Groeneveld, G.J., Veldink, J.H., van der Tweel, I., Kalmijn, S., Beijer, C., de Visser, M., Wokke, J.H.J., Franssen, H., and van den Berg, L.H. (2003). A randomized sequential trial of creatine in amyotrophic lateral sclerosis. Ann Neurol *53*, 437–445.

Gros-Louis, F., Soucy, G., Larivière, R., and Julien, J.P. (2010). Intracerebroventricular infusion of monoclonal antibody or its derived Fab fragment against misfolded forms of SOD1 mutant delays mortality in a mouse model of ALS. J Neurochem *113*, 1188–1199.

Grosskreutz, J., Van Den Bosch, L., and Keller, B.U. (2010). Calcium dysregulation in amyotrophic lateral sclerosis. Cell Calcium *47*, 165–174.

Guo, Y., Zhang, K., Wang, Q., Li, Z., Yin, Y., Xu, Q., Duan, W., and Li, C. (2011). Neuroprotective effects of diallyl trisulfide in SOD1-G93A transgenic mouse model of amyotrophic lateral sclerosis. Brain Res *1374*, 110–115.

Gurney, M.E., Pu, H., Chiu, A.Y., Dal Canto, M.C., Polchow, C.Y., Alexander, D.D., Caliendo, J., Hentati, A., Kwon, Y.W., and Deng, H.X. (1994). Motor neuron degeneration in mice that express a human Cu,Zn superoxide dismutase mutation. Science *264*, 1772–1775.

Guzmán-Lenis, M.-S., Navarro, X., and Casas, C. (2009). Selective sigma receptor agonist 2-(4-morpholinethyl)1-phenylcyclohexanecarboxylate (PRE084) promotes neuroprotection and neurite elongation through protein kinase C (PKC) signaling on motoneurons. Neuroscience *162*, 31–38.

Haidet-Phillips, A.M., Hester, M.E., Miranda, C.J., Meyer, K., Braun, L., Frakes, A., Song, S., Likhite, S., Murtha, M.J., Foust, K.D., et al. (2011). Astrocytes from familial and sporadic ALS patients are toxic to motor neurons. Nat Biotechnol *29*, 824–828.

Hall, A.A., Herrera, Y., Ajmo, C.T., Jr., Cuevas, J., and Pennypacker, K.R. (2009). Sigma receptors suppress multiple aspects of microglial activation. Glia *57*, 744–754.

Hardiman, O., van den Berg, L.H., and Kiernan, M.C. (2011). Clinical diagnosis and management of amyotrophic lateral sclerosis. Nat Rev Neurol *7*, 639–649.

Harrison, A.R., Anderson, B.C., Thompson, L.V., and McLoon, L.K. (2007). Myofiber Length and Three-Dimensional Localization of NMJs in Normal and Botulinum Toxin Treated Adult Extraocular Muscles. Invest Ophthalmol Vis Sci *48*, 3594–3601.

Hashimoto, K., Hayashi, Y., Watabe, K., Inuzuka, T., and Hozumi, I. (2011). Metallothionein-III prevents neuronal death and prolongs life span in amyotrophic lateral sclerosis model mice. Neuroscience *189*, 293–298.

Hayashi, T., and Su, T.-P. (2007). Sigma-1 receptor chaperones at the ER-mitochondrion interface regulate Ca(2+) signaling and cell survival. Cell *131*, 596–610.

Hayashi, T., Hayashi, E., Fujimoto, M., Sprong, H., and Su, T.-P. (2012). The lifetime of UDP-galactose:ceramide galactosyltransferase is controlled by a distinct endoplasmic reticulum-associated degradation (ERAD) regulated by sigma-1 receptor chaperones. J Biol Chem *287*, 43156–43169.

Hegedus, J., Putman, C.T., and Gordon, T. (2009). Progressive motor unit loss in the G93A mouse model of amyotrophic lateral sclerosis is unaffected by gender. Muscle Nerve *39*, 318–327.

Hegedus, J., Putman, C.T., Tyreman, N., and Gordon, T. (2008). Preferential motor unit loss in the SOD1 G93A transgenic mouse model of amyotrophic lateral sclerosis. J Physiol (Lond) *586*, 3337–3351.

Heiman-Patterson, T.D., Deitch, J.S., Blankenhorn, E.P., Erwin, K.L., Perreault, M.J., Alexander,

B.K., Byers, N., Toman, I., and Alexander, G.M. (2005). Background and gender effects on survival in the TgN(SOD1-G93A)1Gur mouse model of ALS. J Neurol Sci *236*, 1–7.

Heiman-Patterson, T.D., Sher, R.B., Blankenhorn, E.A., Alexander, G., Deitch, J.S., Kunst, C.B., Maragakis, N., and Cox, G. (2011). Effect of genetic background on phenotype variability in transgenic mouse models of amyotrophic lateral sclerosis: a window of opportunity in the search for genetic modifiers. Amyotroph Lateral Scler *12*, 79–86.

Henkel, J.S., Beers, D.R., Zhao, W., and Appel, S.H. (2009). Microglia in ALS: the good, the bad, and the resting. J Neuroimmune Pharmacol *4*, 389–398.

Henkel, J.S., Engelhardt, J.I., Siklós, L., Simpson, E.P., Kim, S.H., Pan, T., Goodman, J.C., Siddique, T., Beers, D.R., and Appel, S.H. (2004). Presence of dendritic cells, MCP-1, and activated microglia/macrophages in amyotrophic lateral sclerosis spinal cord tissue. Ann Neurol *55*, 221–235.

Henriques, A., Pitzer, C., Dittgen, T., Klugmann, M., Dupuis, L., and Schneider, A. (2011). CNS-targeted viral delivery of G-CSF in an animal model for ALS: improved efficacy and preservation of the neuromuscular unit. Mol Ther *19*, 284–292.

Hensley, K., Mhatre, M., Mou, S., Pye, Q.N., Stewart, C., West, M., and Williamson, K.S. (2006). On the relation of oxidative stress to neuroinflammation: lessons learned from the G93A-SOD1 mouse model of amyotrophic lateral sclerosis. Antioxid Redox Signal *8*, 2075–2087.

Herskovits, A.Z., and Guarente, L. (2013). Sirtuin deacetylases in neurodegenerative diseases of aging. Cell Res. *23*, 746–758.

Hewitt, C., Kirby, J., Highley, J.R., Hartley, J.A., Hibberd, R., Hollinger, H.C., Williams, T.L., Ince, P.G., McDermott, C.J., and Shaw, P.J. (2010). Novel FUS/TLS mutations and pathology in familial and sporadic amyotrophic lateral sclerosis. Arch Neurol *67*, 455–461.

Highley JR, Kirby J, Heath P, Jansweijer JA, Milo M, Ince PG, and Shaw PJ. (2010). TARDBP mutations, amyotrophic lateral sclerosis and alternative splicing in human fibroblasts. Brain Pathol *20*, Supplement 1.

Hirano, A., Donnenfeld, H., Sasaki, S., and Nakano, I. (1984). Fine structural observations of neurofilamentous changes in amyotrophic lateral sclerosis. J Neuropathol Exp Neurol *43*, 461–470.

Hou, X., Xu, S., Maitland-Toolan, K.A., Sato, K., Jiang, B., Ido, Y., Lan, F., Walsh, K., Wierzbicki, M., Verbeuren, T.J., et al. (2008). SIRT1 regulates hepatocyte lipid metabolism through activating AMP-activated protein kinase. J Biol Chem *283*, 20015–20026.

Howland, D.S., Liu, J., She, Y., Goad, B., Maragakis, N.J., Kim, B., Erickson, J., Kulik, J., DeVito, L., Psaltis, G., et al. (2002). Focal loss of the glutamate transporter EAAT2 in a transgenic rat model of SOD1 mutant-mediated amyotrophic lateral sclerosis (ALS). Proc Natl Acad Sci USA *99*, 1604–1609.

Huang, C., Tong, J., Bi, F., Wu, Q., Huang, B., Zhou, H., and Xia, X.-G. (2012). Entorhinal cortical neurons are the primary targets of FUS mislocalization and ubiquitin aggregation in FUS transgenic rats. Hum Mol Genet *21*, 4602–4614.

Huang, C., Xia, P.Y., and Zhou, H. (2010). Sustained expression of TDP-43 and FUS in motor neurons in rodent's lifetime. Int J Biol Sci *6*, 396–406.

Huang, C., Zhou, H., Tong, J., Chen, H., Liu, Y.-J., Wang, D., Wei, X., and Xia, X.-G. (2011). FUS transgenic rats develop the phenotypes of amyotrophic lateral sclerosis and frontotemporal lobar degeneration. PLoS Genet. *7*, e1002011.

Inghilleri, M., and Iacovelli, E. (2011). Clinical neurophysiology in ALS. Arch Ital Biol *149*, 57–63.

Isaacs, J.D., Dean, A.F., Shaw, C.E., Al-Chalabi, A., Mills, K.R., and Leigh, P.N. (2007). Amyotrophic lateral sclerosis with sensory neuropathy: part of a multisystem disorder? J Neurol Neurosurg Psychiat *78*, 750–753.

Ito, Y., Yamada, M., Tanaka, H., Aida, K., Tsuruma, K., Shimazawa, M., Hozumi, I., Inuzuka, T., Takahashi, H., and Hara, H. (2009). Involvement of CHOP, an ER-stress apoptotic mediator, in both human sporadic ALS and ALS model mice. Neurobiol Dis *36*, 470–476.

Jaarsma, D., Haasdijk, E.D., Grashorn, J.A., Hawkins, R., van Duijn, W., Verspaget, H.W., London, J., and Holstege, J.C. (2000). Human Cu/Zn superoxide dismutase (SOD1) overexpression in mice causes mitochondrial vacuolization, axonal degeneration, and premature motoneuron death and accelerates motoneuron disease in mice expressing a familial amyotrophic lateral sclerosis mutant SOD1. Neurobiol Dis *7*, 623–643.

Jaarsma, D., Teuling, E., Haasdijk, E.D., De Zeeuw, C.I., and Hoogenraad, C.C. (2008). Neuron-specific expression of mutant superoxide dismutase is sufficient to induce amyotrophic lateral sclerosis in transgenic mice. J Neurosci *28*, 2075–2088.

Janko, M., Trontelj, J.V., and Gersak, K. (1989). Fasciculations in motor neuron disease: discharge rate reflects extent and recency of collateral sprouting. J Neurol Neurosurg Psychiat *52*, 1375–1381.

Jeong, J.K., Moon, M.H., Lee, Y.J., Seol, J.W., and Park, S.Y. (2013). Autophagy induced by the class III histone deacetylase Sirt1 prevents prion peptide neurotoxicity. Neurobiol Aging *34*, 146–156.

Jeong, J.-K., Moon, M.-H., Bae, B.-C., Lee, Y.-J., Seol, J.-W., Kang, H.-S., Kim, J.-S., Kang, S.-J., and Park, S.-Y. (2012). Autophagy induced by resveratrol prevents human prion protein-mediated neurotoxicity. Neurosci Res *73*, 99–105.

Jin, F., Wu, Q., Lu, Y.-F., Gong, Q.-H., and Shi, J.-S. (2008). Neuroprotective effect of resveratrol on 6-OHDA-induced Parkinson's disease in rats. Eur J Pharmacol *600*, 78–82.

Johnson, J.O., Mandrioli, J., Benatar, M., Abramzon, Y., Van Deerlin, V.M., Trojanowski, J.Q., Gibbs, J.R., Brunetti, M., Gronka, S., Wuu, J., et al. (2010). Exome sequencing reveals VCP mutations as a cause of familial ALS. Neuron *68*, 857–864.

Julien, J.P. (1997). Neurofilaments and motor neuron disease. Trends Cell Biol *7*, 243–249.

Julien, J.P., Couillard-Després, S., and Meier, J. (1998). Transgenic mice in the study of ALS: the role of neurofilaments. Brain Pathol *8*, 759–769.

Jung, C., Higgins, C.M.J., and Xu, Z. (2002). Mitochondrial electron transport chain complex dysfunction in a transgenic mouse model for amyotrophic lateral sclerosis. J Neurochem *83*, 535–545.

Kabashi, E., Bercier, V., Lissouba, A., Liao, M., Brustein, E., Rouleau, G.A., and Drapeau, P. (2011). FUS and TARDBP but not SOD1 interact in genetic models of amyotrophic lateral sclerosis. PLoS Genet. *7*, e1002214.

Kabashi, E., Valdmanis, P.N., Dion, P., Spiegelman, D., McConkey, B.J., Vande Velde, C., Bouchard, J.-P., Lacomblez, L., Pochigaeva, K., Salachas, F., et al. (2008). TARDBP mutations in individuals with sporadic and familial amyotrophic lateral sclerosis. Nat Genet *40*, 572–574.

Kang, S.H., Li, Y., Fukaya, M., Lorenzini, I., Cleveland, D.W., Ostrow, L.W., Rothstein, J.D., and Bergles, D.E. (2013). Degeneration and impaired regeneration of gray matter oligodendrocytes in amyotrophic lateral sclerosis. Nat Neurosci 1–11.

Kanno, T., Tanaka, K., Yanagisawa, Y., Yasutake, K., Hadano, S., Yoshii, F., Hirayama, N., and Ikeda, J.-E. (2012). A novel small molecule, N-(4-(2-pyridyl)(1,3-thiazol-2-yl))-2-(2,4,6-trimethylphenoxy) acetamide, selectively protects against oxidative stress-induced cell death by activating the Nrf2-ARE pathway: therapeutic implications for ALS. Free Rad Biol Med *53*, 2028–2042.

Kaspar, B.K., Frost, L.M., Christian, L., Umapathi, P., and Gage, F.H. (2005). Synergy of insulin-like growth factor-1 and exercise in amyotrophic lateral sclerosis. Ann Neurol *57*, 649–655.

Kaspar, B.K., Lladó, J., Sherkat, N., Rothstein, J.D., and Gage, F.H. (2003). Retrograde viral delivery of IGF-1 prolongs survival in a mouse ALS model. Science *301*, 839–842.

Kaufman, R.J. (2002). Orchestrating the unfolded protein response in health and disease. J Clin Invest *110*, 1389–1398.

Kaufmann, P., Thompson, J.L.P., Levy, G., Buchsbaum, R., Shefner, J.M., Krivickas, L.S., Katz, J., Rollins, Y., Barohn, R.J., Jackson, C.E., et al. (2009). Phase II trial of CoQ10 for ALS finds insufficient evidence to justify phase III. Ann Neurol *66*, 235–244.

Kawahara, Y., Ito, K., Sun, H., Aizawa, H., Kanazawa, I., and Kwak, S. (2004). Glutamate receptors: RNA editing and death of motor neurons. Nature *427*, 801.

Kawahara, Y., Sun, H., Ito, K., Hideyama, T., Aoki, M., Sobue, G., Tsuji, S., and Kwak, S. (2006). Underediting of GluR2 mRNA, a neuronal death inducing molecular change in sporadic ALS, does not occur in motor neurons in ALS1 or SBMA. Neurosci Res 54, 11–14.

Kennel, P.F., Finiels, F., Revah, F., and Mallet, J. (1996). Neuromuscular function impairment is not caused by motor neurone loss in FALS mice: an electromyographic study. Neuroreport *7*, 1427–1431.

Khandelwal, P.J., Herman, A.M., and Moussa, C.E.H. (2011). Inflammation in the early stages of neurodegenerative pathology. J Neuroimmunol *238*, 1–11.

Khanna, S., Richmonds, C.R., Kaminski, H.J., and Porter, J.D. (2003). Molecular organization of the extraocular muscle neuromuscular junction: partial conservation of and divergence from the skeletal muscle prototype. Invest Ophthalmol Vis Sci *44*, 1918–1926.

Kieran, D., Kalmar, B., Dick, J.R.T., Riddoch-Contreras, J., Burnstock, G., and Greensmith, L. (2004). Treatment with arimoclomol, a coinducer of heat shock proteins, delays disease progression in ALS mice. Nat Med *10*, 402–405.

Kieran, D., Sebastia, J., Greenway, M.J., King, M.A., Connaughton, D., Concannon, C.G., Fenner, B., Hardiman, O., and Prehn, J.H.M. (2008). Control of motoneuron survival by angiogenin. J Neurosci *28*, 14056–14061.

Kim, D., Nguyen, M.D., Dobbin, M.M., Fischer, A., Sananbenesi, F., Rodgers, J.T., Delalle, I., Baur, J.A., Sui, G., and Armour, S.M. (2007). SIRT1 deacetylase protects against neurodegeneration in models for Alzheimer's disease and amyotrophic lateral sclerosis. Embo J *26*, 3169–3179.

Kim, S.U., and de Vellis, J. (2009). Stem cell-based cell therapy in neurological diseases: A review. J Neurosci Res *87*, 2183–2200.

Kirby, J., Halligan, E., Baptista, M.J., Allen, S., Heath, P.R., Holden, H., Barber, S.C., Loynes, C.A., Wood-Allum, C.A., Lunec, J., et al. (2005). Mutant SOD1 alters the motor neuronal transcriptome: implications for familial ALS. Brain *128*, 1686–1706.

Klivenyi, P., Ferrante, R.J., Matthews, R.T., Bogdanov, M.B., Klein, A.M., Andreassen, O.A., Mueller, G., Wermer, M., Kaddurah-Daouk, R., and Beal, M.F. (1999). Neuroprotective effects of creatine in a transgenic animal model of amyotrophic lateral sclerosis. Nat Med *5*, 347–350.

Klivenyi, P., Kiaei, M., Gardian, G., Calingasan, N.Y., and Beal, M.F. (2003). Additive neuroprotective effects of creatine and cyclooxygenase 2 inhibitors in a transgenic mouse model of amyotrophic lateral sclerosis. J Neurochem *88*, 576–582.

Kong, J., and Xu, Z. (1998). Massive mitochondrial degeneration in motor neurons triggers the onset of amyotrophic lateral sclerosis in mice expressing a mutant SOD1. J Neurosci *18*, 3241–3250.

Kourrich, S., Hayashi, T., Chuang, J.-Y., Tsai, S.-Y., Su, T.-P., and Bonci, A. (2013). Dynamic interaction between sigma-1 receptor and Kv1.2 shapes neuronal and behavioral responses to cocaine. Cell *152*, 236–247.

Kraemer, M., Buerger, M., and Berlit, P. (2010). Diagnostic problems and delay of diagnosis in amyotrophic lateral sclerosis. Clin Neurol Neurosurg *112*, 103–105.

Krarup, C. (2011). Lower motor neuron involvement examined by quantitative electromyography in amyotrophic lateral sclerosis. Clin Neurophysiol *122*, 414–422.

Kriz, J., Nguyen, M.D., and Julien, J.P. (2002). Minocycline slows disease progression in a mouse model of amyotrophic lateral sclerosis. Neurobiol Dis *10*, 268–278.

Kuhle, J., Lindberg, R.L.P., Regeniter, A., Mehling, M., Steck, A.J., Kappos, L., and Czaplinski, A. (2009). Increased levels of inflammatory chemokines in amyotrophic lateral sclerosis. Eur J Neurol *16*, 771–774.

Kupershmidt, L., Weinreb, O., Amit, T., Mandel, S., Carrì, M.T., and Youdim, M.B.H. (2009). Neuroprotective and neuritogenic activities of novel multimodal iron-chelating drugs in motor-neuron-like NSC-34 cells and transgenic mouse model of amyotrophic lateral sclerosis. Faseb J *23*, 3766–3779.

Kwak, S., Hideyama, T., Yamashita, T., and Aizawa, H. (2010). AMPA receptor-mediated neuronal death in sporadic ALS. Neuropathology *30*, 182–188.

Kwiatkowski, T.J., Bosco, D.A., Leclerc, A.L., Tamrazian, E., Vanderburg, C.R., Russ, C., Davis, A., Gilchrist, J., Kasarskis, E.J., Munsat, T., et al. (2009). Mutations in the FUS/TLS gene on chromosome 16 cause familial amyotrophic lateral sclerosis. Science *323*, 1205–1208.

Lai, E.C., Felice, K.J., Festoff, B.W., Gawel, M.J., Gelinas, D.F., Kratz, R., Murphy, M.F., Natter, H.M., Norris, F.H., and Rudnicki, S.A. (1997). Effect of recombinant human insulin-like growth factor-I on progression of ALS. A placebo-controlled study. The North America ALS/IGF-I Study Group. Neurology *49*, 1621–1630.

Lan, F., Cacicedo, J.M., Ruderman, N., and Ido, Y. (2008). SIRT1 modulation of the acetylation status, cytosolic localization, and activity of LKB1. Possible role in AMP-activated protein kinase activation. J Biol Chem *283*, 27628–27635.

Lee, D.Y., and Brown, E.J. (2012). Ubiquilins in the crosstalk among proteolytic pathways. Biol Chem *393*, 441–447.

Lee, I.H., Cao, L., Mostoslavsky, R., Lombard, D.B., Liu, J., Bruns, N.E., Tsokos, M., Alt, F.W., and Finkel, T. (2008). A role for the NAD-dependent deacetylase Sirt1 in the regulation of autophagy. Proc Natl Acad Sci USA *105*, 3374–3379.

Lee, J., Ryu, H., and Kowall, N.W. (2009). Motor neuronal protection by L-arginine prolongs survival of mutant SOD1 (G93A) ALS mice. Biochem Biophys Res Commun *384*, 524–529.

Lefebvre, S., Bürglen, L., Reboullet, S., Clermont, O., Burlet, P., Viollet, L., Benichou, B., Cruaud, C., Millasseau, P., and Zeviani, M. (1995). Identification and characterization of a spinal muscular atrophy-determining gene. Cell *80*, 155–165.

Leigh, P.N., and Ray-Chaudhuri, K. (1994). Motor neuron disease. J Neurol Neurosurg Psychiat *57*, 886–896.

Li, S., Yu, W., and Hu, G.-F. (2012). Angiogenin inhibits nuclear translocation of apoptosis inducing factor in a Bcl-2-dependent manner. J Cell Physiol *227*, 1639–1644.

Lin, M.-J., Cheng, C.-W., and Shen, C.-K.J. (2011). Neuronal function and dysfunction of Drosophila dTDP. PLoS ONE *6*, e20371.

Lin, M.T., and Beal, M.F. (2006). Mitochondrial dysfunction and oxidative stress in neurodegenerative diseases. Nature *443*, 787–795.

Lincecum, J.M., Vieira, F.G., Wang, M.Z., Thompson, K., De Zutter, G.S., Kidd, J., Moreno, A., Sanchez, R., Carrion, I.J., Levine, B.A., et al. (2010). From transcriptome analysis to therapeutic anti-CD40L treatment in the SOD1 model of amyotrophic lateral sclerosis. Nat Genet *42*, 392–399.

Lindvall, O., and Kokaia, Z. (2010). Stem cells in human neurodegenerative disorders — time for clinical translation? J Clin Invest *120*, 29–40.

Ling, S.-C., Polymenidou, M., and Cleveland, D.W. (2013). Converging mechanisms in ALS and FTD: disrupted RNA and protein homeostasis. Neuron *79*, 416–438.

Lino, M.M., Schneider, C., and Caroni, P. (2002). Accumulation of SOD1 mutants in postnatal motoneurons does not cause motoneuron pathology or motoneuron disease. J Neurosci *22*,

4825–4832.
Liu, C., Shi, Z., Fan, L., Zhang, C., Wang, K., and Wang, B. (2011). Resveratrol improves neuron protection and functional recovery in rat model of spinal cord injury. Brain Res *1374*, 100–109.
Liu, J., Lillo, C., Jonsson, P.A., Vande Velde, C., Ward, C.M., Miller, T.M., Subramaniam, J.R., Rothstein, J.D., Marklund, S., Andersen, P.M., et al. (2004). Toxicity of familial ALS-linked SOD1 mutants from selective recruitment to spinal mitochondria. Neuron *43*, 5–17.
Lobsiger, C.S., Boillee, S., McAlonis-Downes, M., Khan, A.M., Feltri, M.L., Yamanaka, K., and Cleveland, D.W. (2009). Schwann cells expressing dismutase active mutant SOD1 unexpectedly slow disease progression in ALS mice. Proc Natl Acad Sci USA *106*, 4465–4470.
Lomen-Hoerth, C., Anderson, T., and Miller, B. (2002). The overlap of amyotrophic lateral sclerosis and frontotemporal dementia. Neurology *59*, 1077–1079.
Ludolph, A.C., and Jesse, S. (2009). Evidence-based drug treatment in amyotrophic lateral sclerosis and upcoming clinical trials. Ther Adv Neurol Disord *2*, 319–326.
Ludolph, A.C., Bendotti, C., Blaugrund, E., Chio, A., Greensmith, L., Loeffler, J.-P., Mead, R., Niessen, H.G., Petri, S., and Pradat, P.-F. (2010). Guidelines for preclinical animal research in ALS/MND: A consensus meeting. Amyotroph Lateral Scler *11*, 38–45.
Ludolph, A.C., Bendotti, C., Blaugrund, E., Hengerer, B., Löffler, J.-P., Martin, J., Meininger, V., Meyer, T., Moussaoui, S., Robberecht, W., et al. (2007). Guidelines for the preclinical in vivo evaluation of pharmacological active drugs for ALS/MND: report on the 142nd ENMC international workshop. Amyotroph Lateral Scler *8*, 217–223.
Luty, A.A., Kwok, J.B.J., Dobson-Stone, C., Loy, C.T., Coupland, K.G., Karlström, H., Sobow, T., Tchorzewska, J., Maruszak, A., Barcikowska, M., et al. (2010). Sigma nonopioid intracellular receptor 1 mutations cause frontotemporal lobar degeneration-motor neuron disease. Ann Neurol *68*, 639–649.
Lyras, L.A., Evans, P.J., Shaw, P.J., Ince, P.G., and Halliwell, B. (1996). Oxidative Damage and Motor Neurone Disease Difficulties in the Measurement of Protein Carbonyls in Human Brain Tissue. Free Rad Res *24*, 397-406
Mackenzie, I.R.A., Bigio, E.H., Ince, P.G., Geser, F., Neumann, M., Cairns, N.J., Kwong, L.K., Forman, M.S., Ravits, J., Stewart, H., et al. (2007). Pathological TDP-43 distinguishes sporadic amyotrophic lateral sclerosis from amyotrophic lateral sclerosis with SOD1 mutations. Ann Neurol *61*, 427–434.
Mackenzie, I.R., Rademakers, R., and Neumann, M. (2010). TDP-43 and FUS in amyotrophic lateral sclerosis and frontotemporal dementia. Lancet Neurol *9*, 995–1007.
Maher, P., Dargusch, R., Bodai, L., Gerard, P.E., Purcell, J.M., and Marsh, J.L. (2010). ERK activation by the polyphenols fisetin and resveratrol provides neuroprotection in multiple models of Huntington's disease. Hum Mol Genet *20*, 261–270.
Mancuso, R., Oliván, S., Mancera, P., Pastén-Zamorano, A., Manzano, R., Casas, C., Osta, R., and Navarro, X. (2012a). Effect of genetic background on onset and disease progression in the SOD1-G93A model of amyotrophic lateral sclerosis. Amyotroph Lateral Scler *13*, 302–310.
Mancuso, R., Oliván, S., Rando, A., Casas, C., Osta, R., and Navarro, X. (2012b). Sigma-1R agonist improves motor function and motoneuron survival in ALS mice. Neurotherapeutics *9*, 814–826.
Mancuso, R., Santos-Nogueira, E., Osta, R., and Navarro, X. (2011). Electrophysiological analysis of a murine model of motoneuron disease. Clin Neurophysiol *122*, 1660–1670.
Mancuso, R., Valle, J., Mòdol, L., Martínez, A., Granado-Serrano, A.B., Ramirez-Núñez, O., Pallàs, M., Portero-Otin, M., Osta, R., and Navarro, X. (2014a). Resveratrol Improves Motoneuron Function and Extends Survival in SOD1G93A ALS Mice. Neurotherapeutics doi: 10.1007/s13311-013-0253-y.
Mancuso R, del Valle J, Morell M, Pallás M, Osta R, Navarro X. (2014b). Lack of synergistic effect

of resveratrol and sigma-1 receptor agonist (PRE-084) in SOD1G93A ALS mice: an indication of limited therapeutic opportunity? Neurotherapeutics, Under revision.

Mannen, T., Iwata, M., Toyokura, Y., and Nagashima, K. (1977). Preservation of a certain motoneurone group of the sacral cord in amyotrophic lateral sclerosis: its clinical significance. J Neurol Neurosurg Psychiat *40*, 464–469.

Marinkovic, P., Reuter, M.S., Brill, M.S., Godinho, L., Kerschensteiner, M., and Misgeld, T. (2012). Axonal transport deficits and degeneration can evolve independently in mouse models of amyotrophic lateral sclerosis. Proc Natl Acad Sci USA *109*, 4296–4301.

Marriott, K.-S.C., Prasad, M., Thapliyal, V., and Bose, H.S. (2012). σ -1 receptor at the mitochondrial-associated endoplasmic reticulum membrane is responsible for mitochondrial metabolic regulation. J Pharmacol Exp Ther *343*, 578–586.

Maruyama, H., Morino, H., Ito, H., Izumi, Y., Kato, H., Watanabe, Y., Kinoshita, Y., Kamada, M., Nodera, H., Suzuki, H., et al. (2010). Mutations of optineurin in amyotrophic lateral sclerosis. Nature *465*, 223–226.

Mattiazzi, M., D'Aurelio, M., Gajewski, C.D., Martushova, K., Kiaei, M., Beal, M.F., and Manfredi, G. (2002). Mutated human SOD1 causes dysfunction of oxidative phosphorylation in mitochondria of transgenic mice. J Biol Chem *277*, 29626–29633.

Maurice, T., and Su, T.-P. (2009). The pharmacology of sigma-1 receptors. Pharmacol Ther *124*, 195–206.

Mavlyutov, T.A., Epstein, M.L., Verbny, Y.I., Huerta, M.S., Zaitoun, I., Ziskind-Conhaim, L., and Ruoho, A.E. (2013). Lack of sigma-1 receptor exacerbates ALS progression in mice. Neuroscience *240*, 129–134.

Mavlyutov, T.A., Nickells, R.W., and Guo, L.-W. (2011). Accelerated retinal ganglion cell death in mice deficient in the Sigma-1 receptor. Mol Vis *17*, 1034–1043.

Mazzini, L., Ferrero, I., Luparello, V., Rustichelli, D., Gunetti, M., Mareschi, K., Testa, L., Stecco, A., Tarletti, R., Miglioretti, M., et al. (2010). Mesenchymal stem cell transplantation in amyotrophic lateral sclerosis: A Phase I clinical trial. Exp Neurol *223*, 229–237.

McGoldrick, P., Joyce, P.I., Fisher, E.M.C., and Greensmith, L. (2013). Rodent models of amyotrophic lateral sclerosis. Biochimica Biophysica Acta *1832*, 1421–1436.

Meamar, R., Nasr-Esfahani, M.H., Mousavi, S.A., and Basiri, K. (2013). Stem cell therapy in amyotrophic lateral sclerosis. J Clin Neurosci *20*, 1659-1663.

Meininger, V., Drory, V.E., Leigh, P.N., Ludolph, A., Robberecht, W., and Silani, V. (2009). Glatiramer acetate has no impact on disease progression in ALS at 40 mg/day: a double- blind, randomized, multicentre, placebo-controlled trial. Amyotroph Lateral Scler *10*, 378–383.

Meng, X.-L., Yang, J.Y., Chen, G.-L., Wang, L.-H., Zhang, L.-J., Wang, S., Li, J., and Wu, C.F. (2008). Effects of resveratrol and its derivatives on lipopolysaccharide-induced microglial activation and their structure-activity relationships. Chem Biol Interact *174*, 51–59.

Menzies, F.M., Cookson, M.R., Taylor, R.W., Turnbull, D.M., Chrzanowska-Lightowlers, Z.M.A., Dong, L., Figlewicz, D.A., and Shaw, P.J. (2002). Mitochondrial dysfunction in a cell culture model of familial amyotrophic lateral sclerosis. Brain *125*, 1522–1533.

Miana-Mena, F.J., Muñoz, M.J., Yagüe, G., Mendez, M., Moreno, M., Ciriza, J., Zaragoza, P., and Osta, R. (2005). Optimal methods to characterize the G93A mouse model of ALS. Amyotroph Lateral Scler Other Motor Neuron Disord *6*, 55–62.

Miller, T.M., Pestronk, A., David, W., Rothstein, J., Simpson, E., Appel, S.H., Andres, P.L., Mahoney, K., Allred, P., and Alexander, K. (2013). An antisense oligonucleotide against SOD1 delivered intrathecally for patients with SOD1 familial amyotrophic lateral sclerosis: a phase 1, randomised, first-in-man study. Lancet Neurology *12*, 435-442.

Mills, K.R., and Nithi, K.A. (1998). Peripheral and central motor conduction in amyotrophic lateral sclerosis. J Neurol Sci *159*, 82–87.

Miquel, E., Cassina, A., Martinez-Palma, L., Bolatto, C., Trias, E., Gandelman, M., Radi, R., Barbeito, L.H., and Cassina, P. (2012). Modulation of astrocytic mitochondrial function by dichloroacetate improves survival and motor performance in inherited amyotrophic lateral sclerosis. PLoS ONE *7*, e34776.

Mitchell, J.C., McGoldrick, P., Vance, C., Hortobagyi, T., Sreedharan, J., Rogelj, B., Tudor, E.L., Smith, B.N., Klasen, C., Miller, C.C.J., et al. (2013). Overexpression of human wild-type FUS causes progressive motor neuron degeneration in an age- and dose-dependent fashion. Acta Neuropathol *125*, 273–288.

Mitsumoto, H., Ulug, A.M., Pullman, S.L., Gooch, C.L., Chan, S., Tang, M.-X., Mao, X., Hays, A.P., Floyd, A.G., Battista, V., et al. (2007). Quantitative objective markers for upper and lower motor neuron dysfunction in ALS. Neurology *68*, 1402–1410.

Mitsumoto, H., Santella, R.M., Liu, X., Bogdanov, M., Zipprich, J., Wu, H.-C., Mahata, J., Kilty, M., Bednarz, K., Bell, D., et al. (2008). Oxidative stress biomarkers in sporadic ALS. Amyotroph Lateral Scler *9*, 177–183.

Moreno-Igoa, M., Calvo, A.C., Penas, C., Manzano, R., Oliván, S., Muñoz, M.J., Mancuso, R., Zaragoza, P., Aguilera, J., Navarro, X., et al. (2010). Fragment C of tetanus toxin, more than a carrier. Novel perspectives in non-viral ALS gene therapy. J Mol Med *88*, 297–308.

Mori, K., Weng, S.-M., Arzberger, T., May, S., Rentzsch, K., Kremmer, E., Schmid, B., Kretzschmar, H.A., Cruts, M., Van Broeckhoven, C., et al. (2013a). The C9orf72 GGGGCC repeat is translated into aggregating dipeptide-repeat proteins in FTLD/ALS. Science *339*, 1335–1338.

Mori, T., Hayashi, T., Hayashi, E., and Su, T.-P. (2013b). Sigma-1 Receptor Chaperone at the ER-Mitochondrion Interface Mediates the Mitochondrion-ER-Nucleus Signaling for Cellular Survival. PLoS ONE *8*, e76941.

Mòdol, L., Mancuso, R., Alé, A., Francos-Quijorna, I., and Navarro, X. (2014). Differential effects on KCC2 expression and spasticity of ALS and traumatic injuries to motoneurons. Front Cell Neurosci *8*, 7.

Nagai, M., Re, D.B., Nagata, T., Chalazonitis, A., Jessell, T.M., Wichterle, H., and Przedborski, S. (2007). Astrocytes expressing ALS-linked mutated SOD1 release factors selectively toxic to motor neurons. Nat Neurosci *10*, 615–622.

Nave, K.-A. (2010). Myelination and support of axonal integrity by glia. Nature *468*, 244–252.

Neumann, M., Sampathu, D.M., Kwong, L.K., Truax, A.C., Micsenyi, M.C., Chou, T.T., Bruce, J., Schuck, T., Grossman, M., Clark, C.M., et al. (2006). Ubiquitinated TDP-43 in frontotemporal lobar degeneration and amyotrophic lateral sclerosis. Science *314*, 130–133.

Neymotin, A., Calingasan, N.Y., Wille, E., Naseri, N., Petri, S., Damiano, M., Liby, K.T., Risingsong, R., Sporn, M., Beal, M.F., et al. (2011). Neuroprotective effect of Nrf2/ARE activators, CDDO ethylamide and CDDO trifluoroethylamide, in a mouse model of amyotrophic lateral sclerosis. Free Rad Biol Med *51*, 88–96.

Neymotin, A., Petri, S., Calingasan, N.Y., Wille, E., Schafer, P., Stewart, C., Hensley, K., Beal, M.F., and Kiaei, M. (2009). Lenalidomide (Revlimid) administration at symptom onset is neuroprotective in a mouse model of amyotrophic lateral sclerosis. Exp Neurol *220*, 191–197.

Nimchinsky, E.A., Young, W.G., Yeung, G., Shah, R.A., Gordon, J.W., Bloom, F.E., Morrison, J.H., and Hof, P.R. (2000). Differential vulnerability of oculomotor, facial, and hypoglossal nuclei in G86R superoxide dismutase transgenic mice. J Comp Neurol *416*, 112–125.

Nimmagadda, V.K., Bever, C.T., Vattikunta, N.R., Talat, S., Ahmad, V., Nagalla, N.K., Trisler, D., Judge, S.I.V., Royal, W., Chandrasekaran, K., et al. (2013). Overexpression of SIRT1 protein in neurons protects against experimental autoimmune encephalomyelitis through activation of multiple SIRT1 targets. J Immunol *190*, 4595–4607.

Nishimura, A.L., Mitne-Neto, M., Silva, H.C.A., Richieri-Costa, A., Middleton, S., Cascio, D.,

Kok, F., Oliveira, J.R.M., Gillingwater, T., Webb, J., et al. (2004). A mutation in the vesicle-trafficking protein VAPB causes late-onset spinal muscular atrophy and amyotrophic lateral sclerosis. Am J Hum Genet *75*, 822–831.

Okamoto, K., Hirai, S., Amari, M., Iizuka, T., Watanabe, M., Murakami, N., and Takatama, M. (1993a). Oculomotor nuclear pathology in amyotrophic lateral sclerosis. Acta Neuropathol *85*, 458–462.

Okamoto, K., Hirai, S., Ishiguro, K., Kawarabayashi, T., and Takatama, M. (1991). Light and electron microscopic and immunohistochemical observations of the Onuf's nucleus of amyotrophic lateral sclerosis. Acta Neuropathol *81*, 610–614.

Okamoto, K., Hirai, S., Amari, M., Watanabe, M., and Sakurai, A. (1993b). Bunina bodies in amyotrophic lateral sclerosis immunostained with rabbit anti-cystatin C serum. Neurosci Lett *162*, 125–128.

Okamoto, K., Mizuno, Y., and Fujita, Y. (2008). Bunina bodies in amyotrophic lateral sclerosis. Neuropathology *28*, 109–115.

Orrell, R.W., Lane, R.J.M., and Ross, M. (2005). Antioxidant treatment for amyotrophic lateral sclerosis / motor neuron disease. Cochrane Database Syst Rev doi: 10.1002/14651858.CD002829.pub3

Osei-Lah, A.D., Turner, M.R., Andersen, P.M., Leigh, P.N., and Mills, K.R. (2004). A novel central motor conduction abnormality in D90A-homozygous patients with amyotrophic lateral sclerosis. Muscle Nerve *29*, 790–794.

Ou, S.H., Wu, F., Harrich, D., García-Martínez, L.F., and Gaynor, R.B. (1995). Cloning and characterization of a novel cellular protein, TDP-43, that binds to human immunodeficiency virus type 1 TAR DNA sequence motifs. J Virol *69*, 3584–3596.

Pachter, B.R. (1983). Rat extraocular muscle. 1. Three dimensional cytoarchitecture, component fibre populations and innervation. J Anat *137 (Pt 1)*, 143–159.

Palacios, G., Muro, A., Vela, J.M., Molina-Holgado, E., Guitart, X., Ovalle, S., and Zamanillo, D. (2003). Immunohistochemical localization of the sigma1-receptor in oligodendrocytes in the rat central nervous system. Brain Res *961*, 92–99.

Papadeas, S.T., and Maragakis, N.J. (2009). Advances in stem cell research for Amyotrophic Lateral Sclerosis. Curr Opin Biotechnol *20*, 545–551.

Parakh, S., Spencer, D.M., Halloran, M.A., Soo, K.Y., and Atkin, J.D. (2013). Redox Regulation in Amyotrophic Lateral Sclerosis. Oxid Med Cell Longev *2013*, 1–12.

Parone, P.A., Da Cruz, S., Han, J.S., McAlonis-Downes, M., Vetto, A.P., Lee, S.K., Tseng, E., and Cleveland, D.W. (2013). Enhancing mitochondrial calcium buffering capacity reduces aggregation of misfolded SOD1 and motor neuron cell death without extending survival in mouse models of inherited amyotrophic lateral sclerosis. J Neurosci *33*, 4657–4671.

Pasinelli, P., and Brown, R.H. (2006). Molecular biology of amyotrophic lateral sclerosis: insights from genetics. Nat Rev Neurosci *7*, 710–723.

Pasinelli, P., Belford, M.E., Lennon, N., Bacskai, B.J., Hyman, B.T., Trotti, D., and Brown, R.H., Jr (2004). Amyotrophic lateral sclerosis-associated SOD1 mutant proteins bind and aggregate with Bcl-2 in spinal cord mitochondria. Neuron *43*, 19–30.

Pastor, D., Viso-León, M.C., Jones, J., Jaramillo-Merchán, J., Toledo-Aral, J.J., Moraleda, J.M., and Martínez, S. (2012). Comparative effects between bone marrow and mesenchymal stem cell transplantation in GDNF expression and motor function recovery in a motorneuron degenerative mouse model. Stem Cell Rev *8*, 445–458.

Penas, C., Pascual-Font, A., Mancuso, R., Forés, J., Casas, C., and Navarro, X. (2011). Sigma receptor agonist 2-(4-morpholinethyl)1 phenylcyclohexanecarboxylate (Pre084) increases GDNF and BiP expression and promotes neuroprotection after root avulsion injury. J Neurotrauma *28*, 831–840.

Perry, T.L., Krieger, C., Hansen, S., and Eisen, A. (1990). Amyotrophic lateral sclerosis: Amino acid levels in plasma and cerebrospinal fluid. Ann Neurol *28*, 12–17.

Petri, S., Kiaei, M., Kipiani, K., Chen, J., Calingasan, N.Y., Crow, J.P., and Beal, M.F. (2006). Additive neuroprotective effects of a histone deacetylase inhibitor and a catalytic antioxidant in a transgenic mouse model of amyotrophic lateral sclerosis. Neurobiol Dis *22*, 40–49.

Pollari, E., Savchenko, E., Jaronen, M., Kanninen, K., Malm, T., Wojciechowski, S., Ahtoniemi, T., Goldsteins, G., Giniatullina, R., Giniatullin, R., et al. (2011). Granulocyte colony stimulating factor attenuates inflammation in a mouse model of amyotrophic lateral sclerosis. J Neuroinflamm *8*, 74.

Polymenidou, M., Lagier-Tourenne, C., Hutt, K.R., Huelga, S.C., Moran, J., Liang, T.Y., Ling, S.-C., Sun, E., Wancewicz, E., Mazur, C., et al. (2011). Long pre-mRNA depletion and RNA missplicing contribute to neuronal vulnerability from loss of TDP-43. Nat Neurosci *14*, 459–468.

Porquet, D., Casadesús, G., Bayod, S., Vicente, A., Canudas, A.M., Vilaplana, J., Pelegrí, C., Sanfeliu, C., Camins, A., Pallàs, M., et al. (2013). Dietary resveratrol prevents Alzheimer's markers and increases life span in SAMP8. Age (Dordr) *35*, 1851–1865.

Porter, J.D., and Baker, R.S. (1996). Muscles of a different "color": the unusual properties of the extraocular muscles may predispose or protect them in neurogenic and myogenic disease. Neurology *46*, 30–37.

Porter, J.D., and Hauser, K.F. (1993). Survival of extraocular muscle in long-term organotypic culture: differential influence of appropriate and inappropriate motoneurons. Dev Biol *160*, 39–50.

Porter, J.D., Khanna, S., Kaminski, H.J., Rao, J.S., Merriam, A.P., Richmonds, C.R., Leahy, P., Li, J., and Andrade, F.H. (2001). Extraocular muscle is defined by a fundamentally distinct gene expression profile. Proc Natl Acad Sci USA *98*, 12062–12067.

Porter, J.D. (2002). Extraocular muscle: cellular adaptations for a diverse functional repertoire. Ann NY Acad Sci *956*, 7–16.

Prasad, D.D., Ouchida, M., Lee, L., Rao, V.N., and Reddy, E.S. (1994). TLS/FUS fusion domain of TLS/FUS-erg chimeric protein resulting from the t(16;21) chromosomal translocation in human myeloid leukemia functions as a transcriptional activation domain. Oncogene *9*, 3717–3729.

Price, N.L., Gomes, A.P., Ling, A.J.Y., Duarte, F.V., Martin-Montalvo, A., North, B.J., Agarwal, B., Ye, L., Ramadori, G., Teodoro, J.S., et al. (2012). SIRT1 Is Required for AMPK Activation and the Beneficial Effects of Resveratrol on Mitochondrial Function. Cell Metabolism *15*, 675–690.

Pugdahl, K., Fuglsang-Frederiksen, A., de Carvalho, M., Johnsen, B., Fawcett, P.R.W., Labarre-Vila, A., Liguori, R., Nix, W.A., and Schofield, I.S. (2007). Generalised sensory system abnormalities in amyotrophic lateral sclerosis: a European multicentre study. J Neurol Neurosurg Psychiat *78*, 746–749.

Rabbitts, T.H., Forster, A., Larson, R., and Nathan, P. (1993). Fusion of the dominant negative transcription regulator CHOP with a novel gene FUS by translocation t(12;16) in malignant liposarcoma. Nat Genet *4*, 175–180.

Rakhit, R., Robertson, J., Vande Velde, C., Horne, P., Ruth, D.M., Griffin, J., Cleveland, D.W., Cashman, N.R., and Chakrabartty, A. (2007). An immunological epitope selective for pathological monomer-misfolded SOD1 in ALS. Nat Med *13*, 754–759.

Ralph, G.S., Radcliffe, P.A., Day, D.M., Carthy, J.M., Leroux, M.A., Lee, D.C.P., Wong, L.-F., Bilsland, L.G., Greensmith, L., Kingsman, S.M., et al. (2005). Silencing mutant SOD1 using RNAi protects against neurodegeneration and extends survival in an ALS model. Nat Med *11*, 429–433.

Raoul, C., Abbas-Terki, T., Bensadoun, J.-C., Guillot, S., Haase, G., Szulc, J., Henderson, C.E., and

Aebischer, P. (2005). Lentiviral-mediated silencing of SOD1 through RNA interference retards disease onset and progression in a mouse model of ALS. Nat Med *11*, 423–428.

Reaume, A.G., Elliott, J.L., Hoffman, E.K., Kowall, N.W., Ferrante, R.J., Siwek, D.F., Wilcox, H.M., Flood, D.G., Beal, M.F., Brown, R.H., et al. (1996). Motor neurons in Cu/Zn superoxide dismutase-deficient mice develop normally but exhibit enhanced cell death after axonal injury. Nat Genet *13*, 43–47.

Reiner, A., Medina, L., Figueredo-Cardenas, G., and Anfinson, S. (1995). Brainstem motoneuron pools that are selectively resistant in amyotrophic lateral sclerosis are preferentially enriched in parvalbumin: evidence from monkey brainstem for a calcium-mediated mechanism in sporadic ALS. Exp Neurol *131*, 239–250.

Renton, A.E., Majounie, E., Waite, A., Simón-Sánchez, J., Rollinson, S., Gibbs, J.R., Schymick, J.C., Laaksovirta, H., van Swieten, J.C., Myllykangas, L., et al. (2011). A Hexanucleotide Repeat Expansion in C9ORF72 Is the Cause of Chromosome 9p21-Linked ALS-FTD. Neuron *72*, 257–268.

Ringholz, G.M., Appel, S.H., Bradshaw, M., Cooke, N.A., Mosnik, D.M., and Schulz, P.E. (2005). Prevalence and patterns of cognitive impairment in sporadic ALS. Neurology *65*, 586–590.

Ripps, M.E., Huntley, G.W., Hof, P.R., Morrison, J.H., and Gordon, J.W. (1995). Transgenic mice expressing an altered murine superoxide dismutase gene provide an animal model of amyotrophic lateral sclerosis. Proc Natl Acad Sci USA *92*, 689–693.

Roberts, K., Zeineddine, R., Corcoran, L., Li, W., Campbell, I.L., and Yerbury, J.J. (2012). Extracellular aggregated Cu/Zn superoxide dismutase activates microglia to give a cytotoxic phenotype. Glia *61*, 409–419.

Robinson, D.A. (1970). Oculomotor unit behavior in the monkey. J Neurophysiol *33*, 393–403.

Rosen, D.R. (1993). Mutations in Cu/Zn superoxide dismutase gene are associated with familial amyotrophic lateral sclerosis. Nature *364*, 362.

Rosenfeld, J., King, R.M., Jackson, C.E., Bedlack, R.S., Barohn, R.J., Dick, A., Phillips, L.H., Chapin, J., Gelinas, D.F., and Lou, J.-S. (2008). Creatine monohydrate in ALS: effects on strength, fatigue, respiratory status and ALSFRS. Amyotroph Lateral Scler *9*, 266–272.

Rothstein, J.D. (2003). Of mice and men: reconciling preclinical ALS mouse studies and human clinical trials. Ann Neurol *53*, 423–426.

Saxena, S., Cabuy, E., and Caroni, P. (2009). A role for motoneuron subtype-selective ER stress in disease manifestations of FALS mice. Nat Neurosci *12*, 627–636.

Saxena, S., Roselli, F., Singh, K., Leptien, K., Julien, J.P., Gros-Louis, F., and Caroni, P. (2013). Neuroprotection through Excitabilityand mTOR Required in ALS Motoneurons to Delay Disease and Extend Survival. Neuron *80*, 80–96.

Schmidt, M.L., Carden, M.J., Lee, V.M., and Trojanowski, J.Q. (1987). Phosphate dependent and independent neurofilament epitopes in the axonal swellings of patients with motor neuron disease and controls. Lab Invest *56*, 282–294.

Scott, S., Kranz, J.E., Cole, J., Lincecum, J.M., Thompson, K., Kelly, N., Bostrom, A., Theodoss, J., Nakhala, Al, B.M., Vieira, F.G., et al. (2008). Design, power, and interpretation of studies in the standard murine model of ALS. Amyotroph Lateral Scler *9*, 4–15.

Sephton, C.F., Good, S.K., Atkin, S., Dewey, C.M., Mayer, P., Herz, J., and Yu, G. (2010). TDP-43 is a developmentally regulated protein essential for early embryonic development. J Biol Chem *285*, 6826–6834.

Shaw, P., and Eggett, C.J. (2000). Molecular factors underlying selective vulnerability of motor neurons to neurodegeneration in amyotrophic lateral sclerosis. J Neurol *247*, I17–I27.

Shaw, P.J. (2005). Molecular and cellular pathways of neurodegeneration in motor neurone disease. J Neurol Neurosurg Psychiat *76*, 1046–1057.

Shaw, P.J., Forrest, V., Ince, P.G., Richardson, J.P., and Wastell, H.J. (1995a). CSF and Plasma

Amino Acid Levels in Motor Neuron Disease: Elevation of CSF Glutamate in a Subset of Patients. Neurodegeneration *4*, 209–216.

Shaw, P.J., Ince, P.G., Falkous, G., and Mantle, D. (1995b). Oxidative damage to protein in sporadic motor neuron disease spinal cord. Ann Neurol *38*, 691–695.

Shefner, J.M., Cudkowicz, M.E., Schoenfeld, D., Conrad, T., Taft, J., Chilton, M., Urbinelli, L., Qureshi, M., Zhang, H., Pestronk, A., et al. (2004). A clinical trial of creatine in ALS. Neurology *63*, 1656–1661.

Shefner, J.M., Cudkowicz, M., and Brown, R.H. (2006). Motor unit number estimation predicts disease onset and survival in a transgenic mouse model of amyotrophic lateral sclerosis. Muscle Nerve *34*, 603–607.

Shi, P., Gal, J., Kwinter, D.M., Liu, X., and Zhu, H. (2010). Mitochondrial dysfunction in amyotrophic lateral sclerosis. Biochimica Biophysica Acta *1802*, 45–51.

Shibata, N., Hirano, A., Kobayashi, M., Sasaki, S., Kato, T., Matsumoto, S., Shiozawa, Z., Komori, T., Ikemoto, A., and Umahara, T. (1994). Cu/Zn superoxide dismutase-like immunoreactivity in Lewy body-like inclusions of sporadic amyotrophic lateral sclerosis. Neurosci Lett *179*, 149–152.

Shimazawa, M., Tanaka, H., Ito, Y., Morimoto, N., Tsuruma, K., Kadokura, M., Tamura, S., Inoue, T., Yamada, M., Takahashi, H., et al. (2010). An inducer of VGF protects cells against ER stress-induced cell death and prolongs survival in the mutant SOD1 animal models of familial ALS. PLoS ONE *5*, e15307.

Shin, J.H., Cho, S.I., Lim, H.R., Lee, J.K., Lee, Y.A., Noh, J.S., Joo, I.S., Kim, K.W., and Gwag, B.J. (2007). Concurrent Administration of Neu2000 and Lithium Produces Marked Improvement of Motor Neuron Survival, Motor Function, and Mortality in a Mouse Model of Amyotrophic Lateral Sclerosis. Mol Pharmacol *71*, 965–975.

Simpson, E.P., Henry, Y.K., Henkel, J.S., Smith, R.G., and Appel, S.H. (2004). Increased lipid peroxidation in sera of ALS patients: a potential biomarker of disease burden. Neurology *62*, 1758–1765.

Smith, R.G., Henry, Y.K., Mattson, M.P., and Appel, S.H. (1998). Presence of 4-hydroxynonenal in cerebrospinal fluid of patients with sporadic amyotrophic lateral sclerosis. Ann Neurol *44*, 696–699.

Sobue, G., Sahashi, K., Takahashi, A., Matsuoka, Y., Muroga, T., and Sobue, I. (1983). Degenerating compartment and functioning compartment of motor neurons in ALS: possible process of motor neuron loss. Neurology *33*, 654–657.

Sreedharan, J., Blair, I.P., Tripathi, V.B., Hu, X., Vance, C., Rogelj, B., Ackerley, S., Durnall, J.C., Williams, K.L., Buratti, E., et al. (2008). TDP-43 mutations in familial and sporadic amyotrophic lateral sclerosis. Science *319*, 1668–1672.

Sta, M., Sylva-Steenland, R.M.R., Casula, M., de Jong, J.M.B.V., Troost, D., Aronica, E., and Baas, F. (2011). Innate and adaptive immunity in amyotrophic lateral sclerosis: evidence of complement activation. Neurobiol Dis *42*, 211–220.

Sunico, C.R., Domínguez, G., García-Verdugo, J.M., Osta, R., Montero, F., and Moreno-López, B. (2011). Reduction in the motoneuron inhibitory/excitatory synaptic ratio in an early-symptomatic mouse model of amyotrophic lateral sclerosis. Brain Pathol *21*, 1–15.

Swarup, V., Phaneuf, D., Dupre, N., Petri, S., Strong, M., Kriz, J., and Julien, J.P. (2011). Deregulation of TDP-43 in amyotrophic lateral sclerosis triggers nuclear factor B-mediated pathogenic pathways. J Exp Med *208*, 2429–2447.

Tan, W., Naniche, N., Bogush, A., Pedrini, S., Trotti, D., and Pasinelli, P. (2013). Small peptides against the mutant SOD1/Bcl-2 toxic mitochondrial complex restore mitochondrial function and cell viability in mutant SOD1-mediated ALS. J Neurosci *33*, 11588–11598.

Tanaka, K., Kanno, T., Yanagisawa, Y., Yasutake, K., Hadano, S., Yoshii, F., and Ikeda, J.-E.

(2011). Bromocriptine methylate suppresses glial inflammation and moderates disease progression in a mouse model of amyotrophic lateral sclerosis. Exp Neurol *232*, 41–52.

Tateno, M., Kato, S., Sakurai, T., Nukina, N., Takahashi, R., and Araki, T. (2009). Mutant SOD1 impairs axonal transport of choline acetyltransferase and acetylcholine release by sequestering KAP3. Hum Mol Genet *18*, 942–955.

Tennen, R.I., Michishita-Kioi, E., and Chua, K.F. (2012). Finding a Target for Resveratrol. Cell *148*, 387–389.

Texidó, L., Hernández, S., Martín-Satué, M., Povedano, M., Casanovas, A., Esquerda, J., Marsal, J., and Solsona, C. (2011). Sera from amyotrophic lateral sclerosis patients induce the non-canonical activation of NMDA receptors "in vitro". Neurochem Int *59*, 954–964.

Thorpe, J.W., Moseley, I.F., Hawkes, C.H., MacManus, D.G., McDonald, W.I., and Miller, D.H. (1996). Brain and spinal cord MRI in motor neuron disease. J Neurol Neurosurg Psychiat *61*, 314–317.

Tollervey, J.R., Curk, T., Rogelj, B., Briese, M., Cereda, M., Kayikci, M., König, J., Hortobagyi, T., Nishimura, A.L., Zupunski, V., et al. (2011). Characterizing the RNA targets and position-dependent splicing regulation by TDP-43. Nat Neurosci *14*, 452–458.

Trotti, D., Rolfs, A., Danbolt, N.C., Brown, R.H., and Hediger, M.A. (1999). SOD1 mutants linked to amyotrophic lateral sclerosis selectively inactivate a glial glutamate transporter. Nat Neurosci *2*, 427–433.

Trumbull, K.A., McAllister, D., Gandelman, M.M., Fung, W.Y., Lew, T., Brennan, L., Lopez, N., Morré, J., Kalyanaraman, B., and Beckman, J.S. (2012). Diapocynin and apocynin administration fails to significantly extend survival in G93A SOD1 ALS mice. Neurobiol Dis *45*, 137–144.

Tsao, W., Jeong, Y.H., Lin, S., Ling, J., Price, D.L., Chiang, P.-M., and Wong, P.C. (2012). Rodent models of TDP-43: recent advances. Brain Res *1462*, 26–39.

Tu, P.H., Raju, P., Robinson, K.A., Gurney, M.E., Trojanowski, J.Q., and Lee, V.M. (1996). Transgenic mice carrying a human mutant superoxide dismutase transgene develop neuronal cytoskeletal pathology resembling human amyotrophic lateral sclerosis lesions. Proc Natl Acad Sci USA *93*, 3155–3160.

Tuerxun, T., Numakawa, T., Adachi, N., Kumamaru, E., Kitazawa, H., Kudo, M., and Kunugi, H. (2010). SA4503, a sigma-1 receptor agonist, prevents cultured cortical neurons from oxidative stress-induced cell death via suppression of MAPK pathway activation and glutamate receptor expression. Neurosci Lett *469*, 303–308.

Udan, M., and Baloh, R.H. (2011). Implications of the prion-related Q/N domains in TDP-43 and FUS. Prion *5*, 1–5.

Van Den Bosch, L., Van Damme, P., Bogaert, E., and Robberecht, W. (2006). The role of excitotoxicity in the pathogenesis of amyotrophic lateral sclerosis. Biochimica Biophysica Acta *1762*, 1068–1082.

Van Langenhove, T., van der Zee, J., and Van Broeckhoven, C. (2012). The molecular basis of the frontotemporal lobar degeneration-amyotrophic lateral sclerosis spectrum. Ann Med *44*, 817–828.

Vance, C., Al-Chalabi, A., Ruddy, D., Smith, B.N., Hu, X., Sreedharan, J., Siddique, T., Schelhaas, H.J., Kusters, B., Troost, D., et al. (2006). Familial amyotrophic lateral sclerosis with frontotemporal dementia is linked to a locus on chromosome 9p13.2-21.3. Brain *129*, 868–876.

Verbeeck, C., Deng, Q., DeJesus-Hernandez, M., Taylor, G., Ceballos-Diaz, C., Kocerha, J., Golde, T., Das, P., Rademakers, R., Dickson, D.W., et al. (2012). Expression of Fused in sarcoma mutations in mice recapitulates the neuropathology of FUS proteinopathies and provides insight into disease pathogenesis. Mol Neurodegener *7*, 53.

Vijayalakshmi, K., Alladi, P.A., Ghosh, S., Prasanna, V.K., Sagar, B.C., Nalini, A., Sathyaprabha,

T.N., and Raju, T.R. (2011). Evidence of endoplasmic reticular stress in the spinal motor neurons exposed to CSF from sporadic amyotrophic lateral sclerosis patients. Neurobiol Dis *41*, 695–705.

Vucic, S., and Kiernan, M.C. (2007). Abnormalities in cortical and peripheral excitability in flail arm variant amyotrophic lateral sclerosis. J Neurol Neurosurg Psychiat *78*, 849–852.

Wang, J., Zhang, Y., Tang, L., Zhang, N., and Fan, D. (2011a). Protective effects of resveratrol through the up-regulation of SIRT1 expression in the mutant hSOD1-G93A-bearing motor neuron-like cell culture model of amyotrophic lateral sclerosis. Neurosci Lett *503*, 250–255.

Wang, L.-J., Lu, Y.-Y., Muramatsu, S.-I., Ikeguchi, K., Fujimoto, K.-I., Okada, T., Mizukami, H., Matsushita, T., Hanazono, Y., Kume, A., et al. (2002). Neuroprotective effects of glial cell line-derived neurotrophic factor mediated by an adeno-associated virus vector in a transgenic animal model of amyotrophic lateral sclerosis. J Neurosci *22*, 6920–6928.

Wang, L., Popko, B., and Roos, R.P. (2011). The Unfolded Protein Response in Familial Amyotrophic Lateral Sclerosis. Hum Mol Genet *20*, 1008-1015.

Wang, Q., Zhang, X., Chen, S., Zhang, X., Zhang, S., Youdium, M., and Le, W. (2011b). Prevention of motor neuron degeneration by novel iron chelators in SOD1(G93A) transgenic mice of amyotrophic lateral sclerosis. Neurodegenerative Dis *8*, 310–321.

Wang, W., Li, L., Lin, W.-L., Dickson, D.W., Petrucelli, L., Zhang, T., and Wang, X. (2013). The ALS disease-associated mutant TDP-43 impairs mitochondrial dynamics and function in motor neurons. Hum Mol Genet *22*, 4706-4719.

Waragai, M. (1997). MRI and clinical features in amyotrophic lateral sclerosis. Neuroradiology *39*, 847–851.

Wiedemann, F.R., Winkler, K., Kuznetsov, A.V., Bartels, C., Vielhaber, S., Feistner, H., and Kunz, W.S. (1998). Impairment of mitochondrial function in skeletal muscle of patients with amyotrophic lateral sclerosis. J Neurol Sci *156*, 65–72.

Wiedemann, F.R., Manfredi, G., Mawrin, C., Beal, M.F., and Schon, E.A. (2002). Mitochondrial DNA and respiratory chain function in spinal cords of ALS patients. J Neurochem *80*, 616–625.

Wijesekera, L.C., and Leigh, P.N. (2009). Amyotrophic lateral sclerosis. Orphanet J Rare Dis *4*, 3.

Williams, T.L., Day, N.C., Ince, P.G., Kamboj, R.K., and Shaw, P.J. (1997). Calcium-permeable α-amino-3-hydroxy-5-methyl-4-isoxazole propionic acid receptors: A molecular determinant of selective vulnerability in amyotrophic lateral sclerosis. Ann Neurol *42*, 200–207.

Wong, P.C., Pardo, C.A., Borchelt, D.R., Lee, M.K., Copeland, N.G., Jenkins, N.A., Sisodia, S.S., Cleveland, D.W., and Price, D.L. (1995). An adverse property of a familial ALS-linked SOD1 mutation causes motor neuron disease characterized by vacuolar degeneration of mitochondria. Neuron *14*, 1105–1116.

Wooley, C.M., Sher, R.B., Kale, A., Frankel, W.N., Cox, G.A., and Seburn, K.L. (2005). Gait analysis detects early changes in transgenic SOD1(G93A) mice. Muscle Nerve *32*, 43–50.

Worms, P.M. (2001). The epidemiology of motor neuron diseases: a review of recent studies. J Neurol Sci *191*, 3–9.

Wu, C.-H., Fallini, C., Ticozzi, N., Keagle, P.J., Sapp, P.C., Piotrowska, K., Lowe, P., Koppers, M., McKenna-Yasek, D., Baron, D.M., et al. (2012). Mutations in the profilin 1 gene cause familial amyotrophic lateral sclerosis. Nature *488*, 499–503.

Wu, Y., Li, X., Zhu, J.X., Xie, W., Le, W., Fan, Z., Jankovic, J., and Pan, T. (2011). Resveratrol-Activated AMPK/SIRT1/Autophagy in Cellular Models of Parkinson's Disease. Neurosignals *19*, 163–174.

Xiao, S., Sanelli, T., Dib, S., Sheps, D., Findlater, J., Bilbao, J., Keith, J., Zinman, L., Rogaeva, E., and Robertson, J. (2011). RNA targets of TDP-43 identified by UV-CLIP are deregulated in ALS. Mol Cell Neurosci *47*, 167–180.

Xu, Y.-F., Gendron, T.F., Zhang, Y.-J., Lin, W.-L., D'Alton, S., Sheng, H., Casey, M.C., Tong, J., Knight, J., Yu, X., et al. (2010). Wild-type human TDP-43 expression causes TDP-43 phosphorylation, mitochondrial aggregation, motor deficits, and early mortality in transgenic mice. J Neurosci *30*, 10851–10859.

Yamanaka, K., Chun, S.J., Boillee, S., Fujimori-Tonou, N., Yamashita, H., Gutmann, D.H., Takahashi, R., Misawa, H., and Cleveland, D.W. (2008). Astrocytes as determinants of disease progression in inherited amyotrophic lateral sclerosis. Nat Neurosci *11*, 251–253.

Yang, Y., Hentati, A., Deng, H.X., Dabbagh, O., Sasaki, T., Hirano, M., Hung, W.Y., Ouahchi, K., Yan, J., Azim, A.C., et al. (2001). The gene encoding alsin, a protein with three guanine-nucleotide exchange factor domains, is mutated in a form of recessive amyotrophic lateral sclerosis. Nat Genet *29*, 160–165.

Yong, V.W., and Rivest, S. (2009). Taking advantage of the systemic immune system to cure brain diseases. Neuron *64*, 55–60.

Yong, V.W., Wells, J., Giuliani, F., Casha, S., Power, C., and Metz, L.M. (2004). The promise of minocycline in neurology. Lancet Neurol *3*, 744–751.

Yoo, Y.-E., and Ko, C.-P. (2012). Dihydrotestosterone ameliorates degeneration in muscle, axons and motoneurons and improves motor function in amyotrophic lateral sclerosis model mice. PLoS ONE *7*, e37258.

Zhang, B., Tu, P., Abtahian, F., Trojanowski, J.Q., and Lee, V.M. (1997). Neurofilaments and orthograde transport are reduced in ventral root axons of transgenic mice that express human SOD1 with a G93A mutation. J Cell Biol *139*, 1307–1315.

Zhang, F., Liu, J., and Shi, J.-S. (2010). Anti-inflammatory activities of resveratrol in the brain: role of resveratrol in microglial activation. Eur J Pharmacol *636*, 1–7.

Zhang, H., Tan, C.-F., Mori, F., Tanji, K., Kakita, A., Takahashi, H., and Wakabayashi, K. (2008). TDP-43-immunoreactive neuronal and glial inclusions in the neostriatum in amyotrophic lateral sclerosis with and without dementia. Acta Neuropathol *115*, 115–122.

Zhang, W., Narayanan, M., and Friedlander, R.M. (2003). Additive neuroprotective effects of minocycline with creatine in a mouse model of ALS. Ann Neurol *53*, 267–270.

Zhang, X.-J., Liu, L.-L., Jiang, S.-X., Zhong, Y.-M., and Yang, X.-L. (2011). Activation of the ζ receptor 1 suppresses NMDA responses in rat retinal ganglion cells. Neuroscience *177*, 12–22.

Zhang, Y., Benmohamed, R., Zhang, W., Kim, J., Edgerly, C.K., Zhu, Y., Morimoto, R.I., Ferrante, R.J., Kirsch, D.R., and Silverman, R.B. (2012). Chiral cyclohexane 1,3-diones as inhibitors of mutant SOD1-dependent protein aggregation for the treatment of ALS. ACS Med Chem Lett *3*, 584–587.

Zhao, C.-P., Zhang, C., Zhou, S.-N., Xie, Y.-M., Wang, Y.-H., Huang, H., Shang, Y.-C., Li, W.-Y., Zhou, C., Yu, M.-J., et al. (2007). Human mesenchymal stromal cells ameliorate the phenotype of SOD1-G93A ALS mice. Cytotherapy *9*, 414–426.

Zhong, Z., Ilieva, H., Hallagan, L., Bell, R., Singh, I., Paquette, N., Thiyagarajan, M., Deane, R., Fernandez, J.A., Lane, S., et al. (2009). Activated protein C therapy slows ALS-like disease in mice by transcriptionally inhibiting SOD1 in motor neurons and microglia cells. J Clin Invest *119*, 3437–3449.

Zhu, S., Stavrovskaya, I.G., Drozda, M., Kim, B.Y.S., Ona, V., Li, M., Sarang, S., Liu, A.S., Hartley, D.M., Wu, D.C., et al. (2002). Minocycline inhibits cytochrome c release and delays progression of amyotrophic lateral sclerosis in mice. Nature *417*, 74–78.

Abbreviations

ALS, amyotrophic lateral sclerosis
ANOVA, analysis of variance
BD1036,
CHOP, C/EBP homologous protein
CLIP, cross-linking and immunoprecipitation
CMAP, compound muscle action potential
CNS, central nervous system
CNTF, ciliary neurotrophic factor
CSF, cerebrospinal fluid
CV, coefficient of variation
DNA, deoxyribonucleic acid
EEAT2, excitatory aminoacids transporter 2
EMG, electromyography
ER, endoplasmic reticulum
FALS, familial amyotrophic lateral sclerosis
FTLD, frontotemporal lobar degeneration
GABA, gamma-aminobutyric acid
GDNF, glial derived neurotrophic factor
IGF-1, insulin growth factor -1
IHC, immunohistochemistry
KAP3, kinesin-associated protein 3
MN, motoneuron
MCP1, monocyte chemoattractant protein 1
MEP, motor evoked potential
mnd, motoneuron degenerative
MND, motoneuron disease
MRI, magnetic resonance image
MUNE, motor unit number estimation
NMDA, N-methyl-D-aspartate
SOD1, superoxide dismutase 1
PCR, polymerase chain reaction
PDI, protein disulphide isomerase
PKC, protein kinase C
PL, print length
pmn, progressive motoneuropathy
PRE-084,
ROS, reactive forms of oxygen
RNA, ribonucleic acid
RSV, resveratrol
SALS, sporadic amyotrophic lateral sclerosis
Sigma-1R, sigma 1 receptor
SMA, spinal muscle atrophy
SMN, spinal motoneuron protein
TA, tibialis anterior
TS, toe spreading
UPR, unfolded protein response
UPS, ubiquitin-proteasome system
VEGF, vascular endothelial growth factor
WB, western blot
WT, wild type

Acknowledgments

This thesis would have not been possible without the help of a lot of people. For this reason, I would like to thank:

- Dr. Xavier Navarro, for his supervision and continuous support.
- Dr. Rosario Osta, for her constant collaboration during this entire thesis.
- Dr. Manel Portero-Otín, for his contribution regarding mitochondrial function and biogenesis.
- Dr. Mercè Pallás, for providing us the resveratrol enriched diet.
- All the members of the Group of Neuroplasticity and Regeneration who have contributed in one way or another to the work included in this thesis.

Grant support:

- Centro de Investigación Biomédica en Red sobre Enfermedades Neurodegenerativas (CIBERNED), Instituto de Salud Carlos III.
- Formación de Profesorado Universitario (FPU) Fellowship from the Ministerio de Educación y Ciencia.